

POTENTIAL BENEFITS OF SMART REFRIGERANT DISTRIBUTORS

Final Report

Date Published – December 2002



W. Vance Payne and Piotr A. Domanski

National Institute of Standards and Technology
Building Environment Division
MS 8631, Building 226, Room B114
Gaithersburg, Maryland USA 20899

Prepared for the
AIR-CONDITIONING AND REFRIGERATION TECHNOLOGY INSTITUTE
4100 North Fairfax Drive, Suite 200, Arlington, Virginia 22203

Distribution A – Approved for public release; further dissemination unlimited.

DISCLAIMER

This report was prepared as an account of work sponsored by the Air-conditioning and Refrigeration Technology Institute (ARTI) under its "HVAC&R Research for the 21st Century" (21-CR) program. Neither ARTI, the financial supporters of the 21-CR program, or any agency thereof, nor any of their employees, contractors, subcontractors or employees thereof - makes any warranty, expressed or implied; assumes any legal liability or responsibility for the accuracy, completeness, any third party's use of, or the results of such use of any information, apparatus, product, or process disclosed in this report; or represents that its use would not infringe privately owned rights. Reference herein to any specific commercial product, process, or service by trade name, trademark, manufacturer, or otherwise, does not necessarily constitute nor imply its endorsement, recommendation, or favoring by ARTI, its sponsors, or any agency thereof or their contractors or subcontractors. The views and opinions of authors expressed herein do not necessarily state or reflect those of ARTI, the 21-CR program sponsors, or any agency thereof.

Funding for the 21-CR program provided by (listed in order of support magnitude):

- **U.S.** Department of Energy (DOE Cooperative Agreement No. DE-FC05-99OR22674)
- Air-conditioning & Refrigeration Institute (ARI)
- Copper Development Association (CDA)
- New York State Energy Research and Development Authority (NYSERDA)
- Refrigeration Service Engineers Society (RSES)
- Heating, Refrigeration Air-conditioning Institute of Canada (HRAI)

Available to the public from

U.S. Department of Commerce
National Technical Information Service
5285 Port Royal Road
Springfield, VA 22161
(703) 487-4650

Available to **U.S.** Department of Energy and its contractors in paper from

U.S. Department of Energy
Office of Scientific and Technical Information
P.O. Box 62
Oak Ridge, TN 37831
(423) 576-8401

POTENTIAL BENEFITS OF SMART REFRIGERANT DISTRIBUTORS

Final Report

Date Published – December 2002

W. Vance Payne
Piotr A. Domanski



Prepared for the
AIR-CONDITIONING AND REFRIGERATION TECHNOLOGY INSTITUTE
Under ARTI 21-CR Program Contract Number 605-20050

Use of Non-SI Units in a Non-NIST Publication

It is the policy of the National Institute of Standards and Technology to use the International System of Units (metric units) in all of its publications. However, in North America in the HVAC&R industry, certain non-SI units are so widely used instead of SI units that it is more practical and less confusing to use measurement values for customary units only in figures and tables describing system performance.

EXECUTIVE SUMMARY

The main goal of this study was to investigate the benefits possible for finned tube refrigerant evaporators when refrigerant distribution was precisely controlled to produce a desired equal superheat in each circuit. This goal was accomplished by examining three different finned tube evaporators; a wavy fin, wavy-lanced fin, and a wavy-lanced fin evaporator with tube sheets separated. The effects of non-uniform airflow on capacity were also examined while superheat was controlled in each evaporator circuit. In parallel with the experimental effort, a modeling program was implemented and validated with the experimental results and then used to determine the savings in evaporator core volume possible if refrigerant distribution was controlled by a smart distributor. In extreme cases, the savings in core volume could be as much as 40 %.

Within the experimental part of this study, all three evaporators could avoid significant performance degradation using the ability to control superheat within each of the three finned tube circuits. As an example, with cross-counter flow configuration, uniform airflow, and exit manifold superheat fixed at 5.6°C (10.0°F), the wavy fin and wavy-lanced fin evaporator's capacity dropped by as much as 41 % and 32 %, respectively, as the superheat was allowed to vary between the circuits. Control of superheat was shown to be even more important during cross-parallel refrigerant flow due to the rapid pinching of the refrigerant and air temperatures. For the wavy and lanced finned evaporators in cross-parallel flow, capacity dropped by 85 % and 78 % as superheat changed from 5.6°C (10.0°F) to 16.7°C (30.0°F). As the coil faces were blocked to produce a non-uniform airflow, pressure drop through the coils increased

substantially and control of superheat was shown to restore performance. The non-uniform airflow tests showed that when airflow rate was held constant, the losses in capacity due to low airflow over a portion of the coil could be recovered to within 2% of the original uniform airflow capacity by controlling superheat. The more non-uniform the airflow over the coil, the more capacity was improved by controlling superheat.

A combination of results obtained from laboratory testing and simulations indicate the influence of tube-to-tube heat transfer on capacity degradation. The impact of tube-to-tube heat transfer was negligible in tests with a uniform **5.6 °C (10 °F)** superheat, but it was significant in tests involving **16.7 °C (30 °F)** superheat. Between the two possible conduction mechanisms of heat transfer that may occur, longitudinal fin conduction is responsible for degraded performance rather than longitudinal tube conduction, which has insignificant impact. The upgraded version of the **EVAP5** evaporator model, which accounts for tube-to-tube heat transfer based on tube temperatures, was able to predict key return bend temperatures which indicated the occurrence of tube-to-tube heat transfer. However, the study also confirmed that longitudinal heat conduction is affected by the fin design, air-side heat transfer coefficient, and moisture removal process.

ACKNOWLEDGEMENT

This work was sponsored by the Air-conditioning and Refrigeration Technology Institute (ARTI) under ARTI 21-CR Program Contract Number 605-20050. We acknowledge the comments and support from people associated with the sponsoring organizations and all members of the ARTI 21-CR Equipment Energy Efficiency Subcommittee. John Wamsley provided technician support for all of the experimental efforts, and Jong Min Choi assisted greatly with his technical comments and skillful support. David Yashar contributed the analysis on longitudinal tube conduction and provided many helpful comments for the final draft of this report.

TABLE OF CONTENTS

EXECUTIVE SUMMARY	i
ACKNOWLEDGMENTS	iii
LIST OF TABLES	vi
LIST OF FIGURES	viii
NOMENCLATURE.....	xii
CHAPTER 1. SCOPE OF THE STUDY	1
CHAPTER 2. BACKGROUND AND LITERATURE REVIEW	3
CHAPTER 3. LABORATORY EXPERIMENT	7
3.1 Experimental Setup.....	7
3.2 Evaporators Selected for Testing	11
3.3 Test Conditions and Experimental Procedure	14
3.4 Experimental Results	19
3.4.1 Cross-Counter Air/Refrigerant Flow Configuration Tests	19
3.4.1.1 Non-Uniform Superheat Tests	19
3.4.1.2 Effects of Airflow Rate on Coil Capacity	29
3.4.1.3 Effects of Non-Uniform Airflow on Coil Capacity	31
3.4.2 Cross-Parallel Air/Refrigerant Flow Configuration Tests	48
CHAPTER 4. EVAPORATOR MODELING AND SIMULATIONS	52
4.1 Background on Evaporator Model EVAP5	52
4.2 Description of EVAP5	53
4.2.1 Modeling Approach	53.
4.2.2 Heat Transfer and Pressure Drop Correlations	55

4.3 Modeling Issues	58
4.3.1 Refrigerant Distribution	58
4.3.2 Air-Side Heat Transfer Correlations	62
4.3.3 Internal Heat Transfer in a Finned Tube Evaporator	65
4.3.3.1 Longitudinal Tube Conduction	66
4.3.3.2 Tube-to-Tube Heat Transfer via Fins	71
4.4 Validation and Simulations with EVAP5	77
4.4.1 Validation of EVAPS	77
4.4.2 Possible Savings in Heat Transfer Area Due to Optimized Superheat	93
4.4.2.1 Cross-Counter Flow Configuratin with Uniform Air Flow Distribution	93
4.4.2.2 Cross-Parallel Flow Configuration with Uniform Air Flow Distribution	95
4.4.2.3 Cross-Counter Flow Arrangement With Non-Uniform Air Flow Distribution	97
CHAPTER 5. CONCLUSIONS	102
APPENDIX A. SUMMARY OF TEST RESULTS	104
APPENDIX B. CAPACITY UNCERTAINTY	166
APPENDIX C. USER'S INSTRUCTION FOR THE EVAP-COND VERSION USED IN THIS STUDY	167
BIBLIOGRAPHY	178

LIST OF TABLES

Table 3.1.1 : Essential Control Parameters	10
Table 3.3.1 Experimental Test Conditions	14
Table 3.3.2 Evaporator Tests	16
Table 3.3.3 Test Number and Conditions for Each Evaporator Test	16
Table 3.4.1.1 .1. Non-Uniform Superheat Test Data for COIL-W and COIL-E	20
Table 3.4.1.2.1 : Capacity of the Test Evaporators at Varying Airflow Rates	30
Table 3.4.1.3.1 : COIL-W Performance with Non-Uniform Airflow.....	32
Table 3.4.1.3.2: COIL-E Performance with Non-Uniform Airflow	33
Table 3.4.2.1: Counter and Parallel Flow Performance of COIL-W and COIL-E	49
Table 4.4.1.1: Measured and Simulated Capacities for COIL-W in Cross-Counter Flow Configuration	81
Table 4.4.1.2: Measured and Simulated Capacities for COIL-E in Cross-Counter Flow Configuration	82
Table 4.4.1.3: Measured and Simulated Capacities for COIL-EC in Cross-Counter Flow Configuration.....	83
Table 4.4.1.4a: EVAPS Validations for COIL-W, SI Units	84
Table 4.4.1.4b: EVAPS Validations for COIL-W, IP Units	85
Table 4.4.1.5a: EVAPS Validations for COIL-E, SI Units	86
Table 4.4.1.5b: EVAPS Validations for COIL-E, IP Units	87
Table 4.4.1.6a: EVAPS Validations for COIL-EC, SI Units	88
Table 4.4.1.6a: EVAPS Validations for COIL-EC, IP Units	88
Table 4.4.2.3.1 : Simulated Capacities and Refrigerant Distributions for Non-Uniform Inlet Air Velocity Profile	99
Table 4.4.2.3.2: Savings in Coil Volume Relative to COIL-W due to Optimized Refrigerant for 1:2.5 and 1:4 Air Velocity Ratios	101

Table A.1.1: Wavy Fin Evaporators in Cross-Counter Flow	104
Table A.2.1: Wavy Fin Evaporator in Cross-Parallel Flow	114
Table A.3.1: Enhanced Fin (Wavy Lanced) Evaporators in Cross-Counter Flow	119
Table A.4.1: Enhanced Fin (Wavy-Lanced) Evaporators in Cross-Parallel Flow	132
Table A.5.1: Enhanced-Cut Fin (Wavy-Lanced) Evaporator in Cross-Counter Flow .	137
Table A.6.1: Wavy Fin Evaporator with Non-Uniform Airflow	146
Table A.7.1: Enhanced Fin (Wavy-Lanced) Evaporator with Non-Uniform Airflow	153
Table B.1: Relative Uncertainties of Two Evaporator Tests	166

LIST OF FIGURES

Figure 3.1.1: Schematic diagram of the experimental setup.....	7
Figure 3.1.2: Condensing unit used to precisely control refrigerant conditions	8
Figure 3.2.1: COIL-EC showing separated tube depth rows	12
Figure 3.2.2: A schematic side view of refrigerant circuitry	12
Figure 3.2.3: A schematic side view of refrigerant circuitry for COIL-EC	13
Figure 3.2.4: Circuiting of all three evaporators.....	13
Figure 3.3.1 : Capacity ratio for different shape fins relative to the capacity at test 9 for the wavy coil	18
Figure 3.4.1.1.1 : Capacity of evaporators for tests 5 through 12.....	21
Figure 3.4.1.1.2: Capacity ratio at different superheat conditions relative to test 9 for COIL-W and COIL-E	21
Figure 3.4.1.1.3: Capacity ratio for COIL-W relative to test 9 for wet and test 5 for dry conditions	23
Figure 3.4.1.1.4: Capacity ratio for COIL-E relative to test 9 for wet and test 5 for dry conditions	23
Figure 3.4.1.1.5: COIL-W, test 9. circuit bend temperatures for cross-counter flow	26
Figure 3.4.1.1.6: COIL-W, test 12. circuit bend temperatures for cross-counter flow	26
Figure 3.4.1.1.7. Capacity of COIL-E and COIL-EC relative to COIL-E, test 9 at two different airflow rates	27
Figure 3.4.1.1.8. COIL-EC and COIL-E bend temperatures for test 9.....	27
Figure 3.4.1.1.9: COIL-EC and COIL-E bend temperatures for test 10.....	28
Figure 3.4.1.1.10: COIL-EC and COIL-E bend temperatures for test 13.....	28
Figure 3.4.1.1.11 : COIL-EC and COIL-E bend temperatures for test 14.....	29
Figure 3.4.1.2.1: Capacity as a function of air flow rate for wet coil conditions	31

Figure 3.4.1.3.1 : Idealized velocity profile over evaporator with upper half partially blocked	32
Figure 3.4.1.3.2: Uniform airflow velocity (ft/min) contour map for COIL-W	35
Figure 3.4.1.3.3: Non-uniform velocity (1:1.5) (ft/min) contour map for COIL-W	36
Figure 3.4.1.3.4: Non-uniform velocity (1:2) (ft/min) contour map for COIL-W	37
Figure 3.4.1.3.5: Relative capacities for COIL-W non-uniform airflow	38
Figure 3.4.1.3.6: Uniform velocity (ft/min) contour map for COIL-E	40
Figure 3.4.1.3.7: Non-uniform velocity (1:1.26) (ft/min) contour map for COIL-E	41
Figure 3.4.1.3.8: Non-uniform velocity (1:1.36) (ft/min) contour map for COIL-E	42
Figure 3.4.1.3.9: Non-uniform velocity (1:1.62) (ft/min) contour map for COIL-E	43
Figure 3.4.1.3.10: Non-uniform velocity (1:1.75) (ft/min) contour map for COIL-E ..	44
Figure 3.4.1.3.11: Non-uniform velocity (1:2.59) (ft/min) contour map for COIL-E ..	45
Figure 3.4.1.3.12: Capacity relative to uniform airflow for COIL-E	47
Figure 3.4.2.1 : Cross-parallel flow capacity comparison for COIL-W and COIL-E relative to their performance at test 9 with cross-counter flow	50
Figure 4.2.1.1 : Representation of air distribution and refrigerant circuitry in EVAP5	54
Figure 4.3.1.1 : Possible refrigerant pressure profiles in a three-circuit evaporator fed by a refrigerant distributor	59
Figure 4.3.1.2: EVAP-COND refrigerant input data options for evaporator simulations	60
Figure 4.3.1.3: EVAP-COND input data window for simulations involving a refrigerant distributor	60
Figure 4.3.1.4: EVAP-COND input data window for simulations with specified overall evaporator exit saturation temperature and superheat	61

Figure 4.3.2.1: Comparison of air-side heat transfer correlations	64
Figure 4.3.3.1: Tested and predicted capacities for COIL-E and COIL-EC at 5.6 °C (10 °F) and 16.7 °C (30 °F) superheats	66
Figure 4.3.3.1.1: Refrigerant circuitry configuration for the analyzed R-22 evaporator	68
Figure 4.3.3.1.2: EVAP-COND window with evaporator design information	69
Figure 4.3.3.1.3: EVAP-COND window with evaporator operating conditions	69
Figure 4.3.3.2.1: Schematic graph for longitudinal fin conduction between two adjacent tubes	74
Figure 4.3.3.2.2: Schematic of refrigerant circuitry for COIL-W, COIL-E and COIL-EC in cross-counter flow configuration	75
Figure 4.3.3.2.3: COIL-E measured and simulated capacities for tests with 5.6 °C (10 °F) and 16.7 °C (30 °F) superheats	76
Figure 4.4.1.1: Design parameters for COIL-W	78
Figure 4.4.1.2: Correction parameters for COIL-W and COIL-E	79
Figure 4.4.1.3: Difference between simulated and measured capacities for all wet coil tests for COIL-W, COIL-E, and COIL-EC	89
Figure 4.4.1.4: Difference between simulated and measured capacities for all dry coil tests for COIL-W, COIL-E, and COIL-EC	89
Figure 4.4.1.5: Tube numbering and refrigerant exit temperatures for individual tubes for test 9 and test 12 for COIL-W	91
Figure 4.4.1.6: Refrigerant exit qualities for individual tubes for COIL-E and COIL-EC test 10	92
Figure 4.4.2.1.1: Simulation results for alternative coil designs to COIL-W in cross-counter flow configuration	95
Figure 4.4.2.2.1: Simulation results for alternative coil designs to COIL-W in cross-parallel configuration	97
Figure 4.4.2.3.1: Air velocity profile representation for the 1:3 top-to-bottom velocity ratio	99

Figure **4.4.2.3.2**: COIL-W capacities at different air velocity ratios referenced
to capacity at test 9 in cross-counter flow configuration 100

Figure **4.4.2.3.3** Two evaporators with a reduced number of tubes 101

NOMENCLATURE

A_f	= finned surface area, m^2 (ft^2)
A_o	= outside tube and fin area, m^2 (ft^2)
A_p	= pipe mean surface area, m^2 (ft^2)
A_{ps}	= pipe outside surface area, m^2 (ft^2)
A_c	= cross sectional area of the tube available for axial heat conduction, m^2 (ft^2)
C_{min}	= minimum of mass flow rate times heat capacity for either fluid, W/K (Btu/(h·°F))
C_{max}	= maximum of the mass flow rate times the heat capacity for either fluid, W/K (Btu/(h·°F))
C_{pa}	= specific heat at constant pressure for air, kJ/(kg·K) (Btu/(lb·°F))
cfm	= airflow in cubic feet per minute
COP	= coefficient of performance
fpm	= velocity in feet per minute
h_i	= inside-tube heat-transfer coefficient, W/(m^2 ·K), (Btu/(ft^2 ·h·°F))
h_l	= heat-transfer coefficient for condensate layer, W/(m^2 ·K) (Btu/(ft^2 ·h·°F))
h_{pf}	= heat-transfer coefficient for tube/fin contact, W/(m^2 ·K) (Btu/(ft^2 ·h·°F))
h_o	= air-side heat transfer coefficient, W/(m^2 ·K) (Btu/(ft^2 ·h·°F))
i_{fg}	= latent heat of evaporation, kJ/(kg·K) (Btu/(lb·°F))
in WG	= inches of water in gage pressure
IP	= inch-pound or English system of units
K	= material thermal conductivity, W/(m·K) (Btu/(ft·h·°F))
L	= length, m (ft)
m_a	= air mass flow rate, kg/s (lb/h)
NTU	= number of transfer units for the heat exchanger, dimensionless
Q	= capacity or heat transferred, W (Btu/h)
scfm	= airflow in standard cubic feet per minute where flowrate is taken at the air standard density of 0.075 lbm/ ft^3 (ANSI/ASHRAE 51-1985)
SI	= international system of units or metric system of units

T	= temperature, K (°F)
t	= thickness, m (ft)
TXV	= thermostatic expansion valve
U	= overall heat-transfer coefficient, $W/(m^2 \cdot K)$ (Btu/(ft ² ·h·°F))
W	= width, m (ft)
X_p	= thickness of the tube wall, m (ft)
a	= $i_{fgw}(\omega_a - \omega_w)/(C_{pa}(T_a - T_w))$
ϵ	= heat-transfer effectiveness, fraction
ϕ	= fin efficiency, fraction
λ	= longitudinal heat conduction parameter, dimensionless
τ	= tube longitudinal conduction effect factor, fraction
ω_a	= humidity ratio of air at tube inlet, $kg_w/kg_{a,dry}$ (lb _w /lb _{a,dry})
ω_w	= humidity ratio of saturated air at temperature of condensate wetting the tube, $kg_w/kg_{a,dry}$ (lb _w /lb _{a,dry})

Subscripts

a	= air
f	= fin
i	= inlet, inside, or tube numbering index
j	= tube numbering index
nc	= no longitudinal conduction effects
wc	= considering longitudinal conduction effects
r	= refrigerant
sim	= simulation
w	= tube wall or water

1. SCOPE OF THE STUDY

Typically, finned tube evaporators employ parallel refrigerant circuits to obtain an optimal refrigerant mass flux, which affects refrigerant heat transfer coefficient and pressure drop. Each circuit performs optimally when the superheat at its exit matches the desired overall superheat in the exit manifold. Circuit superheat is affected by the refrigerant mass flowrate and the air flowrate associated with each tube.

Most evaporators use an inlet expansion valve with a flow distributor to control the bulk superheat at the evaporator exit manifold. The current practice does not embody means for adjusting refrigerant distribution between different circuits as needed. This means that non-uniform airflow or unintended pressure drops could cause some circuits to have excessive superheat while others may remain two-phase at the evaporator exit. In such situations, some circuits are inefficiently using coil area by transferring heat with superheated vapor instead of two-phase refrigerant. There are also mixing losses associated with reaching the final superheat as two-phase and superheated refrigerant mix in the evaporator exit manifold.

The advances in micro electro-mechanical systems (MEMS) offers the opportunity to develop and place inexpensive flow control valves on each circuit of an evaporator. This would allow control of the refrigerant superheat at the exit of each circuit. This experimental investigation examines the benefits of controlling superheat by placing individual needle valves on each circuit of the evaporators. The study involves three evaporators containing three parallel refrigerant circuits in identical configurations. Two

of these evaporators equipped with enhanced (wavy-lanced) fins, respectively, were tested to examine the benefits of maintaining even superheat when compared to three different scenarios of excessive superheat. The third evaporator with wavy-lanced fins and separated (cut) depth rows facilitates documenting the impact of tube-to-tube heat conduction. Non-uniform superheats are imposed and compared to uniform superheats of 5.6 °C (10.0 °F) and **16.7 °C** (30.0 °F). Non-uniform airflow is also imposed while superheats are allowed to adjust naturally, and while superheats are controlled by the individual expansion valves. The NIST tube-by-tube evaporator model, EVAPS, is also modified and used to simulate the experimental results.

The modeling part of the study discusses longitudinal tube and fin conduction and presents a scheme for including tube-to-tube heat transfer into a tube-by-tube simulation model. Validated results for an upgraded evaporator model are presented.

2. BACKGROUND AND LITERATURE REVIEW

Refrigerant incurs a phase change from the two-phase to the superheat zone in the evaporator. Large refrigerant mass flux not only increases the heat transfer rate, but also increases the pressure drop. Therefore, most refrigerant evaporators employ parallel circuits to provide a balanced effect on the evaporator capacity between the negative effect of refrigerant pressure drop and the positive effect of improved inside-tube heat transfer coefficient.

Even though all refrigerant circuits have the same inlet and outlet conditions, the refrigerant distribution is not uniform; the staggered tube arrangement can cause different heat transfer rates. Non-uniform refrigerant distribution is also due to the thermal resistance in the superheat region increasing more rapidly than in the two-phase region. Superheated vapor at the evaporator exit is necessary to prevent liquid compression and subsequent damage to the compressor, even though superheat reduces the performance of the system.

Refrigerant superheat in a given circuit is affected by the refrigerant mass **flow** rate and the airflow rate over the coil area associated with that circuit. For a given air distribution there is one refrigerant flow rate that results in a desired superheat at the individual circuit exit. When circuits are not well balanced, the target overall superheat **is a** result of mixing a highly superheated refrigerant and two-phase refrigerant leaving different circuits. This causes significant degradation in evaporator capacity because the circuit with superheated refrigerant transfers less heat.

Liang et al.(2001) conducted a numerical study of the refrigerant circuit. The governing equations and control volumes were presented with the simulation procedure for branches, tubes, and control volumes of a coil. Using the model, the heat transfer and fluid flow characteristics of the coils were studied. Compared to a common coil, the researchers found that using a complex refrigerant circuit arrangement where the refrigerant circuits are properly branched or joined may reduce the heat transfer area by around 5 % while maintaining constant capacity. The investigators experimentally validated 6 different refrigerant circuiting arrangements while maintaining the evaporators inlet and exit states. They used an R134a expansion valve inlet condition of **40 °C (104 °F)** saturated liquid with 5.0 °C (2.8 °F) of subcooling and an evaporator exit saturation temperature of 10 °C (50 °F) with 5.0 °C (**2.8 °F**) of superheat. Liang et al. noted that for a given evaporator load, designers must design the refrigerant circuitry to produce a refrigerant mass velocity that produces a maximum heat flux. Maximum heat fluxes vary with refrigerant circuiting due to varying levels of refrigerant pressure drop. Their model was able to predict evaporator capacity within 5 % on four of the six coils while predicting refrigerant pressure drop to within 25 %.

Kirby et al. (1998) experimentally investigated the performance of a 5275 W (18000 Btu/h) window air conditioner under wet and dry coil conditions with non-uniform airflow over the evaporator. The velocity variation over the evaporator varied by as much as a factor of 3, but upon correcting the non-uniformity of airflow, the investigators saw only a minor improvement in performance. This was a system study with no attempt

to maintain constant refrigerant states at the inlet and exit of the evaporator. A round disk was used to block 16 % of the central area of the evaporator while maintaining the original airflow. Tests were conducted with this blockage against the evaporator face and then moved in steps in the upstream direction. They found no capacity degradation greater than 2 %. The authors noted that the blockage caused more of the evaporating refrigerant to exist in the two-phase state; thereby reducing the superheated area of the evaporator and offsetting the inability of the air velocity to compensate for the loss of heat transfer area. Wet-coil tests also showed very little difference in the sensible heat ratio with non-uniform airflow. The authors noted that any non-uniformity in airflow must be noted by designers and used to intelligently circuit the refrigerant to equalize exposure of the evaporating refrigerant to airflow.

Chwalowski et al. (1989) examined computer models and performed experiments using three different evaporators; two V-shaped evaporators with upflow and one vertical slab evaporator with horizontal and angled flow with respect to the approaching airstream. These were evaporator tests with fixed evaporator saturation pressures; therefore, these tests parallel the technique used in the current experimental investigation. The investigators determined coil face velocity for several of the configurations and noted non-uniformity of the airflow. Generally, the evaporator capacity varied with the configuration mainly as a function of the exit superheats at the two evaporator exits. As the coil angle with respect to the approaching airstream was varied, capacity degradations on the order of 20 % were noted. Non-uniformities in superheat were produced by non-uniform airflow that produced differences in heat transfer and pressure drops within the

heat exchangers. The design of the circuitry and various splitting points within the evaporator produced differing capacities as a function of the coil orientation with the airstream. The investigators noted that none of the three evaporator models they considered could accurately predict capacity without some knowledge of the air velocity profile and refrigerant maldistribution.

3. LABORATORY EXPERIMENT

3.1 Experimental Setup

Figure 3.1.1 shows a schematic diagram of the experimental setup. The test rig consisted of three major flow loops: (1) a refrigerant flow loop containing a detachable test section, (2) a water flow loop used for the condensation heat exchanger and (3) an air flow loop used for the evaporation heat exchanger. The design of the rig allowed easy control of operating parameters such as condensing pressure and subcooling at the inlet of the expansion valve (evaporator inlet enthalpy), evaporating pressure at the exit of the evaporator, and superheat at the exit of the evaporator.

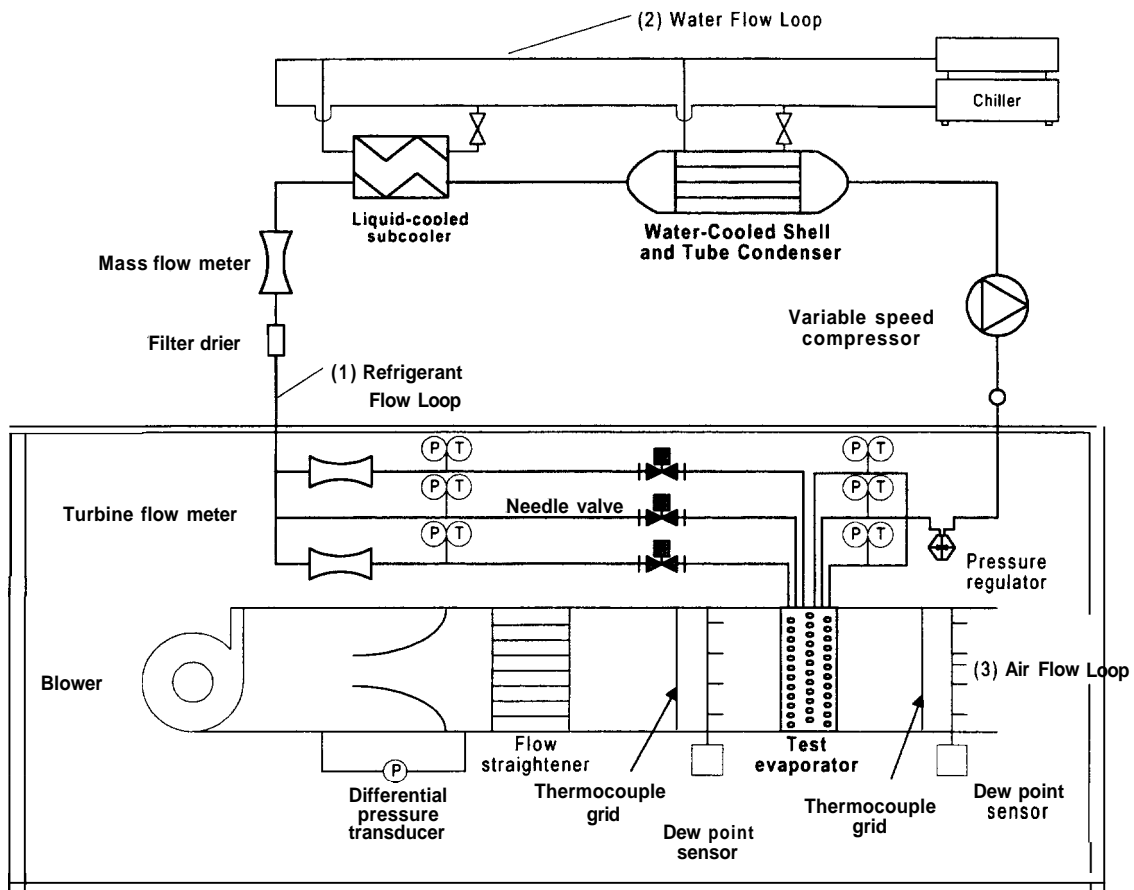


Figure 3.1.1: Schematic diagram of the experimental setup

Figure 3.1.2 is a photo of the specially designed and constructed **R22** condensing unit. The design of this condensing unit allowed complete control of the subcooled **R22** liquid conditions.

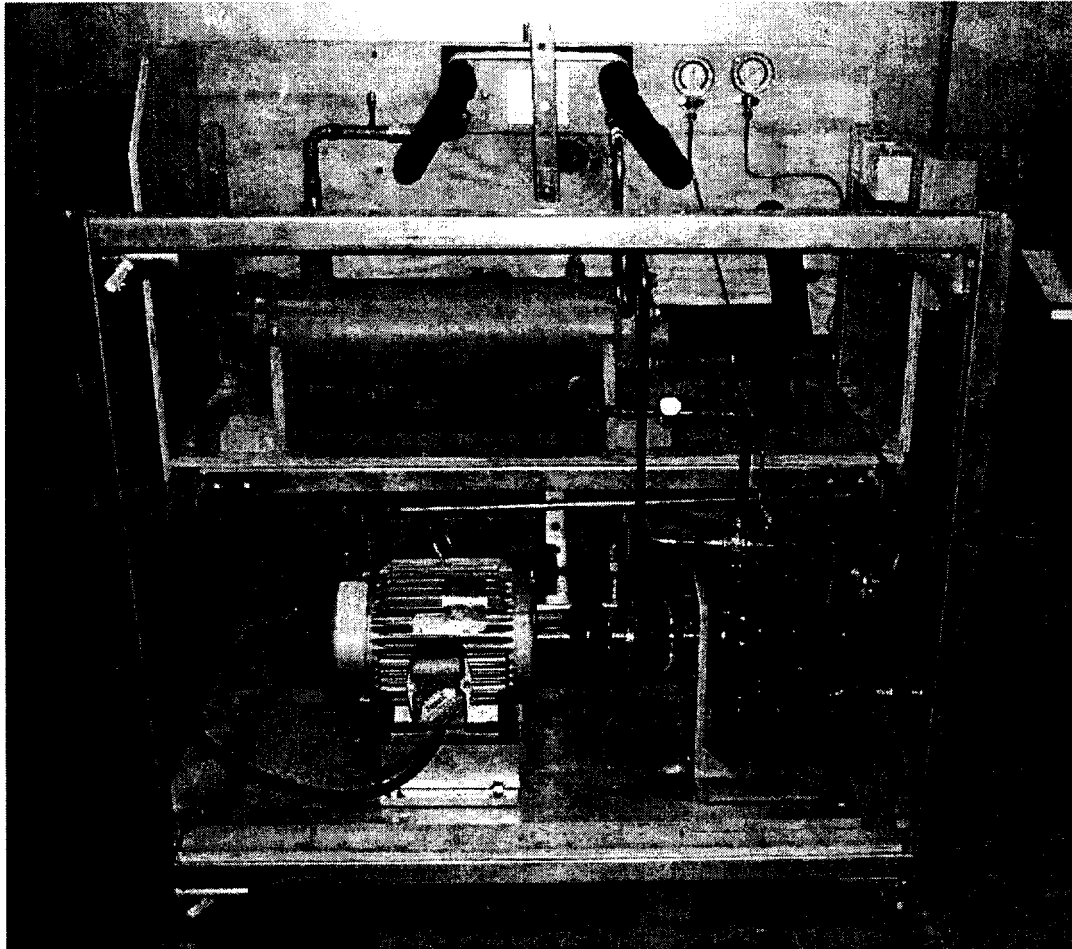


Figure 3.1.2: Condensing unit used to precisely control refrigerant conditions

An open-drive compressor with a variable speed motor provided refrigerant mass flow, set the enthalpy entering the test section, set the condensing pressure, and set the subcooling at the inlet of the expansion valves. We controlled condensing pressure by adjusting cooling water flow using a hand-operated needle valve. To provide additional pressure control for the condenser, we also controlled the entering temperature of the cooling water. Water flow rate and temperature through the subcooler plate type heat

exchanger controlled the refrigerant subcooling at the inlet of the expansion valve. A loop supplying water to the condensing heat exchanger and subcooler consisted of a refrigerator, water storage tank, and a pump. The controls combined to produce evaporator inlet quality of $25 \% \pm 1 \%$.

The test section has three parallel refrigerant paths. The exit pressure of the evaporator was adjusted by a pressure regulating valve which was installed in the refrigerant line. The superheats of the three circuits of the evaporator were adjusted by three manual expansion valves. The design of the test section allowed easy installation and replacement of the evaporators. The pressure and temperature were measured upstream and downstream of the test rig. Flow conditions were also monitored using a sight glass at the inlet of the compressor and expansion valves.

The total refrigerant flow rate was measured by a Coriolis-type mass flow meter in the liquid line between the subcooler and the expansion valves. Two turbine flow meters were installed to measure flow rate in two of the circuits. Flow through the third circuit was calculated by subtracting the flow through two of the circuits from the total mass flow.

Air flow rate was measured in the air flow chamber according to ANSI/ASHRAE 51-1985. Evaporator capacity was calculated using the air enthalpy method and refrigerant enthalpy method following procedures specified in ASHRAE Standard **37** (1998). In the present experiments, the maximum difference between the air and refrigerant side capacity was less than 5% . Air velocity at the face of the evaporator was measured with a hot wire anemometer.

Table 3.1.1 lists the parameters controlled to produce a successful evaporator test. The parameters are listed in the order they were set to produce a controlled test.

Table 3.1.1: Essential Control Parameters

Parameter	Setpoint
Upstream Liquid Saturation Temperature	40.6 °C (105.0 °F): controlled by condenser water flowrate and compressor speed
Liquid Line Subcooling	8.3 °C (15.0 °F): controlled by upstream pressure and refrigerant charge
Evaporator Circuit Superheats	5.6 °C or 16.7 °C (10.0 °F or 30.0 °F): controlled by expansion/needle valve opening and evaporator exit pressure
Evaporator Exit Saturation Temperature	7.2 °C (45.0 °F): controlled by evaporator pressure regulator valve and compressor speed
Evaporator Inlet Liquid Enthalpy	Corresponds to the saturated liquid temperature of 40.6 °C (105.0 °F): when inlet pressures were increased, the inlet enthalpy was always monitored to produce an enthalpy equal to the saturated liquid enthalpy at 40.6 °C (105.0 °F) \pm 1.4 °C (2.5 °F)

3.2 Evaporators Selected for Testing

We used three finned tube heat exchangers of the same outside dimensions, tube spacing, and circuitry as the test evaporators: (1) COIL-W with wavy fins, (2) COIL-E with wavy-lanced (enhanced) fins, and (3) COIL-EC (Figure 3.2.1) with wavy-lanced (enhanced) fins and the tube rows separated to inhibit tube-to-tube heat transfer (enhanced-cut). Figures 3.2.2, 3.2.3, and 3.2.4 show the side views of the refrigerant circuits. The following are the main design parameters:

- (a) 3 depth rows with 25.4 mm (1 in) face spacing and 22.0 mm (0.866 in) row spacing
- (b) 3 refrigerant circuits as shown in Figures 3.2.1 and 3.2.2
- (c) 9.53 mm (0.375 in) diameter round copper tubes, smooth walls, 0.254 mm (0.010 in) wall thickness
- (d) 0.1143 mm (0.0045 in) thick aluminum fins; wavy fins for COIL-W and louvered or slit fins for COIL-E and COIL-EC

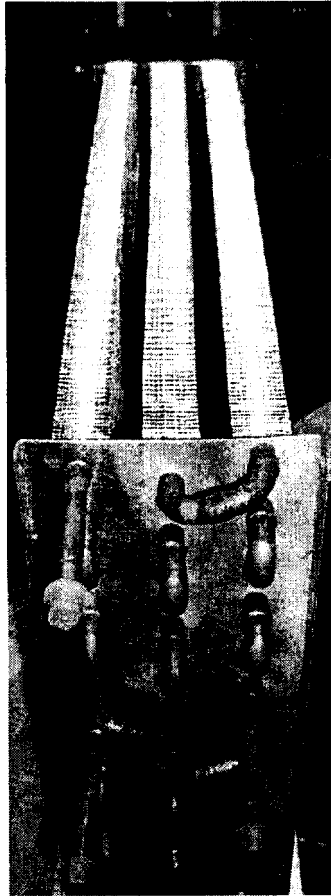


Figure 3.2.1: COIL-EC showing separated tube depth rows

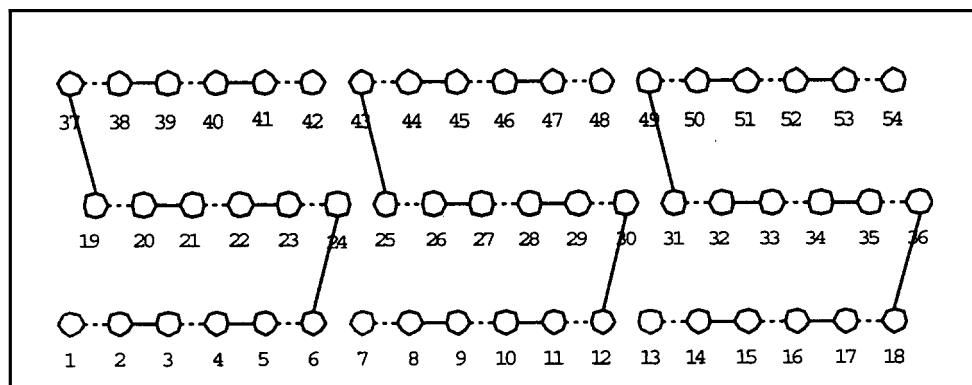


Figure 3.2.2: A schematic side view of refrigerant circuitry

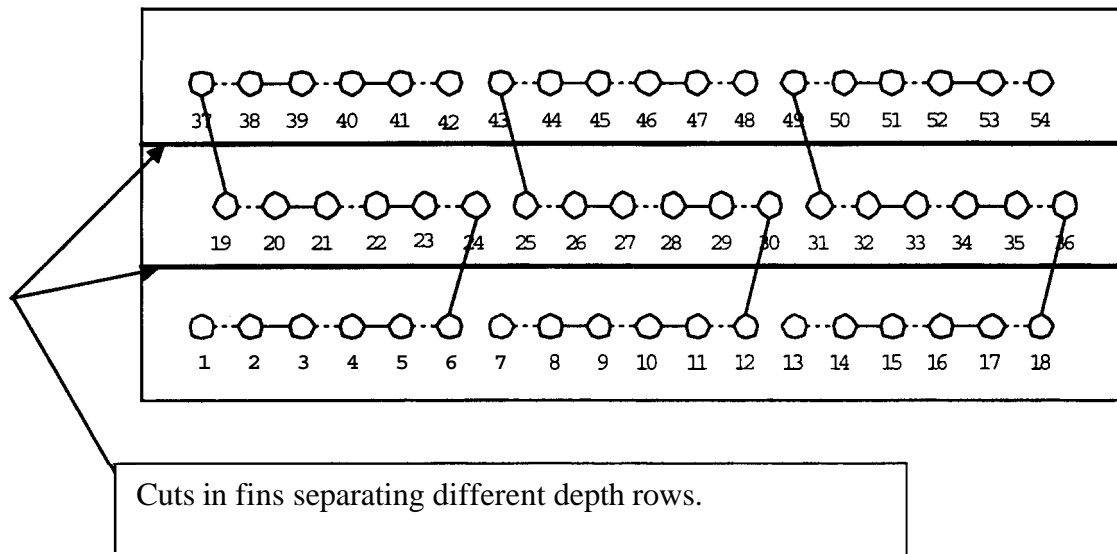


Figure 3.2.3: A schematic side view of refrigerant circuitry for COIL-EC

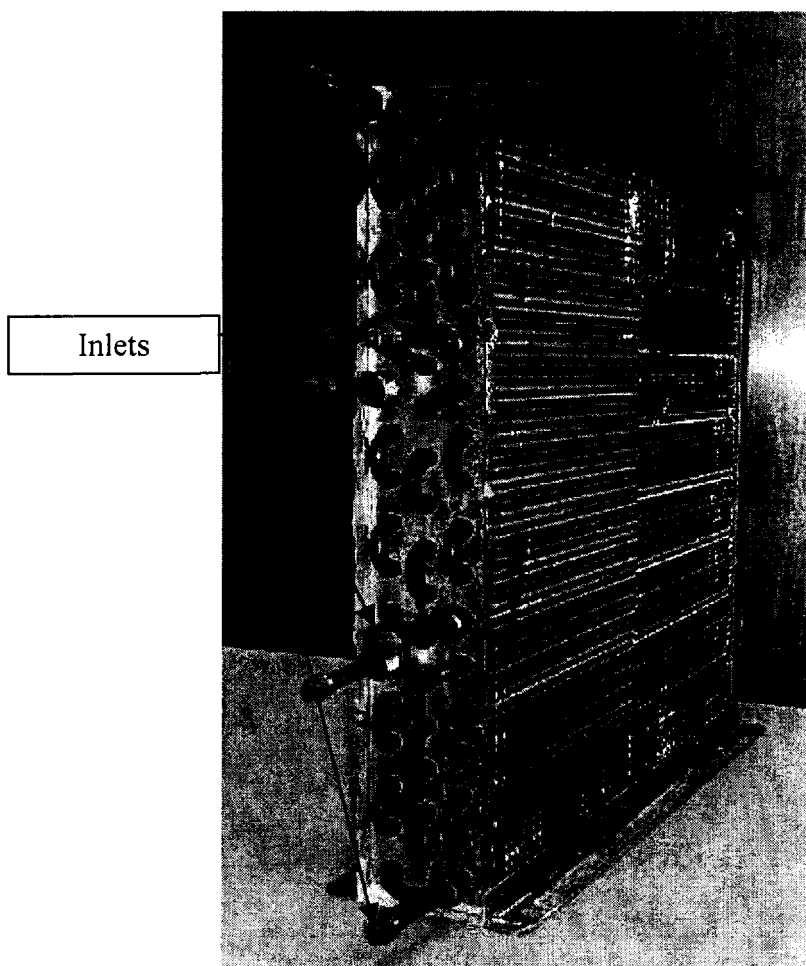


Figure 3.2.4: Circuiting of all three evaporators

3.3 Test Conditions and Experimental Procedure

Table 3.3.1 lists the test parameters and environmental chamber conditions for tests on the three evaporators. All tests were conducted at the same 26.7 °C (80.0 °F) indoor dry-bulb with dew-point varying for wet-coil tests and dry-coil tests. Refrigerant R22 conditions at the inlet to the expansion valves were controlled to maintain an enthalpy equivalent to a 48.9 °C (120.0 °F) saturation temperature with a subcooling of 8.3 °C (15.0 °F) \pm 1.4 °C (2.5 °F). Some tests required increasing the inlet pressure to produce the required superheats at the evaporator circuit exits. When the pressure was increased, the enthalpy and subcooling were adjusted to keep a constant enthalpy at the evaporator inlet.

Table 3.3.1 : Experimental Test Conditions

Variable	Value	Tolerance
Indoor Dry-Bulb	26.7 °C (80.0 °F)	0.28 °C (0.5 °F)
Indoor Dew-Point for Wet-Coil Tests	15.8 °C (60.4 °F)	0.28 °C (0.5 °F)
Evaporator Exit Saturation Temperature	7.2 °C (45.0 °F)	0.28 °C (0.5 °F)
Evaporator/Expansion Valve Inlet Saturation Temperature	48.9 °C (120.0 °F)	1.4 °C (2.5 °F)
Evaporator/Expansion Valve Inlet Subcooling	8.3 °C (15.0 °F)	1.4 °C (2.5 °F)

Once an evaporator coil was mounted in the airflow chamber, indoor dry-bulb and dew-point were stabilized for at least one hour. While indoor psychrometric conditions stabilized, the evaporator inlet R22 pressure and temperature were set by adjusting the

flow control valves on the condensing unit. Water flow to the condenser and subcooler plate heat exchangers was adjusted to establish the evaporator expansion valves inlet pressure and temperature. The evaporator exit saturation temperature was set by adjusting the evaporator pressure regulating valve at the exit of the evaporator. Superheat conditions in the individual circuits were set by adjusting R22 mass flow through each circuit. Airflow rate over the evaporator was adjusted using the variable speed drive on the airflow chamber's pull-thru fan.

Table 3.3.2 and 3.3.3 list the tests performed for the evaporators. Capacity specific airflow rate was initially established at $193 \text{ m}^3/\text{kWh}$ (400 scfm/ton) for test 9. Test 9 required manipulating superheats and airflow rate *to* obtain the desired airflow to capacity ratio. Test 9 capacity was then used to calculate the airflow rate **for** the $169 \text{ m}^3/\text{kWh}$ (300 scfm/ton) and $242 \text{ m}^3/\text{kWh}$ (500 scfm/ton) tests. Tests with **a** cross-parallel flow configuration were performed by switching the refrigerant **flow**.

Non-uniform airflow tests were performed with COIL-W and COIL-E. We established non-uniform air distribution by attaching a series of metal mesh plates to **the** upper half of the coil.

A hot wire anemometer was used to measure airflow rate by traversing the coil **at** a minimum of 25 equally spaced points at the face of the coil. This measurement speed with the chamber airflow within 2 %.

Evaporator	Tests Performed
COIL-W (wavy fins), cross-counter flow	1, 5-13 (10 tests)
COIL-W (wavy fins), cross-parallel flow	9-12 (4 tests)
COIL-E (lanced fins), cross-counter flow	1, 2, 5-14 (12 tests)
COIL-E (lanced fins), cross-parallel flow	9-12 (4 tests)
COIL-EC, cross-counter flow	1, 2, 5, 6, 9, 10, 13, 14 (8 tests)
COIL-W, cross-counter flow, non-uniform airflow	9 (1/2 profile, no superheat adjustment), 9 (1/2 profile, superheat adjusted), 9 (1/3 profile, no superheat adjustment), 9 (1/3 profile, superheat adjusted) [4 tests]
COIL-E, cross-counter flow, non-uniform airflow	9 (1/2 profile, no superheat adjustment), 9 (1/2 profile, superheat adjusted), 9 (1/3 profile, no superheat adjustment), 9 (1/3 profile, superheat adjusted) [4 tests]

Table 3.3.3: Test Number and Conditions for Each Evaporator Test

Test #	Volumetric Flowrate of Air m ³ /h (scfm)			Coil Surface		Overall Superheat			
						Superheats in Individual Circuits			
	145·Q ¹ (300·Q)	193·Q ¹ (400·Q)	242·Q ¹ (500·Q)	Dry	Wet	5.6 °C (10.0 °F) 5.6/5.6/5.6 (10/10/10)	16.7 °C (30.0 °F) 16.7/16.7/16.7 (30/30/30)	5.6 °C (10.0 °F) 16.7/*/16.7 (30/*/30)	5.6 °C (10.0 °F) */16.7/16.7 (*/*/30/30)
1	x				x	1			
2	x				x		2		
3	x				x			3	
4	x				x				4
5		x		x		5			
6		x		x			6		
7		x		x				7	
8		x		x					8
9		x			x	9			
10		x			x		10		
11		x			x			11	
12		x			x				12
13			x		x	13			
14			x		x		14		
15			x		x			15	
16			x		x				16

* Superheat to be controlled such that the desired overall level of superheat is obtained¹

1) SI units of m³/kWh multiplied by capacity (Q) in kW to determine airflow, (IP units of cfm/ton multiplied by capacity (Q) in tons).

In total we performed **54** tests with uniform airflow and 28 tests with imposed non-uniform distribution of air. We conducted a total of 90 tests including repeats and tests that were excluded due to unsteady or non-standard conditions.

The capacity characteristics of the three evaporators are shown below. Figure 3.3.1 shows the capacity ratio at different test conditions to the capacity at test **9** for the wavy coil. Tests **1,9**, and **13** are wet coil tests, and test **5** is a dry coil test. COIL-E and COIL-EC evaporators represented higher capacity than that of the COIL-W evaporator for the wet coil tests. Even though the air-side sensible heat transfer coefficient is much lower than the refrigerant side, the air-side thermal resistance is reduced due to the enhancement of moisture condensation and large finned area. For wet coil tests (tests **1, 9, 13**), the capacity of COIL-E and COIL-EC was larger than that of COIL-W. The COIL-EC produced higher capacity than COIL-E possibly because of the added fin leading edges agitating the boundary layer and increasing the air-side heat transfer coefficient even further in addition to eliminating some tube-to-tube heat transfer.

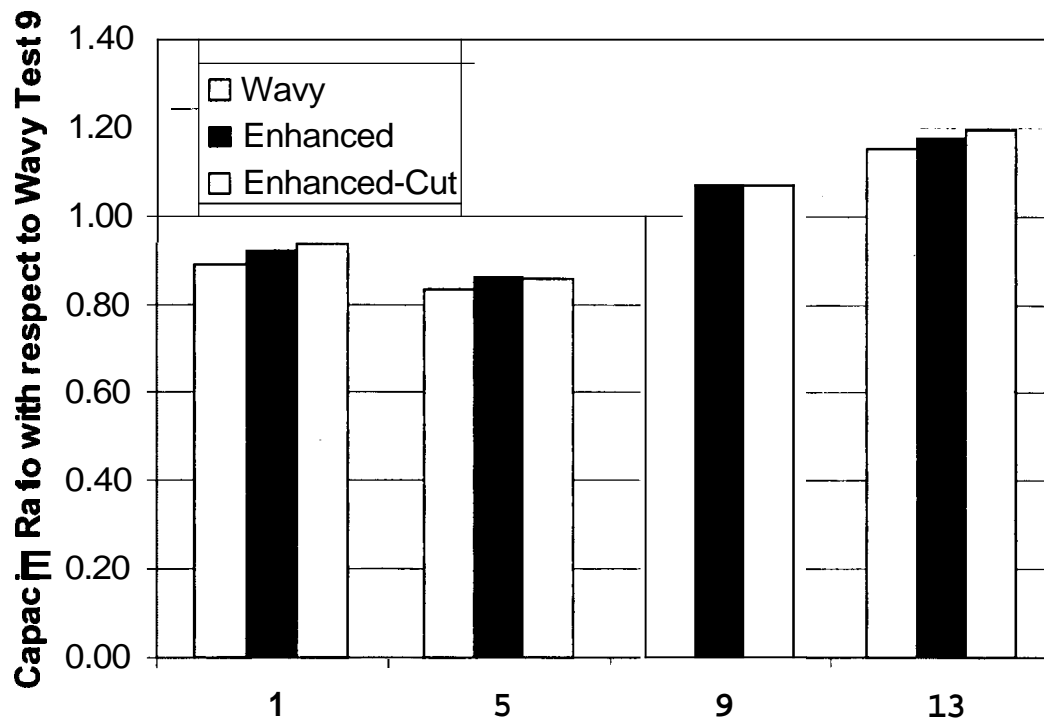


Figure 3.3.1: Capacity ratio for different shape fins relative to the capacity at test 9 for the wavy coil (Test 1: low airflow, wet coil, Test 5: median airflow, dry coil, Test 9: median airflow, wet coil, Test 13: high airflow, wet coil). All tests have a 5.6 °C (10.0 °F) uniform superheat.

3.4 Experimental Results

3.4.1 Cross-Counter Air/Refrigerant Flow Configuration Tests

3.4.1.1 Non-Uniform Superheat Tests

Figure 3.4.1.1.1 shows capacity at different superheat test conditions. These data are shown in Table 3.4.1.1.1. All of the coils showed a rapid decrease in capacity when individual circuit superheat was increased with the overall superheat maintained at 5.6 °C (10 °F). Figure 3.4.1.1.2 shows the relative capacity of COIL-W tests 10 and 12 with respect to test 9. Even though the overall superheat was held at 5.6 °C (10 °F), the non-uniformity of superheat in cases 11 and 12 produced a 41 % loss in capacity. This was almost as severe as the 43 % loss in capacity seen when overall superheat was held at 16.7 °C (30.0 °F).

Test 12 showed similar capacity as test 10 even though overall superheat was lower. At test condition 12, the mass flow rate through the top circuit was much higher than that at test 10. Therefore, the inlet refrigerant temperature of the evaporator for test 10 was higher than test 12 because exit pressure was the same. This means that the temperature difference between air and refrigerant for test 12 was higher than for test 10. This allowed test 12 to have a higher capacity than test 10.

Table 3.4.1.1.1: Non-Uniform Superheat Test Data for COIL-W and COIL-E

Test Name	Test #	Coil Designation	Volumetric Flowrate of Air m ³ /h (cfm)			Coil Surface		Overall Superheat							
								Superheats in Individual Circuits							
			145·Q ^{1a} (300·Q)	193·Q ^{1a} (400·Q)	242·Q ^{1a} (500·Q)	Dry	Wet	5.6 °C (10.0 °F)		16.7 °C (30.0 °F)		5.6 °C (10.0 °F)		5.6 °C (10.0 °F)	
								5.6/5.6/5.6 (10/10/10)	16.7/16.7/16.7 (30/30/30)	16.7/*/16.7 (30/*/30)	*/16.7/16.7 (*/*/30/30)	Q _{test} W (Btu/h)	Q _{test} / Q ^{1b}	Q _{test} W (Btu/h)	Q _{test} / Q ^{1b}
Cross-Counter Air/Refrigerant Flow															
W020225B	5	W		X		X		5428 (18519)	1						
W020228A	6	W		X		X				3569 (12177)	0.66				
W020221A	7	W		X		X						3910 (13341)	0.72		
W020225A	8	W		X		X								3888 (13266)	0.72
W020207B	9	W		X		X		6507 (22203)	1						
W020530A	10	W		X		X				3722 (12701)	0.57				
W020531A	11	W		X		X						3837 (13091)	0.59		
W020215B	12	W		X		X								3830 (13067)	0.59
W020322A	5	E		X		X		5602 (19115)	1						
W020321B	6	E		X		X				4301 (14677)	0.77				
W020322C	7	E		X		X						4797 (16367)	0.86		
W0203228	8	E		X		X								4700 (16037)	0.84
E020607A	9	E		X		X		6955 (23733)	1						
W020318A	10	E		X		X				4865 (16599)	0.70				
W0203188	11	E		X		X						5485 (18715)	0.79		
W020319A	12	E		X		X								4735 (16157)	0.68

* Superheat to be controlled such that the desired overall level of superheat is obtained

1a) SI units of m³/kWh multiplied by capacity (Q) in kW to determine airflow, (IP units of cfm/ton multiplied by capacity (Q) in tons).

1b) Capacity relative to the 5.6 °C (10.0 °F) tests noted by a ratio of 1 in the row above.

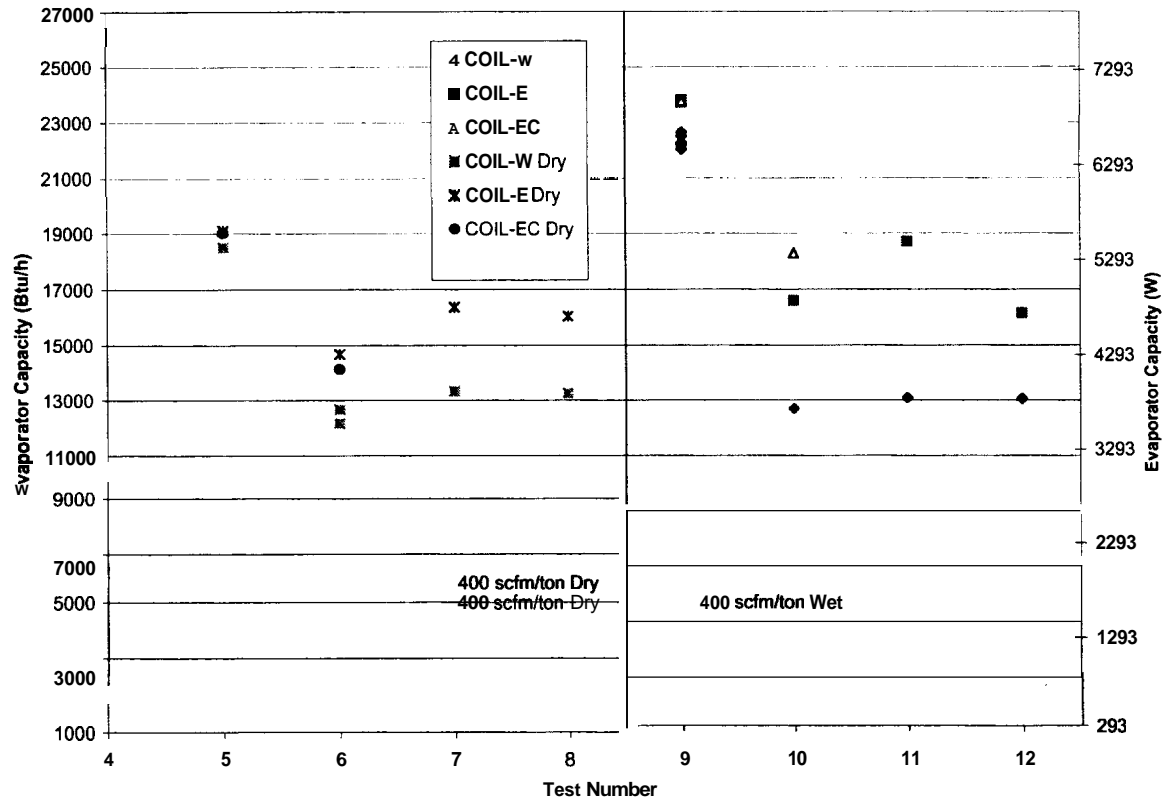


Figure 3.4.1.1.1: Capacity of evaporators for tests 5 through 12

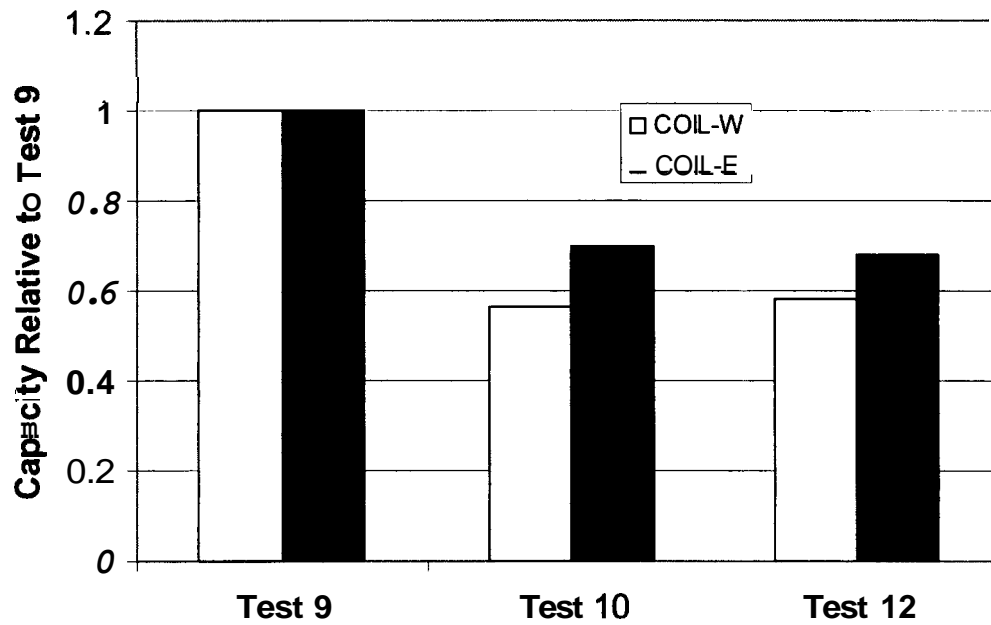


Figure 3.4.1.1.2: Capacity ratio at different superheat conditions relative to test 9 for COIL-W and COIL-E (superheat cases follow Table 3.4.1.1.1).

For COIL-E, the reduction in capacity due to an increase in superheat was lower than COIL-W (Figure 3.4.1.1.1 and 3.4.1.1.2). COIL-E seemed to show a preference as to which flooded circuit (test 11 or 12) produced the higher capacity. When the middle circuit was flooded, the capacity decreased by 21 % compared to 32 % when the top circuit was flooded.

Figure 3.4.1.1.3 shows the relative capacity of COIL-W for tests 10 and 12 with respect to test 9 and for tests 6 and 8 with respect to test 5. The capacity of the dry coil decreased by 28 % with non-uniform circuit superheats with overall superheat fixed at 5.6 °C (10 °F). COIL-E capacity (Figure 3.4.1.1.4) dropped by 16 % with non-uniform superheat under dry conditions; again COIL-E showed that flooding the middle circuit produced a smaller capacity drop than flooding the top circuit while holding overall superheat constant at 5.6 °C (10 °F).

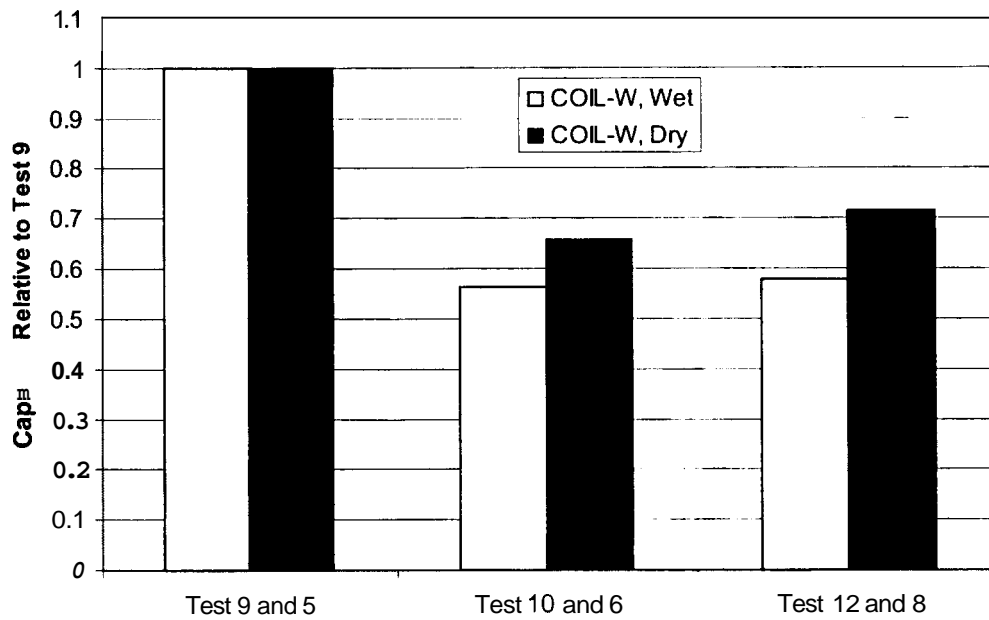


Figure 3.4.1.1.3: Capacity ratio for COIL-W relative to test **9** for wet and test **5** for dry conditions

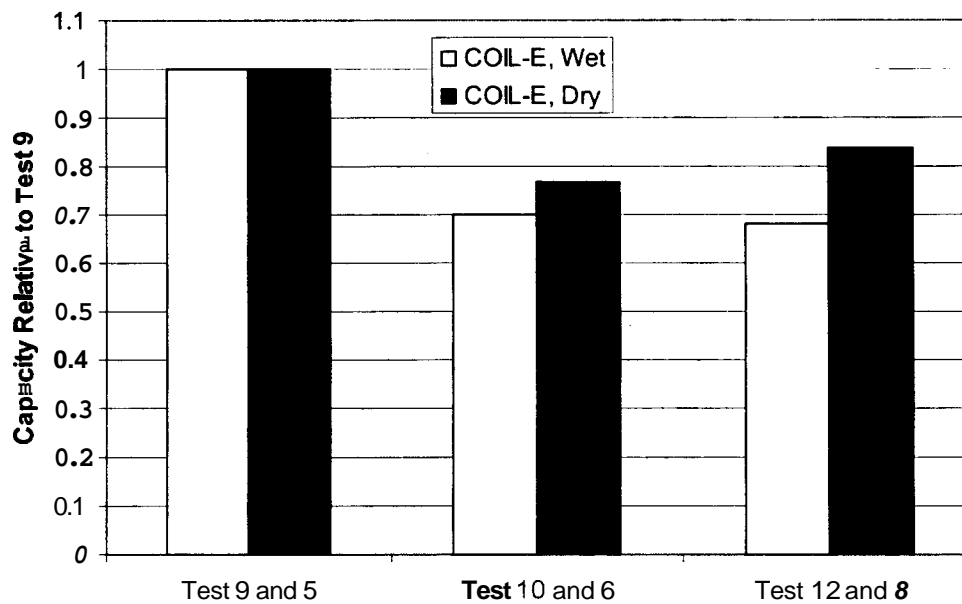


Figure 3.4.1.1.4: Capacity ratio for COIL-E relative to test **9** for wet and test **5** for dry conditions

The experimental investigation was designed to reveal some of the effects of tube-to-tube heat transfer by heat conduction through the fin material. The comparison was done by

examining COIL-E and COIL-EC and comparing their capacity at different levels of superheat. In addition to the capacity comparison between COIL-E and COIL-EC, direct evidence of conduction between tubes was noted from the thermocouple bend temperature data for COIL-W.

Figures 3.4.1.1.5 and 3.4.1.1.6 show bend temperature data for test 9 (6.7 °C (10 °F) superheat on all circuits) and test 12 (flooded top circuit with 16.7 °C (30.0 °F) superheat on the other two circuits). The figure for test 9 shows a uniform temperature distribution between comparable bends in the three refrigerant circuits. The noticeable difference occurs for test 12 where the low temperature, flooded top circuit shows some thermal communication with the final tube passes of the middle circuit. The top circuit is showing an average surface temperature of approximately 9.4 °C (49 °F) throughout all of its tubes, while the middle circuit shows definite superheat at the third and fourth final tube bend with a temperature of 24.0 °C (75.2 °F). This is where the conduction between circuits was obvious; the surface temperature on the final two tubes bend was 22.3 °C (72.2 °F). This is a decrease in temperature due to conduction between the top circuit's tube and the middle circuit's tubes.

The conduction effects were quantified in the tests conducted with COIL-E and COIL-EC; by separating the tube sheets in COIL-EC and thereby removing a majority of the conduction path between tubes. Figure 3.4.1.1.7 shows the capacity of COIL-E and COIL-EC relative to test 9 for COIL-E during cross-counter flow for tests 9, 10, 13, and 14. These two coils used identical fin material and fin type; the only difference was the

tube sheets of COIL-EC were separated. Figure 3.4.1.1.8 shows that for test 9, COIL-E and COIL-EC have very similar bend temperatures. Figure 3.4.1.1.9 shows the same coils with the superheat increased to 16.7 °C (30.0 °F) at the coil exit (test 10). COIL-EC shows lower inlet temperatures than COIL-E even though expansion valve inlet and coil exit conditions are almost identical for both tests. The differences in temperatures seen with tests 9 and 10 are more pronounced for tests 13 and 14 at the higher airflow rate.

These differences in temperatures could have produced the differences in capacity seen between COIL-E and COIL-EC. As noted above, the inlet and exit conditions for these coils were nearly identical, but COIL-EC always showed lower bend temperatures than COIL-E. This would mean that COIL-EC was operating at a higher average temperature difference with respect to the air than COIL-E. The greater average temperature difference for COIL-EC could translate to higher capacity than COIL-E. The test results showed that both coils produced very similar capacities when the overall superheat was at 5.6 °C (10.0 °F). As the superheat was increased to 16.7 °C (30.0 °F), COIL-EC capacity was 10% higher than COIL-E. As the airflow increased for tests 13 and 14, COIL-E and COIL-EC still produced nearly equal capacities at 5.6 °C (10.0 °F) superheat, but when superheat was increased to 16.7 °C (30.0 °F), COIL-EC had a 23 % higher capacity than COIL-E (Figures 3.4.1.1.10 and 3.4.1.1.11). This tends to lend more evidence to conduction effects between the tube sheets; eliminating some conduction paths improved the performance of the enhanced fin coil.

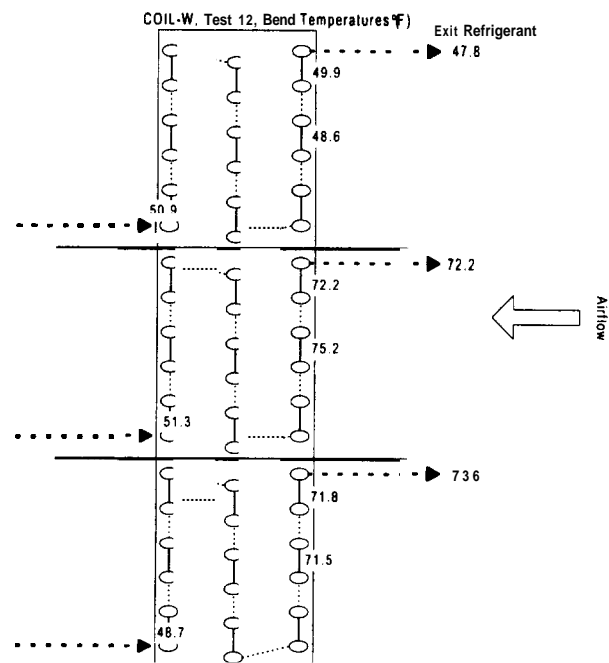
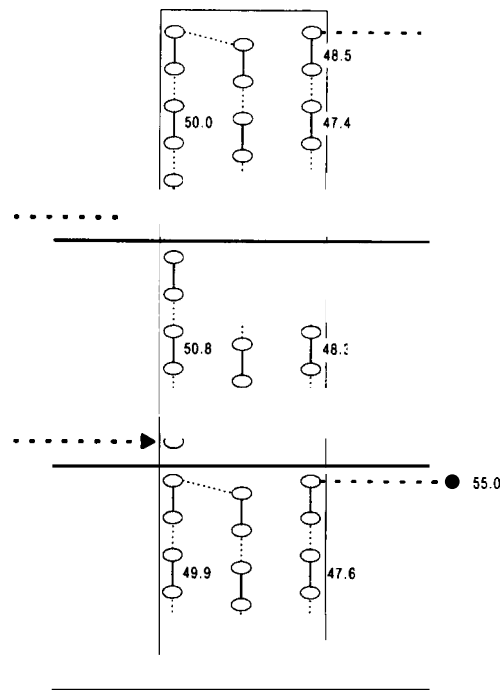


Figure 3.4.1.1.6: COIL-W, test 12, circuit bend temperatures for cross-counter flow (Top circuit flooding with 16.7°C (30.0 °F) superheat on bottom two circuits to yield overall exit superheat of 5.6 °C (10.0 °F); refrigerant exit manifold saturation temperature set to 7.2 °C (45.0 °F))

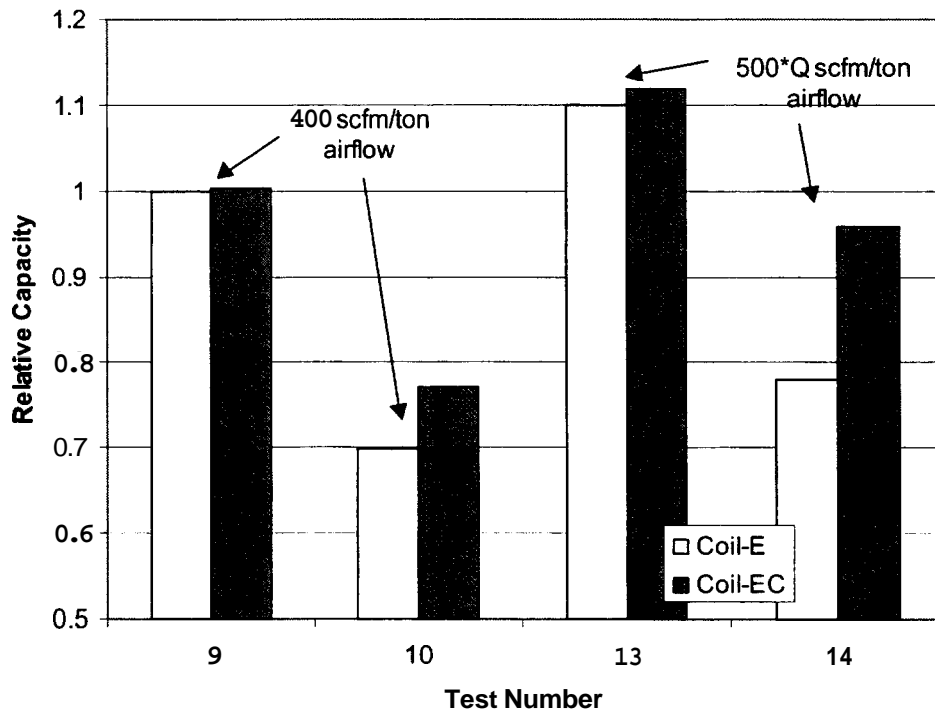


Figure 3.4.1.1.7: Capacity of COIL-E and COIL-EC relative to COIL-E, test 9 at two different airflow rates

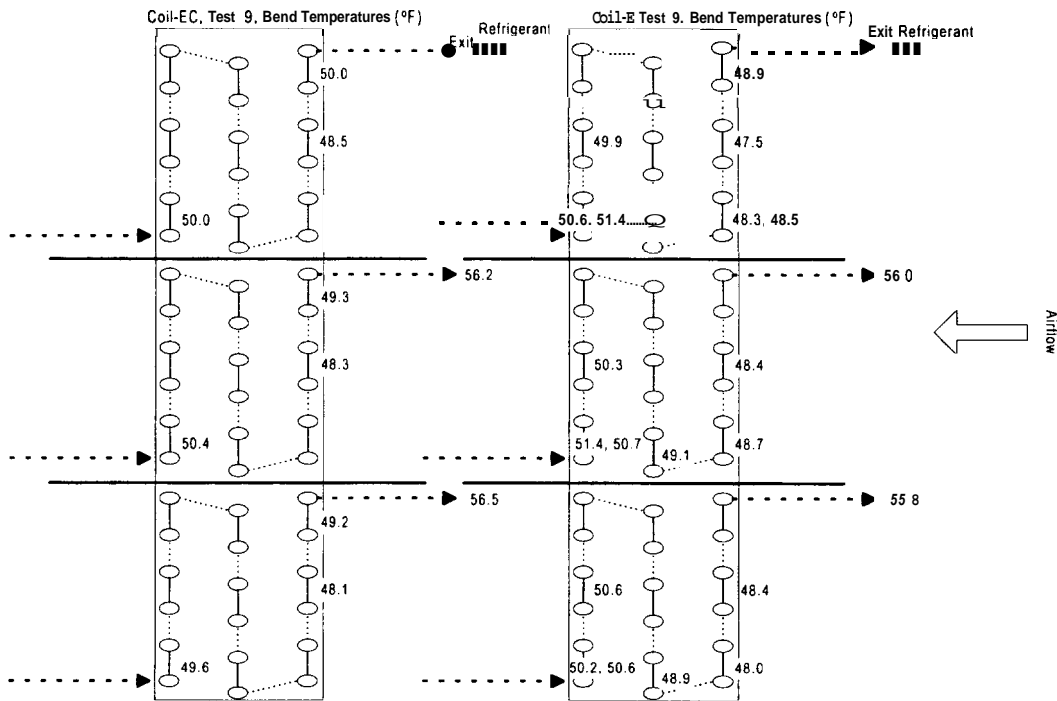


Figure 3.4.1.1.8: COIL-EC and COIL-E bend temperatures for test 9 (cross-counter flow, wet coil, 5.6 °C (10.0 °F) superheat on all circuits)

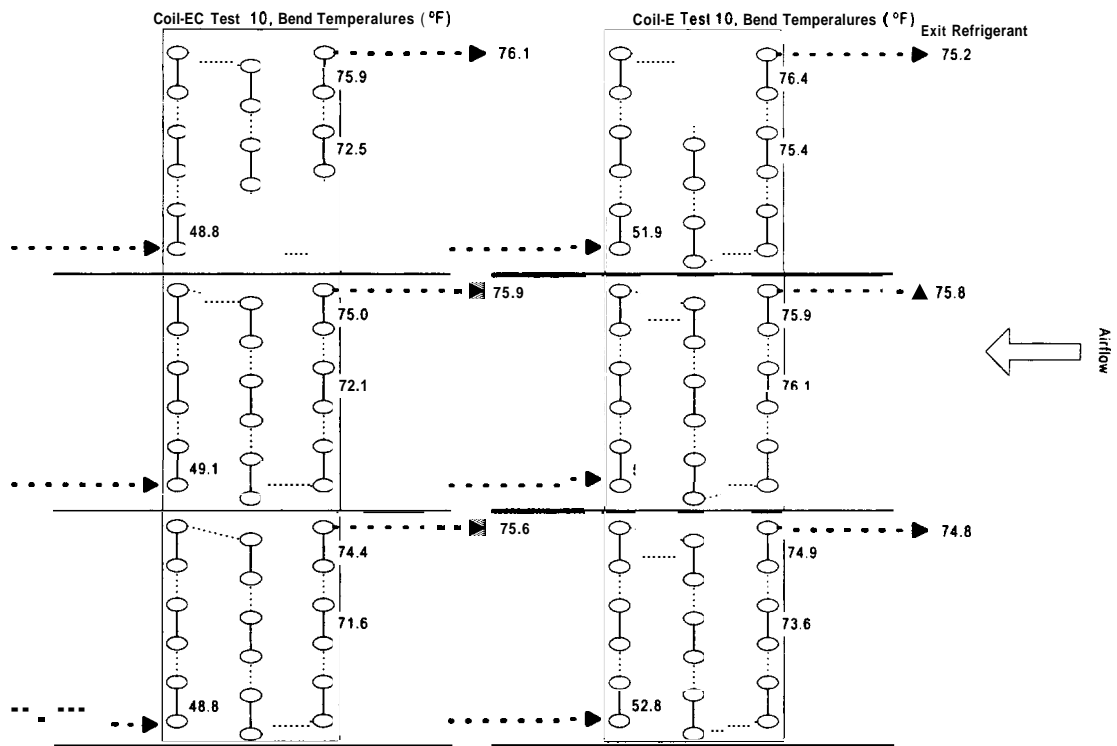
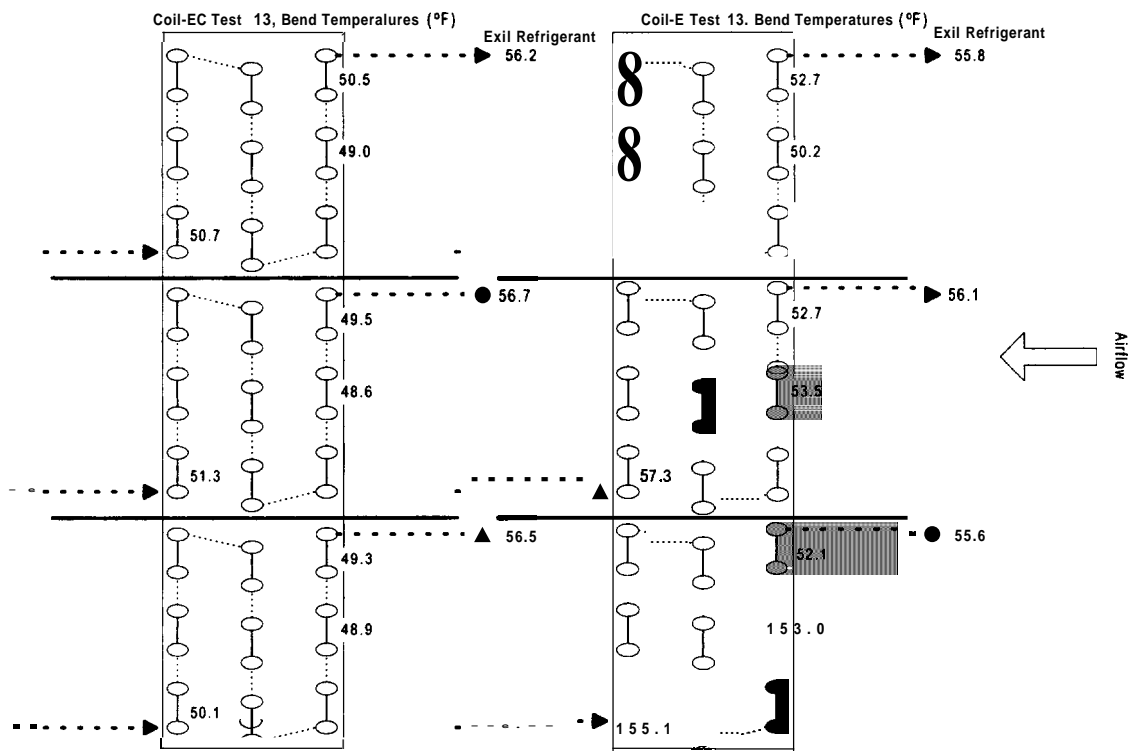


Figure 3.4.1.1.9: COIL-EC and COIL-E bend temperatures for test 10 (cross-counter flow, wet coil, 16.7 °C (30.0 °F) superheat on all circuits)



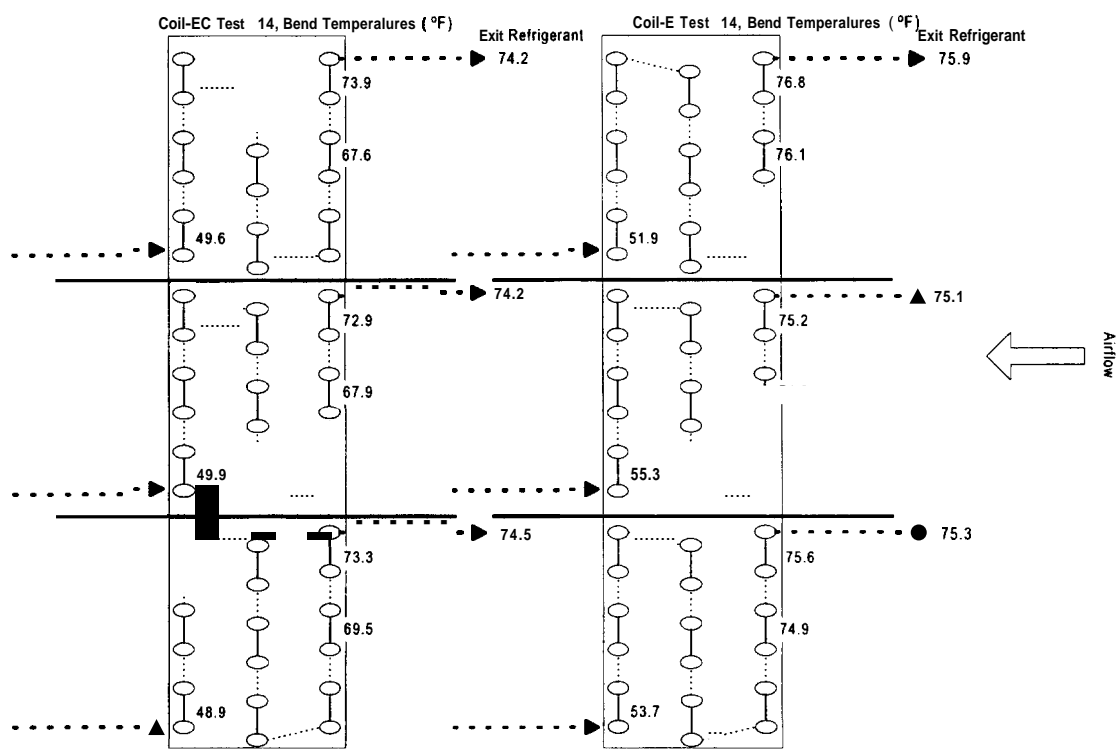


Figure 3.4.1.1.11: COIL-EC and COIL-E bend temperatures for test **14** (cross-counter flow, wet coil, 16.7°C (30.0°F) superheat on all circuits)

3.4.1.2 Effects of Airflow Rate on Coil Capacity

Air flow rate through the evaporator plays an important role in the capacity. When air flow rate is higher than the optimum quantity, the COP of the system decreases due to an increase in the air pressure drop and accompanying fan power consumption. But higher airflow enhances the heat transfer rate of the evaporator on the air-side due to the higher Reynolds number. Table 3.4.1.2.1 and figure 3.4.1.2.1 show the capacity variation of the tested evaporators as a function of air flow rate. As the air flow rate increased, total capacity increased due to the increased air mass flow rate. The latent heat transfer rate changed a little due to the constant evaporator pressure set by the evaporator pressure regulating valve. Other reasons that could play, a small part in the constant latent

capacity may be the condensed water on the surface of tube and fin mixing with the air which is unsaturated before latent heat transfer takes place at the range of these air flow rates. Secondly, the temperature difference between the air and the surface of condensing water decreases because thermal resistance increases due to the condensed water layer. As a result, the dominant increase in total capacity was caused by the increase in the sensible heat transfer rate.

Table 3.4.1.2.1: Capacity of the Test Evaporators at Varying Airflow Rates

Test Name	Coil Designation	Test #	Volumetric Flowrate of Air m ³ /h (scfm)			Coil surface		Overall Superheat			
								Superheats in Individual Circuits			
			145·Q ¹ (300·Q)	193·Q ¹ (400·Q)	242·Q ¹ (500·Q)	Dry	Wet	5.6 °C (10.0 °F)	16.7 °C (30.0 °F)	5.6 °C (10.0 °F)	5.6 °C (10.0 °F)
								5.6/5.6/5.6 (10/10/10)	16.7/16.7/16.7 (30/30/30)	16.7/*/16.7 (30/*/30)	*/16.7/16.7 (*/*/30/30)
								W (Btu/h)	W (Btu/h)	W (Btu/h)	W (Btu/h)
V020226A	W	1	X				X	5788 (19746)			
V020207B	W	9		X			X	6508 (22203)			
V020301A	W	13			X		X	7503 (25598)			
V020320B	E	1	X				X	5998 (20464)			
V020607A	E	9		X			X	6956 (23732)			
V020319B	E	13			X		X	7653 (26109)			
1020417A	EC	1	X				X	6085 (20760)			
102041SA	EC	9		X			X	6972 (23788)			
1020416B	EC	13			X		X	7781 (26546)			

* Superheat to be controlled such that the desired overall level of superheat is obtained

- 1) SI units of m³/kWh multiplied by capacity (Q) in kW to determine airflow, (IP units of cfm/ton multiplied by capacity (Q) in tons).

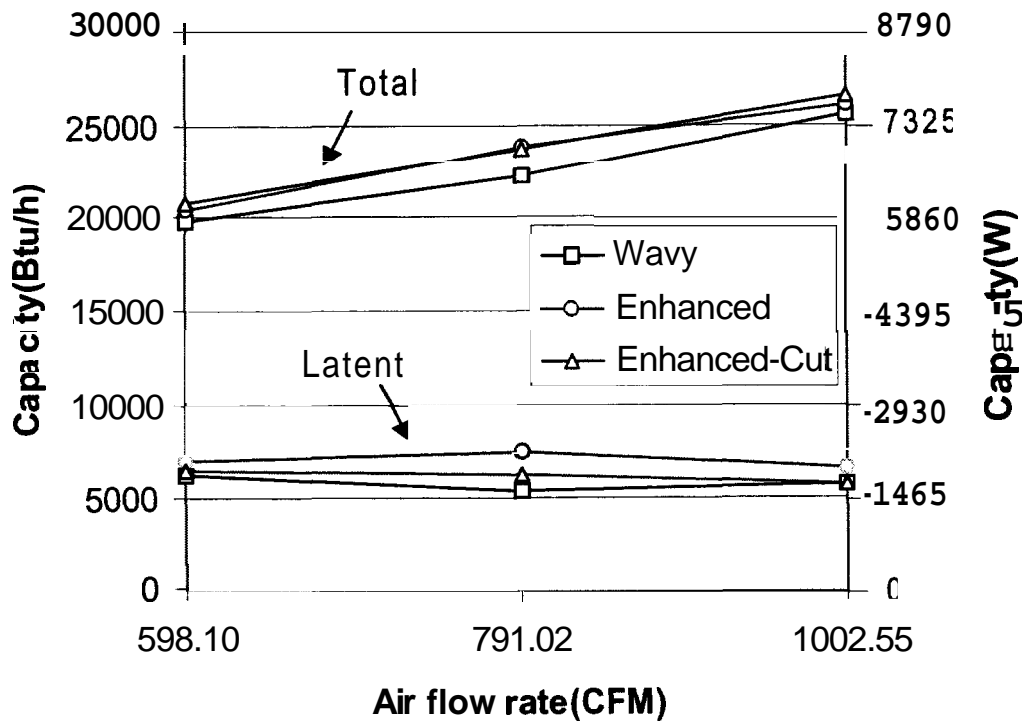


Figure 3.4.1.2.1: Capacity as a function of air flow rate for wet coil conditions

3.4.1.3 Effects of Non-Uniform Airflow on Coil Capacity

The combined effects of non-uniform airflow and evaporator superheat were examined by blocking the upper portion of the test evaporator on COIL-W and COIL-E during cross-counterflow operation for wet coil conditions. Figure 3.4.1.3.1 shows an idealized non-uniform velocity profile for a test coil with the upper half of the coil partially blocked. The velocity ratio was calculated by taking the average of the 15 velocity points on the top half divided by the average of the 15 velocity points on the lower half of the test evaporator. Test 9 conditions of 5.6 °C (10.0 °F) superheat were first performed, then the blockage was applied with no expansion valve adjustment (test 9A), and finally the expansion valves were adjusted to yield 5.6 °C (10.0 °F) superheat on all circuits (test 9B). During these tests the standard airflow rate was held constant; the airflow was not

allowed to drop when the blockage was added regardless of the significantly higher pressure drop. Table 3.4.1.3.1 shows the performance of the coils with varying degrees of airflow blockage.

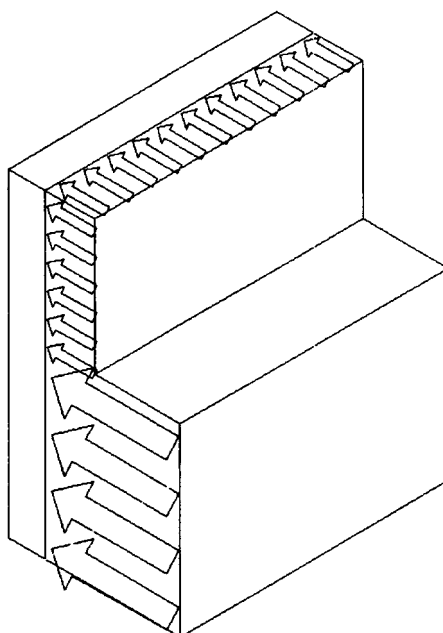


Figure 3.4.1.3.1 : Idealized velocity profile over evaporator with upper half partially blocked

Velocity Ratio (see Figure #)	Test name	Test type ¹	Coil	Airflow, m ³ /h (scfm)	Air-side Capacity, W (Btu/h)	Capacity Ratio, Q/Q _{Test 9}	Coil Air Pressure Drop, Pa (in WG)
1:1 (Fig. 3.4.1.3.2)	W020522 ^A	9	W	1244 (732)	6598 (22515)	1	37.9 (0.152)
1:1.5 (Fig. 3.4.1.3.3)	W020523 ^A	9A	W	1252 (737)	6351 (21670)	0.96	49.6 (0.199)
1:1.5	W020524 ^A	9B	W	1249 (735)	6535 (22298)	0.99	49.8 (0.200)
1:1	W020528 ^B	9	W	1245 (733)	6636 (22644)	1	38.1 (0.153)
1:2 (Fig. 3.4.1.3.4)	W020528 ^C	9A	W	1239 (729)	6179 (21085)	0.93	53.3 (0.214)
1:2	W020529 ^A	9B	W	1237 (728)	6307 (21521)	0.95	58.8 (0.236)

- 1) Test 9: uniform airflow with superheat on all circuits of 5.6 °C (10.0 °F), 9A: same expansion valve setting as test 9 but with non-uniform airflow and no superheat adjustment, 9B: expansion valves adjusted to yield 5.6 °C (10.0 °F) superheat on all circuits with non-uniform airflow.

Table 3.4.1.3.2: COIL-E Performance with Non-Uniform Airflow

Velocity Ratio (see Figure #)	Test name	Test type ¹	Coil	Airflow, m ³ /h (scfm)	Air-side Capacity, W (Btu/h)	Capacity Ratio, Q/Q _{Test 9}	Coil Air Pressure Drop, Pa (in WG)
1:1 (Fig. 3.4.1.3.6)	E020604 A	9	E	1276 (751)	6985 (23833)	1	92.7 (0.372)
1:1.26 (Fig. 3.4.1.3.7)	E020604 B	9A	E	1281 (754)	6933 (23655)	0.99	108.4 (0.435)
1:1.26	E020605 A	9B	E	1281 (754)	7029 (23984)	1.01	106.6 (0.428)
1:1	E020607 A	9	E	1293 (761)	6955 (23733)	1	84.7 (0.340)
1:1.36 (Fig. 3.4.1.3.8)	E020607 B	9A	E	1291 (760)	6797 (23192)	0.98	102.9 (0.413)
1:1.36	E020610 A	9B	E	1286 (757)	6807 (23226)	0.98	101.9 (0.409)
1:1.62 (Fig. 3.4.1.3.9)	E020611 A	9A	E	1290 (759)	6751 (23034)	0.97	101.1 (0.406)
1:1.62	E020612 A	9B	E	1274 (750)	6914 (23591)	0.99	101.4 (0.407)
1:1.75 (Fig. 3.4.1.3.10)	E020613 A	9A	E	1288 (758)	6654 (22705)	0.96	105.4 (0.423)
1:1.75	E020620 A	9B	E	1288 (758)	6877 (23465)	0.99	103.4 (0.415)
1:2.59 (Fig. 3.4.1.3.11)	E020621 A	9A	E	1299 (764)	6575 (22435)	0.95	98.9 (0.397)
1:2.59	E020624 A	9B	E	1290 (759)	6874 (23456)	0.99	101.9 (0.409)

- 1) Test 9: uniform airflow with superheat on all circuits of 5.6 °C (10.0 °F), 9A: same expansion valve setting as test 9 but with non-uniform airflow and no superheat adjustment, 9B: expansion valves adjusted to yield 5.6 °C (10.0 °F) superheat on all circuits with non-uniform airflow.

Figure 3.4.1.3.2 shows the air velocity contour map for COIL-W with no obstructions present. The volumetric flowrate for this test was **1244 m³/h (732 scfm)** with an average velocity of **6437 m/h (352 fpm)** and standard deviation of **512 m/h (28 fpm)**. Any non-uniformity in the unobstructed evaporator's entrance region airflow was due to the dewpoint sampling tree, thermocouple grid, and fin angles. Figure 3.4.1.3.3 shows the

non-uniform velocity contour map for COIL-W when the flow was obstructed to the upper half of the coil. An average of the top half air velocity was compared to the bottom half average air velocity to yield the velocity ratio of 1 to 1.5. The volumetric flowrate for this test was 1252 m³/h (737 scfm) with a 4097 m/h (224 fpm) and 6163 m/h (337 fpm) average velocity on the upper and lower halves of the coil, respectively. Further obstruction was added to produce the velocity contours seen in Figure 3.4.1.3.4 at a velocity ratio of 1 to 2. The average velocities in this case were 4005 m/h (219 fpm) and 8211 m/h (449 fpm) over the upper and lower halves of the coil, respectively.

The imposed airflow blockage in the case of the 1 to 1.5 velocity ratio would have increase fan power by more then 30 *Yo*. For the 1 to 2 velocity ratio case, the fan power would have increased by at least 54 *Yo* relative to the uniform airflow case.

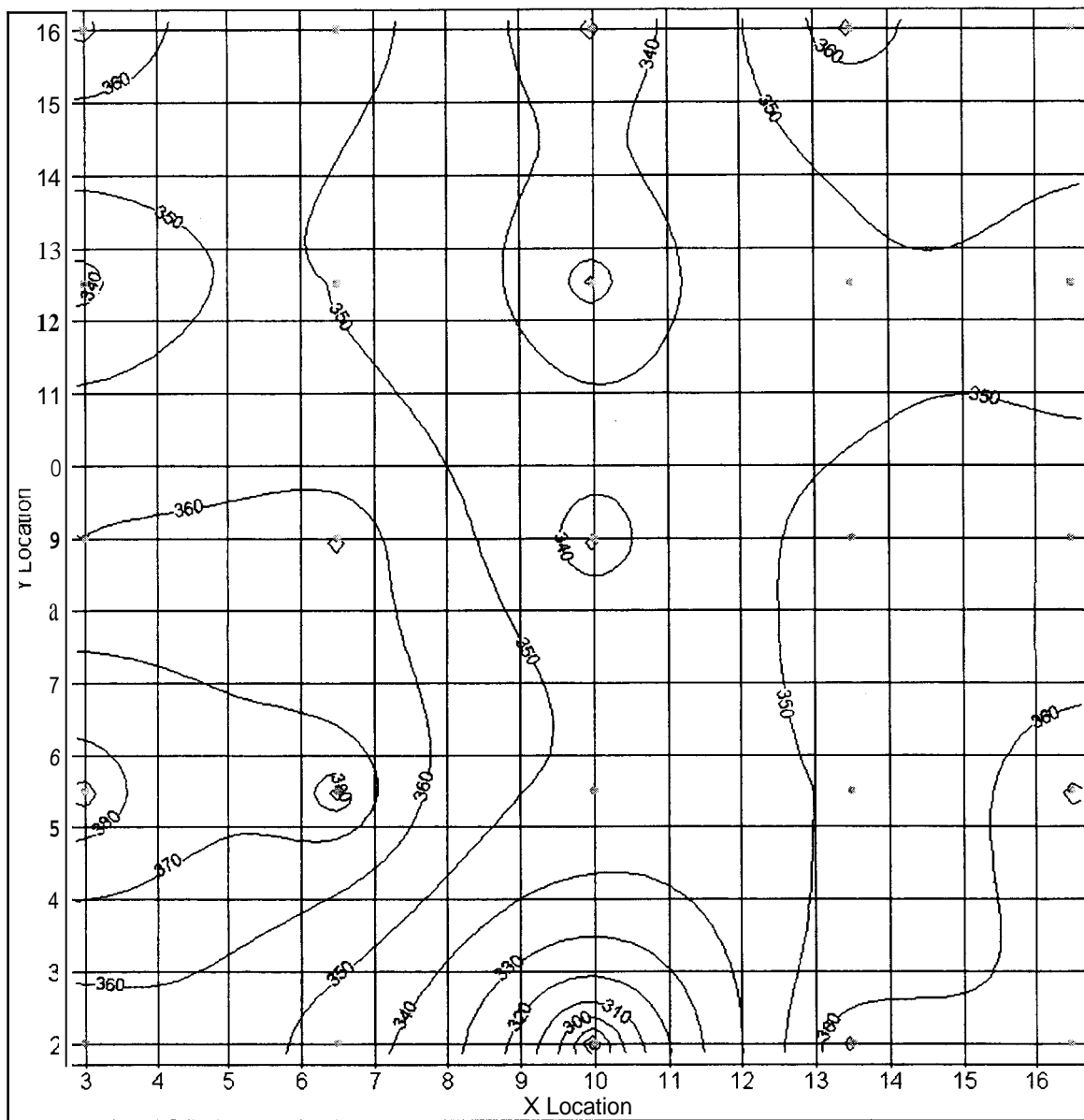


Figure 3.4.1.3.2: Uniform airflow velocity (ft/min) contour **map** for COIL-W

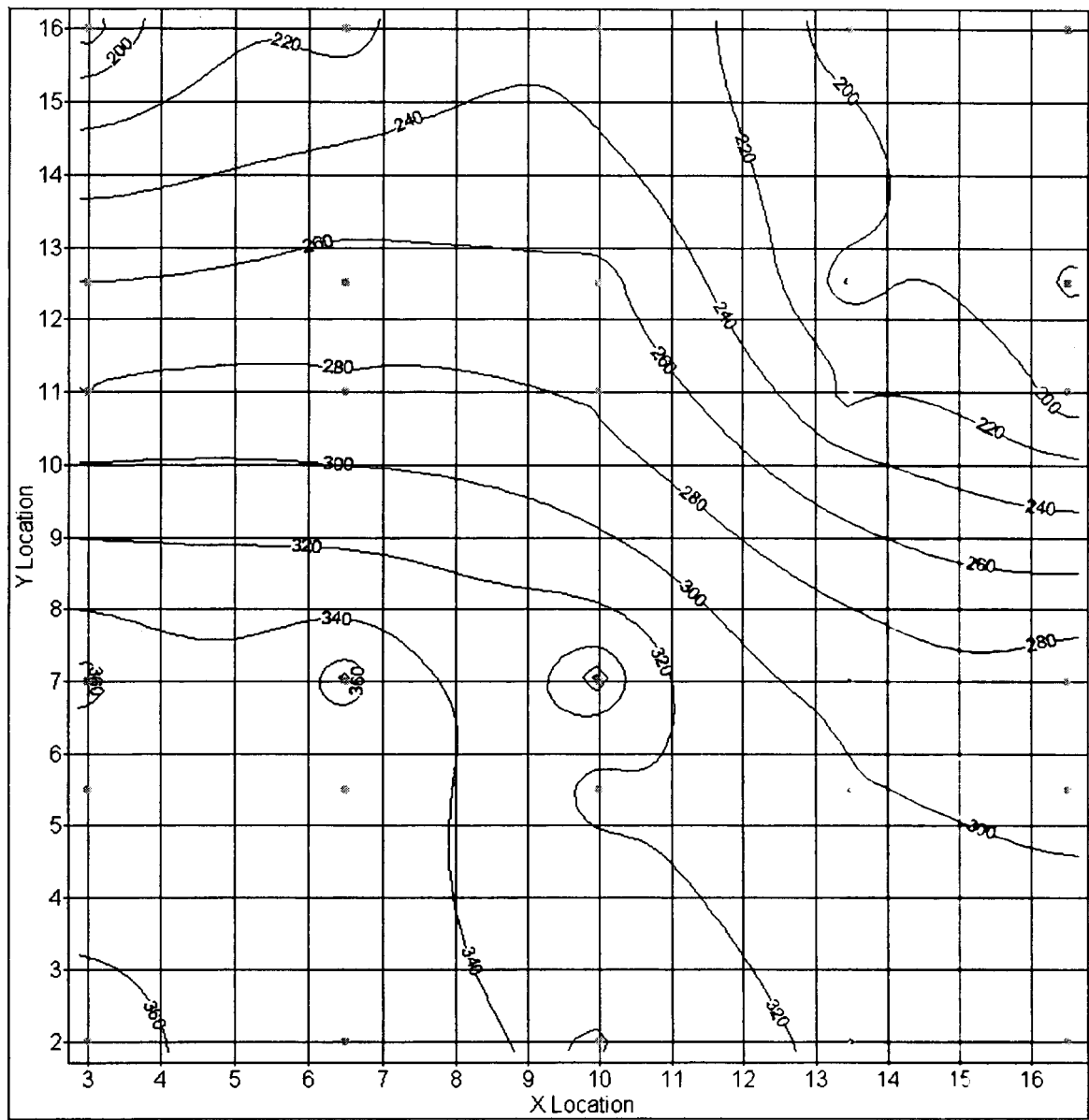


Figure 3.4.1.3.3: Non-uniform velocity (1:1.5) (ft/min) contour map for COIL-W

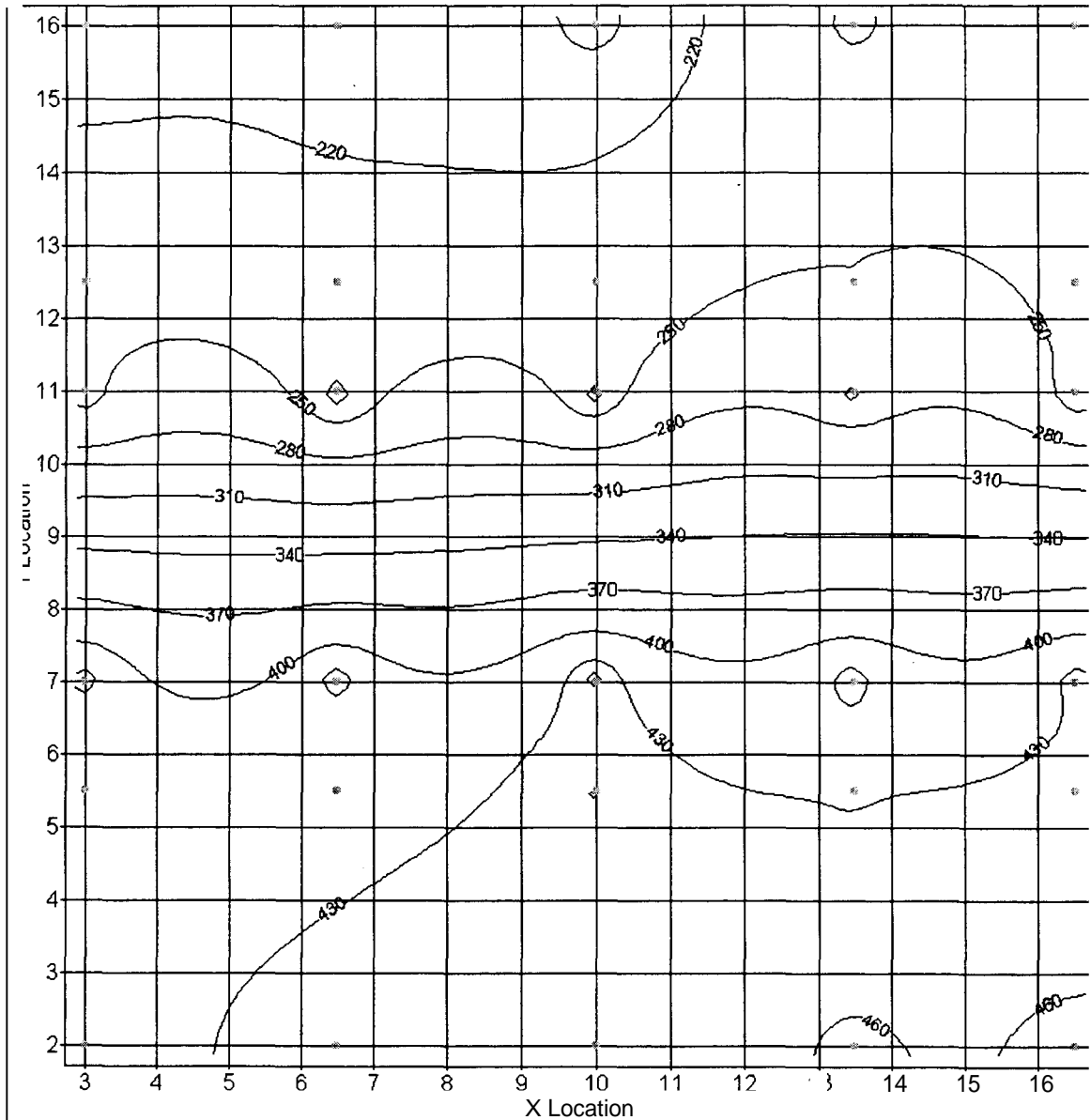


Figure 3.4.1.3.4: Non-uniform velocity (1:2)(ft/min) contour map for COIL-W

Figure 3.4.1.3.5 shows the non-uniform air velocity evaporator capacity relative to the uniform air velocity capacity. The first case shows the effects of an imposed obstruction with a fixed area expansion device. The expansion device would not be able to correct superheat and capacity would drop by 4 % in the 1:1.5 velocity ratio case and by 6.5 % in the 1:2 velocity ratio case. If the expansion device were able to correct each circuit, then the performance would improve closer to pre-obstruction, but for both cases the capacity

still decreased by **1.2 %** and **4.5 %**, respectively. The COIL-W non-uniform velocity results show that a more non-uniform velocity ratio produced a higher drop in capacity; and superheat correction still could not alleviate the entire penalty.

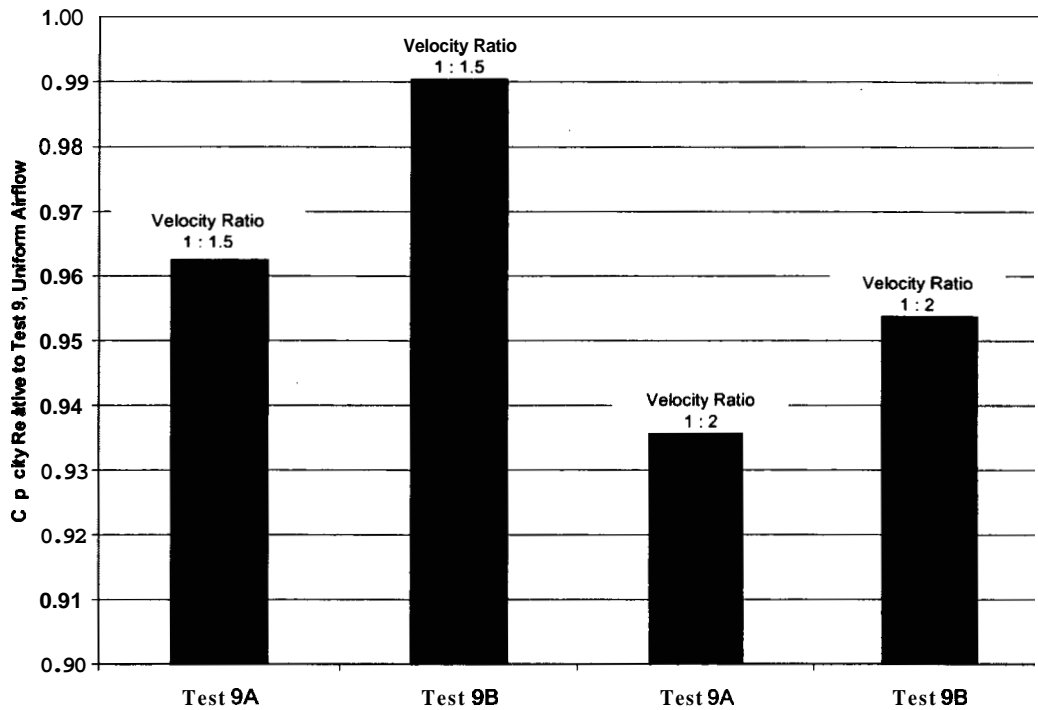


Figure 3.4.1.3.5: Relative capacities for COIL-W non-uniform airflow (refer to Table 3.4.1.3.1 for a description of the actual tests)

Figure 3.4.1.3.6 shows the air velocity contour map for COIL-E with no obstructions present. The volumetric flowrate for this test was **1276 m³/h (751 scfm)** with an average velocity of **6108 m/h (334 fpm)** and standard deviation of **512 m/h (28 fpm)**. Any non-uniformity in the unobstructed evaporator's entrance region airflow was due to the dewpoint sampling tree, thermocouple grid, and fin angles. Figure 3.4.1.3.7 shows the non-uniform velocity contour map for COIL-E when the flow was obstructed to the upper half of the coil. An average of the top half air velocity was compared to the bottom half

average air velocity to yield the velocity ratio of 1 to **1.26**. The volumetric flowrate for this test was **1281 m³/h (754 scfm)** with a **5340 m/h (292 fpm)** and **6748 m/h (369 fpm)** average velocity on the upper and lower halves of the coil, respectively. Further obstruction was added to produce the velocity contours seen in Figure **3.4.1.3.8** at a velocity ratio of 1 to **1.36**. The average velocities in this case were **5340 m/h (292 fpm)** and **7279 m/h (398 fpm)** over the upper and lower halves of the coil, respectively. More obstruction was added to produce a 1 to **1.62** average velocity ratio seen in Figure **3.4.1.3.9**. Average velocities in this case were **4609 m/h (252 fpm)** and **7498 m/h (410 fpm)** over the upper and lower halves of the coil, respectively. Again, obstruction was added to produce a 1 to **1.75** average velocity ratio seen in Figure **3.4.1.3.10**. Average velocities in this case were **3621 m/h (198 fpm)** and **6346 m/h (347 fpm)** over the upper and lower halves of the coil, respectively. The final obstruction was then added to produce a velocity ratio of 1 to **2.59**. Average velocities in this case were **3219 m/h (176 fpm)** and **8358 m/h (457 fpm)** over the upper and lower halves of the coil, respectively.

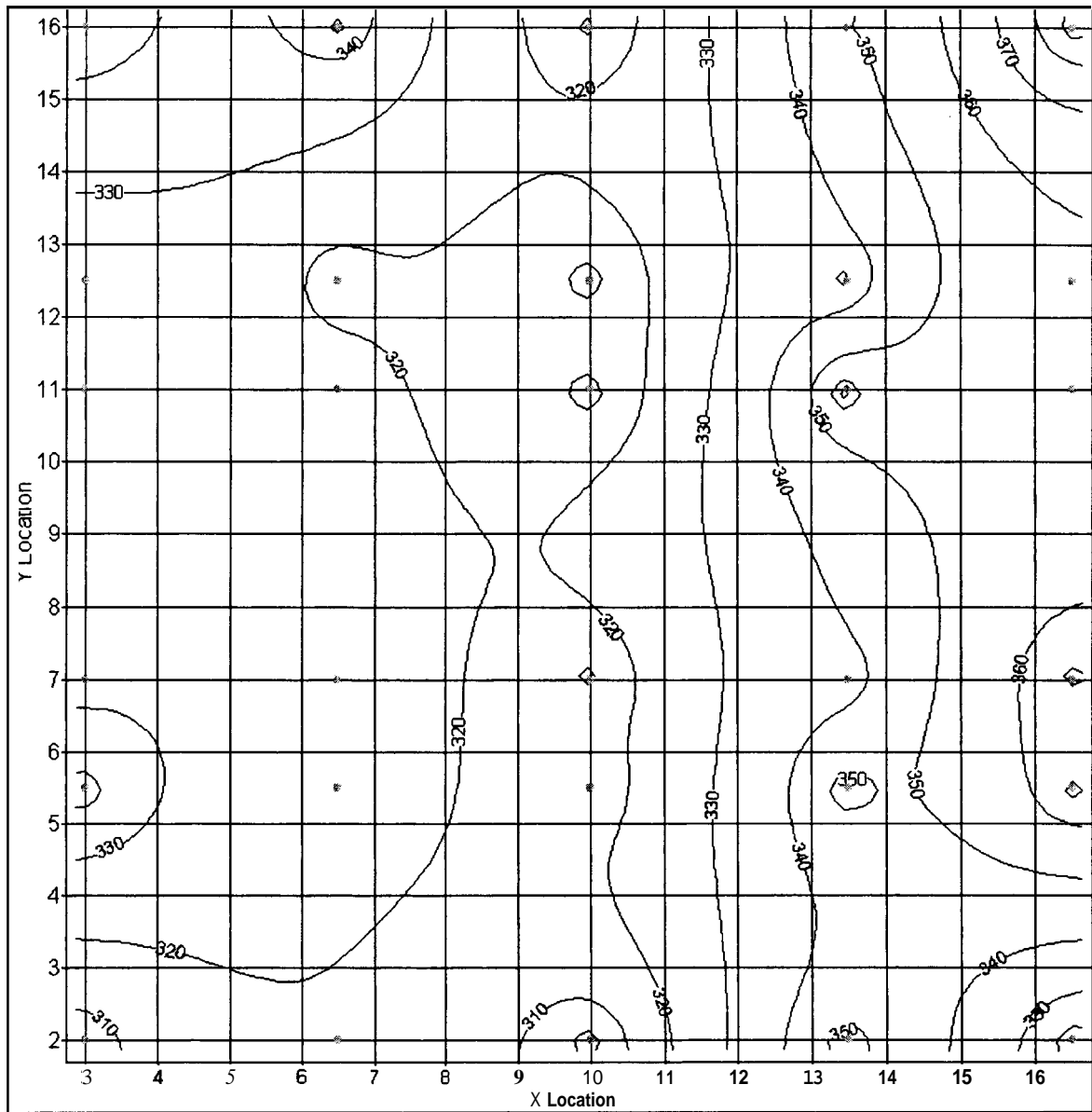


Figure 3.4.1.3.6: Uniform velocity (ft/min) contour map for COIL-E

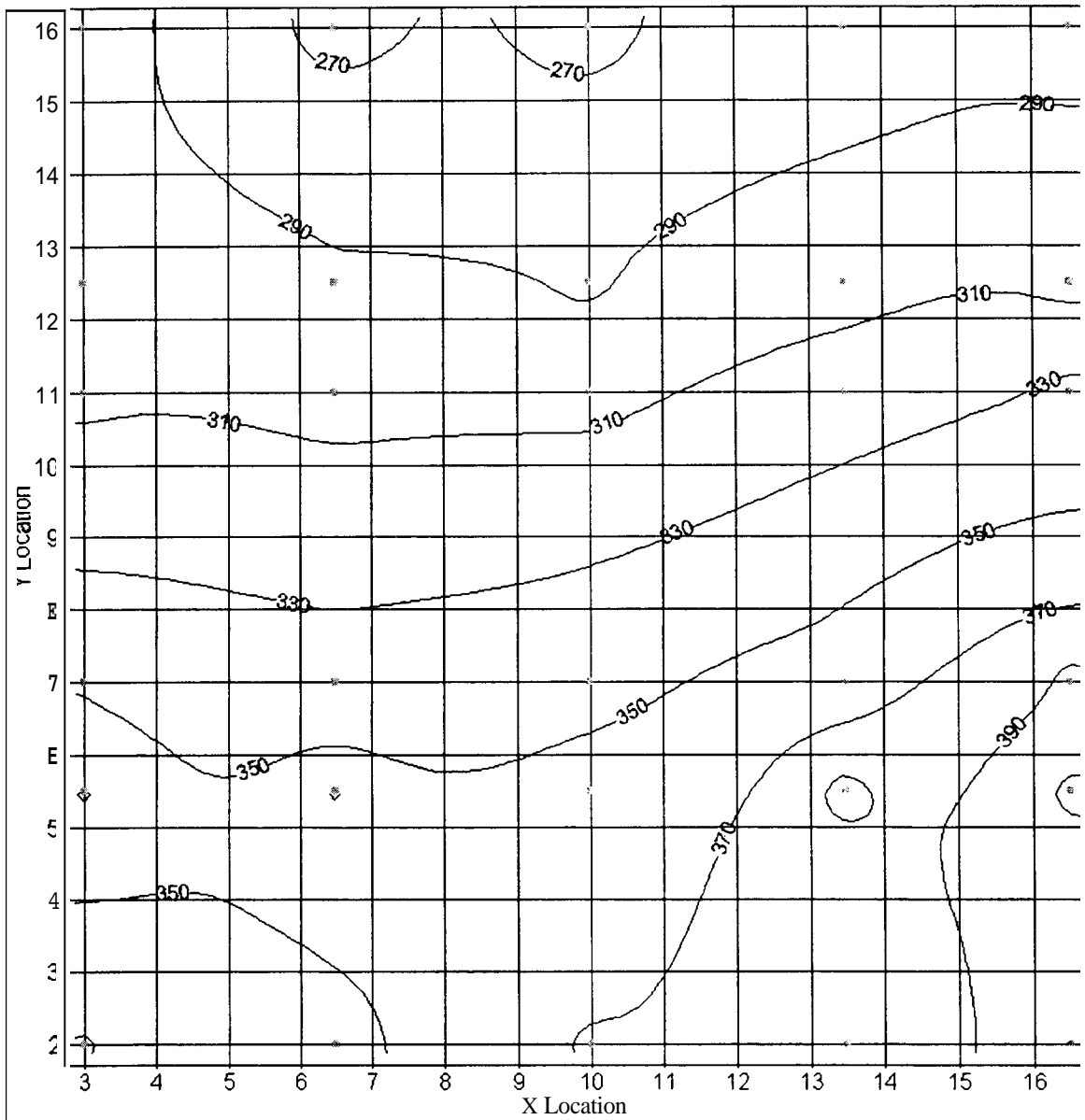


Figure 3.4.1.3.7: Non-uniform velocity (1 :1.26) (ft/min) contour map for COIL-E

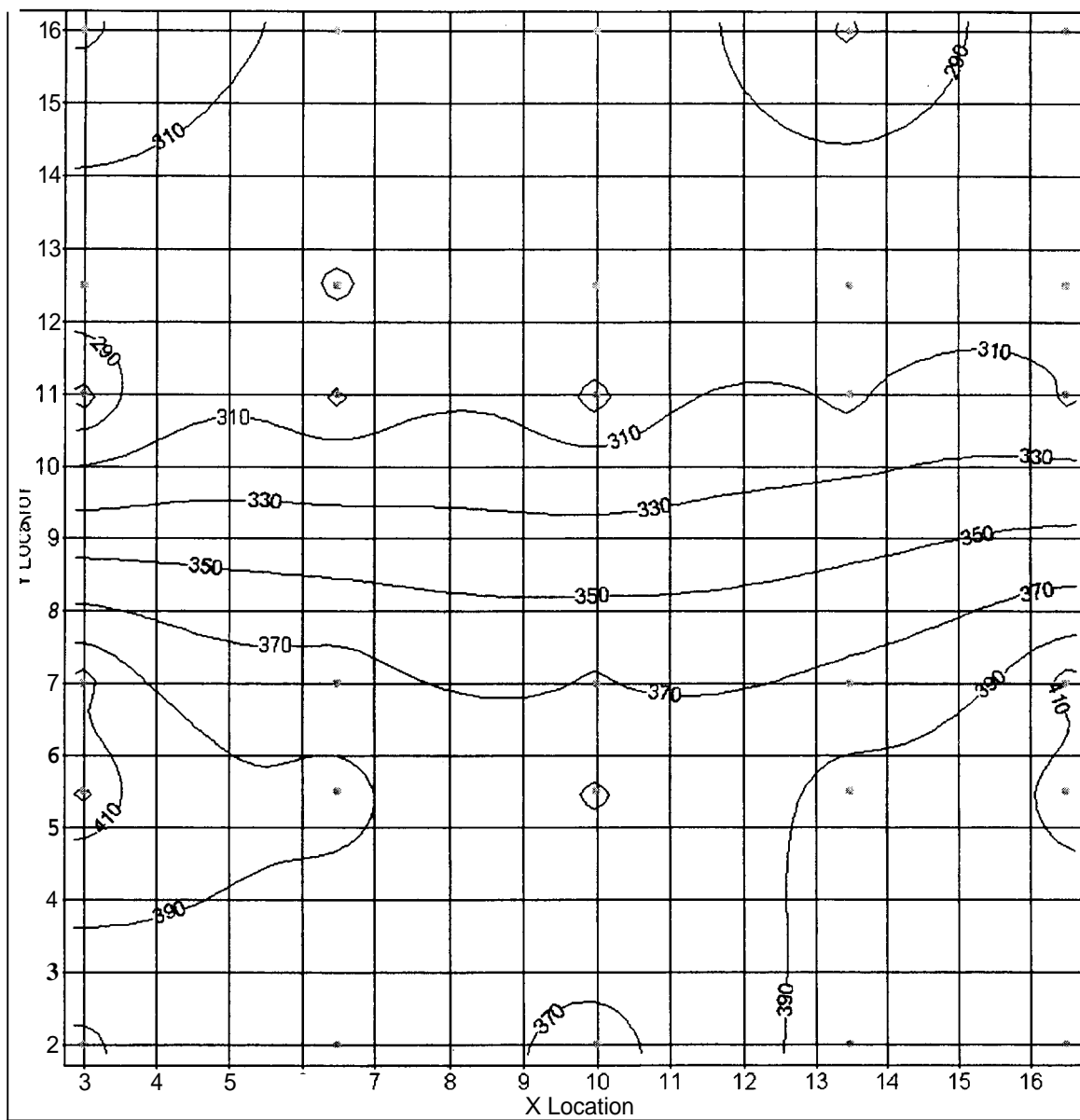


Figure 3.4.1.3.8: Non-uniform velocity (1:1.36) (ft/min) contour map for COIL-E

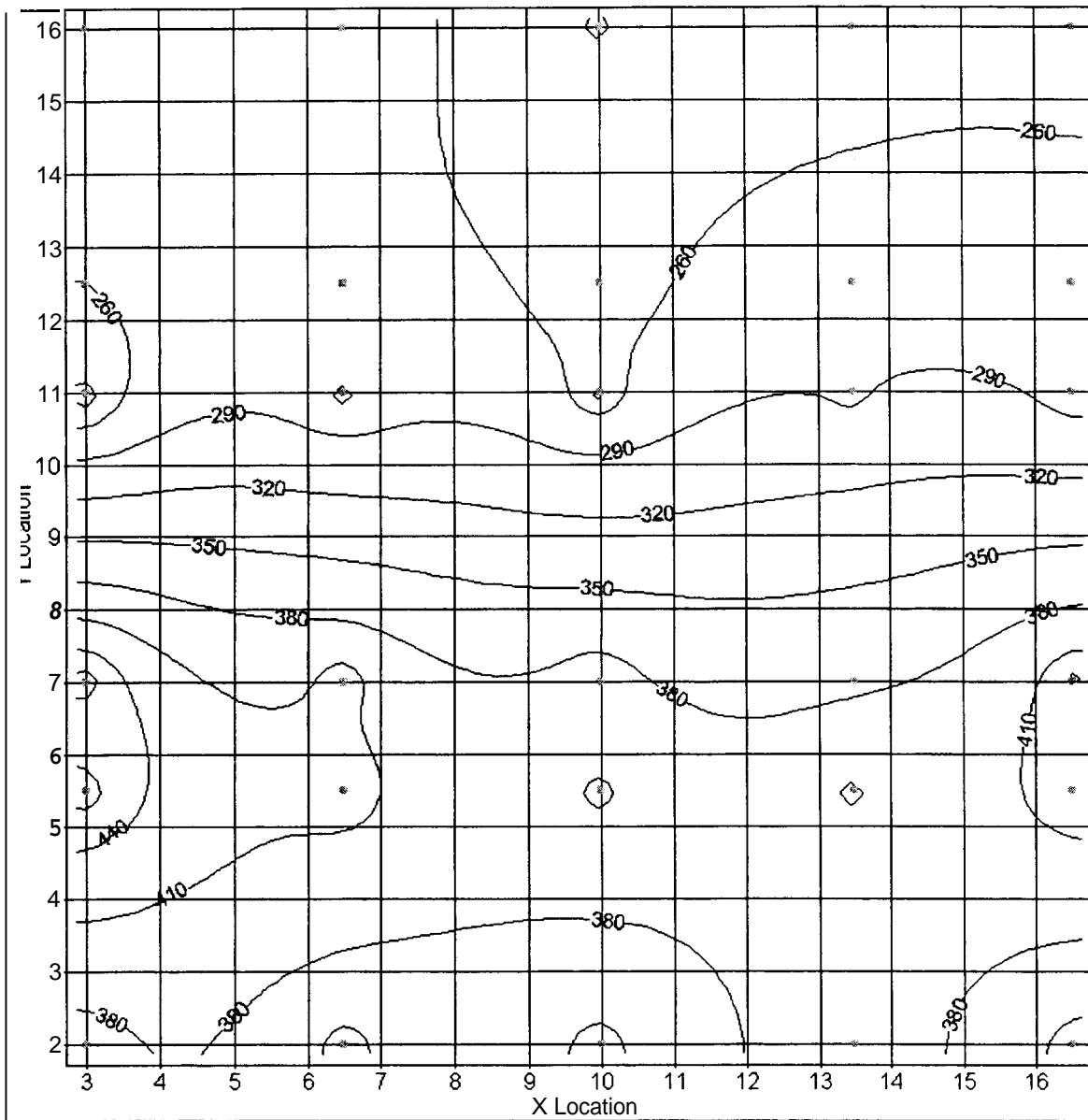


Figure 3.4.1.3.9: Non-uniform velocity (1:1.62) (ft/min) contour map for COIL-E

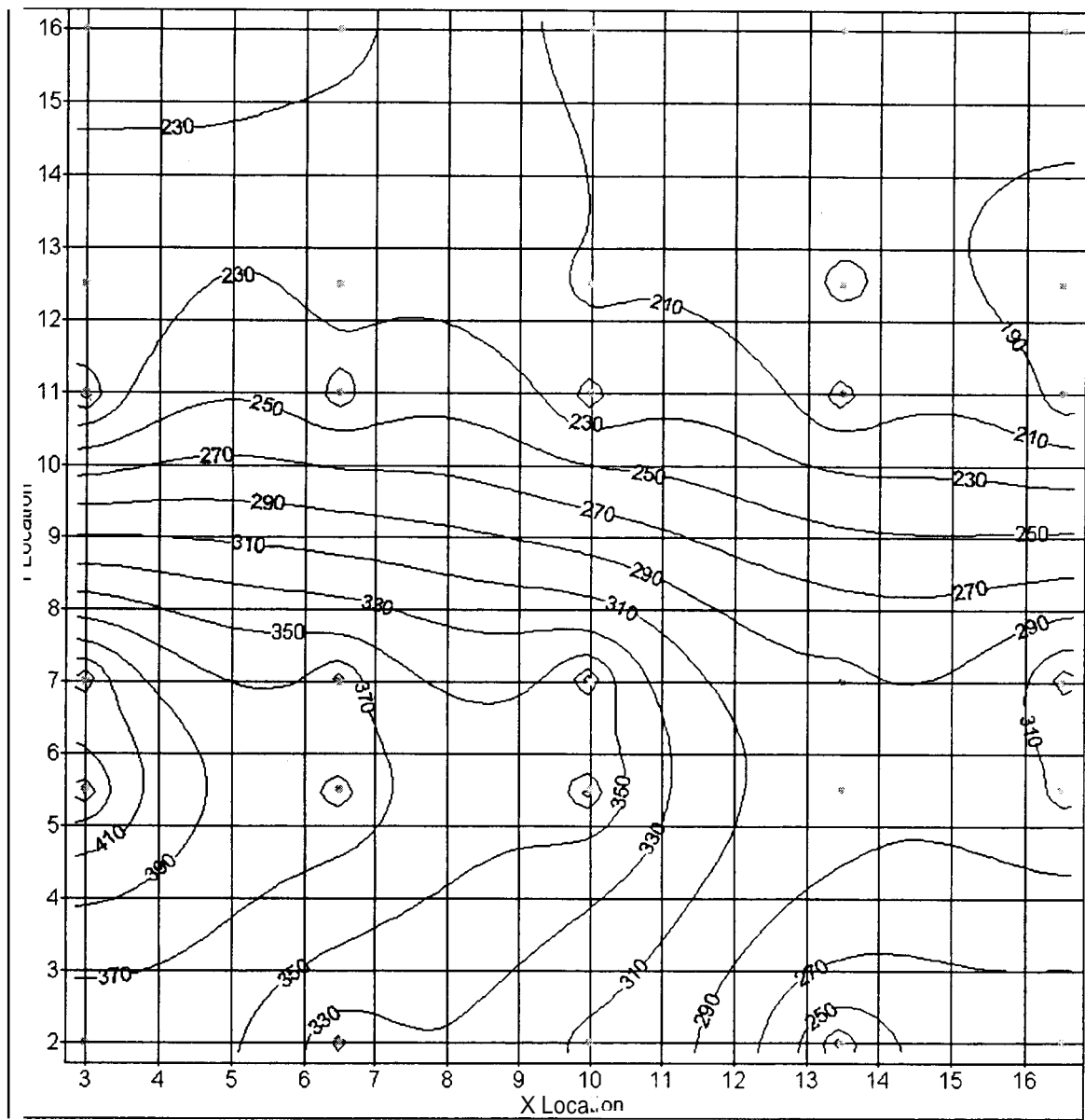


Figure 3.4.1.3.10: Non-uniform velocity (1:1.75) (ft/min) contour **map** for COIL-E

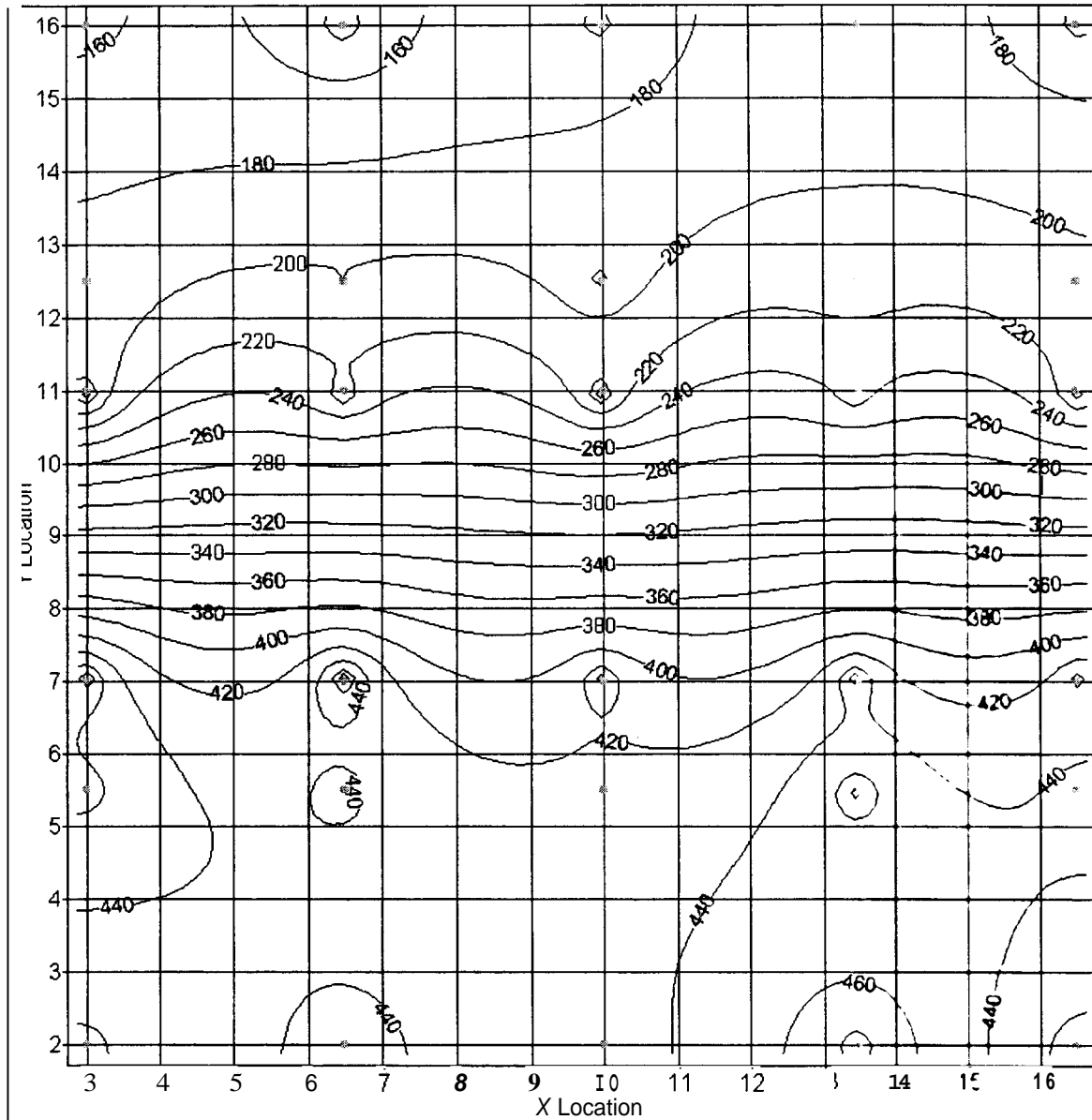


Figure 3.4.1.3.11: Non-uniform velocity (1:2.59) (ft/min) contour map for **COIL-E**

Figure 3.4.1.3.12 shows the non-uniform air velocity evaporator capacity relative to the uniform air velocity capacity for all COIL-E tests represented above and shown in Table 3.4.1.3.2. The cases labeled “Test 9A” show the effects of an imposed obstruction with a fixed area expansion device. Cases labeled “Test 9B” have the superheat adjusted back to 5.6 °C (10.0 °F) on each circuit. The first case had a velocity ratio of 1 to 1.26 and a capacity specific airflow of 183 m³/kWh (378 scfm/ton). Less than 1 % in capacity was

lost due to the obstruction, and this lost capacity was recovered when superheat was corrected (capacity was corrected within the uncertainty of our measurement at approximately 3.5 %). At a higher absolute airflow of $186\text{m}^3/\text{kWh}$ (385 scfdton), the losses in capacity with the obstruction were greater.

The losses in capacity with no superheat correction ranged from slightly more than 2 % at the 1 to 1.36 velocity ratio to approximately 5.5 % at the 1 to 2.59 velocity ratio. When the superheat was corrected, much of the loss in capacity was recovered. Please note that all of these tests were performed at a constant airflow rate. As shown in Table 3.4.1.3.1 and 3.4.1.3.2, the air pressure drop across the evaporator increased substantially when the blockage was imposed. This would translate into much higher fan power requirements and a subsequently lower COP. In the case of the 1 to 1.36 velocity profile, fan power would have increased by 21 % with the imposed blockage (power equals flowrate times the pressure drop). For the 1:1.62 velocity profile, fan power would have increased by 19 %. For the 1:1.75 velocity ratio, fan power would have increased by 24 %. For the highest blockage test with a velocity ratio of 1:2.59, the fan power would have increased by at least 20 %.

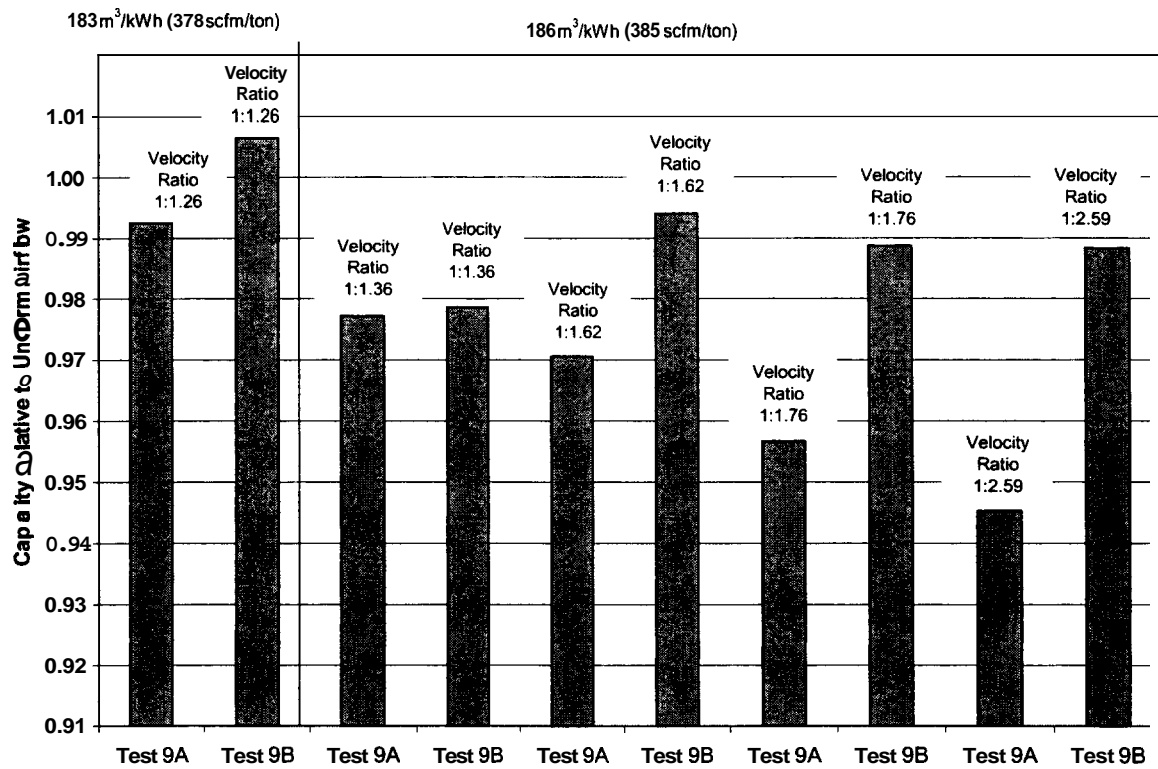


Figure 3.4.1.3.12: Capacity relative to uniform airflow for COIL-E (refer to Table 3.4.1.3.2 for a description of the tests)

3.4.2 Cross-Parallel Air/Refrigerant Flow Configuration Tests

Table **3.4.2.1** shows the performance of COIL-W and COIL-E with refrigerant circuited in cross-counter flow and cross-parallel flow with a capacity specific airflow rate of **193 m³/h (400 scfdton)**. COIL-W airflow rates for parallel flow and counter flow were **912 m³/h (537 scfm)** and **1240 m³/h (730 scfm)**, respectively. COIL-E airflow rates for parallel flow and counter flow were **895 m³/h (527 scfm)** and **1288 m³/h (758 scfm)**, respectively. The main information to be gained from this comparison is the rapid reduction in capacity that follows any increase in superheat during parallel flow (Figure **3.4.2.1**). This was evident for both coils tested under parallel flow conditions.

As the superheat increased from **5.6 °C (10.0 °F)** to **16.7 °C (30.0 °F)**, the refrigerant and air temperatures became pinched very quickly. During all tests the evaporator pressure was fixed to give an evaporating saturation temperature of **7.2 °C (45.0 °F)**. When superheat was increased to **16.7 °C (30.0 °F)**, the exiting refrigerant temperature approached **23.9 °C (75.0 °F)**; pinching of the two streams occurred rapidly. This is evident from examining the capacity of test **10** in parallel flow.

Figure **3.4.2.1** shows that COIL-W capacity in parallel flow decreased by 84.8 % as the superheat increased from **5.6 °C (10.0 °F)** to **16.7 °C (30.0 °F)**; test **9** to test **10**. Tests **11** and **12** also produced very low capacity due to two of the three circuits having a **16.7 °C (30.0 °F)** superheat. Although tests with the center circuit flooding produced higher capacity than the top circuit flooding for both COIL-W and COIL-E.

Table 4.2.1: Counter and Parallel Flow Performance of COIL-W and COIL-E

Test Name	Test #	Coil Designation	Volumetric Flowrate of Air m ³ /h (cfm)			Coil Surface		Overall Superheat							
								Superheats in Individual Circuits							
			145·Q ^{1a} (300·Q)	193·Q ^{1a} (400·Q)	242·Q ^{1a} (500·Q)	Dry	Wet	5.6 °C (10.0 °F)		16.7 °C (30.0 °F)		5.6 °C (10.0 °F)		5.6 °C (10.0 °F)	
								5.6/5.6/5.6 (10/10/10)		16.7/16.7/16.7 (30/30/30)		16.7/*/16.7 (30/*/30)		*/16.7/16.7 (*/*/30/30)	
								Q _{test} W (Btu/h)	Q _{test} / Q ^{1b}	Q _{test} W (Btu/h)	Q _{test} / Q ^{1b}	Q _{test} W (Btu/h)	Q _{test} / Q ^{1b}	Q _{test} W (Btu/h)	Q _{test} / Q ^{1b}
Cross-Counter Air/Refrigerant Flow															
W020207B	9	W		X			X	6507 (22203)	1						
W020530A	10	W		X			X			3722 (12701)	0.57				
W020531A	11	W		X			X					3837 (13091)	0.59		
W020215B	12	W		X			X							3830 (13067)	0.59
E020607A	9	E		X			X	6955 (23733)	1						
W0203 18A	10	E		X			X			4865 (16599)	0.70				
W0203 18B	11	E		X			X					5485 (18715)	0.79		
W0203 19A	12	E		X			X							4735 (16157)	0.68
Cross-Parallel Air/Refrigerant Flow															
W020304A	9	W		X			X	4732 (16146)	1						
W020311B	10	W		X			X			721 (2461)	0.15				
W020306A	11	W		X			X					2605 (8887)	0.55		
W020307A	12	W		X			X							2143 (7311)	0.45
E020403A	9	E		X			X	4549 (15523)	1						
E020404A	10	E		X			X			1017 (3470)	0.22				
E020408A	11	E		X			X					3373 (11508)	0.74		
E020409A	12	E		X			X							2797 (9543)	0.61

 1a : capacity determined at 193 m³/h (400 scfm/ton)

1b : capacity at test 9 for the coil specified.

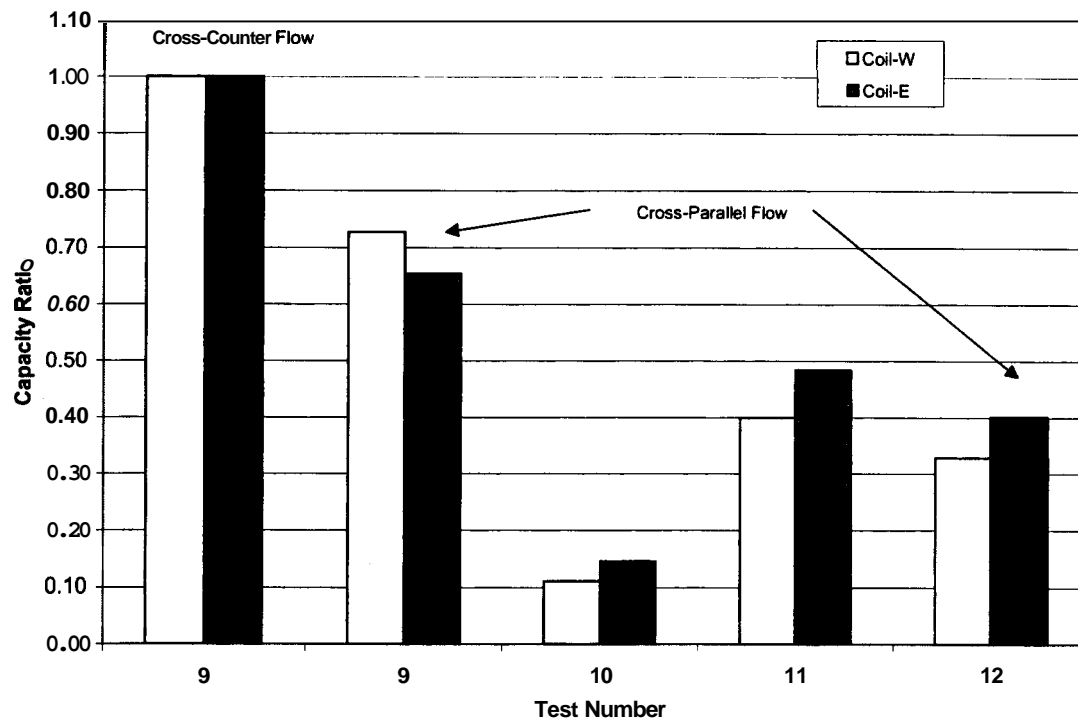


Figure 3.4.2.1: Cross-parallel flow capacity comparison for COIL-W and COIL-E relative to their performance at test 9 with cross-counter flow

COIL-E capacity in parallel flow was **3.9 %** less than COIL-W at the test 9 condition of **193 m³/kWh (400 scfdton)**. This is the opposite of the counter flow capacity results where COIL-E had a **5.4 %** greater capacity than COIL-W. COIL-E produced a slightly lower capacity than COIL-W at the test 9 parallel flow conditions. This was mainly due to the **196 m³/kWh (406 scfm/ton)** for COIL-W and the **193 m³/kWh (399 scfm/ton)** for COIL-E. The ideal airflow would have produced **193 m³/kWh (400 scfm/ton)** for both coils, but COIL-W airflow was high while COIL-E airflow was slightly **low**. These differences in airflow produced the accompanying difference in capacity. Also, a secondary factor in the lower capacity of COIL-E than COIL-W may be due to the more rapid pinching of COIL-E than COIL-W due to the higher air-side heat transfer of the enhanced fins.

COIL-E capacity in parallel flow decreased by 77.6 % as the superheat increased from 5.6 °C (10.0 °F) to 16.7 °C (30.0 °F); test 9 to test 10. Again, rapid pinching of the two fluid streams reduced capacity.

4 EVAPORATOR MODELING AND SIMULATIONS

4.1 Background on Evaporator Model EVAPS

Modeling of finned tube heat exchangers started at NIST with a tube-by-tube simulation model originally formulated by Chi (1979). Over the years, the model underwent significant upgrades, which are documented in Domanski and Didion (1983), Domanski (1991), Lee and Domanski (1997), and Domanski (1999b). These upgrades included the capability to account for air maldistribution and its interaction with refrigerant distribution, the extension to zeotropic mixtures, the extension to new refrigerant property representations, and implementations of new simulation correlations. The 1999 upgrade equipped the evaporator model with a graphical user interface (GUI). The GUI serves as a pre- and post-processor; it facilitates preparation of simulation input data, including the layout of refrigerant circuitry, and allows the user to display detailed performance results for individual tubes after a simulation run is completed. In 2002 under a parallel ARTI-21CR/605-500100 project (Domanski and Payne, 2002), the EVAP-COND simulation package was developed that included the evaporator and condenser models, EVAP5 and COND5, working under the same GUI. Both models were validated with experimental data taken with R22 and R410A heat exchangers at NIST. Since the current project and ARTI-21CR/605-500100 project partially overlapped in time, the EVAP-COND attached to the ARTI-21CR/605-500100 report included some of upgrades developed under this study, e.g. the option to simulate the evaporator together with a refrigerant distributor. Not included in the release version of EVAP-COND are the upgrades to the evaporator model that account for longitudinal fin

conduction, which were needed to perform simulations with controlled refrigerant superheats at individual refrigerant circuits.

4.2 Description of EVAPS

4.2.1 Modeling Approach

Figure 4.2.1.1 presents the refrigerant circuitry and air velocity representation used by EVAPS. The tube-by-tube modeling approach recognizes each tube as a separate entity for which the model performs simulation calculations. These calculations are based on inlet refrigerant and air parameters, their properties, and mass flow rates. The simulation begins with the inlet refrigerant tubes and proceeds to successive tubes along the refrigerant path in the heat exchanger. At the outset of the simulation, the air temperature is only known for the tubes in the first row and has to be estimated for the remaining tubes. A successful simulation run requires several passes (iterations) through the refrigerant circuitry, each time updating inlet air and refrigerant parameters for each tube.

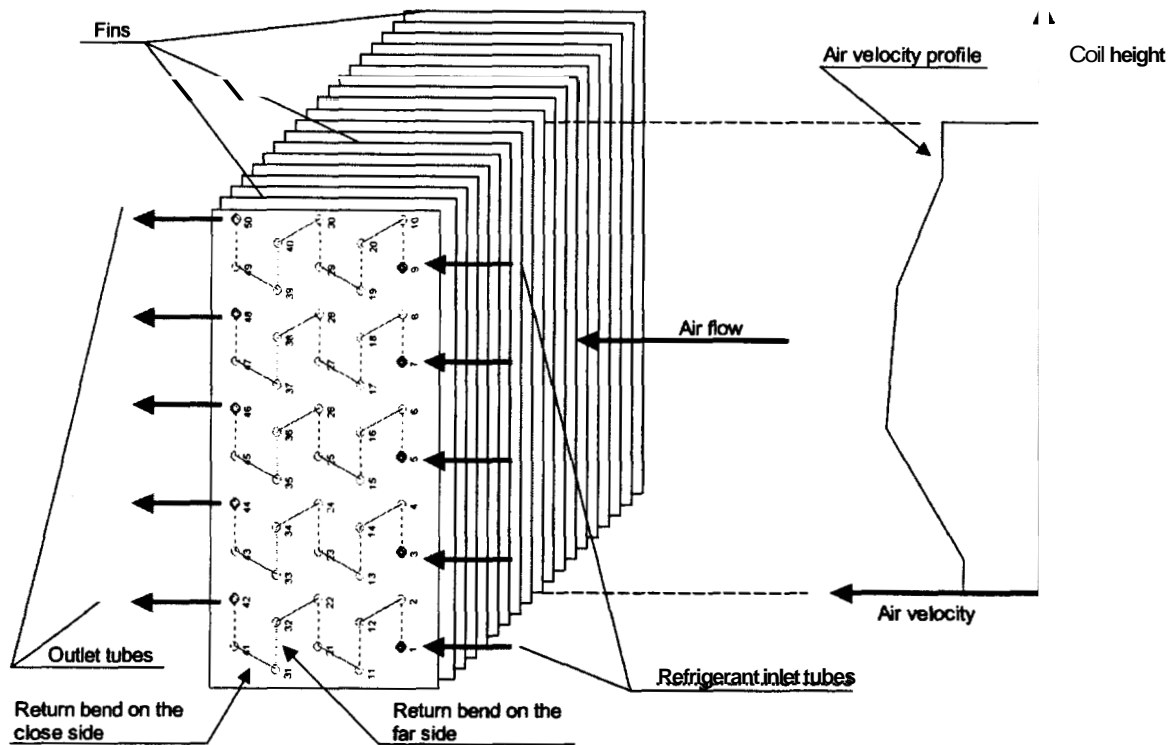


Figure 4.2.1.1 : Representation of air distribution and refrigerant circuitry in **EVAP5**

Heat transfer calculations **start** by calculating the heat-transfer effectiveness, **E**, by one of the applicable relations (Kays and London, 1984). With the air temperature changing due to heat transfer, the selection of the appropriate relation for **E** depends on whether the refrigerant undergoes a temperature change during heat transfer. Once **E** is determined, heat transfer from air to refrigerant is obtained using equation 4.2.1.1.

$$Q_a = m_a C_{pa} (T_{ai} - T_{ri}) \epsilon \quad (4.2.1.1)$$

The overall heat-transfer coefficient, **U**, is calculated by equation 4.2.1.2, which sums up the individual heat-transfer resistances between the refrigerant **and** the air.

$$U = \left[\frac{A_o}{h_i A_{pi}} + \frac{A_o X_p}{A_{pm} K_p} + \frac{1}{h_l} + \frac{A_o}{A_{po} h_{pf}} + \frac{1}{h_o (1 + \alpha) \left(1 - \frac{A_f}{A_o} (1 - \ddot{o}) \right)} \right]^{-1} \quad (4.2.1.2)$$

The first term of equation 4.2.1.2 represents the refrigerant-side convective resistance. The second term is the conduction heat-transfer resistance through the tube wall, and the third term accounts for the conduction resistance through the water layer on the fin and tube. The fourth term represents the contact resistance between the outside tube surface and the fin collar. The fifth term is the convective resistance on the air-side where the multiplier $(1+\alpha)$ in the denominator accounts for the latent heat transfer on the outside surface. For a dry tube $\alpha = 0.0$ and $1/h_l = 0.0$. Once the heat transfer rate from the air to the refrigerant is calculated, the tube wall and fin surface temperatures can be calculated directly using heat-transfer resistances. Then, the humidity ratios for the saturated air at the wall and fin temperatures are calculated, and mass transfer from the moist air to the tube and fin surfaces is determined. For more detailed information on heat transfer calculations refer to Domanski (1991).

4.2.2 Heat Transfer and Pressure Drop Correlations

EVAPS uses the following correlations for calculating heat transfer and pressure drop.

Air Side

- heat-transfer coefficient for flat fins: Wang et al. (2000)
- heat-transfer coefficient for wavy fins: Wang et al. (1999a)
- heat-transfer coefficient for slit fins: Wang et al. (2001)

- heat-transfer coefficient for louver fins: Wang et al. (1999b)
- fin efficiency: Schmidt method, described in McQuiston et al. (1982)

A correlation for calculating the tube-collar junction resistance is not listed because all air-side heat transfer correlations authored by Wang include the heat transfer resistance between the tube and collar.

Refrigerant Side

- single-phase heat-transfer coefficient, smooth tube: McAdams, described in ASHRAE (2001)
- evaporation heat-transfer coefficient **up** to 80% quality, smooth tube: Jung and Didion (1989)
- evaporation heat-transfer coefficient up to 80% quality, rifled tube: Jung and Didion (1989) correlation with a 1.9 enhancement multiplier suggested by Schlager et al. (1989)
- mist flow, smooth and rifled tubes: linear interpolation between heat transfer coefficient values for 80 Y_o and 100 Y_o quality
- single-phase pressure drop, smooth tube: Petukhov (1970)
- two-phase pressure drop, smooth tube, lubricant-free refrigerant: Pierre (1964)
- two-phase pressure drop, rifled tube: Pierre (1964) correlation for smooth tube with a 1.4 multiplier suggested by Schlager et al. (1989)
- single-phase pressure drop, return bend, smooth tube: White, described in Schlichting (1968)
- two-phase pressure drop, return bend, smooth tube: Chisholm, described in Bergles et al. (1981). The length of a return bend depends on the relative locations of the tubes connected by the bend. This length is accounted for in pressure drop calculations.

4.2.3 Representation of Refrigerant Properties

Representation of thermodynamic and transport properties is based on REFPROP6 property routines (McLinden et al., 1998). Because EVAP5 simulations are computationally intensive, using a refrigerant property look-up tables is a practical necessity if simulation runs are expected to take less than 60 seconds. This is particularly true in case of REFPROP6 for which property calculations are several times more CPU demanding than for REFPROP5. EVAP-COND employs a pressure-enthalpy-based system of look-up tables, which includes eight different routines that retrieve the desired state or transport property. The look-up scheme is applicable to single component refrigerants and refrigerant mixtures. If a given refrigerant state falls outside the range of the look-up table, then EVAP-COND calls a REFPROP6 refrigerant property routine directly.

Since REFPROP6 property calculations may not converge occasionally, particularly during phase equilibrium calculations for refrigerant mixtures, EVAP-COND employs an error evasive scheme. Under this scheme, EVAP-COND attempts to obtain a given property even if REFPROP flash calculations do not converge, e.g., if a routine PHFLSH crashes, a routine that uses TPRHO is invoked to attempt to iteratively match TPRHO's enthalpy value with the known (target) value. If both REFPROP flash calculations do not converge, then the data point in the refrigerant look-up table is flagged and look-up table routines iterate properties for this point using refrigerant properties in the neighboring nodes of the table.

4.3 Modeling Issues

The following four sections present four major modeling issues that received special consideration during this study.

4.3.1 Refrigerant Distribution

Simulating refrigerant distribution is an important aspect of heat exchanger simulation because of its impact on the heat exchanger performance. It is also known that in some designs a non-uniform air distribution may affect refrigerant distribution. In a heat exchanger with multiple circuits, refrigerant distributes itself in appropriate proportions so that the refrigerant pressure drop from the inlet to the outlet for all circuits is the same. In the context of simulating refrigerant distribution, a refrigerant circuit starts at the point of the first split of refrigerant stream after leaving the condenser and ends at the final merging point before entering the suction line leading the refrigerant to the compressor. If the refrigerant enters the evaporator by a single tube, the first split, if **any**, will exist within the coil assembly. If the evaporator has several inlet tubes and a refrigerant distributor is used, the first refrigerant split typically occurs at the inlet to the distributor tubes just after the expansion process in a thermostatic expansion valve (TXV) or a short tube restrictor. Note, that in this design, refrigerant pressures and temperatures at different inlet tubes may be different, as graphically **shown** in Figure 4.3.1.1. Such different refrigerant pressure and temperature profiles also occurred during the tests with controlled uneven exit superheats (refrigerant distributions), namely tests **3, 4, 7, 8, 11, and 12**.

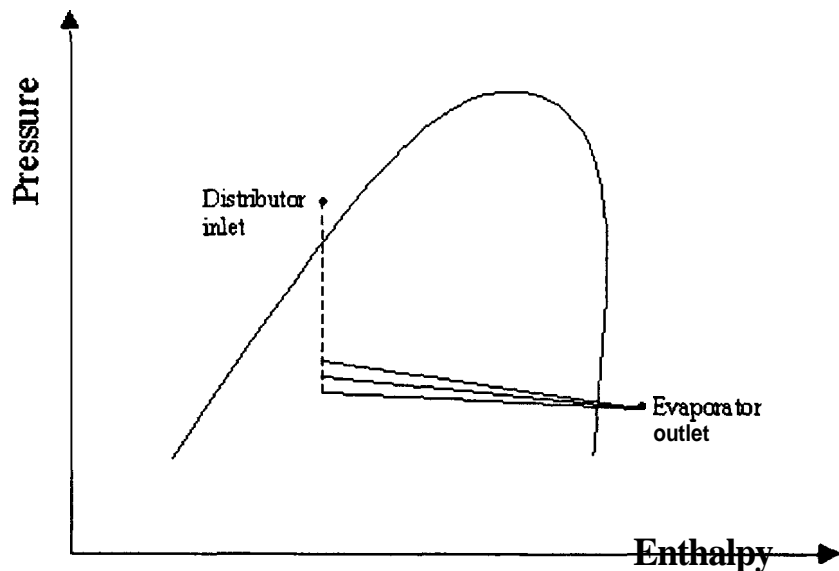


Figure 4.3.1.1 : Possible refrigerant pressure profiles in a three-circuit evaporator fed by a refrigerant distributor

Under this project, two simulation methods were developed to simulate evaporator performance with controlled refrigerant superheats at the evaporator outlet tubes. The first scheme involving a general model for a refrigerant distributor was introduced into EVAP-COND as one of the eight evaporator simulation options. When the evaporator is simulated using this option, the refrigerant operating input data are the condenser exit bubble-point temperature, condenser subcooling, evaporator exit dew-point temperature, and evaporator superheat (in the release version of EVAP-COND, condenser subcooling and evaporator superheat are imposed as 5.0 °C (9.0 °F)). For this option, as the first task EVAP-COND runs preliminary simulations to establish dimensions **of the** refrigerant distributor tubes that would inflict a 70 kPa (**10.2**psi) refrigerant pressure drop. Once the distributor tubes are sized, EVAP-COND proceeds to main simulations in which it

establishes refrigerant distribution between different circuits based on the total pressure **drop**. This total pressure drop includes the pressure drop in a given distributor tube and the refrigerant circuit in the coil assembly it feeds. In the test version used in this study, **EVAP-COND** additionally solicits a “restriction factor” for each distributor tube, which acts as a multiplier to the pressure drop calculated by the program. By inputting values different from 1.0, the user can control refrigerant distribution and refrigerant superheat at different evaporator exit tubes. The program iterates the refrigerant mass flow rate until the overall superheat is reached at the evaporator exit. Figures 4.3.1.2 and 4.3.1.3 present the eight refrigerant input data options and the input data window for **EVAP-COND** simulations involving a refrigerant distributor, respectively.

Outlet pressure and superheat
Outlet pressure and quality
Outlet sat. temp. and superheat
Outlet sat. temp. and quality
Inlet pressure and quality
Inlet sat. temp. and quality
<input checked="" type="checkbox"/> Cond. bubble pt. and evap. sat. temp.
Outlet sat. temp. and min. superheat

Figure 4.3.1.2: EVAP-COND refrigerant input data options for evaporator simulations

Evaporator operating conditions			
Refrigerant			
Cond. bubble pt.	C		40.5
Evap. sat. temp.	C		7.2
Mass flow rate (estimate)	kg/h		54.4
Cond. subcool & evap. superheat	C		5.0
Air			
Inlet temperature	C		26.8
Inlet pressure	kPa		101.325
Inlet relative humidity	fraction		0.51
Volumetric flow rate	m ³ /min		15.19
Units <input checked="" type="checkbox"/> SI Units <input type="checkbox"/> British Units			
		Cancel	OK

Figure 4.3.1.3: EVAP-COND input data window for simulations involving a refrigerant distributor

While the simulation option involving a refrigerant distributor is useful for a coil designer for typical simulations, this option proved to be somewhat impractical for controlling individual exit superheats when we tried to reproduce our test results. This was due to a non-linear dependence of individual exit superheats on the “restriction factors”. For this reason another simulation scheme was developed in which the user directly assigns refrigerant distribution between different circuits. The operating conditions are as shown in Figure 4.3.1.4 with the refrigerant inlet quality and distribution (in fractions) solicited by the follow-up DOS window. While holding the refrigerant distribution constant, the program iterates the overall refrigerant mass flow rate and inlet pressures at individual inlet tubes to converge on the target exit pressure (the same for each exit tube) and overall target superheat. Different individual superheats can be obtained by specifying different refrigerant distributions. Eventually, all simulation results for this study were obtained using the second scheme.

Evaporator operating conditions			
Refrigerant			
Outlet sat. temp.	C		7.2
Superheat	C		5.5
Mass flow rate (estimate)	kg/h		54.4
Inlet quality	fraction		0.20
Air			
Inlet temperature	C		26.9
Inlet pressure	kPa		101.325
Inlet relative humidity	fraction		0.51
Volumetric flow rate	m³/min		15.19
Units: <input checked="" type="checkbox"/> SI Units <input type="checkbox"/> British Units			
		Cancel	OK

Figure 4.3.1.4: EVAP-COND input data window for simulations with specified overall evaporator exit saturation temperature and superheat.

4.3.2. Air-side Heat Transfer Correlations

Often the most significant part of heat transfer resistance between the air and refrigerant is on the air-side of the heat exchanger. For this reason, a literature review on the latest air-side heat transfer correlations was performed at the outset of this study. Of our particular interest were correlations for wavy and lanced (slit) fins – the two fin types used in the evaporators tested under this project.

Figure 4.3.2.1 compares the predictions of different correlations available in the literature. These predictions were calculated for typical fin designs for a three-depth-row heat exchanger. The layout of different prediction lines in the figure may serve as an explanation why predicting performance of a finned-tube heat exchanger may be difficult. For wavy fins, the correlation by Wang et al. (1999a) and Kim et al. (1997) are in a close agreement, while the correlation by Webb (1990) calculates heat transfer coefficients up to 50 % lower than the two first methods. In the air velocity range of 1.8 m/s (5.9 ft/s) to 2.1 m/s (6.9 ft/s), the Webb correlation breaks sharply due to switching between two different algorithms with a changing air-side Reynolds number. At some point the Webb correlations provide a value for the wavy fin heat transfer coefficient that is lower than that for a flat fin, which is not a realistic prediction.

For slit (lanced) fins, the correlations by Nakamura and Xu (1983) and Wang et al. (2001) may differ by more than 40 %, depending on air velocity. This spread may be indicative of the general fact that some correlations do not predict well outside the geometries for which they were developed. A measurement uncertainty in one or both

experiments may also be a contributing factor to this large discrepancy. In addition, it should be noted that the Nakayama and Xu (1983) predictions do not approach zero at air velocities below 2 m/s (6.5 ft/s), the trend exhibited by the other correlations. Regarding louver fins, the correlation by Wang et al. (1999b) shows a step change in the 1.5 m/s (4.9 ft/s) to 1.8 m/s (5.9 ft/s) range caused by using two different algorithms, similar to the Webb correlation for the wavy fins.

The analysis of relative predictions of the air-side heat transfer coefficient provided the reason for replacing the existing correlations in **EVAPS** with correlations published by Wang and his co-workers for all types of fins, i.e., flat, wavy, louver, and slit fins. It was judged that a better degree of prediction consistency can be obtained with all correlations developed by the same author. Still, the reader should note a reservation regarding the louver fin correlation, which did not provide smooth predictions in Figure 4.3.2.1.

In conclusion, we have to recognize the spread in performance between different enhanced fins, either realistic or perhaps, in some instances, overstated by correlations. To accommodate these differences and facilitate accurate evaporator model predictions, **EVAP-COND** provides an option that allows the user to “tune” evaporator simulated performance to the laboratory data by specifying a “correcting parameter” for the air-side heat transfer coefficient (such correcting parameters are also allowed for the refrigerant-side heat transfer coefficient, and refrigerant pressure drop).

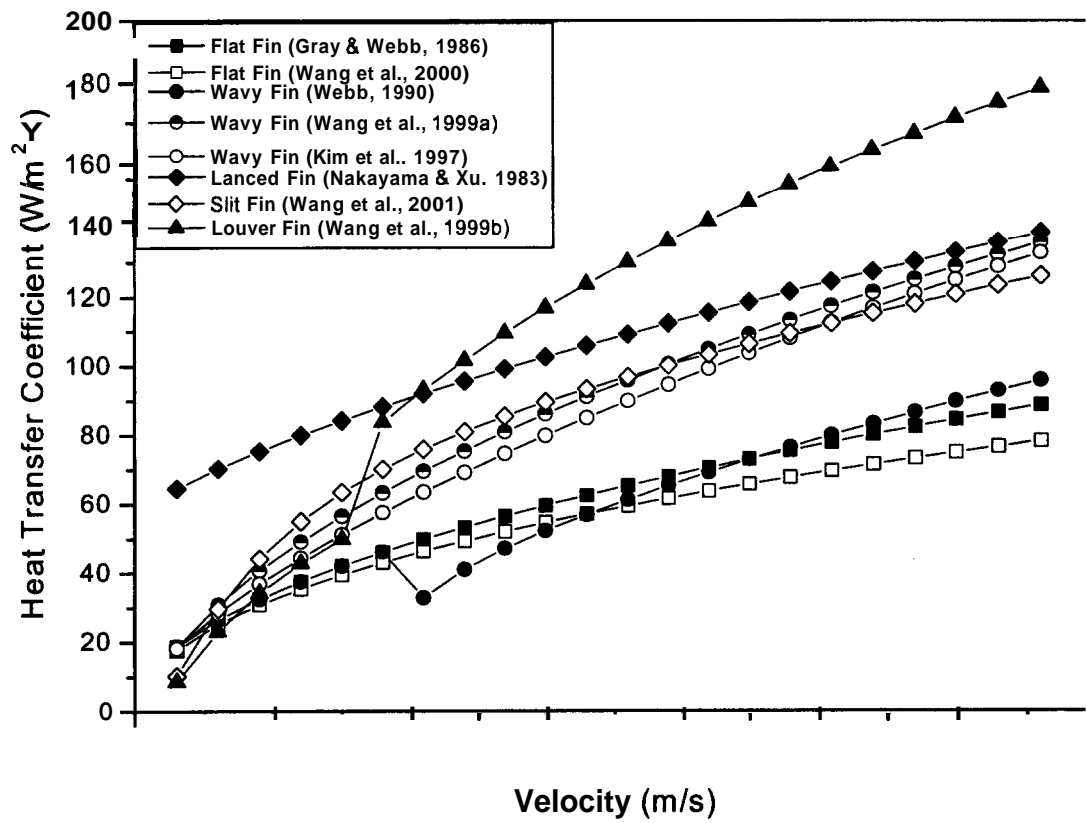


Figure 4.3.2.1: Comparison of air-side heat transfer correlations

4.3.3. Internal Heat Transfer in a Finned-Tube Evaporator

The current study stipulated evaporator tests with a superheat as high as 16.7 °C (30.0 °F) to assess capacity degradation at large and uneven superheats. As presented in previous sections, these tests for COIL-E and COIL-EC produced rather interesting data suggesting that internal heat transfer within the evaporator metal body may be the culprit for significant capacity degradation. Figure 4.3.3.1 presents measured capacities at 193 m³/kWh (400 cfm/ton) and includes capacities predicted by EVAPS (internal heat transfer not considered). The figure shows that tested capacities at 5.6 °C (10 °F) overlap for both coils and are reasonably well predicted by EVAP5. However, at 16.7 °C (30 °F) superheat COIL-E capacity was tested to be 346 W (1180 Btu/h) less than COIL-EC capacity and 966 W (3295 Btu/h) less than the simulated value. The lower capacity degradation for COIL-EC can be explained by the fin cuts, which physically separated different tube depth rows and disallowed heat transfer between neighboring rows.

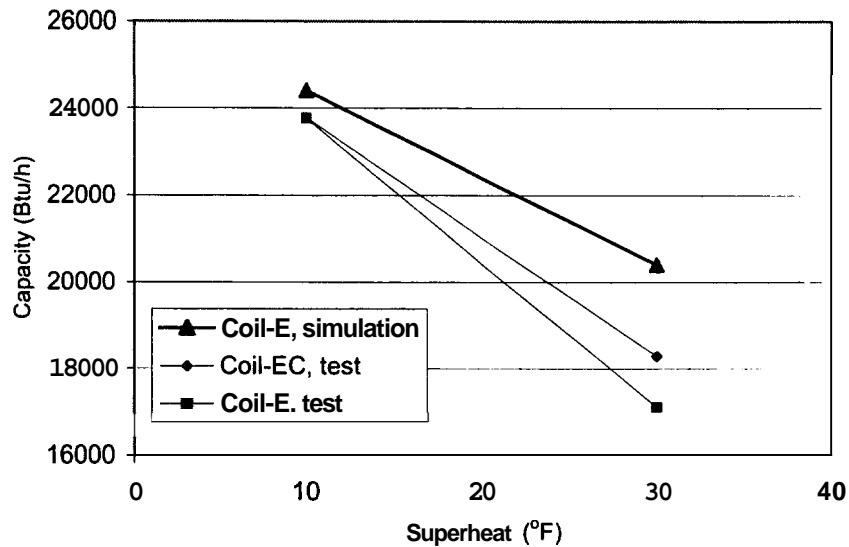


Figure 4.3.3.1: Tested and predicted capacities for COIL-E and COIL-EC at 5.6 °C (10 °F) and 16.7 °C (30 °F) superheats (Test 9 and Test 10 operating conditions. Internal heat transfer within the evaporator **metal** body **not** considered.)

The following two sections discuss the two modes of the internal heat transfer, longitudinal tube conduction and longitudinal fin conduction (tube-to-tube **heat** transfer), and their impact on evaporator performance.

4.3.3.1 Longitudinal Tube Conduction

The general theory states that if a temperature gradient exists in a **wall** of a heat exchanger, then conduction heat transfer **will** occur along that **wall** and **may** therefore degrade the performance of the heat exchanger. Kays and London (1984) identified the major parameters affecting the magnitude of the performance degradation **due** to this phenomenon as follows:

$$\lambda = \frac{kA_w}{LC_{min}}, \quad \frac{C_{min}}{C_{max}}, \quad \text{and} \quad NTU \quad (4.3.3.1.1)$$

The magnitude of the performance degradation becomes larger with increasing λ , C_{min}/C_{max} , and NTU. Kays and London stated that this reduction in performance is seen in heat exchangers designed for high effectiveness ($\epsilon > 0.9$), however, they did not provide much of a quantitative analysis. Ranganayakulu et. al. (1996) carried out a series of finite element simulations to quantify the magnitude of the performance degradation in a heat exchanger due to longitudinal heat conduction.. The results of their simulations are represented by the “conduction effect factor”, τ , in terms of the effectiveness with no longitudinal conduction effects, ϵ_{NC} , and the effectiveness considering longitudinal conduction effects, ϵ_{WC} .

$$\tau = \frac{\epsilon_{NC} - \epsilon_{WC}}{\epsilon_{NC}} \quad (4.3.3.1.2)$$

The conduction effect factor can be read from the charts presented in the paper for given $\epsilon, \lambda, C_{min}/C_{max}$, and NTU. Ranganayakulu et. al. suggested 0.8 as the effectiveness limit below which the impact of longitudinal conduction is negligible.

With the theory and the results from the numerical simulations at hand, the impact of longitudinal tube conduction for a typical finned-tube evaporator was examined. Using **EVAPS**, a 10.6kW (3 ton) evaporator was simulated to identify the tubes with two-phase R-22 (in which the longitudinal heat conduction does not occur) and the tubes with a

superheated refrigerant (in which longitudinal heat conduction does take place). Then the capacity penalty for the superheated tubes was calculated as a fraction of capacity of these tubes and as a fraction of the evaporator capacity.

Figure 4.3.3.1.1 displays an evaporator side view with a schematic of the refrigerant circuitry. Figure 4.3.3.1.2 contains a Coil Design Data window from EVAP-COND with the coil design information, and Figure 4.3.3.1.3 presents the operating conditions of the evaporator.

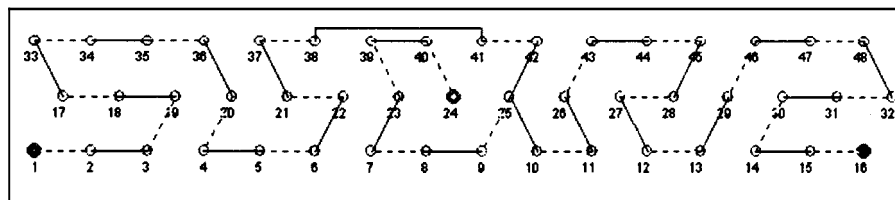


Figure 4.3.3.1.1: Refrigerant circuitry configuration for the analyzed **R-22** evaporator (inlet tube: tube # 24, outlet tubes: tube # 1 and tube # 16;)

Data for a section			Number of repeating sections	
No. of tubes in depth row #1:	16		1	
No. of tubes in depth row #2:	16			
No. of tubes in depth row #3:	16			
No. of tubes in depth row #4:	0			
No. of tubes in depth row #5:	0			

Tube data			Fin data	
Tube length	mm	454	Thickness	mm 0.2032
Inner diameter	mm	9.22	Pitch	mm 2.004
Outer diameter	mm	10.01	Type	Wavy
Tube pitch	mm	25.4	Thermal conductivity	kW/(m.C) 0.2216
Depth row pitch	mm	22.23		
Inner surface		Smooth		
Thermal conductivity	kW/(m.C)	0.386		

☒ SI Units ☐ British Units

Figure 4.3.3.1.2: EVAP-COND window with evaporator design information

Evaporator operating conditions			
Refrigerant		Air	
Inlet pressure	kPa 655	Inlet temperature	C 26.6667
Inlet quality	fraction 0.2	Inlet pressure	kPa 101.325
Mass flow rate	kg/h 100	Inlet relative humidity	fraction 0.5
		Volumetric flow rate	m³/min 14.996

☒ SI Units ☐ British Units

Figure 4.3.3.1.3: EVAP-COND window with evaporator operating conditions

For the evaporator exit superheat of 8.0 °C (14.4 °F), the simulations showed that only 5 of the 48 tubes in the heat exchanger have superheated refrigerant and experience a temperature change. This means that 43 of the tube passes in the heat exchanger will not experience any axial heat conduction because there will be no temperature difference for this to occur (neglecting the marginal drop of saturation temperature due to the pressure

drop). An example of a tube with superheated vapor, tube number **15**, has the following values for the aforementioned parameters.

$$\lambda = \frac{kA_w}{LC_{min}} = \frac{\left(386 \frac{W}{mK}\right)(1.1932E-5m^2)}{(0.454m)\left(9.476 \frac{W}{K}\right)} = 0.0011 \quad (4.3.3.1.3)$$

$$\frac{C_{min}}{C_{max}} = 0.441 \quad (4.3.3.1.4)$$

$$NTU = 0.368 \quad (4.3.3.1.5)$$

These parameters lie below the range of data given by Ranganayakulu. Using extrapolation, it was determined that the conduction effect factor would be approximately 0.0005. This means that this particular tube in the heat exchanger would see a loss in capacity of one twentieth of one percent due to axial heat conduction. When this capacity degradation is summed over all of the tubes in the entire heat exchanger where this effect occurs, the capacity reduction totals **0.13 W (0.45 Btu/h)**, which is insignificant when compared to the predicted performance of the evaporator being **49000 W (16800 Btu/h)**.

It should be noted that the effectiveness of tube **15** is **0.29**. Hence, our result agrees with the general statements by Kays and London and that of Ranganayakulu et. al. that the longitudinal heat transfer has an insignificant effect for heat exchangers with an effectiveness less than 0.8. The negligible impact of the longitudinal tube conduction on evaporator performance permits neglecting this heat transfer in modeling of a finned-tube heat exchanger. It may be further inferred that the same conclusion can be made for the **R407C** zeotropic mixture. Although a **7 °C (12 °F)** glide associated with **R407C** phase change produces a temperature difference promoting longitudinal heat transfer, in the

analyzed evaporator this glide would be distributed over 10 m (33 ft) of tube passes and would result in a small longitudinal temperature gradient.

4.3.3.2 Tube-to-Tube Heat Transfer via Fins

If we recognize that longitudinal tube heat conduction has a negligible impact, then the difference in capacity degradation between COIL-E and COIL-EC at 16.7 °C (30 °F) superheat must be due to longitudinal fin conduction. In COIL-EC, the continuous cuts in the fins separating different depth rows prevent heat transfer between different depth rows. However, the fins join the adjacent tubes in the same depth row, and some heat transfer between them occurs. This is why COIL-EC still experiences a decline in capacity, but not as much as COIL-E.

Our literature review located two publications that shed some light on the longitudinal fin conduction phenomenon. Heun and Crawford (1994) performed analytical study of the effects of longitudinal fin conduction on multipass cross-counterflow single-depth-row heat exchanger. They considered the fins to have one-dimensional temperature distributions and solve them using a system of non-dimensional differential equations. Their results showed that longitudinal fin conduction always degrades heat exchanger performance and this effect is stronger for a low normalized fin resistance and large values of the ratio of air-side conductance to air heat capacity rate.

Romero-Mender et al. (1997) also studied tube-to-tube heat transfer in a single-row finned-tube heat exchanger. They assumed the fins to be continuously and uniformly

distributed along the length of each tube. With his continuum assumption, they solved a system of ordinary differential equations for steady-state refrigerant and tube-wall temperatures. They identified four non-dimensional groups that effected the degradation of evaporator capacity. These group are: (1) the ratio of the thermal conductance for convective heat transfer between the refrigerant and the wall to the product of refrigerants heat capacity and mass flow rate, (2) the ratio of the thermal conductance for external heat transfer from the unfinned portion of the tube to the internal thermal conductance, (3) the ratio of the thermal conductance for convection from the fin to the thermal conductance for conduction along it, and **(4)** the ratio of the thermal conductance for heat conduction along the insulated fin to the thermal conductance between the refrigerant and the wall. Their study also indicated the number of tubes to be an influencing factor. The study by Romero-Mender et al. indicates that tube-to-tube heat transfer always degrades capacity and that the influencing parameters they identified have a non-linear impact on capacity degradation over the wide range of values studied. For some parametric values they found the degradation in a single-row heat exchanger to be as high as **20 %**.

Our literature review have not located a publication that would discuss longitudinal fin conduction in a multi-depth-row evaporator, but it may be safely expected that capacity degradation would be higher than that for a single-depth-row coil. The literature review identified a very recent paper which presents three simulation models for finned-tube single-phase dehumidifying heat exchangers, the most advanced of which accounts for tube-to-tube heat transfer (Oliet et al. (2002)). This model, referred to as

“advancedCHESS”, is based on a finite volume approach with discretization of the heat exchanger domain into a set of control volumes as fin-and-tube elements where both local thermophysical properties and empirical coefficients are computed. While “advancedCHESS” appears to be a research model, two other models are more practical for production simulations. The two less advanced models, called “basicCHESS” and “quickCHESS”, do not consider tube-to-tube heat transfer.

While the above publications are very interesting and valuable, they do not offer a methodology for accounting for tube-to-tube heat transfer in a tube-by-tube simulation model. The number of influencing parameters identified for a dry fin by Romero-Mender et al. (1997) suggests that a fully fundamental approach will be difficult to implement into a tube-by-tube evaporator model, which uses the adiabatic fin tip assumption and considers an individual tube as a separate entity for heat transfer calculations. Our attempts to apply a few algorithms derived from their paper, however, were unsuccessful because we were unable to resolve the “clashes” between the fundamental algorithms and the current simulation scheme used in EVAPS. It appears that merging a fundamental scheme into EVAPS amounts to a separate project that should be dedicated to this task.

To reach the objectives of the project within a stipulated effort and time, a practical scheme was developed, which uses the temperature difference between neighboring tubes as the driving force for heat transfer. This scheme approaches the tube-to-tube heat

transfer problem in a similar way Sheffield (1988) studied fin collar-tube heat transfer resistance as shown in Figure 4.3.3.2.1.

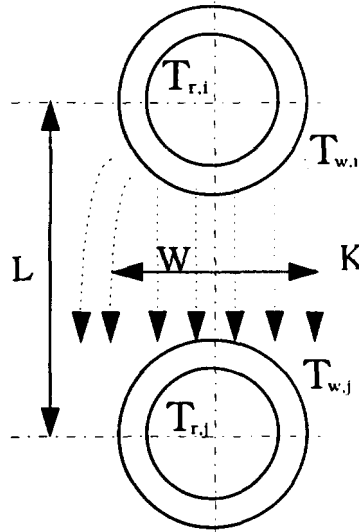


Figure 4.3.3.2.1: Schematic graph for longitudinal fin conduction between two adjacent tubes

To determine the heat transferred, the Fourier Law of Conduction is applied. The effects of the available width and configuration of the conducting material (fin) are represented by a “shape factor” S used in equation 4.9:

$$(Q_{fin})_{i,j} = \left(\frac{W \cdot t_f}{L} K_f \right) (T_{w,i} - T_{w,j}) = S \frac{t_f}{L} \cdot K_f (T_{w,i} - T_{w,j}) \quad (4.3.3.2.1)$$

To show the impact of fin conduction, Lee and Domanski used this scheme considering up to six immediate neighboring tubes. For example, for the circuitry used in the evaporators tested under this project and shown in Figure 4.3.3.2.2 the intermediate neighbors for tube 25 are tubes 7, 8, 26, 44, 43, and 24.

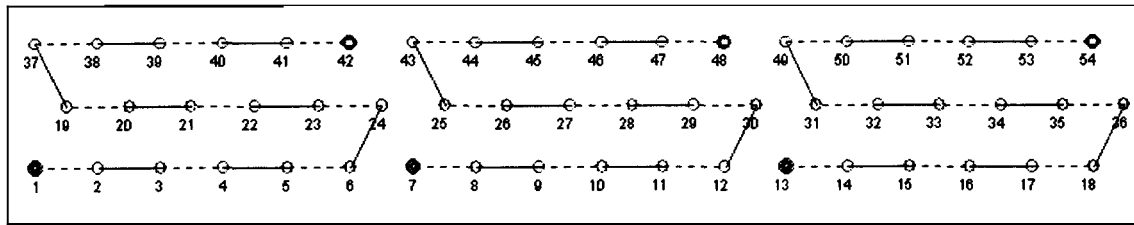


Figure 4.3.3.2.2: Schematic of refrigerant circuitry for COIL-W, COIL-E and COIL-EC in cross-counter flow configuration (inlet tubes: **42, 48, 54**; outlet tubes: **1, 7, 13**)

Extensive experimenting with this scheme for the coils tested under this project indicated that it was important to add additional neighbors to the group of immediate neighbors considered so far. This need demonstrated itself not only in predicted capacity values but also in simulation runs, which **did** not yield gradually changing predictions at small changes in imposed refrigerant superheat at the outlet tubes. Based on these observations, depending on location up to six second-order neighbors were added. These are other tubes in the coil assembly that a given tube “can see”. Tube **25** has four second-order neighbors; they are tubes **6, 9, 45, and 42**. For tube **9**, the immediate neighbors are tube **8, 10, 27, and 26**, and the second-order neighbors are tubes **25, 45, and 28**. In a three-depth-row coil, the maximum number of second-order neighbors is four. A five-depth-row coil is needed for a tube located in the middle depth row to have all six second-order neighbors.

The value of the shape factor depends on a fin design. For flat and wavy fins the fin material is continuous. Lanced fins, however, have numerous cuts, which reduce the fin cross-section area that is available for heat transfer. Hence, the shape factor for flat and wavy fins should be expected to have higher values than for lanced or louver fins. Since

we are not aware of any publication that quantifies the fin shape factor, the values for COIL-W and COIL-E were assigned based on their respective results for test 10. Once these values for shape factors were assigned, they were left unchanged for the remaining simulations. COIL-EC used the same shape factor as COIL-E, however, any tube in COIL-EC could have only two neighbors, the closest two tubes located in the same depth row.

Figure 4.3.3.2.3 shows tested and simulated capacities for COIL-E at conditions of test 1, 2, 9, 10, 13, and 14. For the tests at 5.6 °C (10 °F) superheat (tests 1, 9 and 13), the model predicted measured capacities within 5.1 %. For the tests with 16.7 °C (30 °F) superheat, the differences in between tested and predicted and tested capacities were – 6.7 %, 3.1 %, and - 2.9 %. Without accounting for tube-to-tube heat transfer, EVAP5 would overpredict the capacities at 16.7 °C (30 °F) superheat by approximately 20 %. Section 4.4 presents validation results for all three evaporators.

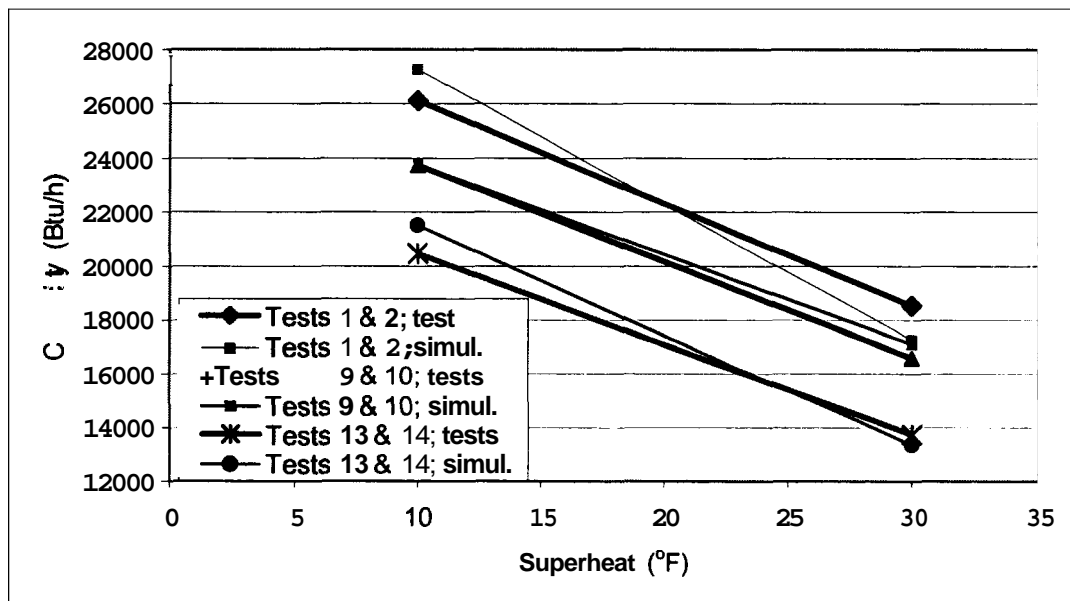


Figure 4.3.3.2.3: COIL-E measured and simulated capacities for tests with 5.6 °C (10 °F) and 16.7 °C (30 °F) superheats (tests 1, 2, 9, 10, 13, 14)

4.4 Validation and Simulations with EVAPS

4.4.1 Validation of EVAPS

The majority of laboratory test data measured in this study are for a cross-counter flow configuration with non-disturbed (uniform) air velocity profile at the coil inlet. These measurements for COIL-W, COIL-E, and COIL-EC were used to validate EVAPS and explore the impact of tube-to-tube heat transfer. The imposed variety of refrigerant superheats at individual exit tubes combined with a wide range of air flow provided a unique set of challenging test data for validating any evaporator model.

The refrigerant circuitry for the tested evaporators has already been presented in Figure 4.3.3.2.2 as it is displayed by the EVAP-COND interface. Also copying from the respective window of EVAP-COND, Figure 4.4.1.1 shows the key design parameters of COIL-W. Except for a different fin design, these parameters were the same for COIL-E and COIL-EC.

At the outset of simulations for each coil, EVAPS was “tuned” to predict the performance of a given evaporator at the conditions of test 9. This was accomplished by inputting “correction parameters” for the refrigerant heat transfer coefficient, refrigerant pressure drop, and air-side heat transfer coefficient. (Section 4.3.2 discusses the reasons for using these parameters in the context of prediction discrepancies between different air-side correlations). Figure 4.4.1.2 presents the correction parameters for COIL-W and COIL-E

as they were input into the EVAP-COND window. The input for COIL-EC was different by the value for the air-side heat transfer coefficient, which was 0.62 instead of 0.65. The 1.6 value for the refrigerant pressure drop parameter accounts for the impact of lubricant, which can be responsible for 35 % pressure drop underprediction. Since the parameter for refrigerant heat transfer coefficient was set to 1.0, the 0.65 or 0.62 value for the air-side heat transfer coefficient accommodates the heat transfer adjustment **on the** air and refrigerant sides. These correction parameters were used in all simulations for the respective coils.

Coil Design Data

Data for a section:

No. of tubes in depth row #1:	18
No. of tubes in depth row #2:	18
No. of tubes in depth row #3:	18
No. of tubes in depth row #4:	0
No. of tubes in depth row #5:	0

W02027B-3 W-counter (9)

Number of repeating sections: 1

Units: ☐ SI Units ☒ British Units

Tube data:

Tube length	in	18
Inner diameter	in	0.3125
Outer diameter	in	0.375
Tube pitch	in	1
Depth row pitch	in	0.866
Inner surface		Smooth
Thermal conductivity	Btu/(ft.h.F)	223

Fin data:

Thickness	in	0.016
Pitch	in	0.0625
Type		Wavy
Thermal conductivity	Btu/(ft.h.F)	128

Cancel OK

Figure 4.4.1.1: Design parameters for COIL-W

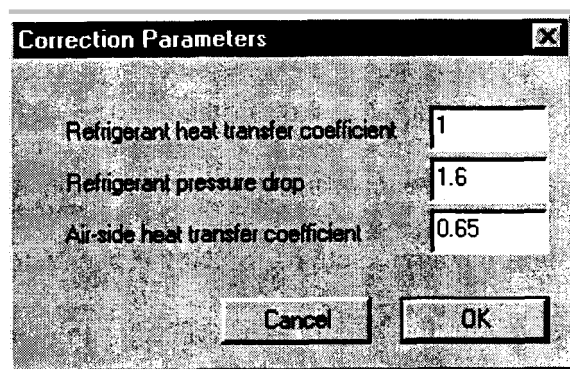


Figure 4.4.1.2: Correction parameters for COIL-W and COIL-E

Tables 4.4.1.1, 4.4.1.2, and 4.4.1.3 show tested and simulated total capacities for COIL-W, COIL-E, and COIL-EC, respectively, in the test matrix format. Tables 4.4.1.4a, 4.4.1.4b, 4.4.1.5a, 4.4.1.5b, 4.4.1.6a, and 4.4.1.6b present total and sensible capacities, sensible heat ratios, and differences between simulated and measured results. It is convenient to screen the accuracy of capacity predictions by reviewing Figures 4.4.1.3 and 4.4.1.4. Figure 4.4.1.3 shows that the maximum error in capacity prediction for wet coil tests was 5.5 % for all air velocities and refrigerant superheat scenarios. For dry coil tests shown in Figure 4.4.1.4, EVAP5 predicted the three capacities at uniform 5.6 °C (10 °F) superheat within 5.0 %. (They are represented by the first bar for each coil). For the remaining six tests at different superheat scenarios, the only capacity predicted within 5.0 % was for COIL-EC (represented by the last bar on the right hand side). Capacities for COIL-W and COIL-E capacities were unpredicted by as much as **20.0 %**. The inability of EVAP5 to account accurately for longitudinal fin conduction for dry coil tests can be explained by the fact that the used algorithm considers only temperature differences between neighboring tubes (the first order effect) and neglects variations in air-side heat transfer. This conclusion agrees with the observation by Romero-Mendez et

al. (1997) who indicated thermal conductance for convection **from** the fin **as** one of the parameters affecting tube-to-tube heat transfer. This and other effects identified by Romero-Mendez et al. (1997) should receive detailed attention **in** a future study dedicated to this challenging modeling issue.

Table 4.4.1.1: Measured and Simulated Capacities for COIL-W in Cross-Counter Flow Configuration

Test Name	Test #	Volumetric Flowrate or Air m ³ /min (cfm)			Coil Surface		Overall Superheat											
							Superheats in Individual Circuits											
		145·Q ¹ (300·Q)	193·Q ¹ (400·Q)	242·Q ¹ (500·Q)	Dry	Wet	5.6 °C (10.0 °F)		16.7 °C (30.0 °F)		5.6 °C (10.0 °F)		16.7 °C (30.0 °F)		5.6 °C (10.0 °F)			
W020226A	1	x				x	Q _{test}	Q _{sim}	Q _{test}	Q _{sim}	Q _{test}	Q _{sim}	Q _{test}	Q _{sim}	Q _{test}	Q _{sim}		
							W (Btu/h)	W (Btu/h)	W (Btu/h)	W (Btu/h)	W (Btu/h)	W (Btu/h)	W (Btu/h)	W (Btu/h)	W (Btu/h)	W (Btu/h)		
							5787	5747					16.7/16.7/16.7	16.7/16.7/16.7	16.7/16.7/16.7	16.7/16.7/16.7	16.7/16.7/16.7	16.7/16.7/16.7
							(19746)	(19609)					(30/30/30)	(30/30/30)	(30/30/30)	(30/30/30)	(30/30/30)	(30/30/30)
W020225B	5		x		x		5428	5417										
W020228A	6		x		x				3595	2953								
W020221A	7		x		x				(12265)	(10076)			3910	3168				
W020225A	8		x		x								(13341)	(10810)				
W020207B	9		x				6507	6485							3888	3360		
W020530A	10		x				(22203)	(22127)							(13267)	(11464)		
W020531A	11		x						3722	3819								
W020215B	12		x						(12701)	(13030)			3837	3819				
W020301A	13			x									(13091)	(13030)	3830	3885		
							7502	7727							(13067)	(13255)		
							(25598)	(26367)										

* Superheat to be controlled such that the desired overall level of superheat is obtained

1) SI units of m³/kWh multiplied by capacity (Q) in kW to determine airflow (IP units of cfm/ton multiplied by capacity (Q) in tons).

Table 4.4.1.2: Measured and Simulated Capacities for COIL-E in Cross-Counter Flow Configuration

Test Name		Test #	Volumetric Flowrate of Air m ³ /h (scfm)			Coil Surface		Overall Superheat											
								Superheats in Individual Circuits											
								5.6 °C (10.0 °F)				16.7 °C (30.0 °F)				5.6 °C (10.0 °F)			
		145-Q ¹ (300-Q)	193-Q ¹ (400-Q)	242-Q ¹ (500-Q)	Dry	Wet	5.6/5.6/5.6 (10/10/10)		16.7/16.7/16.7 (30/30/30)		16.7/16.7/16.7 (30/30/30)		16.7/16.7/16.7 (30/30/30)		5.6/16.7/16.7 (30/30/30)		5.6 °C (10.0 °F) */16.7/16.7 (*30/30)		
		Q _{test} W (Btu/h)	Q _{sim} W (Btu/h)	Q _{test} W (Btu/h)	Q _{sim} W (Btu/h)	Q _{test} W (Btu/h)	Q _{sim} W (Btu/h)	Q _{test} W (Btu/h)	Q _{sim} W (Btu/h)	Q _{test} W (Btu/h)	Q _{sim} W (Btu/h)	Q _{test} W (Btu/h)	Q _{sim} W (Btu/h)	Q _{test} W (Btu/h)	Q _{sim} W (Btu/h)	Q _{test} W (Btu/h)	Q _{sim} W (Btu/h)		
W020320B	1	x					x	5998 (20464)	6239 (21289)										
W020321A	2	x					x			4026 (13737)	3806 (12987)								
E020322A	5		x				x	5603 (19115)	5323 (18163)										
E020321B	6		x				x			4302 (14677)	3466 (11828)								
E020322C	7		x				x					4797 (16367)	3835 (13086)						
E020328B	8		x				x									4700 (16037)	3794 (12945)		
E020607A	9		x					6956 (23733)	6977 (23807)										
E020318A	10		x				x			4865 (16599)	5055 (17249)								
E020318B	11		x				x							5485 (18715)	5181 (17678)				
E020319A	12		x				x									4736 (16157)	4774 (16289)		
W020319B	13			x			x	7033 (26109)	6041 (27389)										
W020320A	14			x			x			5429 (18524)	5693 (19427)								

* Superheat to be controlled such that the desired overall level of superheat is obtained

1 SI units of m³/kWh multiplied by capacity (Q) in kW to determine airflow (IP units of cfm/ton multiplied by capacity (Q) in tons)

Table 4.4.1.3: Measured and Simulated Capacities for COIL-EC in Cross-Counter Flow Configuration

Test Name	Test #	Volumetric Flowrate or Air m ³ /h (scfm)			Coil Surface		Overall Superheat											
							Superheats in Individual Circuits											
		145-Q' (300-Q)	193-Q' (400-Q)	242-Q' (500-Q)	Dry	Wet	5.6 °C (10.0 °F)		16.7 °C (30.0 °F)		5.6 °C (10.0 °F)		16.7 °C (30.0 °F)		5.6 °C (10.0 °F)		16.7 °C (30.0 °F)	
							Q _{test} W (Btu/h)	Q _{sim} W (Btu/h)	Q _{test} W (Btu/h)	Q _{sim} W (Btu/h)	Q _{test} W (Btu/h)	Q _{sim} W (Btu/h)	Q _{test} W (Btu/h)	Q _{sim} W (Btu/h)	Q _{test} W (Btu/h)	Q _{sim} W (Btu/h)	Q _{test} W (Btu/h)	Q _{sim} W (Btu/h)
E020417A	1	x				x	6085 (20760)	6189 (21117)					16.7/16.7/16.7 (30/30/30)				*16.7/16.7 (*30/30)	
E020417B	2	x				x			4647 (15855)	4890 (16684)								
E020418A	5		x		x		5578 (19032)	5356 (18272)										
E020419A	6		x		x				4170 (14226)	4291 (14640)								
E020415A	9		x			x	6972 (23788)	6989 (23845)										
E020509A	10		x			x			5361 (18292)	5467 (18652)								
E020416B	13			x		x	7781 (26546)	7927 (27047)										
E020416A	14			x		x			6653 (22700)	6007 (20496)								

* Superheat to be controlled such that the desired overall level of superheat is obtained

1) SI units of m³/kWh multiplied by capacity (Q) in kW to determine airflow (IP units of cfm/ton multiplied by capacity (Q) in tons).

Table 4.4.1.4a: EVAP5 Validations for COIL-W (evaporator with wavy fins), SI Units

Flow configuration	Test name	Test #	Test results				Simulations with fin conduction included				Simulated capacity w/o fin conduction	
			Results				Difference ¹				Total capacity (watt)	Capacity difference ² (%)
			Total capacity (watt)	Sensible capacity (watt)	Sensible heat ratio (fraction)	Total capacity (watt)	Sensible capacity (watt)	Sensible heat ratio (fraction)	Total Capacity (%)	Sensible heat ratio (%)		
cross-counter	W020226A	1	5788	3953	0.68	5747	3706	0.64	-0.7	-5.9	5837	1.6
cross-counter	W020225B	5	5429	5429	1.00	5418	5418	1.00	-0.2	0.0	5425	0.1
cross-counter	W020228A	6	3595	3595	1.00	2953	2954	1.00	-17.8	0.0	4816	63.1
cross-counter	W020221A	7	3910	3910	1.00	3168	3168	1.00	-19.0	0.0		
cross-counter	W020225A	8	3889	3889	0.76	3360	3360	1.00	-13.6	0.0		
cross-counter	W020207B	9	6508	4914	0.76	6485	4724	0.73	-0.3	-3.7	6499	0.2
cross-counter	W020530A	10	3723	3381	0.91	3819	3014	0.79	2.6	-15.1	5968	56.3
cross-counter	W020531A	11	3837	3372	0.88	3819	2939	0.77	-0.5	-14.2		
cross-counter	W020215B	12	3830	3503	0.91	3885	3013	0.78	1.4	-17.9	7810	1.1
cross-counter	W020301A	13	7503	5820	0.78	7728	5678	0.73	3.0	-5.6		

¹ 100% (simulated value with fin conduction – tested value)/tested value

² 100% (simulated value w/o fin conduction – simulated value with fin conduction)/ simulated value with fin conduction

Table 4.4.1.4b: EVAP5 Validations for COIL-W (evaporator with wavy fins), IP Units

Flow configuration	Test #	Test results				Simulations with fin conduction included				Simulated capacity w/o fin conduction	
		Results				Difference ¹				Total capacity (Btu/h)	Capacity difference ² (%)
		Total capacity (Btu/h)	Sensible capacity (Btu/h)	Sensible heat ratio (fraction)	Total capacity (Btu/h)	Sensible capacity (Btu/h)	Sensible heat ratio (fraction)	Total Capacity (%)	Sensible heat ratio (%)		
cross-counter	W020226A	19746	13488	0.68	19609	12643	0.64	-0.7	-5.9	19916	1.6
cross-counter	W020225B	18521	18521	1.00	18485	18485	1.00	-0.2	0.0	18509	0.1
cross-counter	W020228A	12265	12265	1.00	10076	10077	1.00	-17.8	0.0	16431	63.1
cross-counter	W020221A	13341	13341	1.00	10810	10810	1.00	-19.0	0.0		
cross-counter	W020225A	13267	13267	0.76	11464	11465	1.00	-13.6	0.0		
cross-counter	W020207B	22203	16767	0.76	22127	16119	0.73	-0.3	-3.7	22172	0.2
cross-counter	W020530A	12701	11535	0.91	13030	10283	0.79	2.6	-15.1	20363	56.3
cross-counter	W020531A	13091	11503	0.88	13030	10029	0.77	-0.5	-14.2		
cross-counter	W020215B	13067	11950	0.91	13255	10281	0.78	1.4	-17.9		
cross-counter	W020301A	25598	19857	0.78	26367	19372	0.73	3.0	-5.6	26645	1.1

¹ 100% (simulated value with fin conduction – tested value)/tested value

² 100% (simulated value w/o fin conduction – simulated value with fin conduction)/ simulated value with fin conduction

Table 4.4.1.5a: EVAP5 Validations for COIL-E (evaporator with lanced fins), SI Units

Flow configuration	Test Name	Test #	Test results				Simulations with fin conduction included				Simulated capacity w/o conduction		
			Results				Difference ¹						
			Total capacity (watt)	Sensible capacity (watt)	Sensible heat ratio (fraction)	Total capacity (watt)	Sensible capacity (watt)	Sensible heat ratio (fraction)	Total Capacity (%)	Sensible heat ratio (%)	Total capacity (watt)	Capacity difference ² (%)	
cross-counter	W020320B	1	5998	3959	0.66	6239	3876	0.62	4.0	-5.9	6238	0.0	
cross-counter	W020321A	2	4026	3171	0.79	3806	2733	0.72	-5.5	-8.8	5196	36.5	
cross-counter	E020322A	5	5603	5603	1.0	5323	5323	1.00	-5.0	0.0	5426	1.9	
cross-counter	E020321B	6	4302	4302	1.0	3466	3466	1.00	-19.4	0.0	4572	31.9	
cross-counter	E020322C	7	4797	4797	1.0	3835	3835	1.00	-20.0	0.0			
cross-counter	E020328B	8	4700	4700	1.0	3794	3794	1.00	-19.3	0.0			
cross-counter	E020607A	9	6956	5057	0.73	6977	4677	0.67	0.3	-7.8	6952	-0.4	
cross-counter	E020318A	10	4865	3981	0.82	5055	3810	0.75	3.9	-7.9	5723	13.2	
cross-counter	E020318B	11	5485	4266	0.78	5181	3789	0.73	-5.5	-6.0			
cross-counter	E020319A	12	4736	3943	0.83	4774	3541	0.74	0.8	-10.9			
cross-counter	W020319B	13	7653	5720	0.75	8027	5651	0.70	4.9	-5.8	8004	-0.3	
cross-counter	W020320A	14	5429	4615	0.85	5693	4338	0.76	4.9	-10.4	6395	12.3	

¹ 100% (simulated value with fin conduction – tested value)/tested value

² 100% (simulated value w/o fin conduction – simulated value with fin conduction)/ simulated value with fin conduction

Table A 4.1.5b. EVAPORATOR VALIDATIONS FOR COIL E (COMPARED WITH TESTED VALUE) IN PT. 5

Flow configuration	Test Name	t	Test results				Simulations with fin conduction included				Simulated capacity w/o conduction	
			Results				Difference ¹				Total capacity (Btu/h)	Capacity difference ² (%)
			Total capacity (Btu/h)	Sensible capacity (Btu/h)	Sensible heat ratio (fraction)	Total capacity (Btu/h)	Sensible capacity (Btu/h)	Sensible heat ratio (fraction)	Total Capacity (%)	Sensible heat ratio (%)		
cross-counter	W020320B	1	20464	13506	0.66	21289	13224	0.62	4.0	-5.9	21284	∞
cross-counter	W020321A	2	13737	10819	0.79	12987	9324	0.72	-5.5	-8.8	17730	±6.5
cross-counter	E020322A	5	19115	19115	1.0	18163	18163	1.00	-5.0	0.0	18514	1.0
cross-counter	E020321B	6	14677	14677	1.0	11828	11828	1.00	-19.4	0.0	15602	±1.0
cross-counter	E020322C	7	16367	16367	1.0	13086	13086	1.00	-20.0	0.0		
cross-counter	E020328B	8	16037	16037	1.0	12945	12945	1.00	-19.3	0.0		
cross-counter	E020607A	9	23733	17252	0.73	23807	15957	0.67	0.3	-7.8	23720	4.4
cross-counter	E020318A	10	16599	13581	0.82	17249	13000	0.75	3.9	-7.9	19528	2.2
cross-counter	E020318B	11	18715	14556	0.78	17678	12927	0.73	-5.5	-6.0		
cross-counter	E020319A	12	16157	13452	0.83	16289	12081	0.74	0.8	-10.9		
cross-counter	W020319B	13	26109	19517	0.75	27389	19282	0.70	4.9	-5.8	27312	-0.3
cross-counter	W020320A	14	18524	15744	0.85	19427	14802	0.76	4.9	-10.4	21820	12.3

¹ 100% (simulated value with fin conduction – tested value)/tested value

² 100% (simulated value w/o fin conduction – simulated value with fin conduction)/ simulated value with fin conduction

Table 4.4.1.6a: EVAP5 Validation for COIL-EC (evaporator with lanced fins, cut between tube depth rows), SI Units

Flow configuration	Test name	Test #	Test results				Simulations with fin conduction included				Simulated capacity w/o fin conduction	
			Results				Difference ¹⁾				fin conduction	
			Total capacity (watt)	Sensible capacity (watt)	Sensible heat ratio (fraction)	Total capacity (watt)	Sensible capacity (watt)	Sensible heat ratio (fraction)	Total Capacity (%)	Sensible heat ratio (%)	Total Capacity (watt)	Difference ²⁾ (%)
cross-counter	E020417A	1	6085	4182	0.69	6189	3950	0.64	1.7	-7.7	6196	0.1
cross-counter	E020417B	2	4647	3577	0.77	4890	3329	0.68	5.2	-13.1	4962	1.5
cross-counter	E020418A	5	5578	5578	1.0	5356	5356	1.0	-4.0	0.0	5360	0.1
cross-counter	E020419A	6	4170	4170	1.0	4291	4291	1.0	2.9	0.0	4400	2.5
cross-counter	E020415A	9	6972	5125	0.74	6989	4816	0.69	0.2	-6.7	7005	0.2
cross-counter	E020509A	10	5361	4361	0.81	5467	4044	0.74	2.0	-10.0	5579	2.0
cross-counter	E020416B	13	7781	6083	0.78	7927	5778	0.73	1.9	-7.3	7990	0.8
cross-counter	E020416A	14	6653	5465	0.82	6382	4893	0.77	-4.1	-7.1	6694	4.9

¹ 100% (simulated value with fin conduction – tested value)/tested value

² 100% (simulated value w/o fin conduction – simulated value with fin conduction)/ simulated value with fin conduction

Table 4.4.1.6b: EVAP5 Validation for COIL-EC (evaporator with lanced fins, cut between tube depth rows), IP Units

Flow configuration	Test name	Test #	Test results				Simulations with fin conduction included				Simulated capacity w/o fin conduction	
			Results				Difference ¹⁾				fin conduction	
			Total capacity (Btu/h)	Sensible capacity (Btu/h)	Sensible heat ratio (fraction)	Total capacity (Btu/h)	Sensible capacity (Btu/h)	Sensible heat ratio (fraction)	Total Capacity (%)	Sensible heat ratio (%)	Total Capacity (Btu/h)	Difference ²⁾ (%)
cross-counter	E020417A	1	20760	14269	0.69	21117	13477	0.64	1.7	-7.7	21138	0.1
cross-counter	E020417B	2	15855	12204	0.77	16684	11359	0.68	5.2	-13.1	16928	1.5
cross-counter	E020418A	5	19032	19032	1.0	18272	18273	1.0	-4.0	0.0	18287	0.1
cross-counter	E020419A	6	14226	14226	1.0	14640	14641	1.0	2.9	0.0	15013	2.5
cross-counter	E020415A	9	23788	17485	0.74	23845	16432	0.69	0.2	-6.7	23898	0.2
cross-counter	E020509A	10	18292	14880	0.81	18652	13799	0.74	2.0	-10.0	19033	2.0
cross-counter	E020416B	13	26546	20754	0.78	27047	19713	0.73	1.9	-7.3	27261	0.8
cross-counter	E020416A	14	22700	18645	0.82	21773	16693	0.77	-4.1	-7.1	22840	4.9

¹ 100% (simulated value with fin conduction – tested value)/tested value

² 100% (simulated value w/o fin conduction – simulated value with fin conduction)/ simulated value with fin conduction

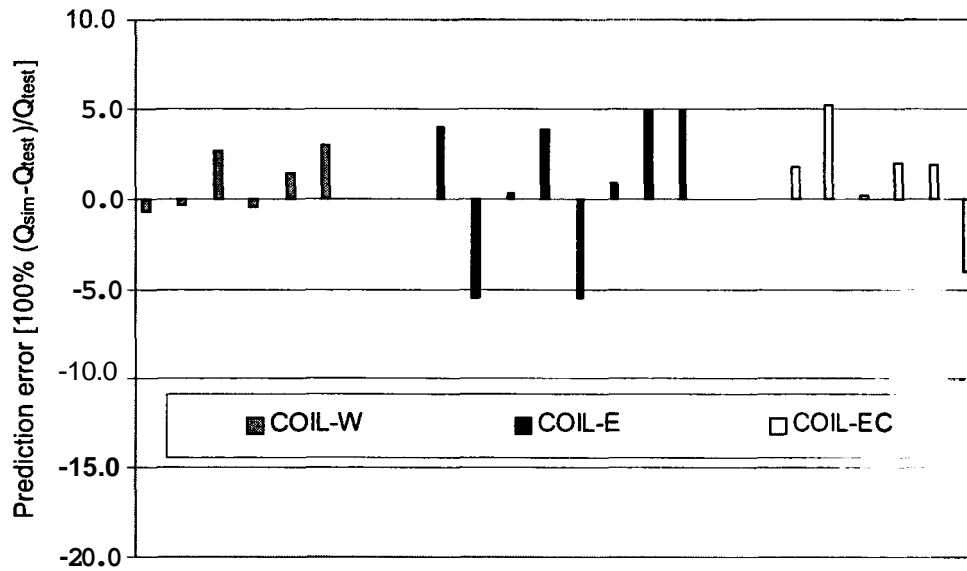


Figure 4.4.1.3: Difference between simulated and measured capacities for all wet coil tests for COIL-W, COIL-E, and COIL-EC

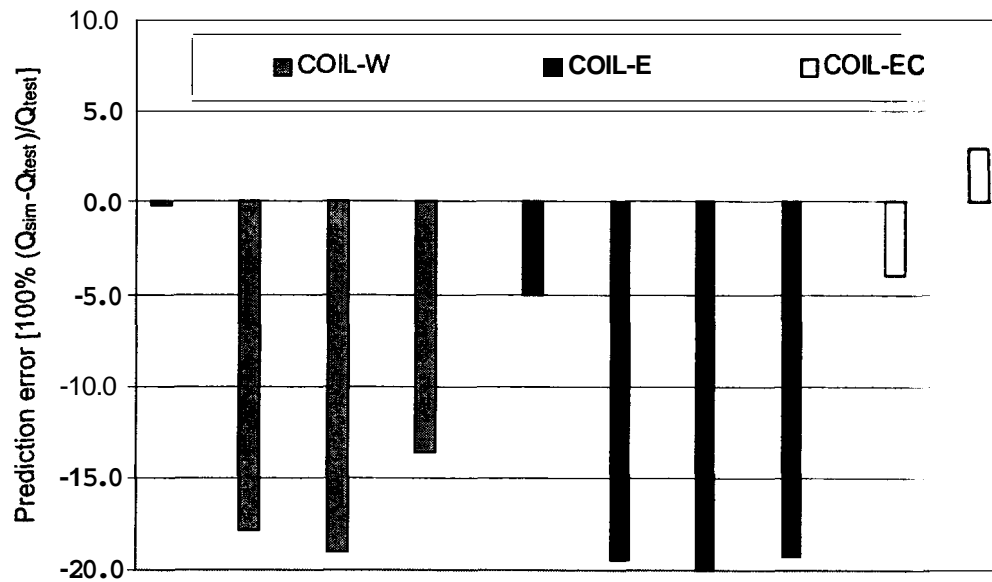
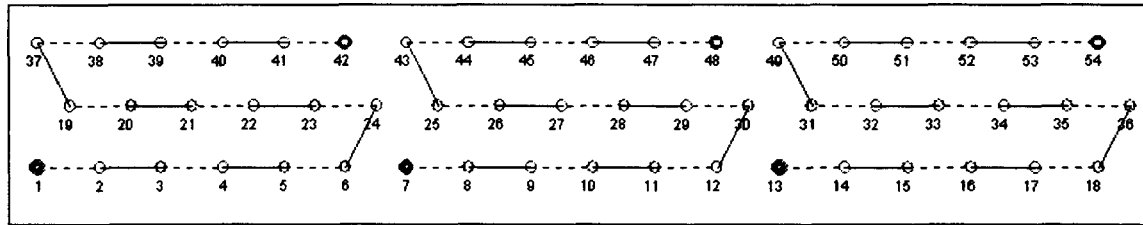


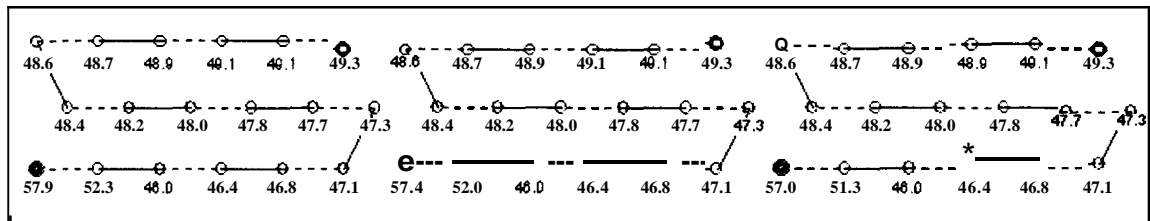
Figure 4.4.1.4: Difference between simulated and measured capacities for all dry coil tests for COIL-W, COIL-E, and COIL-EC

Tube-to-tube heat transfer demonstrates itself in temperatures that can be measured on coils return bends, as it was shown for COIL-W in Figures 3.4.4.1 and 3.4.4.2. Figure 4.4.1.5 shows similar information (refrigerant temperature at tube exits) as it is displayed by **EVAP-COND** for the same tests. For test 9 with even refrigerant superheat, refrigerant temperatures are similar for each circuit; refrigerant temperatures reflect drop in refrigerant pressure until the last two tubes in each circuit (2 and 1, 8 and 7, and 14 and 13) in which the refrigerant is superheated. For test 12, the first circuit is in two-phase flow until the exit tube 1, while the refrigerant leaving two other exit tubes (7 and 13) is highly superheated. Tubes 7 and 8 experience a drop in temperature compared to tube 9 because of their vicinity to the left-hand side circuit with two-phase, low-temperature refrigerant. Tubes 13 and 14 also experience temperature drop, however, it is small because the adjacent tubes are also superheated. This simulation results agree in principle with the measured return bend temperature of Figures 3.4.4.1 and 3.4.4.2.

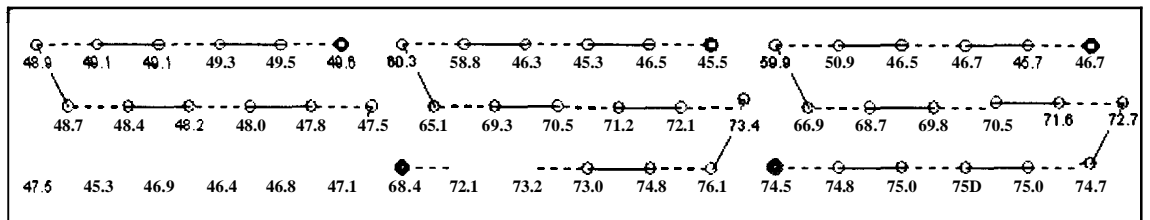


Tube numbering

V
air flow



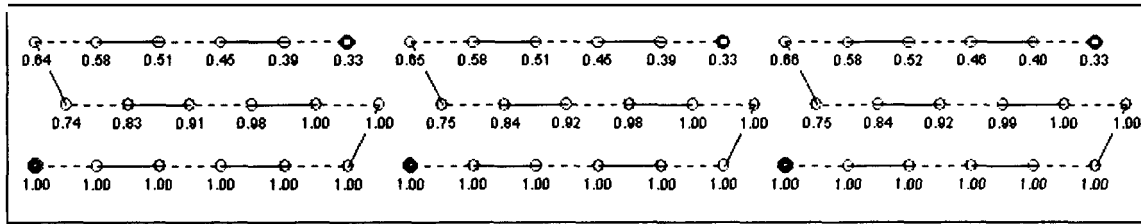
Refrigerant exit temperatures (°F) for COIL-W, test 9



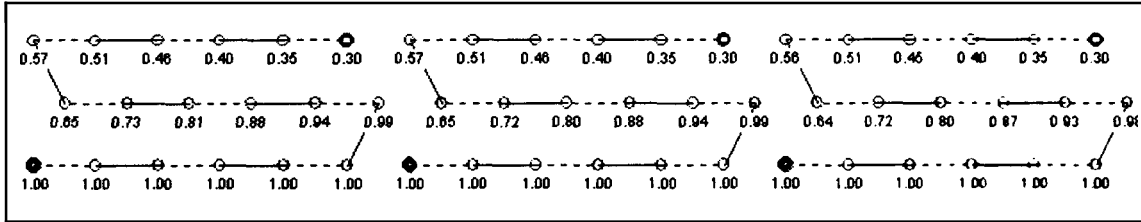
Refrigerant exit temperatures (°F) for COIL-W, test 12

Figure 4.4.15: Tube numbering and refrigerant exit temperatures for individual tubes for test 9 and test 12 for COIL-W, (inlet tubes: 42, 48, 54; outlet tubes: 1, 7, 13)

Figure 4.4.16 presents refrigerant exit qualities for individual tubes for COIL-E and COIL-EC for test 10 (16.7 °C (30 °F) even superheat). The figure shows that refrigerant reaches superheat (quality 1) two tubes earlier in COIL-E than in COIL-EC in each refrigerant circuit. This is a result of heat transfer between different tube depth rows that was allowed in COIL-E and was inhibited in COIL-EC. Corresponding tube temperatures predicted by **EVAPS** agree with those measured during laboratory tests.



Refrigerant exit qualities (fraction) for COIL-E, test 10



Refrigerant exit qualities (fraction) for COIL-EC, test 10

Figure 4.4.1.6: Refrigerant exit qualities for individual tubes for COIL-E and COIL-EC test 10 (16.7 °C (30 °F) even superheat)

The last two columns in Tables 4.4.1.4, 4.4.1.5, and 4.4.1.6 compare simulated capacities that were obtained with and without accounting for tube-to-tube heat transfer. For the tests with a uniform superheat of 5.6 °C (10 °F), the difference in capacities is not greater than 2.7 % for any of the three coils. For the tests with uniform superheat of 16.7 °C (30 °F), the capacities differ by 63.1 % and 56.3 % for COIL-W, 33.6 %, 18.8 %, 19.2 % for COIL-E, and 1.5 %, 2.5 %, 2.5 %, and 4.9 % for COIL-EC. These results demonstrate the impact of fin design on tube-to-tube heat transfer.

The validation of EVAP5 used the full set of COIL-W, COIL-E, and COIL-EC measurements in cross-counter flow configuration, which constituted the majority of the measurements taken in this study. The validation effort was not extended to the eight data points taken in cross-parallel flow configuration because six of these tests that involved 16.7 °C (30 °F) superheat resulted in severe pinching within less than 1 °C (1.8 °F) in at least one of the circuits. Such a close

approach of refrigerant and air causes a profound convergence problem for a tube-by-tube model in which air temperatures upstream of each tube have to be iterated around a target value. Furthermore, for evaluating the potential reduction in heat exchanger volume, only capacity predictions at test 9 with 5.6 °C (10 °F) superheat were needed, and these were attainable with EVAP5.

Test 9 measured capacities for COIL-W and COIL-E were 4729 W (16146 Btu/h) and 4549 W (15522 Btu/h), while EVAP5 predictions were 4796 W (16366 Btu/h) and 5482 W (18705 Btu/h), respectively. This is a very good prediction for COIL-W, within 1.3 %, while the discrepancy for COIL-E is 20.5 %. It should be noted that a higher capacity should be expected for COIL-E than for COIL-W, as it was predicted by EVAPS and always was obtained from laboratory measurements except this time. It is possible that some condensate holdup might have influenced the measured capacity for COIL-E. With this, it was concluded that EVAP5 properly simulated coils in a cross-parallel flow set up. Consequently, COIL-W was applied in a later section to examine potential savings in evaporator core volume for the cross-parallel configuration.

4.4.2 Possible Savings in Heat Transfer Area Due to Optimized Superheat

4.4.2.1 Cross-CounterFlow Configuration with Uniform Air Flow Distribution

Considering similar performance degradations for different refrigerant superheat scenarios, possible savings in heat exchanger material are demonstrated using test 12 of COIL-W as an example. In our simulations, it was assumed that smart refrigerant distributors would optimize refrigerant distribution so the evaporator obtains maximum capacity. In these tests with a

uniform air velocity profile, the evaporators reached maximum capacity when the refrigerant split between the three circuits resulted in uniform superheat at the individual outlet tubes.

For these simulations, five alternative coils were coded with a smaller number of tubes than COIL-W. All simulation runs had the same inlet air condition, refrigerant inlet quality, and refrigerant outlet pressure and superheat at the evaporator exit. Also, inlet air velocity was the same for each coil as for COIL-W. A coil with a smaller face area had a lower volumetric flow rate than COIL-W, proportional to the percentage that its face area was reduced.

Figure 4.4.2.1.1 shows coil designs and simulation results. Four out of five alternative coil designs offered both savings in the heat exchanger core volume and an increase in coil capacity. The coils with a lower volumetric flow of air would also provide savings in fan power.

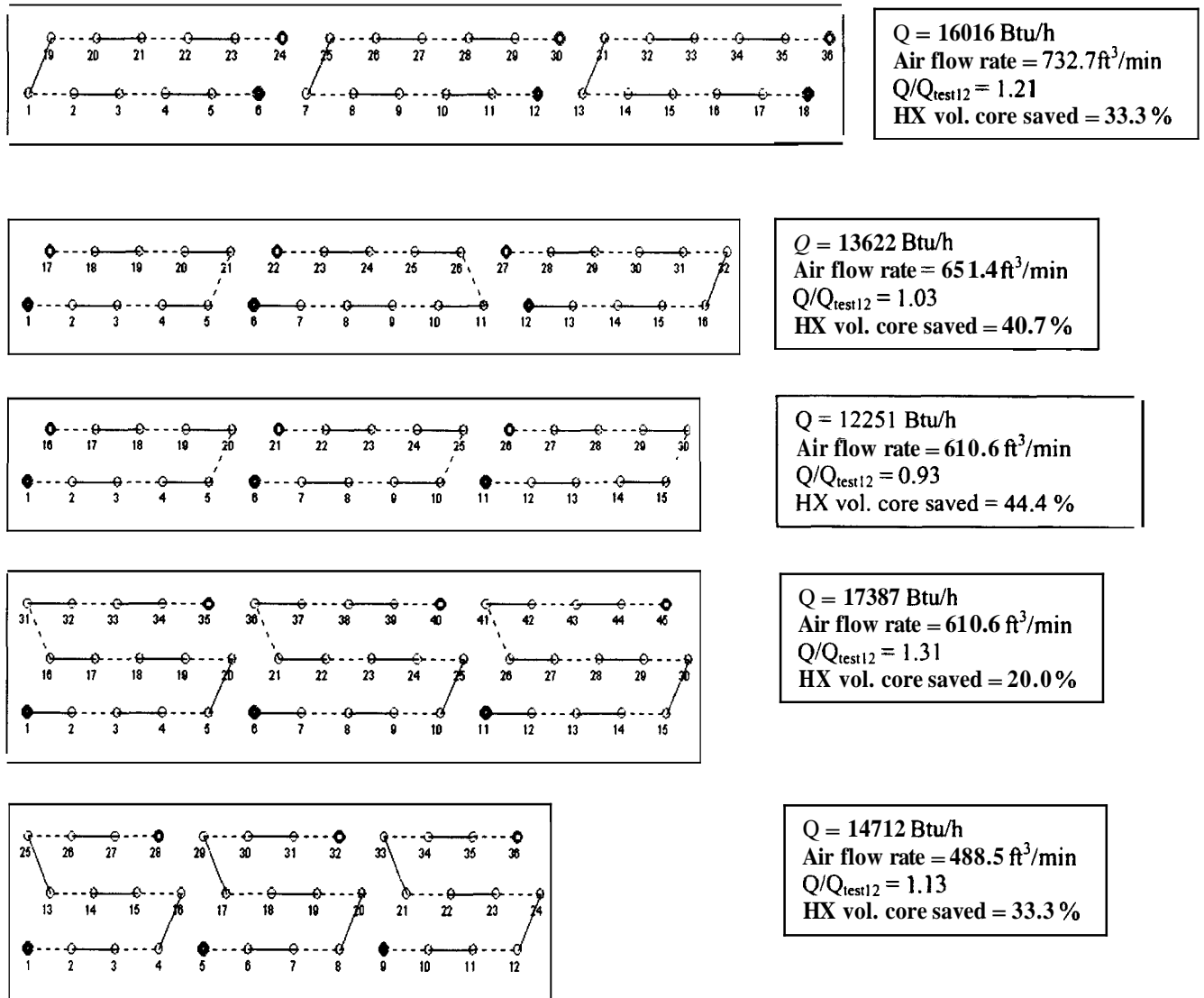


Figure 4.4.2.1.1 : Simulation results for alternative coil designs to COIL-W in cross-counter flow configuration. Performance is compared to COIL-W test 12 with simulated capacity of 13225 Btu/h.

4.4.2.2 Cross-Parallel Flow Configuration with Uniform Air Flow Distribution

Simulations were also performed to demonstrate possible savings in coil material (core volume of the heat exchanger) for COIL-W in cross-parallel configuration. Test 9 (W020304a) was used as a reference. Alternative coil designs with two depth rows were only examined because, in the cross-parallel configuration, more depth rows are not beneficial due to pinching.

All simulations were run using test 9 operating conditions, including **6 °C (10.8 °F)** superheat, with the difference that the volumetric flow of air was adjusted *so* that each coil had the same inlet air velocity as COIL-W. This means that a coil with a smaller face area had a lower volumetric flow rate than COIL-W by the same percentage its face area was reduced.

Figure 4.4.2.2.1 shows coil designs and simulation results. Each of the four presented two-depth row designs offered improved capacity and savings in coil core volume. The coils with a lower volumetric flow of air would also provide savings in fan power. The smallest coil with 12x2 tube arrangement matched the capacity **of** test 12 with a 33.3% savings in coil material.

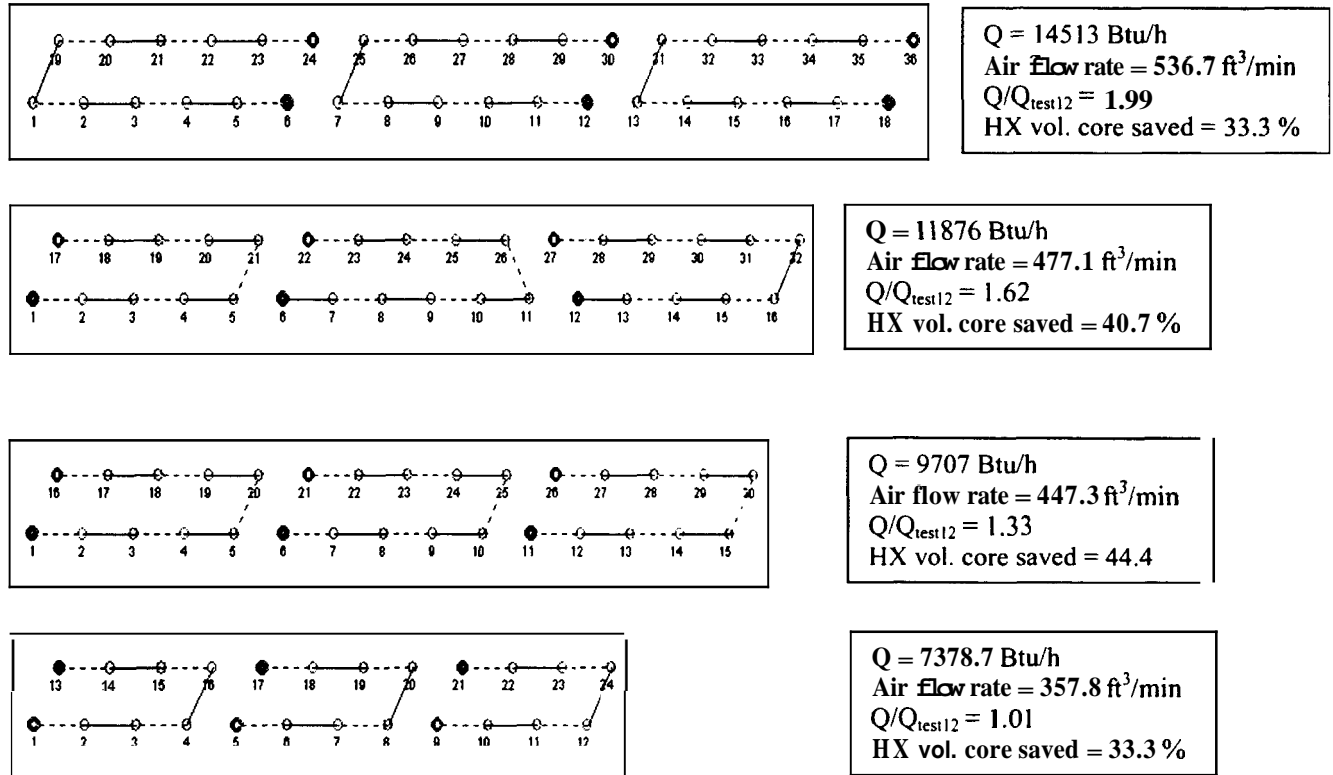


Figure 4.4.2.2.1 : Simulation results for alternative coil designs to COIL-W in cross-parallel configuration. Comparisons are to COIL-W, test 12 with tested capacity of 7311 Btu/h.

4.4.2.3 Cross-Counter Flow Arrangement with Non-Uniform Air Flow Distribution

The tests performed in the lab with non-uniform air distributions resulted in complicated velocity profiles that currently cannot be reproduced in EVAP5 simulations. For this reason, the simulations were performed with one-dimensional, non-uniform velocity profiles that were independent of the tests performed in the lab and represented a different application case scenario. For these simulations, COIL-W test 9 with a uniform air distribution was selected as a reference test, and additional simulations were performed for two-step velocity profiles where the top (left) to bottom (right) velocity ratios were 1:1.5, 1:2.0, 1:2.5, 1:3, 1:3.5, and 1:4.

Two runs were performed for each velocity ratio: the first - with a uniform refrigerant distribution, and the second - with a refrigerant distribution optimized to obtain maximum capacity. During all these tests, the external run parameters (refrigerant inlet state, exit pressure and superheat, air flow rate, etc.) were the same. Figure 4.4.2.3.1 presents a velocity profile representation for the 1:3 ratio as it was input into EVAP-COND. Since our velocity profiles have a near step change, they represent a more radical departure from uniformity than the profiles obtained in the laboratory.

Table 4.4.2.3.1 summarizes simulation results, and Figure 4.4.2.3.2 presents simulated capacities as referenced to the capacity of test 9. The table and figure show that the capacity degrades linearly with degradation of the air velocity. For the 1:4 air velocity ratio and uniform refrigerant distribution, the obtained capacity was only 63 % of the reference test 9 value. However, with optimized refrigerant distribution, as is the purpose of smart distributors, the obtained capacity was within 7 % of the reference capacity.

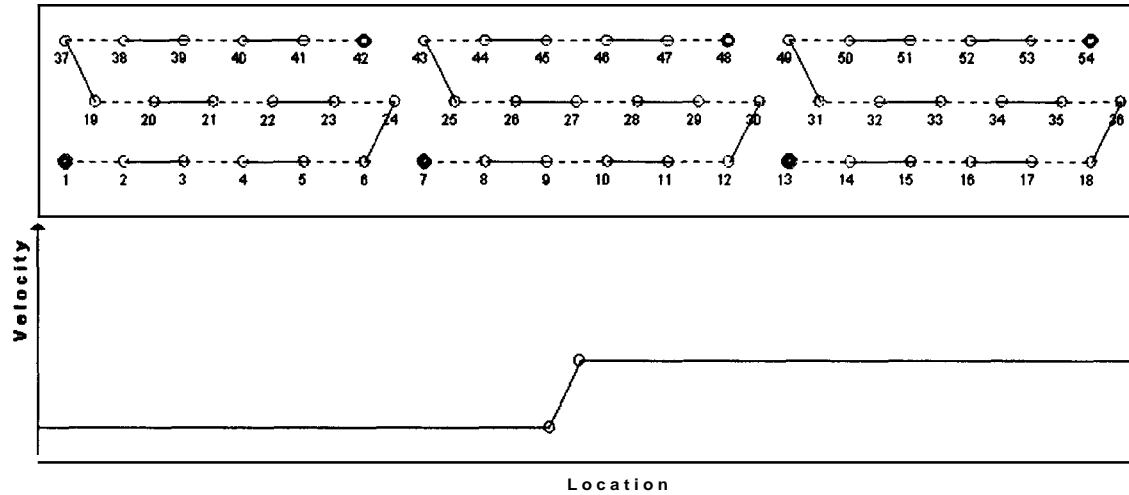


Figure 4.4.2.3.1: Air velocity profile representation for the 1:3 top-to-bottom velocity ratio (during tests the coil was positioned vertically, turned clockwise by 90 °)

Table 4.4.2.3.1: Simulated Capacities and Refrigerant Distributions for Non-Uniform Inlet Air Velocity Profile

Air velocity ratio (top to bottom)		1 : 1	1 : 1.5	1 : 2	1 : 2.5	1 : 3	1 : 3.5	1 : 4
Capacity (watt)	Uniform ref. distribution	7044	6748	6194	5710	5199	4886	4465
	Optimized ref. distribution	7044	7001	6914	6849	6762	6662	6582
Capacity (Btu/h)	Uniform ref. distribution	22127	21197	19456	17935	16331	15347	14024
	Optimized ref. distribution	22127	21997	21718	21515	21240	20928	20675
Optimized refig. distribution (fraction)	top (left) circuit	0.33	0.295	0.265	0.240	0.222	0.210	0.195
	middle circuit	0.33	0.333	0.340	0.340	0.342	0.345	0.350
	bottom (right) circuit	0.33	0.372	0.395	0.420	0.436	0.445	0.455

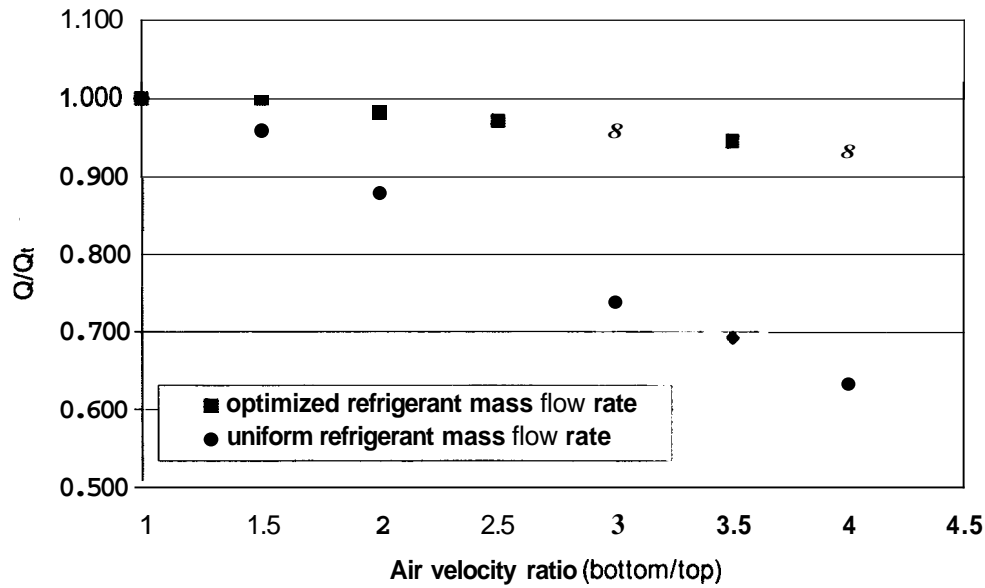
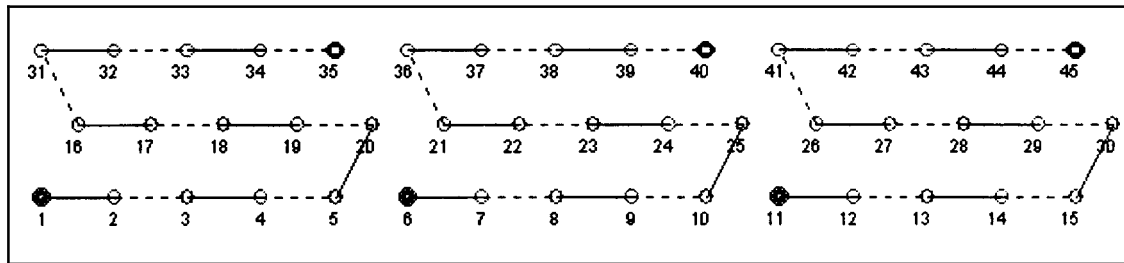
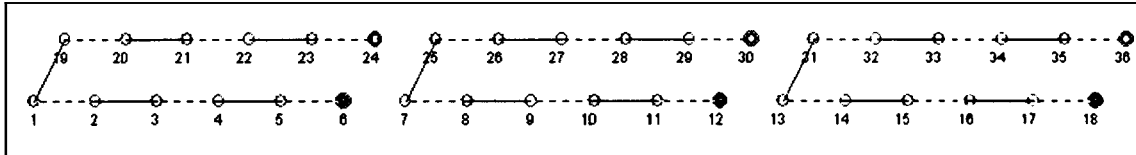


Figure 4.4.2.3.2: **COIL-W** capacities at different air velocity ratios referenced to capacity at test 9 in cross-counter flow configuration

To assess the savings in the heat exchanger material due to optimized control of refrigerant superheat, two evaporators with reduced number of tubes were coded, shown in Figure 4.4.2.3.3, and simulations were performed for 1:2.5 and 1:4 air velocity profiles. The two-depth row evaporator had the same face area as **COIL-W** and was simulated with the same volumetric flow rate of air. For the three-depth-row, the volumetric flow rate was reduced by 16.7 %, which corresponds to the reduction of the coil face area in relation to that of **COIL-W**. The results presented in Table 4.3.3.1.1 show that the benefit of optimizing refrigerant distribution increases with the level of non-uniformity in the air velocity profile. For the 1:4 air velocity ratio, optimizing refrigerant distribution allows a reduction in coil volume of 33.3 %. For the 1:2.5 air velocity ratio, the use of 15x3 coil with a slightly increased volumetric flow rate could produce a 16.7% reduction in the coil volume.



Coil 15x3



Coil 18x2

Figure 4.4.2.3.3: Two evaporators with a reduced number of tubes

Table 4.4.2.3.2: Savings in Coil Volume Relative to COIL-W due to Optimized Refrigerant for 1:2.5 and 1:4 Air Velocity Ratios

Coil	Refrigerant distribution	Air velocity ratio (top to bottom)	Air volumetric flow rate m^3/min	Capacity watt	Air volumetric flow rate ft^3/min	Capacity Btu/h	Savings in coil volume %
COIL-W	uniform	1 : 1	20.7	6485	733	22127	0
COIL-W	optimized	1 : 2.5	20.7	6305	733	21515	0
COIL-W	uniform	1 : 2.5	20.7	5256	733	17935	0
18x2	optimized	1 : 2.5	20.7	4558	733	15553	33.3
15x3	optimized	1 : 2.5	17.3	4890	611	16685	16.7
COIL-W	uniform	1 : 1	20.7	6485	733	22127	0
COIL-W	outimized	1 : 4	20.7	6059	733	20675	0
COIL-W	uniform	1 : 4	20.7	4110	733	13024	0
18x2	optimized	1 : 4	20.7	4335	733	14790	33.3
15x3	optimized	1 : 4	17.3	4474	611	15266	16.7

5 CONCLUSIONS

This collection of experimental data for the three evaporators has revealed interesting results related to non-uniform refrigerant distribution and conduction between tubes through the fins. With cross-counter refrigerant flow, uniform airflow, and exit manifold superheat fixed at 5.6 °C (10.0 °F), the wavy fin and wavy-lanced fin evaporator's capacity dropped by as much as 41 % and 32 %, respectively, as the superheat was allowed to vary between the circuits. Control of superheat was shown to be even more important during cross-parallel refrigerant flow due to the rapid pinching of the refrigerant and air temperatures. For the wavy and lanced finned evaporators in cross-parallel flow, capacity dropped by 85 % and 78 % as superheat changed from 5.6 °C (10.0 °F) to 16.7 °C (30.0 °F).

As the coil's faces were blocked to produce a non-uniform airflow, control of superheat was shown to restore capacity if the volumetric flow of air was unchanged. The tests showed that when airflow rate was held constant, the losses in capacity due to non-uniform airflow could be recovered to within 2 % of the original uniform airflow capacity by controlling superheat. The more non-uniform the airflow over the coil, the greater was the benefit of controlling superheat. For the lanced fin coil, as the airflow ratio between the top half and lower half of the coil varied from 1:1.26 to 1:2.59, superheat control improved capacity by 1.4 % and 4.6 %, respectively.

In parallel with the experimental effort, the NIST evaporator model **EVAPS** was upgraded to control refrigerant distribution and account for tube-to-tube heat transfer. The model was validated with the experimental results and then used to determine the possible savings in

evaporator core volume if refrigerant distribution was controlled by a smart distributor. In extreme cases, the savings in core volume could be as much as 40 %.

A combination of results obtained from laboratory testing and simulations indicated the influence of tube-to-tube heat transfer on capacity degradation. The impact of tube-to-tube heat transfer was negligible in tests with a uniform 5.6 °C (10 °F) superheat, but it was significant in tests involving 16.7 °C (30 °F) superheat. Between two possible conduction mechanisms by which such heat transfer may occur, longitudinal fin conduction was chiefly responsible for degraded performance while longitudinal tube conduction had insignificant effect. The upgraded version of the **EVAPS** evaporator model, which accounts for tube-to-tube heat transfer based on tube temperatures, was able to predict key return bend temperatures that indicated the occurrence of tube-to-tube heat transfer. However, the study also confirmed that longitudinal heat conduction is affected by the fin design, air-side heat transfer coefficient, and moisture removal process. Consequently, a more detailed modeling scheme needs to be developed to capture other effects influencing tube-to-tube heat transfer. Such a study would not only improve the modeling of evaporators but also of condensers and of gas coolers, where internal heat transfer may be even more pronounced.

APPENDIX A. SUMMARY OF TEST RESULTS

A.1 Wavy fin evaporator in cross-counter flow

Table A.1.1: Wavy Fin Evaporators in Cross-Counter Flow

Test names	Test type
W020225B	5
W020228A	6
W020221A	7
W020225A	8
W020207B	9
W020530A	10
W020531A	11
W020215B	12
W020301A	13

SMART DISTRIBUTOR SUMMARY SHEET
 DATA FILENAME: W020225B.DAT SUMMARY FILENAME: W020225B.sum

Air-Side Conditions		Range	Total Air-Side Capacity: 18519.09	Range
Indoor Dry-Bulb :	79.951	0.32	Sensible Cap (Btu/h): 18521.16	356.27
Indoor Inlet Dew (F):	32.006	0.00	Latent Cap (Btu/h): -2.07	356.27
Indoor Exit Dry-Bulb:	57.653	0.20	EvapAir Delta T (F): 22.85	20.64
Indoor Exit Dew (F):	32.009	0.04	Air/Ref Cap Prct Diff: -3.32	0.43
			Sensible Heat Ratio: 1.000	2.05
Indoor Airflow (CFM):	~47.89	7.04	SCFM per Ton: ~82.95	0.0011
Indoor Airflow (SCFM):	~45.32	7.13	(0.075 lb/ft3 standard air)	
Evap Inlet Humidity Ratio (lbH2O/lbAir):			0.003864	
Evap Exit Humidity Ratio (lbH2O/lbAir):			0.003864	
Barometric Pressure (in *G):	29.24		Nozzle Temp (F): 62 ± 6	0 64
Air Chamber Nozzle Pressure Drop (in Water):	1.937	0.037		
Evaporator Coil Air Pressure Drop (in Water):	0.108	0.004		

Refrigerant Side Conditions				
Expansion Valve				
Upstream Pressure (psia):	270.55	0.731	Ref-side Cap (Btu/h):	17904.05
Upstream Temp A (F):	104.58	0.524	Ref-side Cap (tons):	1.49
Upstream Temp B (F):	105.01	0.524	Refrigerant Mdot (lbm/h):	261.38
Upstream Temp C (F):	104.38	0.437	Coriolis Density (lbm/ft3):	69.87
Upstream Average Temp (F):	104.66		Upstream R22 Tsat (F):	119.36
Upstream Subcooling A (F):	14.77	0.594		
Upstream Subcooling B (F):	14.35	0.594		
Upstream Subcooling C (F):	14.98	0.366		
Average Subcooling (F):	14.70			
Evap Exit Pressure (psia):	90.75	0.365	Turbine A Frequency (Hz):	166.38
Evap Exit Avg Temp A:	53.88	1.957	Turb A Vol Flow (ft3/min):	0.0236
Evap Exit Avg Temp B:	53.96	1.727	Turb A Density (lbm/ft3):	70.37
Evap Exit Avg Temp C:	53.99	1.682	Turb A Mass Flow (lb/h):	99.76
Circuit A Superheat (F):	8.42	2.113	Turbine C Frequency (Hz):	146.08
Circuit B Superheat (F):	8.49	1.690	Turb C Vol Flow (ft3/min):	0.0217
Circuit C Superheat (F):	8.53	1.769	Turb C Density (lbm/ft3):	70.40
Overall Superheat (F)	9.75	1.261	Turb C Mass Flow (lb/h):	91.77
			Turb C Calculated Mass Flow (lbm/h):	69.85
Evap Circuit Temp 1 (F):	49.45	1.205	% Total Mass Flow Thru A:	38.17
Evap Circuit Temp 2 (F):	51.08	0.511	% Total Mass Flow Thru B:	26.72
Evap Circuit Temp 3 (F):	48.42	0.372	% Total Mass Flow Thru C:	35.11
Evap Circuit Temp 4 (F):	49.44	1.719		
Evap Circuit Temp 5 (F):	48.47	0.651		
Evap Circuit Temp 6 (F):	51.05	0.557		
Evap Circuit Temp 7 (F):	53.16	1.110		
Evap Circuit Temp 8 (F):	48.39	0.651		
Evap Circuit Temp 9 (F):	49.89	0.092		

SMART DISTRIBUTOR SUMMARY SHEET
 DATA FILENAME: W020221A.DAT SUMMARY FILENAME: W020221A.sum

Air-Side Conditions		Range	Total Air-Side Capacity:	13341.33	Range
Indoor Dry-Bulb :	80.281	0.38	Sensible Cap (Btu/h):	13609.16	317.89
Indoor Inlet Dew (F):	41.520	0.18	Latent Cap (Btu/h):	-267.83	350.52
Indoor Exit Dry-Bulb:	63.768	0.33	EvapAir Delta T (F):	17.01	87.50
Indoor Exit Dew (F):	41.866	0.20	Air/Ref Cap Prcnt Diff:	-2.31	0.22
			Sensible Heat Ratio:	1.020	2.12
Indoor Airflow (CFM):	745.31	9.39	SCFM per Ton:	659.53	0.0065
Indoor Airflow (SCFM):	733.26	9.44	(0.075 lb/ft3 standard air)		
Evap Inlet Humidity Ratio (lbH2O/lbAir):			0.005642		
Evap Exit Humidity Ratio (lbH2O/lbAir):			0.005718		
Barometric Pressure (in HG):	29.24		Nozzle Temp (F):	67.12	0.55
Air Chamber Nozzle Pressure Drop (in Water):	1.899		0.048		
Evaporator Coil Air Pressure Drop (in Water):	0.109		0.006		

Refrigerant Side Conditions					
Expansion Valve					
Upstream Pressure (psia):	270.28	0.609	Ref-side Cap (Btu/h) :	13032.06	125.32
Upstream Temp A (F):	105.46	0.567	Ref-side Cap (tons):	1.09	0.01
Upstream Temp B (F):	107.16	0.610	Refrigerant Mdot (lbm/h):	190.89	1.98
Upstream Temp C (F):	104.32	0.524	Coriolis Density (lbm/ft3):	69.49	0.02
Upstream Average Temp (F):	105.65		Upstream R22 Tsat (F):	119.31	
Upstream Subcooling A (F):	13.84	0.463			
Upstream Subcooling B (F):	12.14	0.464			
Upstream Subcooling C (F):	14.99	0.464			
Average Subcooling (F):	13.66				
Evap Exit Pressure (psia):	89.70	0.730	Turbine A Frequency (Hz):	92.68	1.00
Evap Exit Avg Temp A:	74.78	0.538	Turb A Vol Flow (ft3/min):	0.0138	0.00
Evap Exit Avg Temp B:	47.39	0.558	Turb A Density (lbm/ft3):	70.23	0.09
Evap Exit Avg Temp C:	73.54	0.494	Turb A Mass Flow (lb/h):	58.27	0.63
Circuit A Superheat (F):	30.15	0.854	Turbine C Frequency (Hz):	61.94	1.00
Circuit B Superheat (F):	2.75	0.712	Turb C Vol Flow (ft3/min):	0.0105	0.00
Circuit C Superheat (F):	28.90	0.811	Turb C Density (lbm/ft3):	70.41	0.08
Overall Superheat (F):	11.57	3.499	Turb C Mass Flow (lb/h):	44.35	0.61
			Calculated Mass Flow (lbm/h):	88.27	1.99
Circuit Temp 1 (F):	74.72	0.628	% Total Mass Flow Thru A:	30.53	0.49
Circuit Temp 2 (F):	74.11	0.360	% Total Mass Flow Thru B:	46.24	0.74
Circuit Temp 3 (F):	47.66	0.326	% Total Mass Flow Thru C:	23.23	0.48
Circuit Temp 4 (F):	48.33	0.651			
Circuit Temp 5 (F):	48.79	0.279			
Circuit Temp 6 (F):	53.26	0.322			
Circuit Temp 7 (F):	76.88	0.496			
Circuit Temp 8 (F):	74.72	0.541			
Circuit Temp 9 (F):	50.20	0.650			

SMART DISTRIBUTOR SUMMARY SHEET
 DATA FILENAME: W020225A.DAT SUMMARY FILENAME: W020225A.sum

Air-Side Conditions		Range	Total Air-Side Capacity: 13266.99	Range
Indoor Dry-Bulb	: 79.866	0.32	Sensible Cap (Btu/h): 13267.21	209.99
Indoor Wet-Dew	: 32.006	0.00	Latent Cap (Btu/h): -0.22	209.99
Indoor Exit Dry-Bulb	: 64.004	0.19	EvapAir Delta T (F): 16.53	0.00
Indoor Exit Dew	: 32.006	0.00	Air/Ref Cap Prcnt Diff: -4.70	0.22
			Sensible Heat Ratio: 1.000	1.54
			SCFM per Ton: 667.44	0.0000
Indoor Airflow (CFM):	749.54	7.42		
Indoor Airflow (SCFM):	737.91	7.29	(0.075 lb/ft3 standard air)	
Evap Inlet Humidity Ratio (lbH2O/lbAir):		0.003864		
Evap Exit Humidity Ratio (lbH2O/lbAir):		0.003864		
Barometric Pressure (in HG):	29.24	Nozzle Temp (F): 67.29	0.22	
Air Chamber Nozzle Pressure Drop (in Water):	1.922	0.038		
Evaporator Coil Air Pressure Drop (in Water):	0.108	0.004		

Refrigerant Side Conditions				
Expansion Valve				
Upstream Pressure (psia):	268.55	0.974	Ref-side Cap (Btu/h):	12603.95
Upstream Temp A (F):	104.91	0.438	Ref-side Cap (tons):	1.05
Upstream Temp B (F):	103.59	0.963	Refrigerant Mdot (lbm/h):	184.34
Upstream Temp C (F):	103.95	0.611	Coriolis Density (lbm/ft3):	69.78
Upstream Average Temp (F):	104.15		Upstream R22 Tsat (F):	118.82
Upstream Subcooling A (F):	13.91	0.480		
Upstream Subcooling B (F):	15.23	0.718		
Upstream Subcooling C (F):	14.87	0.751		
Average Subcooling (F):	14.67			
Evap Exit Pressure (psia):	89.70	0.486	Turbine A Frequency (Hz):	156.47
Evap Exit Avg Temp A:	46.78	0.697	Turb A Vol Flow (ft3/min):	0.0236
Evap Exit Avg Temp B:	73.15	0.628	Turb A Density (lbm/ft3):	70.32
Evap Exit Avg Temp C:	74.87	0.516	Turb A Mass Flow (lb/h):	99.74
Circuit A Superheat (F):	2.15	0.756	Turbine C Frequency (Hz):	97.83
Circuit B Superheat (F):	28.52	0.563	Turb C Vol Flow (ft3/min):	0.0153
Circuit C Superheat (F):	30.24	0.586	Turb C Density (lbm/ft3):	70.46
Overall Superheat (F):	9.55	3.225	Turb C Mass Flow (lb/h):	64.64
			Turb C Mass Flow (lbm/h):	19.96
Evap Air Exit Temp 1 (F):	74.75	0.541	% Total Mass Flow Thru A:	54.11
Evap Air Exit Temp 2 (F):	50.67	0.548	% Total Mass Flow Thru B:	10.83
Evap Air Exit Temp 3 (F):	48.88	0.550	% Total Mass Flow Thru C:	35.06
Evap Air Exit Temp 4 (F):	73.84	0.542		
Evap Air Exit Temp 5 (F):	74.78	0.585		
Evap Air Exit Temp 6 (F):	52.67	0.178		
Evap Air Exit Temp 7 (F):	51.49	0.501		
Evap Air Exit Temp 8 (F):	73.03	0.720		
Evap Air Exit Temp 9 (F):	50.18	0.462		

DATA FILENAME: W020207B.DAT SUMMARY FILENAME: W020207B.sum

Air-Side Conditions			Range	Total Air-Side Capacity	22203.15	Range
Indoor Dry-Bulb		79.787	0.39	Sensible Cap (Btu/h)	16766.90	606.34
Indoor Inlet Dew (F)		59.265	0.20	Latent Cap (Btu/h)	5436.25	535.59
Indoor Exit Dry-Bulb		59.520	0.24	Evap/Air Delta T (F)	20.80	242.97
Indoor Exit Dew (F)		55.107	0.15	Air/Ref Cap Prcnt Diff	-1.92	0.44
				Sensible Heat Ratio	0.755	2.93
Indoor Airflow (CFM)		740.40	8.24	SCFM per Ton	395.99	0.01≥9
Indoor Airflow (SCFM)		732.68	8.26	(0.075 lb/ft3 standard air)		
Evap Inlet Humidity Ratio (lbH2O/lbAir)				0.011004		
Evap Exit Humidity Ratio (lbH2O/lbAir)				0.009449		
Barometric Pressure (in HG)		29.24		Nozzle Temp (F)	64.00	0.13
Air Chamber Nozzle Pressure Drop (in Water)				1.885	0.042	
Evaporator Coil Air Pressure Drop (in Water)				0.148	0.008	

Refrigerant Side Conditions						
Expansion Valve						
Upstream Pressure (psia)		274.00	0.731	Ref-side Cap (Btu/h)	2175.54	176.49
Upstream Temp A (F)		105.16	0.866	Ref-side Cap (tons)	1.81	0.01
Upstream Temp B (F)		105.48	0.737	Rp≤rigerant Mdot (lbm/h)	317.95	2.64
Upstream Temp C (F)		104.86	0.910	Coriolis Density (lbm/ft3)	69.81	0.18
Upstream Average Temp (F)		105.16		Upstream R22 Tsat (F)	120.32	
Upstream Subcooling A (F)		15.16	0.796			
Upstream Subcooling B (F)		14.84	0.681			
Upstream Subcooling C (F)		15.46	0.841			
Average Subcooling (F)		15.16				
Evap Exit Pressure (psia)		91.35	0.851	Turbine A Frequency (Hz)	206.85	3.00
Evap Exit Avg Temp A		56.12	2.488	Turb A Vol Flow (ft3/min)	0.0290	0.00
Evap Exit Avg Temp B		56.16	2.094	Turb A Density (lbm/ft3)	70.28	0.13
Evap Exit Avg Temp C		55.82	1.778	Turb A Mass Flow (lb/h)	122.32	1.73
Circuit A Superheat (F)		10.09	2.644	Turbine C Frequency (Hz)	177.75	2.00
Circuit B Superheat (F)		10.14	2.250	Turb C Vol Flow (ft3/min)	0.0260	0.00
Circuit C Superheat (F)		9.80	1.778	Turb C Density (lbm/ft3)	70.32	0.14
Overall Superheat (F)		11.37	1.246	Turb C Mass Flow (lb/h)	109.50	1.18
				Calculated Mass Flow (lbm/h)	86.12	3.08
Circuit Temp 1 (F)		50.39	2.217	% Total Mass Flow Thru A	38.47	0.68
Circuit Temp 2 (F)		49.07	0.650	% Total Mass Flow Thru B	27.09	0.85
Circuit Temp 3 (F)		49.85	0.848	% Total Mass Flow Thru C	34.44	0.51
Circuit Temp 4 (F)		50.84	2.413			
Circuit Temp 5 (F)		48.03	0.707			
Circuit Temp 6 (F)		51.13	0.675			
Circuit Temp 7 (F)		53.55	2.470			
Circuit Temp 8 (F)		48.13	0.656			
Circuit Temp 9 (F)		50.11	0.739			

SMART DISTRIBUTOR SUMMARY SHEET
 DATA FILENAME: W020530A.dat SUMMARY FILENAME: W020530A.sum

Air-Side Conditions		Range			Range
Indoor Dry-Bulb (F)	80.025	0.40	Total Air-Side Capacity	12700.80	282.03
Indoor Inlet Dew (F)	80.331	0.16	Sensible Cap (Btu/h)	11535.04	253.92
Indoor Exit Dry-Bulb (F)	80.020	0.33	Latent Cap (Btu/h)	1165.85	160.77
Indoor Exit Dew (F)	80.510	0.15	EvapAir Delta T (F)	14.37	0.22
			Air/Ref Cap Prcnt Diff	-2.54	3.42
			Sensible Heat Ratio	0.908	0.0115
Indoor Airflow (CFM)	745.80	8.24	SCFM per Tco	688.01	
Indoor Airflow (SCFM)	728.20	8.17	(0.075 lb/ft3 standard air)		
Evap Inlet Humidity Ratio (lbH2O/lbAir)			0.011439		
Evap Exit Humidity Ratio (lbH2O/lbAir)			0.011103		
Barometric Pressure (in HG)	29.24		Nozzle Temp (m)	66.69	0.09
Air Chamber Nozzle Pressure Drop (in Water)			0.720	0.016	
Evaporator Coil Air Pressure Drop (in Water)			0.132	0.006	

Refrigerant Side Conditions					
Expansion Valve					
Upstream Pressure (psia)	276.09	0.487	Ref-side Cap (Btu/h)	12378.19	406.76
Upstream Temp A (F)	104.83	0.252	Ref-side Cap (tons)	1.03	0.04
Upstream Temp B (F)	105.65	0.037	Refrigerant Mdot (lbm/h)	177.51	6.41
Upstream Temp C (F)	104.91	0.611	Coriolis Density (lbm/ft3)	82.69	0.12
Upstream Average Temp (F)	105.13		Upstream R22 Tsat (F)	120.41	
Upstream Subcooling A (F)	15.58	0.262			
Upstream Subcooling E (F)	14.76	0.087			
Upstream Subcooling C (F)	15.50	0.593			
Average Subcooling (F)	15.28				
Evap Exit Pressure (psia)	90.22	0.486	Turbine A Frequency (Hz)	109.56	1.00
Evap Exit Avg Temp A	73.82	0.628	Turb A Vol Flow (ft3/min)	0.0161	0.00
Evap Exit Avg Temp B	73.93	0.629	Turb A Density (lbm/ft3)	70.33	0.04
Evap Exit Avg Temp C	73.69	0.584	Turb A Mass Flow (lb/h)	67.82	0.60
Circuit A Superheat (F)	28.89	0.651	Turbine C Frequency (Hz)	101.78	1.00
Circuit B Superheat (F)	29.00	0.629	Turb C Vol Flow (ft3/min)	0.0158	0.00
Circuit C Superheat (F)	28.76	0.584	Turb C Density (lbm/ft3)	70.32	0.09
Overall Superheat (F)	29.29	0.740	Turb C Mass Flow (lb/h)	66.72	0.65
			Turb C Calculated Mass Flow (lbm/h)	42.96	6.97
Evap Circuit Temp 1 (F)	7322	0.630	% Total Mass Flow Thru A	38.21	1.70
Evap Circuit Temp 2 (F)	4803	0.326	% Total Mass Flow Thru B	24.20	3.07
Evap Circuit Temp 3 (F)	4738	0.373	% Total Mass Flow Thru C	37.59	1.42
Evap Circuit Temp 4 (F)	6786	0.910			
Evap Circuit Temp 5 (F)	6736	0.091			
Evap Circuit Temp 6 (F)	7419	0.812			
Evap Circuit Temp 7 (F)	4990	0.369			
Evap Circuit Temp 8 (F)	7237	0.633			
Evap Circuit Temp 9 (F)	7422	0.902			

SMART DISTRIBUTOR SUMMARY SHEET
 DATA FILENAME: W020531A.dat SUMMARY FILENAME: W020531A.sum

Air-Side Conditions		Range	Total Air-Side Capacity:	13090.69	Range
Indoor Dry-Bulb	80.047	0.23	Sensible Cap (Btu/h):	11502.99	728.87
Indoor Inlet Dew (F)	60.394	0.39	Latent Cap (Btu/h):	1587.70	467.38
Indoor Exit Dry-Bulb	65.142	0.72	EvapAir Delta T (F):	14.33	384.87
Indoor Exit Dew (F)	53.273	0.49	Air/Ref Cap Prcnt Diff:	-0.54	0.44
			Sensible Heat Ratio:	0.879	6.79
Indoor Airflow (CFM):	745.76	10.22	SCFM per Ton:	667.36	0.0228
Indoor Airflow (SCFM):	728.02	10.57	(0.075 lb/ft3 standard air		
Evap Inlet Humidity Ratio (lbH2O/lbAir):	0.011465				
Evap Exit Humidity Ratio (lbH2O/lbAir):	0.011008				
Barometric Pressure (in HG):	29.24	Nozzle Temp (F):	66.79	0	91
Air Chamber Nozzle Pressure Drop (in Water):	0.720		0.020		
Evaporator Coil Air Pressure Drop (in Water):	0.140		0.005		

Refrigerant Side Conditions					
Expansion Valve					
Upstream Pressure (psia):	277.55	2.557	Ref-side Cap (Btu/h):	13018.97	763.62
Upstream Temp A (F):	104.35	1.048	Ref-side Cap (tons):	1.08	0.06
Upstream Temp B (F):	105.59	1.048	R#refrigerant Mdot (lbm/h):	189.68	17.35
Upstream Temp C (F):	103.77	1.049	Coriolis Density (lbm/ft3):	82.54	0.44
Upstream Average Temp (F):	104.57		Upstream R22 Tsat (F):	120.83	
Upstream Subcooling A (F):	16.48	0.663			
Upstream Subcooling B (F):	15.23	0.579			
Upstream Subcooling C (F):	17.06	0.649			
Average Subcooling (F):	16.26				
Evap Exit Pressure (psia):	90.36	0.730	Turbine A Frequency (Hz):	95.85	2.00
Evap Exit Avg Temp A:	75.21	0.448	Turb A Vol Flow (ft3/min):	0.0143	0.00
Evap Exit Avg Temp B:	47.61	1.115	Turb A Density (lbm/ft3):	70.40	0.16
Evap Exit Avg Temp C:	72.59	0.540	Turb A Mass Flow (lb/h):	60.20	1.13
Circuit A Superheat (F):	30.07	0.505	Turbine C Frequency (Hz):	32.75	7.00
Circuit B Superheat (F):	2.46	0.880	Turb C Vol Flow (ft3/min):	0.0066	0.00
Circuit C Superheat (F):	27.44	0.776	Turb C Density (lbm/ft3):	70.49	0.16
Overall Superheat (F):	11.12	3.861	Turb C Mass Flow (lb/h):	27.93	3.93
			Turb C Calculated Mass Flow (lbm/h):	101.55	9.23
Evap Circuit Temp 1 (F):	70.50	0.588	% Total Mass Flow Thru A:	31.74	1.92
Evap Circuit Temp 2 (F):	47.59	0.653	% Total Mass Flow Thru B:	53.54	3.10
Evap Circuit Temp 3 (F):	47.19	0.606	% Total Mass Flow Thru C:	14.72	2.30
Evap Circuit Temp 4 (F):	67.21	0.637			
Evap Circuit Temp 5 (F):	66.65	0.638			
Evap Circuit Temp 6 (F):	74.16	0.718			
Evap Circuit Temp 7 (F):	49.54	1.115			
Evap Circuit Temp 8 (F):	69.63	0.318			
Evap Circuit Temp 9 (F):	75.05	0.811			

SMART DISTRIBUTOR SUMMARY SHEET
 DATA FILENAME: W020215B.DAT SUMMARY FILENAME: W020215B.sum

Air-Side Conditions		Range	Total Air-Side Capacity: 13066.57	Range
Indoor Dry-Bulb :	79.301	0.18	Sensible Cap (Btu/h): 11950.49	353.33
Indoor Inlet Dew (F) :	58.305	0.05	Latent Cap (Btu/h): 1116.08	217.05
Indoor Exit Dry-Bulb: 65.873	0.18	EvapAir Delta T (F): 14.83		136.28
Indoor Exit Dew (F) : 57.875	0.10	Air/Ref Cap Prcnt Diff: 0.46		0.22
		Sensible Heat Ratio: 0.915		3.04
		SCFM per Ton: 672.23		0.0081
Indoor Airflow (CFM): 748.84	4.67	(0.075 lb/ft3 standard air)		
Indoor Airflow (SCFM): 731.98	4.61	0.010704		
Evap Inlet Humidity Ratio (lbH2O/lbAir):		0.010384		
Evap Exit Humidity Ratio (lbH2O/lbAir):				
Barometric Pressure (in HG): 29.24	Nozzle Temp (F): 68.79	0.01		
Air Chamber Nozzle Pressure Drop (in Water): 1.905	0.024			
Evaporator Coil Air Pressure Drop (in Water): 0.132	0.004			

Refrigerant Side Conditions				
Expansion Valve				
Upstream Pressure (psia):	277.28	0.487	Ref-side Cap (Btu/h): 13125.68	92.23
Upstream Temp A (F):	108.74	0.522	Ref-Time Cap (Btu/h): 1.09	0.01
Upstream Temp B (F):	103.63	0.050	Refrigerant Mdot (lbm/h): 193.41	1.32
Upstream Temp C (F):	107.75	0.433	Coriolis Density (lbm/ft3): 69.17	0.04
Upstream Average Temp (F):	106.71		Upstream R22 Tsat (F): 121.29	
Upstream Subcooling A (F):	12.55	0.480		
Upstream Subcooling B (F):	17.66	0.050		
Upstream Subcooling C (F):	13.54	0.458		
Average Subcooling (F):	14.59			
Evap Exit Pressure (psia):	90.57	0.486	Turbine A Frequency (Hz): 139.51	1.00
Evap Exit Avg Temp A:	47.78	0.788	Turb A Vol Flow (ft3/min): 0.0230	0.00
Evap Exit Avg Temp B:	72.17	0.223	Turb A Density (lbm/ft3): 69.72	0.08
Evap Exit Avg Temp C:	73.81	0.539	Turb A Mass Flow (lb/h): 117.33	0.85
Circuit A Superheat (F):	2.55	0.945	Turbine C Frequency (Hz): 118.78	1.00
Circuit B Superheat (F):	26.94	0.393	Turb C Vol Flow (ft3/min): 0.0191	0.00
Circuit C Superheat (F):	28.58	0.649	Turb C Density (lbm/ft3): 69.88	0.07
Overall Superheat (F)	10.11	1.904	Turb C Mass Flow (lb/h): 75.82	0.83
			Turb C Calculated Mass Flow (lbm/h): 0.27	1.34
Evap Cir pit Temp 1 (F):	73.26	0.357	% Total Mass Flow Thru A:	0.83
Evap Cir pit Temp 2 (F):	49.12	0.324	% Total Mass Flow Thru B:	0.35
Evap Cir pit Temp 3 (F):	51.36	0.602	% Total Mass Flow Thru C:	0.09
Evap Cir pit Temp 4 (F):	72.64	0.085		
Evap Cir pit Temp 5 (F):	75.34	0.541		
Evap Cir pit Temp 6 (F):	52.93	0.745		
Evap Cir pit Temp 7 (F):	51.65	0.411		
Evap Cir pit Temp 8 (F):	72.31	0.360		
Evap Cir pit Temp 9 (F):	49.82	0.649		

SMART DISTRIBUTOR SUMMARY SHEET
 DATA FILENAME: W020301A.DAT SUMMARY FILENAME: W020301A.sum

Air-Side Conditions		Range
Indoor Dry-Bulb :	30.471	856.04
Indoor Inlet Dew (F) :	±0.264	726.72
Indoor Exit Dry-Bulb :	±1.646	451.86
Indoor Exit Dew (F) :	36.949	0.43
Indoor Airflow (CFM) :	940.48	3.44
Indoor Airflow (SCFM) :	926.34	0.0176
Evap Inlet Humidity Ratio (lbH2O/lbAir) :	0.011411	
Evap Exit Humidity Ratio (lbH2O/lbAir) :	0.010112	
Barometric Pressure (in HG) :	29.24	
Air Chamber Nozzle Pressure Drop (in Water) :	1.867	0.058
Evaporator Coil Air Pressure Drop (in Water) :	0.224	0.010

Refrigerant Side Conditions		
Expansion Valve		
Upstream Pressure (psia) :	317.57	335.91
Upstream Temp A (F) :	105.66	0.03
Upstream Temp B (F) :	105.98	4.95
Upstream Temp C (F) :	105.44	0.07
Upstream Average Temp (F) :	105.69	
Upstream Subcooling A (F) :	26.35	
Upstream Subcooling B (F) :	26.02	
Upstream Subcooling C (F) :	26.57	
Average Subcooling (F) :	26.31	
Evap Exit Pressure (psia) :	91.29	
Evap Exit Avg Temp A :	56.21	
Evap Exit Avg Temp B :	57.07	
Evap Exit Avg Temp C :	56.51	
Circuit A Superheat (F) :	10.00	
Circuit B Superheat (F) :	10.86	
Circuit C Superheat (F) :	10.30	
Overall Superheat (F) :	11.46	
Circuit B Calculated Mass Flow (lbm/h) :		
Circuit Temp 1 (F) :	51.28	2.00
Circuit Temp 2 (F) :	51.53	0.00
Circuit Temp 3 (F) :	51.21	0.03
Circuit Temp 4 (F) :	51.80	1.28
Circuit Temp 5 (F) :	49.78	1.00
Circuit Temp 6 (F) :	52.38	0.00
Circuit Temp 7 (F) :	53.55	0.60
Circuit Temp 8 (F) :	49.47	1.10
Circuit Temp 9 (F) :	51.32	0.53
Turbine A Frequency (Hz) :		
Turb A Vol Flow (ft3/min) :	0.0340	
Turb A Density (lbm/ft3) :	70.20	
Turb A Mass Flow (lb/h) :	143.13	
Turbine C Frequency (Hz) :	210.33	
Turb C Vol Flow (ft3/min) :	0.0303	
Turb C Density (lbm/ft3) :	70.24	
Turb C Mass Flow (lb/h) :	127.69	
% Total Mass Flow Thru A :	102.87	
% Total Mass Flow Thru B :	38.30	
% Total Mass Flow Thru C :	27.53	
	34.17	

A.2 Wavy fin evaporator in cross-parallel flow

Test names	Test type
W020304A	9
W020311B	10
W020306A	11
W020307A	12

SMART DISTRIBUTOR SUMMARY SHEET
 DATA FILENAME: W020304A.DAT SUMMARY FILENAME: W020304A.sim

Air-Side Conditions		Range	Total Air-Side Capacity	16146.00	Range
Indoor Dry-Bulb	: 30.044	0.31	Sensible Cap (Btu/h)	: 12113.40	333.86
Indoor Inlet Dew	(F): 80.110	0.20	Latent Cap (Btu/h)	: 4032.60	173.85
Indoor Exit Dry-Bulb	: 80.190	0.17	EvapAir Delta T (m)	: 20.50	165.48
Indoor Exit Dew	(F): 88.020	0.20	Air/Ref Cap Prnt Diff	: 3.44	0.00
			Sensible Heat Ratio	: 0.750	2.06
Indoor Airflow (CFM)	: 543.06	7.69	SCFM per Ton	: 393.87	0.0054
Indoor Airflow (SCFM)	: 536.68	7.65	(0.075 lb/ft3 standard air)		
Evap Inlet Humidity Ratio (lbH2O/lbAir)	: 0.011348				
Evap Exit Humidity Ratio (lbH2O/lbAir)	: 0.009773				
Barometric Pressure (in HG)	: 29.24	Nozzle Temp (F): 68.01	0.88		
Air Chamber Nozzle Pressure Drop (in Water)	: 0.628	0.018			
Evaporator Coil Air Pressure Drop (in Water)	: 0.088	0.004			

Refrigerant Side Conditions					
Expansion Valve					
Upstream Pressure (psia)	: 274.31	0.809	Ref-side Cap (Btu/h)	: 18700.38	88.35
Upstream Temp A (F)	: 105.86	0.323	Ref-side Cap (tons)	: 1.39	0.01
Upstream Temp B (F)	: 106.23	0.324	Refrigerant Mdot (lbm/h)	: 244.37	1.10
Upstream Temp C (F)	: 105.40	0.808	Coriolis Density (lbm/ft3)	: 69.85	0.03
Upstream Average Temp (F)	: 105.83		Upstream R22 Tsat (F)	: 120.39	
Upstream Subcooling A (F)	: 14.54	0.593			
Upstream Subcooling B (F)	: 14.16	0.662			
Upstream Subcooling C (F)	: 14.99	0.620			
Average Subcooling (F)	: 14.56				
Evap Exit Pressure (psia)	: 90.59	0.486	Turbine A Frequency (Hz)	: 186.94	1.00
Evap Exit Avg Temp A	: 54.68	0.365	Turb A Vol Flow (ft3/min)	: 0.0237	0.00
Evap Exit Avg Temp B	: 56.50	0.275	Turb A Density (lbm/ft3)	: 70.17	0.08
Evap Exit Avg Temp C	: 55.35	0.436	Turb A Mass Flow (lb/h)	: 99.79	0.66
Circuit A Superheat (F)	: 9.39	0.377	Turbine C Frequency (Hz)	: 133.10	2.00
Circuit B Superheat (F)	: 11.22	0.432	Turb C Vol Flow (ft3/min)	: 0.0200	0.00
Circuit C Superheat (F)	: 10.07	0.571	Turb C Density (lbm/ft3)	: 70.24	0.09
Overall Superheat (F)	: 10.84	0.786	Turb C Mass Flow (lb/h)	: 84.26	1.12
Circuit B Calculated Mass Flow (lbm/h):				60.82	1.15
Evap Circuit Temp 1 (F)	: 49.39	0.645	% Total Mass Flow Thru A	: 40.75	0.34
Evap Circuit Temp 2 (F)	: 48.82	0.089	% Total Mass Flow Thru B	: 24.84	0.40
Evap Circuit Temp 3 (F)	: 54.41	0.599	% Total Mass Flow Thru C	: 34.41	0.49
Evap Circuit Temp 4 (F)	: 48.25	0.089			
Evap Circuit Temp 5 (F)	: 48.30	0.369			
Evap Circuit Temp 6 (F)	: 57.70	0.173			
Evap Circuit Temp 7 (F)	: 55.01	0.407			
Evap Circuit Temp 8 (F)	: 48.80	0.368			
Evap Circuit Temp 9 (F)	: 56.44	0.365			

SMART DISTRIBUTOR SUMMARY SHEET
 DATA FILENAME: W020311B.DAT SUMMARY FILENAME: W020311B.sum

Air-Side Conditions		Range	Total Air-Side Capacity:	2461.30	Range
Indoor Dry-Bulb :	79.792	0.27	Sensible Cap (Btu/h):	3078.41	188.16
Indoor Inlet Dew (F) :	60.549	0.07	Latent Cap (Btu/h):	-617.11	135.79
Indoor Exit Dry-Bulb:	75.282	0.27	EvapAir Delta T (F):	5.20	149.23
Indoor Exit Dew (F) :	61.121	0.16	Air/Ref Cap Prcnt Diff:	11.08	0.22
			Sensible Heat Ratio:	1.251	9.87
			SCFM per Ton:	2617.04	0.0755
Indoor Airflow (CFM):	559.56	6.70	(0.075 lb/ft3 standard air)		
Indoor Airflow (SCFM):	536.78	6.58			
Evap Inlet Humidity Ratio (lbH2O/lbAir):			0.011529		
Evap Exit Humidity Ratio (lbH2O/lbAir):			0.011771		
Barometric Pressure (in HG):	29.24		Nozzle Temp (F):	75.49	0.58
Air Chamber Nozzle Pressure Drop (in Water):			1.077	0.026	
Evaporator Coil Air Pressure Drop (in Water):			0.070	0.003	

Refrigerant Side Conditions					
Expansion Valve					
Upstream Pressure (psia):	307.47	1.348	Ref-side Cap (Btu/h) :	2732.66	102.12
Upstream Temp A (F) :	105.67	0.378	Ref-side Cap (tons):	0.23	0.01
Upstream Temp B (F) :	106.10	0.379	Refrigerant Mdot (lbm/h):	39.31	1.54
Upstream Temp C (F) :	105.60	0.378	Coriolis Density (lbm/ft3):	68.20	0.04
Upstream Average Temp (F) :	105.79		Upstream R22 Tsat (F):	129.48	
Upstream Subcooling A (F) :	23.81	0.324			
Upstream Subcooling B (F) :	23.38	0.098			
Upstream Subcooling C (F) :	23.88	0.324			
Average Subcooling (F) :	23.69				
Evap Exit Pressure (psia):	89.60	1.946	Turbine A Frequency (Hz):	18.57	1.00
Evap Exit Avg Temp A:	74.28	0.313	Turb A Vol Flow (ft3/min):	0.0040	0.00
Evap Exit Avg Temp B:	74.05	0.691	Turb A Density (lbm/ft3):	70.20	0.14
Evap Exit Avg Temp C:	76.15	0.577	Turb A Mass Flow (lb/h):	16.74	0.59
Circuit A Superheat (F) :	29.88	0.906	Turbine C Frequency (Hz):	21.90	2.00
Circuit B Superheat (F) :	29.65	1.270	Turb C Vol Flow (ft3/min):	0.0052	0.00
Circuit C Superheat (F) :	31.74	0.888	Turb C Density (lbm/ft3):	70.21	0.14
Overall Superheat (F)	30.26	1.194	Turb C Mass Flow (lb/h):	21.72	1.11
			Circuit B Calculated Mass Flow (lbm/h):	0.84	1.85
Evap Circuit Temp 1 (F) :	48.64	1.586	% Total Mass Flow Thru A:	42.60	2.65
Evap Circuit Temp 2 (F) :	71.56	0.902	% Total Mass Flow Thru B:	2.14	4.69
Evap Circuit Temp 3 (F) :	73.85	0.629	% Total Mass Flow Thru C:	55.26	3.07
Evap Circuit Temp 4 (F) :	50.06	6.634			
Evap Circuit Temp 5 (F) :	70.52	1.360			
Evap Circuit Temp 6 (F) :	74.23	0.627			
Evap Circuit Temp 7 (F) :	55.80	5.294			
Evap Circuit Temp 8 (F) :	68.68	4.634			
Evap Circuit Temp 9 (F) :	76.45	0.401			

WARM DISTRIBUTION SUMMARY SHEET
 DATA FILENAME W02030 A.D.M SUMMARY MILENAME W020306A SUM

Indoor Conditions	Range	Total Air-Side Capacity	Range
Indoor Dry-Bulb : 80.396	0.30	Sensible Cap (Btu/h) : 3887.11	111.33
Indoor Inlet Dew (F) : 80.252	0.10	Latent Cap (Btu/h) : 1178.87	109.55
Indoor Exit Dry-Bulb : 88.001	0.20	EvapAir Delta T (F) : 13.03	0.00
Indoor Exit Dew (F) : 89.117	0.08	Air/Ref Cap Prcnt Diff : 4.83	23.08
		Sensible Heat Ratio : 0.867	0.012
Indoor Airflow (CFM) : 551.47	7.81	SCFM per Ton : 724.51	
Indoor Airflow (SCFM) : 536.57	7.63	(0.075 lb/ft3 standard air)	
Evap Inlet Humidity Ratio (lbH2O/lbAir) : 0.011406			
Evap Exit Humidity Ratio (lbH2O/lbAir) : 0.010945			
Barometric Pressure (in HG) : 29.24	Nozzle Temp (F) : 70.38	4.40	
Air Chamber Nozzle Pressure Drop (in Water) : 1.061	0.030		
Evaporator Coil Air Pressure Drop (in Water) : 0.081	0.003		

Refrigerant Side Conditions			
Expansion Valve			
Upstream Pressure (psia) : 273.97	0.974	Ref-side Cap (Btu/h) : 3316.15	2432.86
Upstream Temp A (F) : 103.36	0.524	Ref-side Cap (tons) : 0.78	0.20
Upstream Temp B (F) : 111.52	0.784	Refrigerant Mdot (lbm/h) : 136.90	35.63
Upstream Temp C (F) : 104.76	0.743	Coriolis Density (lbm/ft3) : 64.97	1.17
Upstream Average Temp (F) : 106.55		Upstream R22 Tsat (F) : 120.39	
Upstream Subcooling A (F) : 17.03	0.490		
Upstream Subcooling B (F) : 8.87	0.715		
Upstream Subcooling C (F) : 15.63	0.743		
Average Subcooling (F) : 13.84			
Evap Exit Pressure (psia) : 90.80	1.095	Turbine A Frequency (Hz) : 29.07	1.00
Evap Exit Avg Temp A : 70.24	0.406	Turb A Vol Flow (ft3/min) : 0.0054	0.00
Evap Exit Avg Temp B : 51.46	1.848	Turb A Density (lbm/ft3) : 70.55	0.08
Evap Exit Avg Temp C : 72.44	0.518	Turb A Mass Flow (lb/h) : 22.74	0.59
Circuit A Superheat (F) : 25.03	1.022	Turbine C Frequency (Hz) : 32.19	2.00
Circuit B Superheat (F) : 6.25	2.199	Turb C Vol Flow (ft3/min) : 0.0065	0.00
Circuit C Superheat (F) : 27.23	1.055	Turb C Density (lbm/ft3) : 70.34	0.11
Overall Superheat (F) : 11.74	1.251	Turb C Mass Flow (lb/h) : 27.55	1.13
		Turb C Calculated Mass Flow (lbm/h) : 86.61	36.19
Evap Circuit Temp 1 (F) : 48.56	0.647	% Total Mass Flow Thru A : 16.68	4.59
Evap Circuit Temp 2 (F) : 69.49	2.179	% Total Mass Flow Thru B : 63.12	10.51
Evap Circuit Temp 3 (F) : 69.92	0.816	% Total Mass Flow Thru C : 20.21	5.92
Evap Circuit Temp 4 (F) : 50.51	0.648		
Evap Circuit Temp 5 (F) : 49.61	0.648		
Evap Circuit Temp 6 (F) : 51.42	0.835		
Evap Circuit Temp 7 (F) : 54.68	1.661		
Evap Circuit Temp 8 (F) : 62.05	7.423		
Evap Circuit Temp 9 (F) : 72.71	0.587		

DATA FILENAME: W020307A.DAT SUMMARY FILENAME: W020307A.sum

Air-Side Conditions			Range
Indoor Dry-Bulb	73.931	0.27	200.11
Indoor Inlet Dew (F)	60.090	0.21	164.86
Indoor Exit Dry-Bulb	63.811	0.23	153.90
Indoor Exit Dew (F)	53.759	0.25	0.22
Indoor Airflow (CFM)	554.06	8.18	3.69
Indoor Airflow (SCFM)	538.18	7.84	0.0201
Evap Inlet Humidity Ratio (lbH2O/lbAir)	0.011339		
Evap Exit Humidity Ratio (lbH2O/lbAir)	0.011204		
Barometric Pressure (in HG)	29.24	Nozzle Temp (F)	69.52
Air Chamber Nozzle Pressure Drop (in Water)	1.069		0.63
Evaporator Coil Air Pressure Drop (in Water)	0.080		

Refrigerant Side Conditions			
Expansion Valve			
Upstream Pressure (psia)	265.64	1.461	8082.88
Upstream Temp A (F)	104.59	0.877	144.34
Upstream Temp B (F)	100.08	4.034	0.67
Upstream Temp C (F)	101.52	2.015	16.63
Upstream Average Temp (F)	102.06		69.77
Upstream Subcooling A (F)	13.40	0.680	17.98
Upstream Subcooling B (F)	17.91	4.176	
Upstream Subcooling C (F)	16.46	1.874	
Average Subcooling (F)	15.92		
Evap Exit Pressure (psia)	90.38	0.730	165.03
Evap Exit Avg Temp A	49.25	1.320	0.034
Evap Exit Avg Temp B	72.79	0.449	70.37
Evap Exit Avg Temp C	74.44	0.426	99.00
Circuit A Superheat (F)	4.24	1.554	27.73
Circuit B Superheat (F)	27.78	0.764	0.039
Circuit C Superheat (F)	29.44	1.030	70.83
Overall Superheat (F)	9.75	1.418	25.22
Circuit B Calculated Mass Flow (lbm/h)			
Evap Circuit Temp 1 (F)	50.37	1.848	-7.58
Evap Circuit Temp 2 (F)	49.31	0.934	84.88
Evap Circuit Temp 3 (F)	48.20	0.650	-6.50
Evap Circuit Temp 4 (F)	67.81	0.812	21.62
Evap Circuit Temp 5 (F)	72.33	0.997	
Evap Circuit Temp 6 (F)	69.41	0.644	
Evap Circuit Temp 7 (F)	54.67	0.932	
Evap Circuit Temp 8 (F)	71.66	1.896	
Evap Circuit Temp 9 (F)	74.97	0.629	

Turbine A Frequency (Hz)			
Turb A Vol Flow (ft3/min)			0.034
Turb A Density (lbm/ft3)			70.37
Turb A Mass Flow (lb/h)			99.00
Turbine C Frequency (Hz)			27.73
Turb C Vol Flow (ft3/min)			0.039
Turb C Density (lbm/ft3)			70.83
Turb C Mass Flow (lb/h)			25.22
% Total Mass Flow Thru A			-7.58
% Total Mass Flow Thru B			84.88
% Total Mass Flow Thru C			-6.50
			21.62
			0.82

A.3 Enhanced fin (wavy-lanced) evaporator in cross-counter flow

Table A.3.1: Enhanced Fin (Wavy Lanced) Evaporators in Cross-Counter Flow

	Test type
W020320B	1
W020321A	2
W020322A	5
W02032 1B	6
W020322C	7
W020322B	8
E020607A	9
W0203 18A	10
W0203 18B	11
W020319A	12
W020319B	13
W020320A	14

SMART DISTRIBUTOR SUMMARY SHEET
 DATA FILENAME: W020320B.DAT SUMMARY FILENAME: W020320B.sum

Air-Side Conditions		Range	Total Air-Side Capacity:	20463.67	Range
Indoor Dry-Bulb :		30.050	Sensible Cap (Btu/h):	13506.42	511.47
Indoor Inlet Dew (F):		≤0.805	Latent Cap (Btu/h):	6957.25	433.45
Indoor Exit Dry-Bulb:		39.937	EvapAir Delta T (F):	20.62	195.51
Indoor Exit Dew (F):		34.342	Air/Ref Cap Prcnt Diff:	-1.54	0.43
			Sensible Heat Ratio:	0.660	2.19
Indoor Airflow (CFM):		601.63	SCFM per Ton:	348.88	0.0094
Indoor Airflow (SCFM):		594.94	(0.075 lb/ft3 standard air)		
Evap Inlet Humidity Ratio (lbH2O/lbAir):		0.011637			
Evap Exit Humidity Ratio (lbH2O/lbAir):		0.009185			
Barometric Pressure (in HG):		29.24	Nozzle Temp (F):	63.00	0.55
Air Chamber Nozzle Pressure Drop (in Water):		1.282	0.034		
Evaporator Coil Air Pressure Drop (in Water):		0.166	0.005		
Refrigerant Side Conditions		-----			
Expansion Valve		-----			
Upstream Pressure (psia):		271.78	0.437	Ref-side Cap (Btu/h) :	20106.95
Upstream Temp A (F):		105.01	0.282	Ref-side Cap (tons) :	214.83
Upstream Temp B (F):		105.14	0.587	Refrigerant Mdot (lbm/h):	1.68
Upstream Temp C (F):		104.76	0.035	Coriolis Density (lbm/ft3):	293.36
Upstream Average Temp (F):		104.97	.	Upstream R22 Tsat (F):	70.21
Upstream Subcooling A (F):		14.68	0.332		119.69
Upstream Subcooling B (F):		14.55	0.567		
Upstream Subcooling C (F):		14.93	0.225		
Average Subcooling (F):		14.72	.		
Evap Exit Pressure (psia):		90.57	0.608	Turbine A Frequency (Hz):	185.79
Evap Exit Avg Temp A:		55.72	2.870	Turb A Vol Flow (ft3/min):	0.0262
Evap Exit Avg Temp B:		56.18	1.563	Turb A Density (lbm/ft3):	0.04
Evap Exit Avg Temp C:		56.55	2.066	Turb A Mass Flow (lb/h):	1.14
Circuit A Superheat (F):		10.27	2.635	Turbine C Frequency (Hz):	172.72
Circuit B Superheat (F):		10.74	1.563	Turb C Vol Flow (ft3/min):	0.0253
Circuit C Superheat (F):		11.11	2.222	Turb C Density (lbm/ft3):	0.01
Overall Superheat (F)		13.18	0.874	Turb C Mass Flow (lb/h):	106.70
		Circuit B Calculated Mass Flow (lbm/h):			
Circuit Temp 1 (F):		53.82	2.307	% Total Mass Flow Thru A:	76.11
Circuit Temp 2 (F):		49.80	0.324	% Total Mass Flow Thru B:	37.69
Circuit Temp 3 (F):		53.05	0.555	% Total Mass Flow Thru C:	25.94
Circuit Temp 4 (F):		51.74	1.946		36.37
Circuit Temp 5 (F):		51.98	0.647		
Circuit Temp 6 (F):		56.36	0.597		
Circuit Temp 7 (F):		53.80	2.217		
Circuit Temp 8 (F):		53.31	0.600		
Circuit Temp 9 (F):		54.18	0.277		

SMART DISTRIBUTOR SUMMARY SHEET
 DATA FILENAME: W020321A.DAT SUMMARY FILENAME: W020321A.sum

Air-Side Conditions		Range	Total Air-Side Capacity:	13737.21	Range
Indoor Dry-Bulb (F)	30.071	0.27	Sensible Cap (Btu/h)	10818.72	461.23
Indoor Wet-Dew (F)	30.627	0.10	Latent Cap (Btu/h)	2918.49	382.69
Indoor Exit Dry-Bulb (F)	34.222	0.16	EvapAir Delta T (F)	16.45	219.40
Indoor Exit Dew (F)	38.072	0.10	Air/Ref Cap Prnt Diff:	-3.58	0.43
			Sensible Heat Ratio:	0.788	4.38
			SCFM per Ton:	521.14	0.0118
Indoor Airflow (CFM)	608.69	11.13	(0.075 lb/ft3 standard air)		
Indoor Airflow (SCFM)	536.58	10.93			
Evap Inlet Humidity Ratio (lbH2O/lbAir)			0.011562		
Evap Exit Humidity Ratio (lbH2O/lbAir)			0.010536		
Barometric Pressure (in HG)	29.24		Nozzle Temp (F)	66.56	0.45
Air Chamber Nozzle Pressure Drop (in Water)			1.301	0.047	
Evaporator Coil Air Pressure Drop (in Water)			0.129	0.005	

Refrigerant Side Conditions					
Expansion Valve					
Upstream Pressure (psia)	270.29		0.365	Ref-side Cap (Btu/h)	13203.77
Upstream Temp A (F)	105.71		0.481	Ref-side Cap (tons)	227.41
Upstream Temp B (F)	105.90		0.610	Refrigerant Mdot (lbm/h)	0.02
Upstream Temp C (F)	105.54		0.619	Coriolis Density (lbm/ft3)	190.17
Upstream Average Temp (F)	105.72			Upstream R22 Tsat (F)	69.91
Upstream Subcooling A (F)	13.60		0.481		119.31
Upstream Subcooling B (F)	13.41		0.610		
Upstream Subcooling C (F)	13.76		0.619		
Average Subcooling (F)	13.59				
Evap Exit Pressure (psia)	90.41		0.486	Turbine A Frequency (Hz)	2.00
Evap Exit Avg Temp A (F)	74.48		0.470	Turb A Vol Flow (ft3/min)	0.00
Evap Exit Avg Temp B (F)	76.45		0.534	Turb A Density (lbm/ft3)	0.07
Evap Exit Avg Temp C (F)	75.17		0.398	Turb A Mass Flow (lb/h)	1.13
Circuit A Superheat (F)	29.43		0.623	Turbine C Frequency (Hz)	73.64
Circuit B Superheat (F)	31.40		0.710	Turb C Vol Flow (ft3/min)	1.00
Circuit C Superheat (F)	30.12		0.569	Turb C Density (lbm/ft3)	0.00
Overall Superheat (F)	30.67		0.768	Turb C Mass Flow (lb/h)	70.22
				Turb C Mass Flow (lbm/h)	0.66
				% Total Mass Flow Thru A	41.13
				% Total Mass Flow Thru B	38.73
				% Total Mass Flow Thru C	21.63
					39.65
Circuit B Calculated Mass Flow (lbm/h)					
Evap Circuit Temp 1 (F)	76.63		0.755		
Evap Circuit Temp 2 (F)	75.42		0.728		
Evap Circuit Temp 3 (F)	52.54		0.555		
Evap Circuit Temp 4 (F)	77.08		0.815		
Evap Circuit Temp 5 (F)	76.80		0.804		
Evap Circuit Temp 6 (F)	56.76		0.641		
Evap Circuit Temp 7 (F)	77.43		0.883		
Evap Circuit Temp 8 (F)	75.87		0.806		
Evap Circuit Temp 9 (F)	53.66		0.464		

SMART DISTRIBUTOR SUMMARY SHEET
DATA FILENAME: W020322A.DAT SUMMARY FILENAME: W020322A.sum

Air-Side Conditions		Range	Total Air-Side Capacity:	19115.01	412.43
Indoor Dry-Bulb :	80.098	0.37	Sensible Cap (Btu/h) :	19115.23	412.43
Indoor Wet-Dew (F) :	32.006	0.00	Latent Cap (Btu/h) :	-0.22	0.00
Indoor Exit Dry-Bulb:	57.457	0.22	EvapAir Delta T (F) :	23.19	0.22
Inroom Exit Dew (F) :	32.006	0.00	Air/Ref Cap Prnt Diff: -4.37	2.42	
			Sensible Heat Ratio: 1.000	0.0000	
Indoor Airflow (CFM) :	760.02	9.45	SCFM per Ton: 478.64		
Indoor Airflow (SCFM) :	757.65	9.55	(0.075 lb/ft3 standard air)		
Evap Inlet Humidity Ratio (lbH2O/lbAir) :			0.003864		
Evap Exit Humidity Ratio (lbH2O/lbAir) :			0.003864		
Barometric Pressure (in HG) :	29.24		Nozzle Temp (F) :	60.88	0.84
Air Chamber Nozzle Pressure Drop (in Water) :	1.276	0.032			
Evaporator Coil Air Pressure Drop (in Water) :	0.131	0.004			

Refrigerant Side Conditions					
Expansion Valve					
Upstream Pressure (psia) :	272.97	0.487	Ref-side Cap (Btu/h) :	18279.72	241.19
Upstream Temp A (F) :	105.01	0.524	Ref-side Cap (tons) :	1.52	0.02
Upstream Temp B (F) :	105.18	0.693	Refrigerant Mdot (lbm/h) :	266.22	3.19
Upstream Temp C (F) :	104.77	0.524	Coriolis Density (lbm/ft3) :	70.21	0.02
Upstream Average Temp (F) :	104.99		Upstream R22 Tsat (F) :	120.02	
Upstream Subcooling A (F) :	15.01	0.593			
Upstream Subcooling B (F) :	14.84	0.762			
Upstream Subcooling C (F) :	15.25	0.482			
Average Subcooling (F) :	15.03				
Evap Exit Pressure (psia) :	90.14	0.486	Turbine A Frequency (Hz) :	170.89	2.00
Evap Exit Avg Temp A :	55.43	2.086	Turb A Vol Flow (ft3/min) :	0.0242	0.00
Evap Exit Avg Temp B :	55.13	1.732	Turb A Density (lbm/ft3) :	70.30	0.08
Evap Exit Avg Temp C :	56.00	2.454	Turb A Mass Flow (lb/h) :	102.20	1.12
Circuit A Superheat (F) :	10.35	2.244	Turbine C Frequency (Hz) :	151.21	2.00
Circuit B Superheat (F) :	10.04	1.830	Turb C Vol Flow (ft3/min) :	0.0224	0.00
Circuit C Superheat (F) :	10.91	2.454	Turb C Density (lbm/ft3) :	70.34	0.08
Overall Superheat (F) :	13.38	1.086	Turb C Mass Flow (lb/h) :	94.58	1.21
			Circuit B Calculated Mass Flow (lbm/h) :	69.44	3.35
Evap Circuit Temp 1 (F) :	54.25	6.450	% Total Mass Flow Thru A :	38.39	0.58
Evap Circuit Temp 2 (F) :	49.21	0.847	% Total Mass Flow Thru B :	26.08	1.04
Evap Circuit Temp 3 (F) :	53.40	0.403	% Total Mass Flow Thru C :	35.53	0.61
Evap Circuit Temp 4 (F) :	51.86	1.191			
Evap Circuit Temp 5 (F) :	54.36	0.843			
Evap Circuit Temp 6 (F) :	56.74	0.596			
Evap Circuit Temp 7 (F) :	54.66	1.862			
Evap Circuit Temp 8 (F) :	53.21	0.899			
Evap Circuit Temp 9 (F) :	55.06	0.564			

SMART DISTRIBUTOR SUMMARY SHEET
 DATA FILENAME: W020321B.DAT SUMMARY FILENAME: W020321B.sum

Air-Side Conditions		Range	Total Air-Side Capacity	10076.52	192.51
Indoor Dry-Bulb	: 79.773	0.20	Ensemble Cap (Btu/h)	: 1018.79	198.01
Indoor Inlet Dew (F)	: 44.526	0.00	Latent p (Btu/h)	: -342.27	86.94
Indoor Exit Dry-Bulb	: 62.101	0.13	EvapAir lta T (w)	: 18.30	0.00
Indoor Exit Dew (F)	: 44.915	0.00	Air/Ref Cap rcnf Dief	: -7.09	1.73
Indoor Airflow (CFM)	: 11.16	10.07	Sensible heat Ratio	: 1.023	0.0001
Indoor Airflow (SCFM)	: 30.87	9.91	SCFM per Ton	: 613.93	
Evaporator Inlet Humidity Ratio (lbH2O/lbAir)	: 0.006339		10.075 lb/ft3 standard air		
Evaporator Exit Humidity Ratio (lbH2O/lbAir)	: 0.00435				
Evaporator Pressure (in HG)	: 29.24		Nozzle emp (m)	: 64 7z 0 30	
Air Chamber Nozzle Pressure Drop (in Water)	: 267	0.033			
Evaporator Coil Air Pressure Drop (in Water)	: 134	0.004			

Refrigerant Side Conditions					
Expansion Valve					
Upstream Pressure (psia)	: 209.73	0.48	Ref-side Cap (Btu/h)	: 13636.52	222.68
Upstream Temp A (F)	: 104.74	0.52	Ref-side Cap (tons)	: 1.14	0.02
Upstream Temp B (F)	: 104.93	0.08	Refrigerant Mdot (lbm/h)	: 195.05	2.97
Upstream Temp C (F)	: 104.60	0.50	Refrigerant Density (lbm/ft3)	: 70.16	0.05
Upstream Average Temp (F)	: 104.76		Upstream R22 Tsat (F)	: 119.14	
Upstream Subcooling A (F)	: 14.41	0.559			
Upstream Subcooling B (F)	: 14.21	0.262			
Upstream Subcooling C (F)	: 14.55	0.567			
Average Subcooling (F)	: 14.39				
Evaporator Exit Pressure (psia)	: 90.47	0.008	Turbine A Frequency (Hz)	: 124.95	2.00
Evaporator Exit Avg Temp A	: 73.99	0.359	Turb A Vol Flow (ft3/min)	: 0.0181	0.00
Evaporator Exit Avg Temp B	: 75.87	0.027	Turb A Density (lbm/ft3)	: 70.34	0.08
Evaporator Exit Avg Temp C	: 74.77	0.358	Turb A Mass Flow (lb/h)	: 76.48	1.14
Circuit A Superheat (F)	: 28.91	0.316	Turb C Mass Flow (lb/h)	: 120.20	1.00
Circuit B Superheat (F)	: 30.79	0.784	Turb C Vol Flow (ft3/min)	: 0.0183	0.00
Circuit C Superheat (F)	: 29.70	0.516	Turb C Density (lbm/ft3)	: 70.36	0.09
Overall Superheat (F)	: 30.09	0.593	Turb C Mass Flow (lb/h)	: 77.15	0.66
Circuit B Calculated Mass Flow (lbm/h)					
Evaporator Temp 1 (F)	: 76.17	0.357	Total Mass Flow Thru A	: 19.21	0.82
Evaporator Temp 2 (F)	: 73.24	0.632	Total Mass Flow Thru B	: 21.24	1.20
Evaporator Temp 3 (F)	: 52.92	0.647	Total Mass Flow Thru C	: 39.55	0.58
Evaporator Temp 4 (F)	: 76.36	0.855			
Evaporator Temp 5 (F)	: 76.62	0.629			
Evaporator Temp 6 (F)	: 56.40	0.642			
Evaporator Temp 7 (F)	: 76.98	0.540			
Evaporator Temp 8 (F)	: 74.18	0.316			
Evaporator Temp 9 (F)	: 54.92	1.755			

SMART DISTRIBUTOR SUMMARY SHEET

DATA FILENAME: W020322C.DAT SUMMARY FILENAME: W020322C.sum

Air-Side Conditions		Range	Total Air-Side Capacity:	1≤B≤7.24	19≤2.29
Indoor Dry-Bulb	: 30.050	0.28	Sensible Cap	1≤B≤7.46	19≤2.29
Indoor Inlet Dew (F)	: 32.00±	0.00	Latent Cap	-0.22	0.00
Indoor Exit Dry-Bulb	: ≤0.≤63	0.20	EvapAir Delta T (F)	19.96	2.15
Indoor Exit Dew (F)	: 32.00±	0.00	Air/Ref Cap Prcnt Diff:	-5.37	13.02
			Sensible Heat Ratio:	1.000	0.0000
Indoor Airflow (CFM)	: 760.98	12.30	SCFM per Ton:	552.7±	
Indoor Airflow (SCFM)	: 753.93	12.21	(0.075 lb/ft3 standard air)		
Evap Inlet Humidity Ratio (lbH2O/lbAir)	:		0.0038±4		
Evap Exit Humidity Ratio (lbH2O/lbAir)	:		0.0038±4		
Barometric Pressure (in HG)	: 29.24	Nozzle Temp (m):	63 59 0 55		
Air Chamber Nozzle Pressure Drop (in Water):	1.271	0.041			
Evaporator Coil Air Pressure Drop (in Water):	0.132	0.006			

Refrigerant Side Conditions					
Expansion Valve					
Upstream Pressure (psia):	278.74	2.923	Ref-side Cap (Btu/h) :	15478.92	222.72
Upstream Temp A (F):	106.91	0.127	Ref-side Cap (tons):	1.29	0.02
Upstream Temp B (F):	107.25	0.347	Refrigerant Mdot (lbm/h):	227.86	2.64
Upstream Temp C (F):	106.65	0.170	Coriolis Density (lbm/ft3):	69.87	0.06
Upstream Average Temp (F):	106.94	.	Upstream R22 Tsat (F):	121.70	
Upstream Subcooling A (F):	14.79	0.754			
Upstream Subcooling B (F):	14.46	0.754			
Upstream Subcooling C (F):	15.05	0.754			
Average Subcooling (F):	14.77				
Evap Exit Pressure (psia):	90.79	2.311	Turbine A Frequency (Hz):	127.38	2.00
Evap Exit Avg Temp A:	74.01	0.495	Turb A Vol Flow (ft3/min):	0.0184	0.00
Evap Exit Avg Temp B:	47.36	0.558	Turb A Density (lbm/ft3):	70.01	0.02
Evap Exit Avg Temp C:	74.32	0.539	Turb A Mass Flow (lb/h):	77.47	1.11
Circuit A Superheat (F):	28.59	1.481	Turbine C Frequency (Hz):	103.21	2.00
Circuit B Superheat (F):	1.94	1.531	Turb C Vol Flow (ft3/min):	0.0160	0.00
Circuit C Superheat (F):	28.90	1.872	Turb C Density (lbm/ft3):	70.05	0.03
Overall Superheat (F):	11.45	3.853	Turb C Mass Flow (lb/h):	67.27	1.11
Circuit B Calculated Mass Flow (lbm/h):					
8v4 Circuit Temp 1 (F):	76.62	6.583	% Total Mass Flow Thru A:	83.13	4.07
8v4 Circuit Temp 2 (F):	72.82	1.716	% Total Mass Flow Thru B:	34.00	0.85
8v4 Circuit Temp 3 (F):	53.43	0.135	% Total Mass Flow Thru C:	36.48	1.40
8v4 Circuit Temp 4 (F):	51.27	0.556		29.52	0.66
8v4 Circuit Temp 5 (F):	55.05	0.277			
8v4 Circuit Temp 6 (F):	57.46	2.941			
8v4 Circuit Temp 7 (F):	76.80	5.038			
8v4 Circuit Temp 8 (F):	77.12	1.167			
8v4 Circuit Temp 9 (F):	55.42	0.599			

SMART DISTRIBUTOR SUMMARY SHEET
 DATA FILENAME: W020322B.DAT SUMMARY FILENAME: W020322B.sum

Air-Side Conditions		Range	Moal Air-Side Capacity:	6037.21	244.39
Indoor Dry-Bulb :	79.955	0.2°	Sensible Cap (Btu/h):	6037.43	244.39
Indoor Inlet Dew (F):	32.006	0.0°	Latent Cap (Btu/h):	-0.22	0.00
Indoor Exit Dry-Bulb:	61.106	0.1°	EvapAir Delta T (F):	19.60	0.22
Indoor Exit Dew (F):	32.006	0.0°	Air/Ref Cap Prnt Diff:	-6.22	1.61
			Sensible Heat Ratio:	1.000	0.0000
Indoor Airflow (CFM):	760.08	6.71	SCFM per Ton:	562.90	
Indoor Airflow (SCFM):	752.40	6.84	(0.075 lb/ft3 standard air)		
Evap Inlet Humidity Ratio (lbH2O/lbAir):			0.003864		
Evap Exit Humidity Ratio (lbH2O/lbAir):			0.003864		
Barometric Pressure (in HG):	29.24		Nozzle Temp (F):	53.07	0.50
Air Chamber Nozzle Pressure Drop (in Water):	1.267		0.023		
Evaporator Coil Air Pressure Drop (in Water):	0.132		0.004		

Refrigerant Side Conditions					
Expansion Valve					
Upstream Pressure (psia):	276.86	0.244	Ref-side Cap (Btu/h):	15039.85	234.64
Upstream Temp A (F):	105.34	0.347	Ref-side Cap (tons):	1.25	0.02
Upstream Temp B (F):	105.23	0.524	Refrigerant Mdot (lbm/h):	219.73	3.08
Upstream Temp C (F):	105.11	0.085	Coriolis Density (lbm/ft3):	70.13	0.07
Upstream Average Temp (F):	105.23		Upstream R22 Tsat (F):	121.16	
Upstream Subcooling A (F):	15.82	0.347			
Upstream Subcooling B (F):	15.93	0.593			
Upstream Subcooling C (F):	16.05	0.154			
Average Subcooling (F):	15.93				
Evap Exit Pressure (psia):	91.03	0.365	Turbine A Frequency (Hz):	167.48	1.00
Evap Exit Avg Temp A:	47.22	0.486	Turb A Vol Flow (ft3/min):	0.0238	0.00
Evap Exit Avg Temp B:	74.24	0.357	Turb A Density (lbm/ft3):	70.25	0.05
Evap Exit Avg Temp C:	75.32	0.269	Turb A Mass Flow (lb/h):	100.21	0.63
Circuit A Superheat (F):	1.69	0.565	Turbine C Frequency (Hz):	122.48	1.00
Circuit B Superheat (F):	28.71	0.448	Turb C Vol Flow (ft3/min):	0.0186	0.00
Circuit C Superheat (F):	29.80	0.347	Turb C Density (lbm/ft3):	70.29	0.01
Overall Superheat (F):	10.93	3.666	Turb C Mass Flow (lb/h):	78.34	0.58
Circuit B Calculated Mass Flow (lbm/h):					
4V800 Circuit Temp 1 (F):	76.78	0.625	% Total Mass Flow Thru A:	41.18	3.77
4V800 Circuit Temp 2 (F):	49.73	0.603	% Total Mass Flow Thru B:	45.61	0.80
4V800 Circuit Temp 3 (F):	53.96	0.322	% Total Mass Flow Thru C:	18.74	1.49
4V800 Circuit Temp 4 (F):	75.62	0.584		35.65	0.69
4V800 Circuit Temp 5 (F):	76.51	0.357			
4V800 Circuit Temp 6 (F):	56.66	0.553			
4V800 Circuit Temp 7 (F):	54.14	0.598			
4V800 Circuit Temp 8 (F):	74.96	0.358			
4V800 Circuit Temp 9 (F):	55.71	0.643			

SMART DISTRIBUTOR SUMMARY SHEET
 DATA FILENAME: E020607A.dat SUMMARY FILENAME: E020607A.sum

Air-Side Conditions		Range	Total Air-Side Capacity	23732.88	Range
Indoor Dry-Bulb	79.851	0.39	Sensible Cap (Btu/h)	17252.27	459.67
Indoor Inlet Dew (F)	60.360	0.11	Latent Cap (Btu/h)	6480.61	350.17
Indoor Exit Dry-Bulb	59.725	0.19	EvapAir Delta T (F)	20.59	153.02
Indoor Exit Dew (F)	55.721	0.15	Air/Ref Cap Prcnt Diff	-0.48	0.22
			Sensible Heat Ratio	0.72	3.41
Indoor Airflow (CFM)	7±9.76	7.65	SCFM per Ton	384.7±	0.00±2
Indoor Airflow (SCFM)	7±0.95	7.53	(0.075 lb/ft3 standard air)		
Evap Inlet Humidity Ratio (lbH2O/lbAir)			0.011451		
Evap Exit Humidity Ratio (lbH2O/lbAir)			0.009666		
Barometric Pressure (in HG)	29.24	Nozzle Temp (m)	60 70 0 ±4		
Air Chamber Nozzle Pressure Drop (in Water)	0.77±	0.01±			
Evaporator Coil Air Pressure Drop (in Water)	0.34±	0.00±			

Refrigerant Side Conditions					
Expansion Valve					
Upstream Pressure (psia)	273.97	0.609	Ref-side Cap (Btu/h)	23619.08	522.63
Upstream Temp A (F)	105.06	0.610	Ref-side Cap (tons)	1.97	0.0±
Upstream Temp B (F)	105.52	0.262	Refrigerant Mdot (lbm/h)	344.39	7.73
Upstream Temp C (F)	105.08	0.524	Coriolis Density (lbm/ft3)	82.28	0.03
Upstream Average Temp (F)	105.22		Upstream R22 Tsat (F)	119.69	
Upstream Subcooling A (F)	14.63	0.644			
Upstream Subcooling B (F)	14.17	0.297			
Upstream Subcooling C (F)	14.62	0.524			
Average Subcooling (F)	14.47				
Evap Exit Pressure (psia)	90.83	0.486	Turbine A Frequency (Hz)	221.44	1.00
Evap Exit Avg Temp A	55.78	1.263	Turb A Vol Flow (ft3/min)	0.0309	0.00
Evap Exit Avg Temp B	55.97	1.747	Turb A Density (lbm/ft3)	70.29	0.09
Evap Exit Avg Temp C	55.76	2.343	Turb A Mass Flow (lb/h)	130.53	0.71
Circuit A Superheat (F)	10.04	1.419	Turbine C Frequency (Hz)	198.44	1.00
Circuit B Superheat (F)	10.23	1.668	Turb C Vol Flow (ft3/min)	0.0287	0.00
Circuit C Superheat (F)	10.02	2.656	Turb C Density (lbm/ft3)	70.29	0.08
Overall Superheat (F)	12.83	1.228	Turb C Mass Flow (lb/h)	121.09	0.59
Circuit B Calculated Mass mlow (lbm/h)					
92.76					8.08
37.90					0.93
26.93					1.81
35.16					0.93
Circuit A Superheat (F)					
49.92					
51.11					
50.37					
49.15					
49.04					
49.12					
53.23					
49.02					
49.96					

SMART DISTRIBUTOR SUMMARY SHEET
 DATA FILENAME: W020318A.DAT SUMMARY FILENAME: W020318A.sum

Air-Side Conditions		Range	Total Air-Side Capacity: 16598.91		Range
Indoor Dry-Bulb :	30.345	0.17	Sensible Cap (Btu/h):	13581.22	484.67
Indoor Wet Dew (F) :	30.173	0.15	Latent Cap (Btu/h):	3017.69	116.88
Indoor Exit Dry-Bulb :	34.613	0.26	Evap Air Delta T (F):	16.23	0.43
Indoor Exit Dew (F) :	38.083	0.15	Air/Ref Cap Prnt Diff:	-3.92	2.95
			Sensible Heat Ratio:	0.818	0.0084
Indoor Airflow (CFM):	775.54	7.57	SCFM per Ton:	548.99	
Indoor Airflow (SCFM):	759.38	7.39	(0.075 lb/ft3 standard air)		
Evap Inlet Humidity Ratio (lbH2O/lbAir):			0.011373		
Evap Exit Humidity Ratio (lbH2O/lbAir):			0.010540		
Barometric Pressure (in HG):	29.24		Nozzle Temp (F):	66.26	0 ≤4
Air Chamber Nozzle Pressure Drop (in Water):			2.106	0.041	
Evaporator Coil Air Pressure Drop (in Water):			0.212	0.008	

Refrigerant Side Conditions					
Expansion Valve					
Upstream Pressure (psia):	273.41	0.487	Ref-side Cap (Btu/h):	15947.48	236.80
Upstream Temp A (F):	105.24	0.262	Ref-side Cap (tons):	1.33	0.02
Upstream Temp B (F):	105.29	0.524	Refrigerant Mdot (lbm/h):	228.43	4.18
Upstream Temp C (F):	105.06	0.524	Coriolis Density (lbm/ft3):	70.18	0.06
Upstream Average Temp (F):	105.20		Upstream R22 Tsat (F):	120.13	
Upstream Subcooling A (F):	14.94	0.366			
Upstream Subcooling B (F):	14.90	0.663			
Upstream Subcooling C (F):	15.13	0.455			
Average Subcooling (F):	14.99				
Evap Exit Pressure (psia):	90.51	0.486	Turbine A Frequency (Hz):	137.33	2.00
Evap Exit Avg Temp A:	75.20	0.425	Turb A Vol Flow (ft3/min):	0.0198	0.00
Evap Exit Avg Temp B:	75.81	0.134	Turb A Density (lbm/ft3):	70.27	0.04
Evap Exit Avg Temp C:	74.79	0.404	Turb A Mass Flow (lb/h):	83.33	1.12
Circuit A Superheat (F):	29.99	0.582	Turbine C Frequency (Hz):	144.83	1.00
Circuit B Superheat (F):	30.61	0.427	Turb C Vol Flow (ft3/min):	0.0216	0.00
Circuit C Superheat (F):	29.59	0.449	Turb C Density (lbm/ft3):	70.29	0.08
Overall Superheat (F):	30.39	0.851	Turb C Mass Flow (lb/h):	90.93	0.61
Circuit B Calculated Mass Flow (lbm/h):			54.23	4.64	
Evap Circuit Temp 1 (F):	76.35	0.583	% Total Mass Flow Thru A:	36.47	0.89
Evap Circuit Temp 2 (F):	75.92	0.359	% Total Mass Flow Thru B:	23.73	1.60
Evap Circuit Temp 3 (F):	52.34	0.092	% Total Mass Flow Thru C:	39.80	0.79
Evap Circuit Temp 4 (F):	76.32	0.629			
Evap Circuit Temp 5 (F):	76.23	0.540			
Evap Circuit Temp 6 (F):	55.96	0.642			
Evap Circuit Temp 7 (F):	78.23	0.356			
Evap Circuit Temp 8 (F):	74.36	0.541			
Evap Circuit Temp 9 (F):	53.94	0.323			

SMAAM DISTRIBUTOR SUMMARY SHEET									
DATA FILENAME W020318B.SMT SUMMARY FILENAME W020318B SUM									
Air-Side Conditions		Range	Total Air-Side Capacity: 18714.97				Range		
Indoor Dry-Bulb : 30.289		0.34	Sensible Cap (Btu/h): 14556.00				277.25		
Indoor Inlet Dew (F): 30.077		0.10	Latent Cap (Btu/h): 4158.97				169.33		
Indoor Exit Dry-Bulb: 33.435		0.14	EvapAir Delta T (F): 17.40				0.22		
Indoor Exit Dew (F): 37.148		0.10	Air/Ref Cap Prct Diff: -1.67				2.30		
Indoor Airflow (CFM): 773.75		9.07	Sensible Heat Ratio: 0.778				0.0068		
Indoor Airflow (SCFM): 759.46		8.91	SCFM per Ton: 486.97						
Evap Inlet Humidity Ratio (lbH2O/lbAir):		0.011334	(0.075 lb/ft3 standard air)						
Evap Exit Humidity Ratio (lbH2O/lbAir):		0.010186							
Barometric Pressure (in HG): 29.24			Nozzle Temp (F): 65 Z0 0 60						
Air Chamber Nozzle Pressure Drop (in Water):		2.101	0.049						
Evaporator Coil Air Pressure Drop (in Water):		0.228	0.010						

Refrigerant Side Conditions									
Expansion Valve									
Upstream Pressure (psia):		269.16	0.731	Ref-side Cap (Btu/h) :		18401.73	293.95		
Upstream Temp A (F):		102.85	0.262	Ref-side Cap (tons):		1.53	0.02		
Upstream Temp B (F):		103.15	0.349	Refrigerant Mdot (lbm/h):		266.99	3.96		
Upstream Temp C (F):		102.69	0.611	Coriolis Density (lbm/ft3):		70.50	0.04		
Upstream Average Temp (F):		102.90		Upstream R22 Tsat (F):		118.95			
Upstream Subcooling A (F):		16.10	0.316						
Upstream Subcooling B (F):		15.80	0.011						
Upstream Subcooling C (F):		16.27	0.303						
Average Subcooling (F):		16.06							
Evap Exit Pressure (psia):		90.08	0.486	Turbine A Frequency (Hz):		138.54	1.00		
Evap Exit Avg Temp A:		75.05	0.538	Turb A Vol Flow (ft3/min):		0.0199	0.00		
Evap Exit Avg Temp B:		46.96	0.350	Turb A Density (lbm/ft3):		70.63	0.04		
Evap Exit Avg Temp C:		73.57	0.404	Turb A Mass Flow (lb/h):		84.44	0.61		
Circuit A Superheat (F):		29.94	0.695	Turbine C Frequency (Hz):		134.36	1.00		
Circuit B Superheat (F):		1.85	0.446	Turb C Vol Flow (ft3/min):		0.0202	0.00		
Circuit C Superheat (F):		28.47	0.562	Turb C Density (lbm/ft3):		70.66	0.09		
Overall Superheat (F)		8.08	3.255	Turb C Mass Flow (lb/h):		85.47	0.62		
				Circuit B Calculated Mass Flow (lbm/h):		97.07	4.53		
Evap Circuit Temp 1 (F):		76.37	0.540	% Total Mass Flow Thru A:		31.63	0.68		
Evap Circuit Temp 2 (F):		75.49	0.315	% Total Mass Flow Thru B:		36.36	1.16		
Evap Circuit Temp 3 (F):		51.99	0.370	% Total Mass Flow Thru C:		32.01	0.54		
Evap Circuit Temp 4 (F):		51.30	0.370						
Evap Circuit Temp 5 (F):		52.50	0.556						
Evap Circuit Temp 6 (F):		57.06	0.365						
Evap Circuit Temp 7 (F):		78.01	0.539						
Evap Circuit Temp 8 (F):		76.11	0.270						
Evap Circuit Temp 9 (F):		53.54	0.091						

SMART DISTRIBUTOR SUMMARY SHEET
 DATA FILENAME: W020319A.DAT SUMMARY FILENAME: W020319A.sum

Air-Side Conditions		Range	Total Air-Side Capacity	16157.00	574.90
Indoor Dry-Bulb	: 73.951	0.39	Sensible Cap (Btu/h)	: 13451.72	416.34
Indoor Inlet Dew (F)	: 80.169	0.10	Latent Cap (Btu/h)	: 2705.28	226.59
Indoor Exit Dry-Bulb	: 88.635	0.14	EvapAir Delta T (F)	: 16.00	0.43
Indoor Exit Dew (F)	: 83.311	0.15	Air/Ref Cap Prcnt Diff	: 0.54	3.90
			Sensible Heat Ratio	: 0.833	0.0112
Indoor Airflow (CFM)	: 779.33	6.30	SCFM per Ton	: 566.71	
Indoor Airflow (SCFM)	: 763.02	6.13	(0.075 lb/ft3 standard air)		
Evap Inlet Humidity Ratio (lbH2O/lbAir)	: 0.011372				
Evap Exit Humidity Ratio (lbH2O/lbAir)	: 0.010629				
Barometric Pressure (in HG)	: 29.24	Nozzle Temp (F)	: 66.13	0	72
Air Chamber Nozzle Pressure Drop (in Water)	: 2.126	0.034			
Evaporator Coil Air Pressure Drop (in Water)	: 0.212	0.005			

Refrigerant Side Conditions					
Expansion Valve					
Upstream Pressure (psia)	: 275.15	0.487	Ref-Side Cap (Btu/h)	: 10242.23	243.60
Upstream Temp A (F)	: 105.64	0.609	Res-side Ca (tons)	: 1.33	0.02
Upstream Temp B (F)	: 105.62	0.524	Refrigerant Mdot (lbm/h)	: 237.93	3.30
Upstream Temp C (F)	: 105.38	0.524	Coriolis Density (lbm/ft3)	: 70.08	0.13
Upstream Average Temp (F)	: 105.55		Upstr'am R22 Tsat (F)	: 120.63	
Upstream Subcooling A (F)	: 15.04	0.643			
Upstream Subcooling B (F)	: 15.06	0.559			
Upstream Subcooling C (F)	: 15.30	0.524			
Average Subcooling (F)	: 15.13				
Evap Exit Pressure (psia)	: 90.56	0.486	Turbine A Frequency (Hz)	: 137.48	2.00
Evap Exit Avg Temp A	: 47.14	0.630	Turb A Vol Flow (ft3/min)	: 0.0278	0.00
Evap Exit Avg Temp B	: 74.83	0.269	Turb A Density (lbm/ft3)	: 70.20	0.09
Evap Exit Avg Temp C	: 75.28	0.425	Turb A Mass Flow (lb/h)	: 116.95	1.22
Circuit A Superheat (F)	: 1.87	0.558	Turbine C Frequency (Hz)	: 143.52	1.00
Circuit B Superheat (F)	: 29.56	0.379	Turb C Vol Flow (ft3/min)	: 0.0214	0.00
Circuit C Superheat (F)	: 30.01	0.513	Turb C Density (lbm/ft3)	: 70.24	0.08
Overall Superheat (F)	: 9.96	3.499	Turb C Mass Flow (lb/h)	: 90.13	0.65
			Turb C Calculated Mass Flow (lbm/h)	: 30.91	3.74
Evap Circuit Temp 1 (F)	: 76.87	0.270	% Total Mass Flow Thru A	: 49.14	0.90
Evap Circuit Temp 2 (F)	: 50.12	0.467	% Total Mass Flow Thru B	: 12.99	1.40
Evap Circuit Temp 3 (F)	: 53.65	0.554	% Total Mass Flow Thru C	: 37.87	0.74
Evap Circuit Temp 4 (F)	: 76.40	0.540			
Evap Circuit Temp 5 (F)	: 77.30	0.827			
Evap Circuit Temp 6 (F)	: 56.01	0.597			
Evap Circuit Temp 7 (F)	: 53.01	0.843			
Evap Circuit Temp 8 (F)	: 75.59	0.672			
Evap Circuit Temp 9 (F)	: 53.97	0.555			

SMART DISTRIBUTOR SUMMARY SHEET
 DATA FILENAME: W020319B.dat SUMMARY FILENAME: W020319B.sum

Air-Side Conditions		Range	Total Air-Side Capacity: 26108.83	Range
Indoor Dry-Bulb :	79.699	0.49	Sensible Cap (Btu/h):	19517.33
Indoor Inlet Dew (F):	60.531	0.11	Latent Cap (Btu/h):	6591.50
Indoor Exit Dry-Bulb:	62.441	0.24	EvapAir Delta T (F):	17.87
Indoor Exit Dew (F):	56.993	0.20	Air/Ref Cap Prnt Diff:	-1.19
			Sensible Heat Ratio:	0.748
			SCFM per Ton:	455.73
Indoor Airflow (CFM):	1008.70	8.47	(0.075 lb/ft3 standard air)	
Indoor Airflow (SCFM):	991.62	8.25	0.011522	
Evap Inlet Humidity Ratio (lbH2O/lbAir):			0.010128	
Evap Exit Humidity Ratio (lbH2O/lbAir):			Nozzle Temp (F):	64.50
Barometric Pressure (in HG):	29.24		Pressure Drop (in Water):	1.321
Air Chamber Nozzle Pressure Drop (in Water):			0.022	
Evaporator Coil Air Pressure Drop (in Water):			0.381	0.012

Refrigerant Side Conditions				
Expansion Valve				
Upstream Pressure (psia):	273.73	0.731	Ref-side Cap (Btu/h):	25796.98
Upstream Temp A (F):	104.55	0.262	Ref-side Cap (tons):	2.15
Upstream Temp B (F):	104.78	0.525	R _p refrigerant Mdot (lbm/h):	375.15
Upstream Temp C (F):	104.42	0.567	Coriolis Density (lbm/ft3):	70.28
Upstream Average Temp (F):	104.58		Upstream R22 Tsat (F):	120.19
Upstream Subcooling A (F):	15.63	0.401		
Upstream Subcooling B (F):	15.41	0.594		
Upstream Subcooling C (F):	15.77	0.636		
Average Subcooling (F):	15.60			
Evap Exit Pressure (psia):	90.74	0.730	Turbine A Frequency (Hz):	240.70
Evap Exit Avg Temp A:	56.77	1.240	Turb A Vol Flow (ft3/min):	0.0335
Evap Exit Avg Temp B:	54.10	1.378	Turb A Density (lbm/ft3):	70.37
Evap Exit Avg Temp C:	55.63	1.793	Turb A Mass Flow (lb/h):	141.49
Circuit A Superheat (F):	9.87	1.396	Turbine C Frequency (Hz):	221.52
Circuit B Superheat (F):	10.20	1.534	Turb C Vol Flow (ft3/min):	0.0318
Circuit C Superheat (F):	9.73	1.811	Turb C Density (lbm/ft3):	70.39
Overall Superheat (F)	12.60	0.982	Turb C Mass Flow (lb/h):	134.28
Circuit B Calculated Mass Flow (lbm/h):				
Evap Circuit Temp 1 (F):	53.56	0.877	Total Mass Flow Thru A:	99.38
Evap Circuit Temp 2 (F):	50.68	0.557	Total Mass Flow Thru B:	37.71
Evap Circuit Temp 3 (F):	55.23	0.599	Total Mass Flow Thru C:	26.49
Evap Circuit Temp 4 (F):	53.06	0.601		35.79
Evap Circuit Temp 5 (F):	53.09	0.555		
Evap Circuit Temp 6 (F):	58.84	0.088		
Evap Circuit Temp 7 (F):	54.63	0.598		
Evap Circuit Temp 8 (F):	53.77	0.277		
Evap Circuit Temp 9 (F):	56.19	0.553		

SMART DISTRIBUTOR SUMMARY SHEET

DATA FILENAME: W020320A.DAT SUMMARY FILENAME: W020320A.SUM

Air-Side Conditions		Range	Total Air-Side Capacity: 18523.84	Range
Indoor Dry-Bulb :		79.855	Sensible Cap (Btu/h): 15744.03	650.3Z
Indoor Inlet Dew (F):		50.782	Latent Cap (Btu/h): 2779.82	836.7Z
Indoor Exit Dry-Bulb:		56.088	EvapAir Delta T (F): 14.38	656.3Z
Indoor Exit Dew (F):		59.354	Air/Ref Cap Prcnt Diff: -4.23	0.65
			Sensible Heat Ratio: 0.850	4.10
Indoor Airflow (CFM):		1017.56	SCFM per Ton: 643.26	0.034Z
Indoor Airflow (SCFM):		992.98	(0.075 lb/ft3 standard air)	
Evap Inlet Humidity Ratio (lbH2O/lbAir):		0.011628		
Evap Exit Humidity Ratio (lbH2O/lbAir):		0.011041		
Barometric Pressure In HG):		29.24	Nozzle Temp (F): 67.54	0.27
Air Chamber Nozzle Pressure Drop (in Water):		1.334	0.038	
Evaporator Coil Air Pressure Drop (in Water):		0.329	0.009	
Refrigerant Side Conditions				
Expansion Valve				
Upstream Pressure (psia):		271.74	0.4Z7	Ref-side Cap (Btu/h) : 0.1738.75
Upstream Temp A (F):		103.20	0.5Z7	Ref-side Cap (tons): 1.48
Upstream Temp B (F):		103.43	0.2Z2	Refrigerant Mdot (lbm/h): 251.93
Upstream Temp C (F):		103.17	0.5Z7	Coriolis Density (lbm/ft3): 70.48
Upstream Average Temp (F):		103.27		Upstream R22 Tsat (F): 119.70
Upstream Subcooling A (F):		16.50	0.567	
Upstream Subcooling B (F):		16.27	0.332	
Upstream Subcooling C (F):		16.52	0.706	
Average Subcooling (F):		16.43		
Evap Exit Pressure (psia):		90.54	0.486	Turbine A Frequency (Hz): 147.04
Evap Exit Avg Temp A:		75.88	0.559	Turb A Vol Flow (ft3/min): 0.0211
Evap Exit Avg Temp B:		75.08	0.607	Turb A Density (lbm/ft3): 70.58
Evap Exit Avg Temp C:		75.31	0.673	Turb A Mass Flow (lb/h): 89.17
Circuit A Superheat (F):		30.55	0.537	Turbine C Frequency (Hz): 153.19
Circuit B Superheat (F):		29.75	0.607	Turb C Vol Flow (ft3/min): 0.0227
Circuit C Superheat (F):		29.98	0.538	Turb C Density (lbm/ft3): 70.58
Overall Superheat (F):		30.44	0.616	Turb C Mass Flow (lb/h): 96.03
				Turb C Calculated Mass Flow (lbm/h): 66.73
Circuit Temp 1 (F):		77.00	0.625	% Total Mass Flow Thru A: 35.39
Circuit Temp 2 (F):		76.63	0.540	% Total Mass Flow Thru B: 26.49
Circuit Temp 3 (F):		53.30	0.645	% Total Mass Flow Thru C: 38.12
Circuit Temp 4 (F):		75.65	0.584	
Circuit Temp 5 (F):		74.86	0.541	
Circuit Temp 6 (F):		56.91	0.087	
Circuit Temp 7 (F):		78.70	1.077	
Circuit Temp 8 (F):		75.74	0.623	
Circuit Temp 9 (F):		54.81	0.644	

A.4 Enhanced fin (wavy-lanced) evaporator in cross-parallel flow

Table A.4.1: Enhanced Fin (Wavy-Lanced) Evaporators in Cross-Parallel Flow

Test names	Test type
E020403A	9
E020404A	10
E020408A	11
E020409A	12

DATA FILENAME E02040				T DISTRIBUTOR SUMMARY SHEET			
at SUMMARY FILENAME E020403A.SUM							
Air-Side Conditions		Range	Total Air-Side Capacity:	15522.67	Range	330.44	
Indoor Dry-Bulb : 80.1B2		0.40	Sensible Cap (Btu/h):	10855.53		193.09	
Indoor Inlet Dew (F) : 80.7B1		0.27	Latent Cap (Btu/h):	4667.14		184.87	
Indoor Exit Dry-Bulb : 81.800		0.33	EvapAir Delta T (F):	18.77		0.22	
Indoor Exit Dew (F) : 85.9B9		0.30	Air/Ref Cap Prcnt Diff:	0.98		3.60	
			Sensible Heat Ratio:	0.699		0.0107	
Indoor Airflow (CFM): 533.03		6.06	SCFM per Ton:	405.92			
Indoor Airflow (SCFM): 525.08		5.97	(0.075 lb/ft3 standard air)				
Evap Inlet Humidity Ratio (lbH2O/lbAir):			0.011614				
Evap Exit Humidity Ratio (lbH2O/lbAir):			0.009751				
Barometric Pressure (in HG): 29.24			Nozzle Temp (F): 65.08	0 59			
Air Chamber Nozzle Pressure Drop (in Water):			0.623	0.014			
Evaporator Coil Air Pressure Drop (in Water):			0.135	0.005			

Refrigerant Side Conditions							
Expansion Valve							
Upstream Pressure (psia):		271.30	0.852	Ref-side Cap (Btu/h):	15674.41	478.40	
Upstream Temp A (F):		104.13	0.617	Ref-side Cap (tons):	1.31	0.04	
Upstream Temp B (F):		104.30	0.698	Refrigerant Mdot (lbm/h):	227.91	6.96	
Upstream Temp C (F):		104.03	0.740	Coriolis Density (lbm/ft3):	82.14	0.11	
Upstream Average Temp (F):		104.16		Upstream R22 Tsat (F):	119.00		
Upstream Subcooling A (F):		14.87	0.741				
Upstream Subcooling B (F):		14.70	0.698				
Upstream Subcooling C (F):		14.96	0.635				
Average Subcooling (F):		14.84					
Evap Exit Pressure (psia):		90.75	0.243	Turbine A Frequency (Hz):	134.83	1.00	
Evap Exit Avg Temp A:		55.71	0.508	Turb A Vol Flow (ft3/min):	0.0194	0.00	
Evap Exit Avg Temp B:		55.76	0.461	Turb A Density (lbm/ft3):	70.44	0.09	
Evap Exit Avg Temp C:		55.18	0.596	Turb A Mass Flow (lb/h):	82.13	0.67	
Circuit A Superheat (F):		10.36	0.621	Turbine C Frequency (Hz):	141.57	1.00	
Circuit B Superheat (F):		10.40	0.526	Turb C Vol Flow (ft3/min):	0.0211	0.00	
Circuit C Superheat (F):		9.82	0.573	Turb C Density (lbm/ft3):	70.45	0.11	
Overall Superheat (F):		10.92	0.675	Turb C Mass Flow (lb/h):	89.29	0.71	
				Turb C Calculated Mass Flow (lbm/h):	56.49	7.50	
Circuit Temp 1 (F):		52.38	0.621	% Total Mass Flow Thru A:	36.04	1.16	
Circuit Temp 2 (F):		49.79	0.558	% Total Mass Flow Thru B:	24.78	2.54	
Circuit Temp 3 (F):		61.63	0.780	% Total Mass Flow Thru C:	39.18	1.43	
Circuit Temp 4 (F):		51.69	0.655				
Circuit Temp 5 (F):		51.98	0.556				
Circuit Temp 6 (F):		63.51	0.636				
Circuit Temp 7 (F):		53.75	0.733				
Circuit Temp 8 (F):		52.56	0.739				
Circuit Temp 9 (F):		60.70	0.508				

SMART DISTRIBUTOR SUMMARY SHEET
DATA FILENAME: E020404A.DAT SUMMARY FILENAME: E020404A.sum

Air-Side Conditions		Range	Total Air-Side Capacity:	3469.93	Range
Indoor Dry-Bulb : 80 155		0.25	Sensible Cap (Btu/h):	3877.22	343.64
Indoor Inlet Dew (F): 60 865		0.11	Latent Cap (Btu/h):	-407.28	283.77
Indoor Exit Dry-Bulb: 73 938		0.15	EvapAir Delta T (F):	6.63	118.68
Indoor Exit Dew (F): 61 245		0.15	Air/Ref Cap Prctn Diff: -5.87	11.71	0.03
Indoor Airflow (CFM): 551.04		6.93	Sensible Heat Ratio: 1.117	0.0399	
Indoor Airflow (SCFM): 529.90		6.63	SCFM per Ton: 1832.50		
Evap Inlet Humidity Ratio (lbH2O/lbAir):		0.011662	(0.075 lb/ft3 standard air)		
Evap Exit Humidity Ratio (lbH2O/lbAir):		0.011824			
Barometric Pressure (in HG): 29.24		Nozzle Temp (m : 74 30 0 53			
Air Chamber Nozzle Pressure Drop (in Water): 0.650		0.016			
Evaporator Coil Air Pressure Drop (in Water): 0.084		0.004			
Refrigerant Side Conditions					
Expansion Valve					
Upstream Pressure (psia):	287.28	1.096	Ref-side Cap (Btu/h) :	3284.20	286.12
Upstream Temp A (F):	105.41	0.785	Ref-side Cap (tons):	0.27	0.02
Upstream Temp B (F):	105.99	0.699	Refrigerant Mdot (lbm/h):	46.98	4.12
Upstream Temp C (F):	106.05	0.786	Coriolis Density (lbm/ft3):	84.78	0.11
Upstream Average Temp (F):	105.82		Upstream R22 Tsat (F):	123.58	
Upstream Subcooling A (F):	18.17	0.517			
Upstream Subcooling B (F):	17.59	0.491			
Upstream Subcooling C (F):	17.53	0.651			
Average Subcooling (F):	17.76				
Evap Exit Pressure (psia):	90.21	1.946	Turbine A Frequency (Hz):	24.09	1.00
Evap Exit Avg Temp A:	73.88	0.292	Turb A Vol Flow (ft3/min):	0.0047	0.00
Evap Exit Avg Temp B:	73.46	0.606	Turb A Density (lbm/ft3):	70.24	0.12
Evap Exit Avg Temp C:	73.55	0.539	Turb A Mass Flow (lb/h):	19.84	0.58
Circuit A Superheat (F):	29.09	1.150	Turbine C Frequency (Hz):	36.17	1.00
Circuit B Superheat (F):	28.67	1.263	Turb C Vol Flow (ft3/min):	0.0071	0.00
Circuit C Superheat (F):	28.76	1.308	Turb C Density (lbm/ft3):	70.14	0.12
Overall Superheat (F):	28.88	1.123	Turb C Mass Flow (lb/h):	29.71	0.60
			Turb C Calculated Mass Flow (lbm/h):	-2.58	4.12
Evap Circuit Temp 1 (F):	52.30	2.824	% Total Mass Flow Thru A:	42.27	3.70
Evap Circuit Temp 2 (F):	72.64	2.171	% Total Mass Flow Thru B:	-5.56	9.30
Evap Circuit Temp 3 (F):	75.80	0.540	% Total Mass Flow Thru C:	33.29	5.61
Evap Circuit Temp 4 (F):	52.47	3.334			
Evap Circuit Temp 5 (F):	70.86	3.262			
Evap Circuit Temp 6 (F):	76.17	0.540			
Evap Circuit Temp 7 (F):	56.97	3.270			
Evap Circuit Temp 8 (F):	60.35	6.607			
Evap Circuit Temp 9 (F):	75.32	0.541			

SMART DISTRIBUTOR SUMMARY SHEET
 DATA FILENAME: E020408A.DAT SUMMARY FILENAME: E020408A.sum

Air-Side Conditions		Range	Total Air-Side Capacity:	11507.75	Range
Indoor Dry-Bulb :		30.129	0.15	Sensible Cap (Btu/h):	9384.29
Indoor Inlet Dew (F) :		≤0.343	0.09	Latent Cap (Btu/h):	2123.46
Indoor Exit Dry-Bulb:		≤4.462	0.22	EvapAir Delta T (F):	16.19
Indoor Exit Dew (F) :		38.231	0.05	Air/Ref Cap Prcnt Diff:	0.19
				Sensible Heat Ratio:	0.815
Indoor Airflow (CFM):		536.99	6.49	SCFM per Ton:	548.56
Indoor Airflow (SCFM):		526.06	6.26	(0.075 lb/ft3 standard air)	
Evap Inlet Humidity Ratio (lbH2O/lbAir):				0.011444	
Evap Exit Humidity Ratio (lbH2O/lbAir):				0.010598	
Barometric Pressure (in Hg):		29.24	Nozzle Temp (F):	67.37	0.≤3
Air Chamber Nozzle Pressure Drop (in Water):			0.629	0.015	
Evaporator Coil Air Pressure Drop (in Water):			0.121	0.004	
Refrigerant Side Conditions					
Expansion Valve					
Upstream Pressure (psia):		273.06	0.852	Ref-side Cap (Btu/h):	11529.24
Upstream Temp A (F):		104.61	0.524	Ref-side Cap (tons):	0.96
Upstream Temp B (F):		105.25	0.567	Refrigerant Mdot (lbm/h):	168.32
Upstream Temp C (F):		104.59	0.567	Coriolis Density (lbm/ft3):	82.46
Upstream Average Temp (F):		104.82		Upstream R22 Tsat (F):	119.58
Upstream Subcooling A (F):		14.97	0.≤B4		
Upstream Subcooling B (F):		14.32	0.≤02		
Upstream Subcooling C (F):		14.98	0.≤B6		
Average Subcooling (F):		14.76			
Evap Exit Pressure (psia):		90.58	0.486	Turbine A Frequency (Hz):	≤9.08
Evap Exit Avg Temp A:		63.32	0.701	Turb A Vol Flow (ft3/min):	0.0107
Evap Exit Avg Temp B:		47.25	0.558	Turb A Density (lbm/ft3):	70.3≤
Evap Exit Avg Temp C:		63.07	0.270	Turb A Mass Flow (lb/h):	45.13
Circuit A Superheat (F):		18.14	0.949	Turbine C Frequency (Hz):	79.13
Circuit B Superheat (F):		2.07	0.715	Turb C Vol Flow (ft3/min):	0.0123
Circuit C Superheat (F):		17.89	0.505	Turb C Density (lbm/ft3):	70.37
Overall Superheat (F)		10.10	0.906	Turb C Mass Flow (lb/h):	54.02
				Turb C Mass Flow (lbm/h):	69.17
Circuit Temp 1 (F):		51.32	0.644	Total Mass Flow Thru A:	26.82
Circuit Temp 2 (F):		49.04	0.649	Total Mass Flow Thru B:	41.03
Circuit Temp 3 (F):		68.89	1.267	Total Mass Flow Thru C	32.10
Circuit Temp 4 (F):		52.24	0.601		
Circuit Temp 5 (F):		52.41	0.646		
Circuit Temp 6 (F):		55.49	0.743		
Circuit Temp 7 (F):		52.71	1.388		
Circuit Temp 8 (F):		52.08	0.323		
Circuit Temp 9 (F):		67.92	0.177		

SMART DISTRIBUTOR SUMMARY SHEET
 DATA FILENAME: E020409A.DAT SUMMARY FILENAME: E020409A.sum

Air-Side Conditions				Range
Indoor Dry-Bulb :	30.006	Range	Total Air-Side Capacity:	9542.99
Indoor Inlet Dew (F) :	≤0.361	0.52	Sensible Cap (Btu/h) :	7901.04
Indoor Exit Dry-Bulb: :	≤8.911	0.31	Latent Cap (Btu/h) :	1641.95
Indoor Exit Dew (F) :	33.748	0.42	EvapAir Delta T (F) :	13.57
		0.39	Air/Ref Cap Prnt Diff: :	-0.27
			Sensible Heat Ratio: :	0.828
Indoor Airflow (CFM) :	541.60	8.59	SCFM per Ton: :	664.02
Indoor Airflow (SCFM) :	528.06	8.74	(0.075 lb/ft3 standard air)	
Evap Inlet Humidity Ratio (lbH2O/lbAir) :			0.011451	
Evap Exit Humidity Ratio (lbH2O/lbAir) :			0.010800	
Barometric Pressure (in HG) :	29.24	Nozzle Temp (F) :	69.37	0 ≤3
Air Chamber Nozzle Pressure Drop (in Water) :	0.637	0.020		
Evaporator Coil Air Pressure Drop (in Water) :	0.106	0.003		

Refrigerant Side Conditions				
Expansion Valve				
Upstream Pressure (psia) :	274.70	0.244	Ref-side Cap (Btu/h) :	9515.76
Upstream Temp A (F) :	104.15	0.654	Ref-side Cap (tons) :	0.79
Upstream Temp B (F) :	103.60	0.698	Refrigerant Mdot (lbm/h) :	138.13
Upstream Temp C (F) :	103.47	0.173	Coriolis Density (lbm/ft3) :	82.30
Upstream Average Temp (F) :	103.74	.	Upstream R22 Tsat (F) :	120.05
Upstream Subcooling A (F) :	15.90	0.654		
Upstream Subcooling B (F) :	16.45	0.681		
Upstream Subcooling C (F) :	16.58	0.173		
Average Subcooling (F) :	16.31			
Evap Exit Pressure (psia) :	90.61	0.730	Turbine A Frequency (Hz) :	139.20
Evap Exit Avg Temp A: :	46.71	0.650	Turb A Vol Flow (ft3/min) :	0.0200
Evap Exit Avg Temp B: :	69.85	0.360	Turb A Density (lbm/ft3) :	70.43
Evap Exit Avg Temp C: :	68.68	0.721	Turb A Mass Flow (lb/h) :	84.58
Circuit A Superheat (F) :	1.63	0.581	Turbine C Frequency (Hz) :	64.16
Circuit B Superheat (F) :	24.77	0.606	Turb C Vol Flow (ft3/min) :	0.0108
Circuit C Superheat (F) :	23.60	0.755	Turb C Density (lbm/ft3) :	70.54
Overall Superheat (F) :	10.76	2.618	Turb C Mass Flow (lb/h) :	45.69
Circuit B Calculated Mass Flow (lbm/h) :				
Evap Circuit Temp 1 (F) :	51.00	1.113	% Total Mass Flow Thru A: :	7.87
Evap Circuit Temp 2 (F) :	49.84	0.557	% Total Mass Flow Thru B: :	≤1.24
Evap Circuit Temp 3 (F) :	50.73	1.067	% Total Mass Flow Thru C: :	5.68
Evap Circuit Temp 4 (F) :	51.94	2.825		33.08
Evap Circuit Temp 5 (F) :	56.65	7.969		
Evap Circuit Temp 6 (F) :	73.43	0.716		
Evap Circuit Temp 7 (F) :	53.62	0.599		
Evap Circuit Temp 8 (F) :	51.44	0.648		
Evap Circuit Temp 9 (F) :	72.13	0.904		

Range				
418.13				
292.10				
182.38				
0.43				
6.54				
0.0155				
0.03				
5.86				
0.10				
1.17				
1.00				
0.00				
0.03				
0.58				
6.38				
2.96				
4.34				
1.71				

A.5 Enhanced-Cut fin (wavy-lanced)evaporator in cross-counter flow

Test names	Test type
E020417A	1
E020417B	2
E020418A	5
E020419A	6
E020415A	9
E020509A	10
E020416B	13

DATA FILENAME: E020417A.DAT SUMMARY FILENAME: E020417A.sum

Air-Side Conditions			Range	Total Air-Side Capacity:	20760.16	428.20
Indoor Dry-Bulb			79.9-9	Sensible Cap (Btu/h):	14269.36	468.38
Indoor Inlet Dew (F):			60.3-7	Latent Cap (Btu/h):	6490.80	180.28
Indoor Exit Dry-Bulb:			58.5-8	EvapAir Delta T (F):	21.86	0.65
Indoor Exit Dew (F):			54.3-3	Air/R _{ef} C _A Part Diff	1.19	3.53
				Sensible Heat Ratio:	0.687	0.00-2
Indoor Airflow (CFM):			5-8.10	SCFM per Ton:	342.83	
Indoor Airflow (SCFM):			5-3.10	(0.075 lb/ft ³ standard air)		
Evap Inlet Humidity Ratio (lb _x 2o/lbAir):			0.0114-7			
Evap Exit Humidity Ratio (lb _x 2o/lbAir):			0.00-172			
Barometric Pressure (in HG)			2-24	Nozzle Temp (m):	59.68	±0
Air Chamber Nozzle Pressure Drop (in Col _{pr})			1.270	0.024		
Evaporator Coil Air Pressure Drop (in Water):			0.157	0.005		

Refrigerant Side Conditions						
Expansion Valve						
Upstream Pressure (psia):			275.47	0.852	Ref-side Cap (Btu/h):	21005.77
Upstream Temp A (F):			104.55	0.524	Ref-side Cap (tons):	1.75
Upstream Temp B (F):			104.69	0.262	Refrigerant Mdot (lbm/h):	305.27
Upstream Temp C (F):			104.39	0.524	Coriolis Density (lbm/ft ³):	82.16
Upstream Average Temp (F):			104.54		Upstream R22 Tsat (F):	120.18
Upstream Subcooling A (F):			15.63	0.593		
Upstream Subcooling B (F):			15.49	0.366		
Upstream Subcooling C (F):			15.79	0.515		
Average Subcooling (F):			15.64			
Evap Exit Pressure (psia):			90.50	0.608	Turbine A Frequency (Hz):	199.27
Evap Exit Avg Temp A:			55.36	1.931	Turb A Vol Flow (ft ³ /min):	0.0280
Evap Exit Avg Temp B:			54.85	1.310	Turb A Density (lbm/ft ³):	70.37
Evap Exit Avg Temp C:			56.24	2.159	Turb A Mass Flow (lb/h):	118.23
Circuit A Superheat (F):			9.90	2.037	Turbine C or Q _{max} (K):	171.80
Circuit B Superheat (F):			9.40	1.310	Turb C 1 Flow (ft ³ /min):	0.0252
Circuit C Superheat (F):			10.79	2.271	Turb C Density (lbm/ft ³):	70.40
Overall Superheat (F)			13.18	0.956	Turb C Mass Flow (lb/h):	106.26
					Turb C Calculated Mass Flow (lbm/h):	80.78
Circuit Temp 1 (F):			50.12	1.484	% Total Mass Flow Thru A:	38.73
Circuit Temp 2 (F):			48.55	0.558	% Total Mass Flow Thru B:	26.46
Circuit Temp 3 (F):			49.69	0.605	% Total Mass Flow Thru C:	34.81
Circuit Temp 4 (F):			49.16	0.743		
Circuit Temp 5 (F):			47.56	0.280		
Circuit Temp 6 (F):			50.81	0.649		
Circuit Temp 7 (F):			51.45	1.203		
Circuit Temp 8 (F):			48.11	0.743		
Circuit Temp 9 (F):			49.80	0.605		

SMART DISTRIBUTOR SUMMARY SHEET
 DATA FILENAME: E020417B.DAT SUMMARY FILENAME: E020417B.sum

Air-Side Conditions		Range	Total Air-Side Capacity: 15855.26	Range
Inoor Dry-Bulb :	80.014	0.12	Sensible Cap (Btu/h): 12203.85	298.26
Inoor Inlet Dew (F) :	60.375	0.02	Latent Cap (Btu/h): 3651.40	260.58
Inoor Exit Dry-Bulb :	61.822	0.18	EvapAir Delta T (F): 18.70	102.26
Inoor Exit Dew (F) :	57.092	0.06	Air/Ref Cap Prct Diff: -3.21	0.22
			Sensible Heat Ratio: 0.770	3.50
			SCFM per Ton: 448.44	0.0060
Indoor Airflow (CFM):	601.66	8.27	(0.075 lb/ft3 standard air)	
Indoor Airflow (SCFM):	592.51	8.10	(0.011458	
Evap Inlet Humidity Ratio (lbH2O/lbAir):			0.010165	
Evap Exit Humidity Ratio (lbH2O/lbAir):				
Barometric Pressure (in HG):	29.24	Nozzle Temp (F): 62.65	0.41	
Air Chamber Nozzle Pressure Drop (in Water):	1.277	0.035		
Evaporator Coil Air Pressure Drop (in Water):	0.142	0.006		

Refrigerant Side Conditions				
Expansion Valve				
Upstream Pressure (psia):	297.86	0.731	Ref-side Cap (Btu/h) :	15346.55
Upstream Temp A (F) :	102.90	0.569	Ref-side Cap (tons):	44.96
Upstream Temp B (F) :	103.07	0.525	Refrigerant Mdot (lbm/h):	0.04
Upstream Temp C (F) :	102.75	0.351	Coriolis Density (lbm/ft3):	6.59
Upstream Average Temp (F) :	102.91		Upstream R22 Tsat (F):	0.19
Upstream Subcooling A (F) :	23.49	0.623		
Upstream Subcooling B (F) :	23.33	0.611		
Upstream Subcooling C (F) :	23.65	0.548		
Average Subcooling (F) :	23.49			
Evap Exit Pressure (psia):	90.84	0.486	Turbine A Frequency (Hz) :	139.28
Evap Exit Avg Temp A:	76.02	0.360	Turb A Vol Flow (ft3/min):	0.0200
Evap Exit Avg Temp B:	76.73	0.268	Turb A Density (lbm/ft3):	0.09
Evap Exit Avg Temp C:	75.23	0.538	Turb A Mass Flow (lb/h):	0.67
Circuit A Superheat (F) :	30.62	0.517	Turbine C Frequency (Hz):	129.36
Circuit B Superheat (F) :	31.33	0.425	Turb C Vol Flow (ft3/min):	0.0195
Circuit C Superheat (F) :	29.82	0.616	Turb C Density (lbm/ft3):	0.05
Overall Superheat (F) :	31.06	0.673	Turb C Mass Flow (lb/h):	82.64
			Turb C Calculated Mass Flow (lbm/h):	49.95
			% Total Mass Flow Thru A:	39.03
			% Total Mass Flow Thru B:	22.97
			% Total Mass Flow Thru C:	38.01
				1.04
Circuit Temp 1 (F) :	75.45	0.223		
Circuit Temp 2 (F) :	72.93	0.726		
Circuit Temp 3 (F) :	48.37	0.653		
Circuit Temp 4 (F) :	76.19	0.723		
Circuit Temp 5 (F) :	73.76	0.679		
Circuit Temp 6 (F) :	49.53	0.462		
Circuit Temp 7 (F) :	77.76	0.672		
Circuit Temp 8 (F) :	71.55	0.635		
Circuit Temp 9 (F) :	49.21	0.605		

SMART DISTRIBUTOR SUMMARY SHEET
 DATA FILENAME: E020418A.DAT SUMMARY FILENAME: E020418A.sum

Air-Side Conditions		Range	Total Air-Side Capacity	19031.65	517.13
Indoor Dry-Bulb : 79.855		0.49	Sensible Cap (Btu/h):	19485.39	562.65
Indoor Inlet Dew (F) : 48.872		0.21	Latent Cap (Btu/h):	-453.74	66.94
Indoor Exit Dry-Bulb: 57.438		0.39	EvapAir Delta T (F):	22.80	0.43
Indoor Exit Dew (F) : 49.299		0.21	Air/Ref Cap Prcnt Diff:	-1.20	4.20
			Sensible Heat Ratio:	1.024	0.0035
Indoor Airflow (CFM): 784.81		13.11	SCFM per Ton:	492.16	
Indoor Airflow (SCFM): 780.56		13.05	(0.075 lb/ft3 standard air)		
Evap Inlet Humidity Ratio (lbH2O/lbAir):		0.007484			
Evap Exit Humidity Ratio (lbH2O/lbAir):		0.007606			
Barometric Pressure (in HG): 29.24		Nozzle Temp (F): 58.43	0 ≤ 5		
Air Chamber Nozzle Pressure Drop (in Water): 0.811		0.027			
Evaporator Coil Air Pressure Drop (in Water): 0.168		0.007			
Refrigerant Side Conditions					
Expansion Valve					
Upstream Pressure (psia): 276.43		0.731	Ref-side Cap (Btu/h):	18802.24	432.99
Upstream Temp A (F): 105.93		0.612	Ref-side Cap (tons):	1.57	0.04
Upstream Temp B (F): 106.00		0.569	Refrigerant Mdot (lbm/h):	274.77	6.41
Upstream Temp C (F): 105.73		0.262	Coriolis Density (lbm/ft3):	82.52	0.16
Upstream Average Temp (F): 105.89			Upstream R22 Tsat (F):	120.46	
Upstream Subcooling A (F): 14.53		0.716			
Upstream Subcooling B (F): 14.46		0.638			
Upstream Subcooling C (F): 14.73		0.469			
Average Subcooling (F): 14.57					
Evap Exit Pressure (psia): 90.97		0.730	Turbine A Frequency (Hz):	177.61	1.00
Evap Exit Avg Temp A: 55.72		2.571	Turb A Vol Flow (ft3/min):	0.0251	0.00
Evap Exit Avg Temp B: 55.69		2.391	Turb A Density (lbm/ft3):	70.16	0.09
Evap Exit Avg Temp C: 55.54		4.962	Turb A Mass Flow (lb/h):	105.75	0.70
Circuit A Superheat (F): 10.10		2.259	Turbine C Frequency (Hz):	157.36	2.00
Circuit B Superheat (F): 10.08		2.313	Turb C Vol Flow (ft3/min):	0.0232	0.00
Circuit C Superheat (F): 9.92		4.806	Turb C Density (lbm/ft3):	70.19	0.04
Overall Superheat (F): 13.54		1.654	Turb C Mass Flow (lb/h):	97.84	1.08
			Turb C Calculated Mass Flow (lbm/h):	71.18	6.34
Circuit Temp 1 (F): 50.04		2.784	% Total Mass Flow Thru A:	38.49	1.02
Circuit Temp 2 (F): 48.21		0.464	% Total Mass Flow Thru B:	25.90	2.01
Circuit Temp 3 (F): 49.38		0.557	% Total Mass Flow Thru C:	35.61	1.08
Circuit Temp 4 (F): 49.12		1.673			
Circuit Temp 5 (F): 47.46		0.654			
Circuit Temp 6 (F): 50.40		0.603			
Circuit Temp 7 (F): 51.37		1.158			
Circuit Temp 8 (F): 48.17		0.327			
Circuit Temp 9 (F): 49.81		0.652			

SMART DISTRIBUTOR SUMMARY SHEET
 DATA FILENAME: E020419A.DAT SUMMARY FILENAME: E020419A.sum

Air-Side Conditions		Range	Total Air-Side Capacity: 14125.73	Range
Indoor Dry-Bulb :	73.724	0.32	Sensible Cap (Btu/h): 14523.20	490.90
Indoor Inlet Dew (F):	40.502	0.16	Latent Cap (Btu/h): -397.4	504.52
Indoor Exit Dry-Bulb:	63.019	0.37	EvapAir Delta T (F): 17.08	76.25
Indoor Exit Dew (F):	40.883	0.15	Air/Ref Cap Prcnt Diff: -5.67	0.44
			Sensible Heat Ratio: 1.028	6.95
Indoor Airflow (CFM):	789.23	8.25	SCFM per Ton: 59.78	0.0053
Indoor Airflow (SCFM):	776.63	7.86	(0.075 lb/ft3 standard air)	
Evap Inlet Humidity Ratio (lbH2O/lbAir):			0.007380	
Evap Exit Humidity Ratio (lbH2O/lbAir):			0.007487	
Barometric Pressure (in HG):	29.24		Nozzle Temp (F): 63.73	0.55
Air Chamber Nozzle Pressure Drop (in Water):			0.812	0.016
Evaporator Coil Air Pressure Drop (in Water):			0.170	0.008

Refrigerant Side Conditions				
Expansion Valve				
Upstream Pressure (psia):	277.85	2.192	Ref-side Cap (Btu/h): 13323.55	373.13
Upstream Temp A (F):	107.88	1.179	Ref-side Cap (tons):	1.11
Upstream Temp B (F):	108.09	1.136	Refrigerant Mdot (lbm/h):	192.94
Upstream Temp C (F):	107.62	1.135	Coriolis Density (lbm/ft3):	83.35
Upstream Average Temp (F):	107.87		Upstream R22 Tsat (F):	120.91
Upstream Subcooling A (F):	13.03	0.852		
Upstream Subcooling B (F):	12.82	0.747		
Upstream Subcooling C (F):	13.29	0.887		
Average Subcooling (F):	13.05			
Evap Exit Pressure (psia):	91.02	0.486	Turbine A Frequency (Hz):	127.60
Evap Exit Avg Temp A:	76.68	0.717	Turb A Vol Flow (ft3/min):	0.0185
Evap Exit Avg Temp B:	77.23	0.605	Turb A Density (lbm/ft3):	69.86
Evap Exit Avg Temp C:	77.04	0.628	Turb A Mass Flow (lb/h):	77.42
Circuit A Superheat (F):	31.18	0.628	Turbine C Frequency (Hz):	110.12
Circuit B Superheat (F):	31.73	0.481	Turb C Vol Flow (ft3/min):	0.0169
Circuit C Superheat (F):	31.54	0.605	Turb C Density (lbm/ft3):	69.90
Overall Superheat (F):	31.90	0.770	Turb C Mass Flow (lb/h):	70.99
			Turb C Calculated Mass Flow (lbm/h):	44.52
Circuit B Calculated Mass Flow (lbm/h):				
Circuit Temp 1 (F):	77.70	0.539	% Total Mass Flow Thru A:	40.13
Circuit Temp 2 (F):	74.36	1.175	% Total Mass Flow Thru B:	23.07
Circuit Temp 3 (F):	48.34	0.806	% Total Mass Flow Thru C:	36.80
Circuit Temp 4 (F):	76.94	0.310		
Circuit Temp 5 (F):	75.66	0.586		
Circuit Temp 6 (F):	49.54	0.804		
Circuit Temp 7 (F):	78.43	1.077		
Circuit Temp 8 (F):	76.15	0.832		
Circuit Temp 9 (F):	48.94	0.853		

SMART DISTRIBUTOR SUMMARY SHEET				
DATA FILENAME: E020415A.DAT SUMMARY FILENAME: E020415A.sum				
Air-Side Conditions				
	Range	Total Air-Side Capacity:		Range
Indoor Dry-Bulb :	80.121	0.42	Sensible Cap (Btu/h):	23788.22 627.38
Indoor Inlet Dew (F):	60.369	0.47	Latent Cap (Btu/h):	17485.19 457.67
Indoor Exit Dry-Bulb:	60.258	0.37	EvapAir Delta T (F):	20.32 279.03
Indoor Exit Dew (F):	55.995	0.39	Air/Ref Cap Prcnt Diff:	-0.68 0.44
			Sensible Heat Ratio:	0.735 2.68
			SCFM per Ton:	394.12 0.0113
Indoor Airflow (CFM):	791.02	9.05	(0.075 lb/ft3 standard air)	
Indoor Airflow (SCFM):	781.29	9.07	0.011455	
Evap Inlet Humidity Ratio (lbH2O/lbAir):			0.009764	
Evap Exit Humidity Ratio (lbH2O/lbAir):			Nozzle Temp (F):	83.09 0.82
Barometric Pressure (in HG):	29.24		1.369 0.031	
Air Chamber Nozzle Pressure Drop (in Water):			0.254 0.006	
Evaporator Coil Air Pressure Drop (in Water):				

Refrigerant Side Conditions				
Expansion Valve				
Upstream Pressure (psia):	295.10	0.731	Ref-side Cap (Btu/h):	23625.71 519.24
Upstream Temp A (F):	106.36	0.611	Ref-side Cap (tons):	1.97 0.04
Upstream Temp B (F):	106.39	0.786	Refrigerant Mdot (lbm/h):	346.04 7.32
Upstream Temp C (F):	106.19	0.524	Coriolis Density (lbm/ft3):	82.62 0.27
Upstream Average Temp (F):	106.31		Upstream R22 Tsat (F):	125.57
Upstream Subcooling A (F):	19.22	0.578		
Upstream Subcooling B (F):	19.18	0.731		
Upstream Subcooling C (F):	19.38	0.557		
Average Subcooling (F):	19.26			
Evap Exit Pressure (psia):	90.94	0.486	Turbine A Frequency (Hz):	226.62 2.00
Evap Exit Avg Temp A:	55.82	3.720	Turb A Vol Flow (ft3/min):	0.0316 0.00
Evap Exit Avg Temp B:	56.22	3.719	Turb A Density (lbm/ft3):	70.09 0.09
Evap Exit Avg Temp C:	56.55	3.557	Turb A Mass Flow (lb/h):	133.06 1.20
Circuit A Superheat (F):	9.88	3.720	Turbine C Frequency (Hz):	195.31 1.00
Circuit B Superheat (F):	10.28	3.774	Turb C Vol Flow (ft3/min):	0.0283 0.00
Circuit C Superheat (F):	10.61	3.479	Turb C Density (lbm/ft3):	70.12 0.08
Overall Superheat (F)	13.26	2.197	Turb C Mass Flow (lb/h):	119.04 0.70
Circuit B Calculated Mass Flow (lbm/h):				
Evap Circuit Temp 1 (F):	50.62	1.159	Total Mass Flow Thru A:	93.95 6.96
Evap Circuit Temp 2 (F):	49.01	0.746	Total Mass Flow Thru B:	38.45 0.86
Evap Circuit Temp 3 (F):	50.49	0.651	Total Mass Flow Thru C:	27.15 1.46
Evap Circuit Temp 4 (F):	49.71	0.745		34.40 0.70
Evap Circuit Temp 5 (F):	48.28	0.511		
Evap Circuit Temp 6 (F):	52.07	0.738		
Evap Circuit Temp 7 (F):	51.75	0.738		
Evap Circuit Temp 8 (F):	48.88	0.652		
Evap Circuit Temp 9 (F):	50.67	0.604		

SMART DISTRIBUTOR SUMMARY SHEET
 DATA FILENAME: E020509A.dat SUMMARY FILENAME: E020509A.sum

Air-Side Conditions		Range	Total Air-Side Capacity:	18291.86	Range
Indoor Dry-Bulb :	79.875	0.24	Sensible Cap (Btu/h):	14879.62	685.26
Indoor Wet-Bulb Dew (F) :	60.358	0.10	Latent Cap (Btu/h):	3412.24	619.90
Indoor Exit Dry-Bulb :	63.170	0.13	EvapAir Delta T (F):	17.26	107.75
Indoor Exit Dew (F) :	58.071	0.07	Air/Ref Cap Prcnt Diff:	-4.19	0.43
			Sensible Heat Ratio:	0.813	4.45
					0.0081
Indoor Airflow (CFM):	796.91	13.83	SCFM per Ton:	513.29	
Indoor Airflow (SCFM):	782.42	13.62	(0.075 lb/ft3 standard air)		
Evap Inlet Humidity Ratio (lbH2O/lbAir):		0.011451			
Evap Exit Humidity Ratio (lbH2O/lbAir):		0.010536			
Barometric Pressure (in HG):	29.24	Nozzle Temp (F):	64.04	0.59	
Air Chamber Nozzle Pressure Drop (in Water):	0.825	0.028			
Evaporator Coil Air Pressure Drop (in Water):	0.226	0.008			

Refrigerant Side Conditions					
Expansion Valve					
Upstream Pressure (psia):	271.33	0.731	Ref-side Cap (Btu/h):	17523.19	551.53
Upstream Temp A (F):	103.34	0.347	Ref-side Cap (tons):	1.46	0.05
Upstream Temp B (F):	103.54	0.305	Refrigerant Mdot (lbm/h):	248.82	7.78
Upstream Temp C (F):	103.15	0.610	Coriolis Density (lbm/ft3):	81.81	0.14
Upstream Average Temp (F):	103.34		Upstream R22 Tsat (F):	119.04	
Upstream Subcooling A (F):	15.70	0.382			
Upstream Subcooling B (F):	15.50	0.340			
Upstream Subcooling C (F):	15.89	0.810			
Average Subcooling (F):	15.70				
Evap Exit Pressure (psia):	91.31	0.486	Turbine A Frequency (Hz):	157.80	1.00
Evap Exit Avg Temp A:	76.06	0.537	Turb A Vol Flow (ft3/min):	0.0225	0.00
Evap Exit Avg Temp B:	75.89	0.403	Turb A Density (lbm/ft3):	70.56	0.05
Evap Exit Avg Temp C:	75.56	0.425	Turb A Mass Flow (lb/h):	95.20	0.63
Circuit A Superheat (F):	30.26	0.650	Turbine C Frequency (Hz):	142.88	1.00
Circuit B Superheat (F):	30.09	0.537	Turb C Vol Flow (ft3/min):	0.0213	0.00
Circuit C Superheat (F):	29.75	0.649	Turb C Density (lbm/ft3):	70.59	0.09
Overall Superheat (F)	30.54	0.892	Turb C Mass Flow (lb/h):	90.20	0.62
Circuit B Calculated Mass Flow (lbm/h):				63.42	7.75
3V300 Circuit Temp 1 (F):	75.77	0.826	% Total Mass Flow Thru A:	38.26	1.20
3V300 Circuit Temp 2 (F):	73.07	0.830	% Total Mass Flow Thru B:	25.48	2.32
3V300 Circuit Temp 3 (F):	49.31	0.649	% Total Mass Flow Thru C:	36.26	1.23
3V300 Circuit Temp 4 (F):	75.44	0.541			
3V300 Circuit Temp 5 (F):	72.22	0.631			
3V300 Circuit Temp 6 (F):	50.75	0.801			
3V300 Circuit Temp 7 (F):	77.72	0.355			
3V300 Circuit Temp 8 (F):	72.43	0.831			
3V300 Circuit Temp 9 (F):	49.87	0.648			

SMART DISTRIBUTOR SUMMARY SHEET
 DATA FILENAME: E020416B.DAT SUMMARY FILENAME: E020416B.sum

Air-Side Conditions		Range	Total Air-Side Capacity: 26546.29	Range
Indoor Dry-Bulb :	≤0.142	0.28	Sensible Cap (Btu/h): 20754.50	745.84
Indoor Inlet Dew (F):	≤0.258	0.52	Latent Cap (Btu/h): 5791.80	771.24
Indoor Exit Dry-Bulb:	≤1.442	0.32	EvapAir Delta T (F): 19.08	509.00
Indoor Exit Dew (F):	≤7.130	0.34	Air/Ref Cap Prcnt Diff: -0.79	0.44
			Sensible Heat Ratio: 0.782	4.28
			SCFM per Ton 446.36	0.0169
Indoor Airflow (CFM):	1002.55	17.60		
Indoor Airflow (SCFM):	987.44	17.77	10.07# lb/f=3 #standard air)	
Evap Inlet Humidity Ratio (lbH2O/lbAir):			0.011009	
Evap Exit Humidity Ratio (lbH2O/lbAir):			0.010179	
Barometric Pressure (in HG):	29.24		Nozzle Temp (F): 63 44 0 ≤0	
Air Chamber Nozzle Pressure Drop (in water):			1.323 0.047	
Evaporator Coil Air Pressure Drop (in Water)			0 374 0 012	

Refrigerant Side Conditions				
Expansion Valve				
Upstream Pressure (psia):	274.04	0.731	Ref-side Cap (Btu/h) :	26335.16
Upstream Temp A (F):	105.19	0.524	Ref-side Cap (tons):	2.19
Upstream Temp B (F):	105.32	0.524	Refrigerant Mdot (lbm/h):	383.61
Upstream Temp C (F):	104.94	0.568	Coriolis Density (lbm/ft3):	82.25
Upstream Average Temp (F):	105.15		Upstream R22 Tsat (F):	119.72
Upstream Subcooling A (F):	14.53	0.539		
Upstream Subcooling B (F):	14.39	0.664		
Upstream Subcooling C (F):	14.78	0.619		
Average Subcooling (F):	14.57			
Evap Exit Pressure (psia):	90.76	0.486	Turbine A Frequency (Hz):	250.13
Evap Exit Avg Temp A:	56.18	1.951	Turb A Vol Flow (ft3/min):	0.0348
Evap Exit Avg Temp B:	56.73	2.799	Turb A Density (lbm/ft3):	70.27
Evap Exit Avg Temp C:	56.51	2.848	Turb A Mass Flow (lb/h):	146.58
Circuit A Superheat (F):	10.26	2.084	Turbine C Frequency (Hz):	218.50
Circuit B Superheat (F):	10.82	2.644	Turb C Vol Flow (ft3/min):	0.0314
Circuit C Superheat (F):	10.60	2.848	Turb C Density (lbm/ft3):	70.31
Overall Superheat (F):	13.48	1.740	Turb C Mass Flow (lb/h):	132.43
			Calculated Mass Flow (lbm/h):	104.61
SV200 Circuit Temp 1 (F):	50.69	1.205	% Total Mass Flow Thru A:	38.21
SV200 Circuit Temp 2 (F):	49.54	0.326	% Total Mass Flow Thru B:	27.27
SV200 Circuit Temp 3 (F):	51.16	0.603	% Total Mass Flow Thru C:	34.52
SV200 Circuit Temp 4 (F):	49.88	0.652		
SV200 Circuit Temp 5 (F):	48.62	0.653		
SV200 Circuit Temp 6 (F):	52.93	0.692		
SV200 Circuit Temp 7 (F):	52.31	1.111		
SV200 Circuit Temp 8 (F):	49.65	0.652		
SV200 Circuit Temp 9 (F):	51.21	0.651		

SMART DISTRIBUTOR SUMMARY SHEET
 DATA FILENAME: E020416A.DAT SUMMARY FILENAME: E020416A.sum

Air-Side Conditions		Range	Total Air-Side Capacity	22768.45	Range
Indoor Dry-Bulb	: 30.037	0.29	Sensible Cap (Btu/h):	18645.28	680.51
Indoor Inlet Dew (F)	: 30.534	0.37	Latent Cap (Btu/h):	4123.17	510.26
Indoor Exit Dry-Bulb	: 33.363	0.35	EvapAir Delta T (F):	17.05	349.67
Indoor Exit Dew (F)	: 38.372	0.37	Air/Ref Cap Prnt Diff:	-3.52	0.22
			Sensible Heat Ratio:	0.819	4.43
			SCFM per Ton:	523.03	0.0110
Indoor Airflow (CFM):	1011.50	19.34	(0.075 lb/ft3 standard air)		
Indoor Airflow (SCFM):	992.38	19.44	0.011524		
Evap Inlet Humidity Ratio (lbH2O/lbAir):			0.010652		
Evap Exit Humidity Ratio (lbH2O/lbAir):			Nozzle Temp (F):	65.00	0.55
Barometric Pressure (in HG):	29.24		1.341	0.052	
Air Chamber Nozzle Pressure Drop (in Water):			0.347	0.010	
Evaporator Coil Air Pressure Drop (in Water):					

Refrigerant Side Conditions					
Expansion Valve					
Upstream Pressure (psia):	270.94	0.974	Ref-side Cap (Btu/h):	21986.14	576.47
Upstream Temp A (F):	103.42	0.613	Ref-side Cap (tons):	1.83	0.05
Upstream Temp B (F):	103.44	0.089	Refrigerant Mdot (lbm/h):	312.41	8.42
Upstream Temp C (F):	103.22	0.613	Coriolis Density (lbm/ft3):	81.76	0.11
Upstream Average Temp (F):	103.36		Upstream R22 Tsat (F):	118.87	
Upstream Subcooling A (F):	15.45	0.823			
Upstream Subcooling B (F):	15.43	0.440			
Upstream Subcooling C (F):	15.65	0.709			
Average Subcooling (F):	15.51				
Evap Exit Pressure (psia):	90.50	0.243	Turbine A Frequency (Hz):	203.68	1.00
Evap Exit Avg Temp A:	74.20	0.561	Turb A Vol Flow (ft3/min):	0.0286	0.00
Evap Exit Avg Temp B:	74.23	0.853	Turb A Density (lbm/ft3):	70.54	0.09
Evap Exit Avg Temp C:	74.45	0.584	Turb A Mass Flow (lb/h):	121.00	0.72
Circuit A Superheat (F):	28.69	0.783	Turbine C Frequency (Hz):	175.48	1.00
Circuit B Superheat (F):	28.72	0.853	Turb C Vol Flow (ft3/min):	0.0256	0.00
Circuit C Superheat (F):	28.94	0.806	Turb C Density (lbm/ft3):	70.57	0.09
Overall Superheat (F):	29.39	0.604	Turb C Mass Flow (lb/h):	108.61	0.70
			Turb C Calculated Mass Flow (lbm/h):	82.79	8.69
Evap Circuit Temp 1 (F):	74.73	0.541	% Total Mass Flow Thru A:	38.73	1.19
Evap Circuit Temp 2 (F):	68.13	1.636	% Total Mass Flow Thru B:	26.50	2.13
Evap Circuit Temp 3 (F):	50.12	0.326	% Total Mass Flow Thru C:	34.77	1.08
Evap Circuit Temp 4 (F):	73.35	1.084			
Evap Circuit Temp 5 (F):	68.01	1.590			
Evap Circuit Temp 6 (F):	51.52	0.556			
Evap Circuit Temp 7 (F):	75.74	0.585			
Evap Circuit Temp 8 (F):	70.28	1.088			
Evap Circuit Temp 9 (F):	50.01	0.279			

A.6 Wavy fin evaporator with non-uniform airflow

Test names	Test type¹	Velocity ratio
W020522A	9	1:1
W020523A	9A	1:1.5
W020524A	9B	1:1.5
W020528B	9	1:1
W020528C	9A	1:2
W020529A	9B	1:2

SMART DISTRIBUTOR SUMMARY SHEET

DATA FILENAME: W020522A.dat SUMMARY FILENAME: W020522A.sum

Air-Side Conditions		Range	Total Air-Side Capacity:	22514.69	Range
Indoor Dry-Bulb :	79.9E0	0.36	Sensible Cap (Btu/h):	16410.41	769.28
Indoor Inlet Dew (F):	60.3E5	0.44	Latent Cap (Btu/h):	6104.28	555.80
Indoor Exit Dry-Bulb :	60.1E4	0.34	EvapAir Delta T (F):	20.35	358.61
Indoor Exit Dew (F):	59.8E5	0.34	Air/Ref Cap Frnt Diff:	1.56	0.44
			Sensible Heat Ratio:	0.729	4.23
			SCFM per Ton:	90.26	0.0150
Indoor Airflow (CFM):	740.98	9.54			
Indoor Airflow (SCFM):	732.22	9.38	(0.075 lb/ft3 stand air)		
Evap Inlet Humidity Ratio (lbH2O/lbAir):	0.011461				
Evap Exit Humidity Ratio (lbH2O/lbAir):	0.009714				
Barometric Pressure (in HG):	29.24		Nozzle Temp (F):	1.66	0.59
Air Chamber Nozzle Pressure Drop (in Water):	0.719	0.078			
Evaporator Coil Air Pressure Drop (in Water):	0.152	0.005			

Refrigerant Side Conditions					
Expansion Valve					
Upstream Pressure (psia):	306.67	1.4E1	Ref-side Cap (Btu/h):	22864.18	1037.16
Upstream Temp A (F):	105.20	0.0E6	Ref-side Cap (tons):	1.91	0.09
Upstream Temp B (F):	105.56	0.5E7	Refrigerant Mdot (lbm/h):	334.30	15.10
Upstream Temp C (F):	105.25	0.5E7	Coriolis Density (lbm/ft3):	82.44	0.21
Upstream Average Temp (F):	105.34		Upstream R22 Tsat (F):	128.66	
Upstream Subcooling A (F):	23.46	0.3E2			
Upstream Subcooling B (F):	23.10	0.6E3			
Upstream Subcooling C (F):	23.41	0.502			
Average Subcooling (F):	23.33				
Evap Exit Pressure (psia):	90.98	0.730	Turbine A Frequency (Hz):	215.95	2.00
Evap Exit Avg Temp A:	54.60	2.254	Turb A Vol Flow (ft3/min):	0.0302	0.00
Evap Exit Avg Temp B:	55.08	2.390	Turb A Density (lbm/ft3):	70.27	0.01
Evap Exit Avg Temp C:	54.97	2.163	Turb A Mass Flow (lb/h):	127.42	1.12
Circuit A Superheat (F):	8.74	1.942	Turbine C Frequency (Hz):	187.18	2.00
Circuit B Superheat (F):	9.22	2.096	Turb C Vol Flow (ft3/min):	0.0272	0.00
Circuit C Superheat (F):	9.11	2.163	Turb C Density (lbm/ft3):	70.26	0.09
Overall Superheat (F)	10.71	1.731	Turb C Mass Flow (lb/h):	114.72	1.26
			Circuit B Calculated Mass Flow (lbm/h):	92.17	14.97
Evap Circuit Temp 1 (F):	49.77	0.558	% Total Mass Flow Thru A:	38.12	1.74
Evap Circuit Temp 2 (F):	51.18	0.557	% Total Mass Flow Thru B:	27.56	3.27
Evap Circuit Temp 3 (F):	50.46	0.278	% Total Mass Flow Thru C:	34.32	1.53
Evap Circuit Temp 4 (F):	49.54	0.371			
Evap Circuit Temp 5 (F):	48.64	0.650			
Evap Circuit Temp 6 (F):	49.05	0.603			
Evap Circuit Temp 7 (F):	52.98	0.366			
Evap Circuit Temp 8 (F):	49.05	0.604			
Evap Circuit Temp 9 (F):	49.63	1.115			

SMART DISTRIBUTOR SUMMARY SHEET
 DATA FILENAME: W020523A.dat SUMMARY FILENAME: W020523A.sum

Air-Side Conditions	Range	Total Air-Side Capacity	Range
Indoor Dry-Bulb : 78.900	0.30	Sensible Cap (Btu/h): 21369.58	550.13
Indoor Inlet Dew (F) : 60.247	0.10	Latent Cap (Btu/h): 16030.95	471.81
Indoor Exit Dry-Bulb: 60.624	0.12	EvapAir Heat T (F): 18.75	178.27
Indoor Exit Dew (F) : 54.098	0.05	Air/Ref Cap Prct Diff: 2.88	0.43
		Sensible Heat Ratio: 0.740	3.55
Indoor Airflow (CFM): 746.69	7.28	SCFM per Ton: 408.17	0.0073
Indoor Airflow (SCFM): 737.07	7.12	(0.075 lb/ft3 standard air)	
Evap Inlet Humidity Ratio (lbH2O/lbAir):	0.011405		
Evap Exit Humidity Ratio (lbH2O/lbAir):	0.009801		
Barometric Pressure (in HG): 2.224	Nozzle Temp (F): 61.88	0.64	
Air Chamber Nozzle Pressure Dro (in Water):	0.729	0.014	
Evaporator Coil Air Pressure Dro (in Water):	0.199	0.008	

Refrigerant Side Conditions			
Expansion Valve			
Upstream Pressure (psia): 271.86	0.852	Ref-side Cap (Btu/h) : 22292.27	552.09
Upstream Temp A (F): 105.78	0.524	Ref-side Cap (tons):	1.86
Upstream Temp B (F): 106.14	0.524	Refrigerant Mdot (lbm/h):	330.43
Upstream Temp C (F): 105.72	0.567	Coriolis Density (lbm/ft3):	82.44
Upstream Average Temp (F): 105.88		Upstream R22 Tsat (F):	119.13
Upstream Subcooling A (F): 13.35	0.524		
Upstream Subcooling B (F): 12.98	0.594		
Upstream Subcooling C (F): 13.41	0.664		
Average Subcooling (F): 13.25			
Evap Exit Pressure (psia): 90.87	0.365	Turbine A Frequency (Hz):	214.67
Evap Exit Avg Temp A: 46.16	0.441	Turb A Vol Flow (ft3/min):	0.0300
Evap Exit Avg Temp B: 59.17	1.051	Turb A Density (lbm/ft3):	70.18
Evap Exit Avg Temp C: 62.86	1.024	Turb A Mass Flow (lb/h):	126.54
Circuit A Superheat (F): 0.36	0.441	Turbine C Frequency (Hz):	186.76
Circuit B Superheat (F): 13.37	1.160	Turb C Vol Flow (ft3/min):	0.0272
Circuit C Superheat (F): 17.06	1.024	Turb C Density (lbm/ft3):	70.19
Overall Superheat (F): 1.14	0.729	Turb C Mass Flow (lb/h):	114.36
		Turb C Calculated Mass Flow (lbm/h):	89.53
Evap <Circuits Temp 1 (F): 49.89	0.558	% Total Mass Flow Thru A:	38.30
Evap <Circuits Temp 2 (F): 50.53	0.741	% Total Mass Flow Thru B:	27.09
Evap <Circuits Temp 3 (F): 49.87	0.557	% Total Mass Flow Thru C:	34.61
Evap <Circuits Temp 4 (F): 49.13	0.696		
Evap <Circuits Temp 5 (F): 48.43	0.279		
Evap <Circuits Temp 6 (F): 49.07	0.558		
Evap <Circuits Temp 7 (F): 52.45	0.645		
Evap <Circuits Temp 8 (F): 49.36	0.558		
Evap <Circuits Temp 9 (F): 48.36	0.512		

SMART DISTRIBUTOR SUMMARY SHEET
 DATA FILENAME: W020524A.dat SUMMARY FILENAME: W020524A.sum

Air-Side Conditions		Range	Total Air-Side Capacity: 22297.78	Range
Indoor Dry-Bulb : 79.59		0.65	Sensible Cap (Btu/h): 1261.99	425.38
Indoor Inlet Dew (F): 60.65		0.26	Latent Cap (Btu/h): 2035.79	405.47
Indoor Exit Dry-Bulb: 60.28		0.41	EvapAir Delta T (F): 20.10	279.77
Indoor Exit Dew (F): 55.04		0.30	Air/Ref Cap Prnt Diff: 0.28	0.44
			Sensible Heat Ratio: 0.723	3.09
Indoor Airflow (CFM): 203.96		5.75	SCFM per Ton: 395.42	0.0110
Indoor Airflow (SCFM): 234.82		5.95	(0.075 lb/ft3 standard air)	
Evap Inlet Humidity Ratio (lbH2O/lbAir): 0.011453				
Evap Exit Humidity Ratio (lbH2O/lbAir): 0.009731				
Barometric Pressure (in xG): 29.24		Nozzle Temp (F): 61.23	0.011	
Air Chamber Nozzle Pressure Drop (in Water): 0.724			0.011	
Evaporator Coil Air Pressure Drop (in Water): 0.200			0.008	
Refrigerant Side Conditions				
Expansion Valve				
Upstream Pressure (psia): 279.51		0.731	Ref-side Cap (Btu/h): 22358.83	522.64
Upstream Temp A (F): 105.36		0.086	Ref-side Cap (tons): 1.86	0.04
Upstream Temp B (F): 105.77		0.611	Refrigerant Mdot (lbm/h): 326.72	7.41
Upstream Temp C (F): 105.44		0.524	Coriolis Density (lbm/ft3): 82.37	0.14
Upstream Average Temp (F): 105.53			Upstream R22 Tsat (F): 121.32	
Upstream Subcooling A (F): 15.95		0.224		
Upstream Subcooling B (F): 15.54		0.611		
Upstream Subcooling C (F): 15.88		0.558		
Average Subcooling (F): 15.79				
Evap Exit Pressure (psia): 90.79		0.486	Turbine A Frequency (Hz): 192.30	1.00
Evap Exit Avg Temp A: 56.12		1.630	Turb A Vol Flow (ft3/min): 0.0271	0.00
Evap Exit Avg Temp B: 57.04		1.812	Turb A Density (lbm/ft3): 70.25	0.01
Evap Exit Avg Temp C: 57.12		2.202	Turb A Mass Flow (lb/h): 114.12	0.58
Circuit A Superheat (F): 10.42		1.475	Turbine C Frequency (Hz): 198.00	2.00
Circuit B Superheat (F): 11.33		1.812	Turb C Vol Flow (ft3/min): 0.0287	0.00
Circuit C Superheat (F): 11.41		2.201	Turb C Density (lbm/ft3): 70.24	0.08
Overall Superheat (F): 12.16		1.257	Turb C Mass Flow (lb/h): 120.75	1.08
Circuit B Calculated Mass Flow (lbm/h): 34.93		% Total Mass Flow Thru A: 28.11		
Evap Circuit Temp 1 (F): 49.34		0.324	% Total Mass Flow Thru B: 36.96	1.00
Evap Circuit Temp 2 (F): 50.10		0.604		
Evap Circuit Temp 3 (F): 49.20		0.743		
Evap Circuit Temp 4 (F): 48.60		0.139		
Evap Circuit Temp 5 (F): 47.86		0.559		
Evap Circuit Temp 6 (F): 48.70		0.414		
Evap Circuit Temp 7 (F): 51.89		0.601		
Evap Circuit Temp 8 (F): 48.80		0.650		
Evap Circuit Temp 9 (F): 52.45		3.981		

DATA FILENAME: W020528B.dat SUMMARY FILENAME: W020528B.sum

SMART DISTRIBUTOR SUMMARY SHEET

Air-Side Conditions				Range	
Indoor Dry-Bulb	: 30.028	Range	Total Air-Side Capacity	22603	≤1
Indoor Inlet Dew (F)	: 30.360	0.45	Sensible Cap (Btu/h)	16466.36	489.00
Indoor Exit Dry-Bulb	: 30.090	0.17	Latent Cap (Btu/h)	≤177.2	251.94
Indoor Exit Dew (F)	: 33.773	0.23	EvapAir Delta T (m)	20.41	0.43
		0.20	Air/Ref Cap Prcnt Diff	0.69	4.12
			Sensible Heat Ratio	0.727	0.0109
Indoor Air Flow (CFM)	741.52	8.10	SCFM per Ton	388	38
Indoor Airflow (SCFM)	732.8	8.24	(0.075 g/fc3 standard air)		
Evap Inlet Humidity Ratio (lbH2O/lbAir)			0.011451		
Evap Exit Humidity Ratio (lbH2O/lbAir)			0.009684		
Barometric Pressure (in HG)	: 29.24	Nozzle Temp (F)	: 61.33	0.64	
Air Chamber Nozzle Pressure Drop (in Water)	: 0.720	0.016			
Evaporator Coil Air Pressure Drop (in Water)	: 0.153	0.006			

Refrigerant Side Conditions					
Expansion Valve					
Upstream Pressure (psia)	: 277.49	0.452	Ref-side Cap (Btu/h)	: 22798.19	090.12
Upstream Temp A (F)	: 105.26	0.324	Ref-Sub Temp	: 1.90	0.04
Upstream Temp B (F)	: 105.75	0.324	Refrigerant Mol (lbm/h)	: 333.16	≤.96
Upstream Temp C (F)	: 105.23	0.411	Coriolis Density (lbm/ft3)	: 82.40	0.15
Upstream Average Temp (F)	: 105.41		Upstr-Sub R22 Tsat (F)	: 120.72	
Upstream Subcooling A (m)	: 15.46	0.524			
Upstream Subcooling B (F)	: 14.98	0.643			
Upstream Subcooling C (F)	: 15.49	0.611			
Average Subcooling (F)	: 15.31				
Evap Exit Pressure (psia)	: 90.80	0.608	Turbine A Frequency (Hz)	: 215.22	1.00
Evap Exit Avg Temp A	: 56.32	1.102	Turb A Vol Flow (ft3/min)	: 0.0301	0.00
Evap Exit Avg Temp B	: 55.29	0.896	Turb A Density (lbm/ft3)	: 70.26	0.08
Evap Exit Avg Temp C	: 55.85	1.379	Turb A Mass Flow (lb/h)	: 126.99	0.49
Circuit A Superheat (F)	: 10.62	1.102	Turbine C Frequency (Hz)	: 187.44	1.00
Circuit B Superheat (F)	: 9.60	1.029	Turb C Vol Flow (ft3/min)	: 0.0272	0.00
Circuit C Superheat (m)	: 0.16	1.535	Turb C Density (lbm/ft3)	: 70.27	0.09
Overall Superheat (m)	: 1.61	1.139	Turb C Mass Flow (lb/h)	: 114.87	0.47
			Circuit B Calculated Mass Flow (g/m/h)	: 91.30	7.39
Evap Circuit temp 1 (F)	: 49.89	0.746	% Total Mass Flow thru A	: 38.12	0.05
Evap Circuit temp 2 (F)	: 50.99	0.357	% Total Mass Flow thru B	: 27.40	1.16
Evap Circuit temp 3 (F)	: 50.48	0.550	% Total Mass Flow thru C	: 34.48	0.43
Evap Circuit temp 4 (F)	: 49.77	0.697			
Evap Circuit temp 5 (F)	: 49.17	0.976			
Evap Circuit temp 6 (F)	: 48.88	0.403			
Evap Circuit temp 7 (F)	: 53.19	1.020			
Evap Circuit temp 8 (F)	: 49.55	1.023			
Evap Circuit temp 9 (F)	: 50.69	1.425			

SMART DISTRIBUTOR SUMMARY SHEET
 DATA FILENAME: W020528C.dat SUMMARY FILENAME: W020528C.sum

Air-Side Conditions		Range	Total Air-Side Capacity:	21085.08	Range
Indoor Dry-Bulb :	73.941	0.34	Sensible Cap (Btu/h):	15581.68	449.83
Indoor Inlet Dew (F) :	50.424	0.10	Latent Cap (Btu/h):	5503.40	399.80
Indoor Exit Dry-Bulb :	50.960	0.17	EvapAir Delta T (F):	19.40	160.10
Indoor Exit Dew (F) :	50.361	0.15	Air/Ref Cap Prct Diff:	5.17	0.43
			Sensible Heat Ratio:	0.739	4.14
			SCFM per Ton:	415.14	0.0092
Indoor Airflow (CFM):	739.51	7.97	(0.075 lb/ft3 standard air)		
Indoor Airflow (SCFM):	729.45	7.82	0.011478		
Evap Inlet Humidity Ratio (lbH2O/lbAir):			0.009896		
Evap Exit Humidity Ratio (lbH2O/lbAir):			Nozzle Temp (F):	62.18	0 ≤4
Barometric Pressure (in HG):	29.24		Nozzle Temp (F):	0.715	0.015
Air Chamber Nozzle Pressure Drop (in Water):			0.214	0.010	
Evaporator Coil Air Pressure Drop (in Water):					

Refrigerant Side Conditions					
Expansion Valve					
Upstream Pressure (psia):	269.87	1.218	Ref-side Cap (Btu/h):	22173.27	535.33
Upstream Temp A (F):	103.87	0.524	Ref-side Cap (tons):	1.85	0.04
Upstream Temp B (F):	104.35	0.525	Refrigerant Mdot (lbm/h):	325.78	7.87
Upstream Temp C (F):	103.86	0.481	Coriolis Density (lbm/ft3):	81.91	0.18
Upstream Average Temp (F):	104.03		Upstream R22 Tsat (F):	118.55	
Upstream Subcooling A (F):	14.68	0.663			
Upstream Subcooling B (F):	14.20	0.420			
Upstream Subcooling C (F):	14.70	0.517			
Average Subcooling (F):	14.52				
Evap Exit Pressure (psia):	91.43	0.486	Turbine A Frequency (Hz):	209.64	3.00
Evap Exit Avg Temp A:	46.33	0.372	Turb A Vol Flow (ft3/min):	0.0294	0.00
Evap Exit Avg Temp B:	58.24	0.824	Turb A Density (lbm/ft3):	70.48	0.08
Evap Exit Avg Temp C:	64.31	0.363	Turb A Mass Flow (lb/h):	124.23	1.55
Circuit A Superheat (F):	0.26	0.527	Turbine C Frequency (Hz):	182.45	1.00
Circuit B Superheat (F):	12.16	0.980	Turb C Vol Flow (ft3/min):	0.0266	0.00
Circuit C Superheat (F):	18.24	0.441	Turb C Density (lbm/ft3):	70.48	0.07
Overall Superheat (F):	0.90	0.436	Turb C Mass Flow (lb/h):	112.40	0.68
			Turb C Calculated Mass Flow (lbm/h):	89.14	7.53
Evap Inlet Temp 1 (F):	50.19	0.557	% Total Mass Flow Thru A:	38.14	0.86
Evap Inlet Temp 2 (F):	50.65	0.650	% Total Mass Flow Thru B:	27.36	1.68
Evap Inlet Temp 3 (F):	49.90	0.650	% Total Mass Flow Thru C:	34.50	0.98
Evap Inlet Temp 4 (F):	49.61	0.558			
Evap Inlet Temp 5 (F):	48.98	0.651			
Evap Inlet Temp 6 (F):	49.47	0.558			
Evap Inlet Temp 7 (F):	52.53	0.600			
Evap Inlet Temp 8 (F):	49.91	0.325			
Evap Inlet Temp 9 (F):	48.85	0.651			

DATA FILENAME: W020529A.dat SUMMARY FILENAME: W020529A.sum

Air-Side Conditions			Range	Total Air-Side Capacity:	21520.92	640.29
Indoor Dry-Bulb	73.933	0.50	Sensible Cap (Btu/h):	15838.75	469.14	
Indoor Inlet Dew (F)	60.230	0.21	Latent Cap (Btu/h):	5682.17	361.99	
Indoor Exit Dry-Bulb:	60.603	0.24	EvapAir Delta T (F):	19.75	0.43	
Indoor Exit Dew (F):	54.033	0.25	Air/Ref Cap Prcnt Diff:	0.26	3.87	
			Sensible Heat Ratio:	0.736	0.0159	
Indoor Airflow (CFM):	737.94	9.18	SCFM per Ton:	406.15		
Indoor Airflow (SCFM):	728.40	9.17	(0.075 lb/ft3 standard air)			
Evap Inlet Humidity Ratio (lbH2O/lbAir)			0.011422			
Evap Exit Humidity Ratio (lbH2O/lbAir)			0.009787			
Barometric Pressure (in HG):	29.24		Nozzle Temp (F):	61.76	0.55	
Air Chamber Nozzle Pressure Drop (in Water):			0.712	0.018		
Evaporator Coil Air Pressure Drop (in Water):			0.236	0.006		

Refrigerant Side Conditions						
Expansion Valve						
Upstream Pressure (psia):	321.32	1.218	Ref-side Cap (Btu/h):	21575.13	53.24	
Upstream Temp A (F):	104.25	0.262	Ref-side Cap (tons):	1.80	0.05	
Upstream Temp B (F):	104.91	0.524	Refrigerant Mdot (lbm/h):	314.00	9.43	
Upstream Temp C (F):	104.48	0.306	Coriolis Density (lbm/ft3):	82.37	0.12	
Upstream Average Temp (F):	104.55		Upstream R22 Tsat (F):	132.44		
Upstream Subcooling A (F):	28.18	0.385				
Upstream Subcooling B (F):	27.52	0.448				
Upstream Subcooling C (F):	27.96	0.399				
Average Subcooling (F):	27.89					
Evap Exit Pressure (psia):	91.11	0.486	Turbine A Frequency (Hz):	173.30	2.00	
Evap Exit Avg Temp A:	55.99	1.378	Turb A Vol Flow (ft3/min):	0.0245	0.00	
Evap Exit Avg Temp B:	55.99	1.493	Turb A Density (lbm/ft3):	70.42	0.04	
Evap Exit Avg Temp C:	55.87	2.022	Turb A Mass Flow (lb/h):	103.72	1.13	
Circuit A Superheat (F):	10.17	1.378	Turbine C Frequency (Hz):	199.25	1.00	
Circuit B Superheat (F):	10.17	1.493	Turb C Vol Flow (ft3/min):	0.0288	0.00	
Circuit C Superheat (F):	10.05	2.022	Turb C Density (lbm/ft3):	70.38	0.05	
Overall Superheat (F)	11.47	1.166	Turb C Mass Flow (lbm/h):	121.71	0.63	
			Calculated Mass Flow (lbm/h):	88.57	9.20	
Circuit Temp 1 (F):	49.26	0.369	% Total Mass Flow Thru A:	33.03	0.94	
Circuit Temp 2 (F):	50.18	0.557	% Total Mass Flow Thru B:	28.20	2.10	
Circuit Temp 3 (F):	49.06	0.651	% Total Mass Flow Thru C:	38.76	1.30	
Circuit Temp 4 (F):	48.60	0.279				
Circuit Temp 5 (F):	47.81	0.559				
Circuit Temp 6 (F):	48.80	0.649				
Circuit Temp 7 (F):	51.84	0.501				
Circuit Temp 8 (F):	49.01	0.279				
Circuit Temp 9 (F):	53.97	3.328				

A.7 Enhanced fin (wavy-lanced) evaporator with non-uniform airflow

Table A.7.1: Enhanced-Cut Fin (Wavy-Lanced) Evaporator with Non-Uniform Airflow

Test names	Test type ¹	Velocity ratio
E020604A	9	1:1
E020604B	9A	1:1.26
E020605A	9B	1:1.26
E020607A	9	1:1
E020607B	9A	1:1.36
E020610A	9B	1:1.36
E020611A	9A	1:1.62
E020612A	9B	1:1.62
E020613A	9A	1:1.75
E020620A	9B	1:1.75
E020621A	9A	1:2.59
E020624A	9B	1:2.59

airflow and no superheat adjustment, 9B: expansion valves adjusted to yield 5.6 °C (10.0 °F) superheat on all circuits with non-uniform airflow.

SMART DISTRIBUTOR SUMMARY SHEET
 DATA FILENAME: E020604A.dat SUMMARY FILENAME: E020604A.sum

Air-Side Conditions		Rate	Total Air-Side Capacity:	Range
Indoor Dry-Bulb :	80.206	Q47	Sensible Cap (Btu/h): 23833.08	462.48
Indoor Inlet Dew (F):	80.500	Q26	Latent Cap (Btu/h): 17220.20	445.58
Indoor Exit Dry-Bulb:	89.854	Q33	EvapAir Delta T (F): 20.83	271.87
Indoor Exit Dew (F):	85.712	Q25	Air/Ref Cap Prcnt Diff: -1.50	0.43
			Sensible Heat Ratio: 0.723	3.11
			SCFM per Ton: 378.03	0.0110
Indoor Airflow (CFM):	759.74	10.21	(0.075 lb/ft3 standard air)	
Indoor Airflow (SCFM):	750.80	10.05	0.011509	
Evap Inlet Humidity Ratio (lbH2O/lbAir):			0.009663	
Barometric Pressure (in HG):	29.24	Nozzle Temp (F):	61.3	0.37
Air Chamber Nozzle Pressure Drop (in Water):	0.756		0.020	
Evaporator Coil Air Pressure Drop (in Water):	0.372		0.016	

Refrigerant Side Conditions				
Expansion Valve				
Upstream Pressure (psia):	275.71	0.731	Ref-side Cap (Btu/h):	23476.20
Upstream Temp A (F):	103.90	0.043	Ref-side Cap (tons):	1.96
Upstream Temp B (F):	104.21	0.306	Refrigerant Mdot (lbm/h):	340.40
Upstream Temp C (F):	104.02	0.524	Coriolis Density (lbm/ft3):	81.94
Upstream Average Temp (F):	104.04		Upstream R22 Tsat (F):	120.22
Upstream Subcooling A (F):	16.32	0.208		
Upstream Subcooling B (F):	16.01	0.401		
Upstream Subcooling C (F):	16.20	0.782		
Average Subcooling (F):	16.18			
Evap Exit Pressure (psia):	91.05	0.973	Turbine A Frequency (Hz):	215.39
Evap Exit Avg Temp A:	56.46	2.755	Turb A Vol Flow (ft3/min):	0.0301
Evap Exit Avg Temp B:	56.19	3.166	Turb A Density (lbm/ft3):	70.47
Evap Exit Avg Temp C:	55.97	4.415	Turb A Mass Flow (lb/h):	127.46
Circuit A Superheat (F):	10.53	2.773	Turbine C Frequency (Hz):	197.67
Circuit B Superheat (F):	10.26	3.166	Turb C Vol Flow (ft3/min):	0.0286
Circuit C Superheat (F):	10.04	4.393	Turb C Density (lbm/ft3):	70.45
Overall Superheat (F)	12.80	1.178	Turb C Mass Flow (lb/h):	120.94
		Circuit B	Calculated Mass Flow (lbm/h):	92.00
ΣV300 Circuit Temp 1 (F):	50.01	0.557	% Total Mass Flow Thru A:	37.45
ΣV300 Circuit Temp 2 (F):	50.00	0.372	% Total Mass Flow Thru B:	27.02
ΣV300 Circuit Temp 3 (F):	49.88	0.557	% Total Mass Flow Thru C:	35.53
ΣV300 Circuit Temp 4 (F):	48.93	0.558		
ΣV300 Circuit Temp 5 (F):	48.77	0.279		
ΣV300 Circuit Temp 6 (F):	49.34	0.558		
ΣV300 Circuit Temp 7 (F):	51.88	0.646		
ΣV300 Circuit Temp 8 (F):	49.06	0.558		
ΣV300 Circuit Temp 9 (F):	50.57	0.557		

SMART DISTRIBUTOR SUMMARY SHEET
 DATA FILENAME: E020604B.dat SUMMARY FILENAME: E020604B.sum

Air-Side Conditions		Range
Indoor Dry-Bulb	73.937	336.15
Indoor Inlet Dew (F)	60.484	317.97
Indoor Exit Dry-Bulb	53.911	294.02
Indoor Exit Dew (F)	53.688	0.22
Indoor Airflow (CFM)	762.89	1.89
Indoor Airflow (SCFM)	753.71	0.0113
Evap Inlet Humidity Ratio (lbH2O/lbAir)	0.011503	
Evap Exit Humidity Ratio (lbH2O/lbAir)	0.009654	
Barometric Pressure (in HG)	29.24	
Air Chamber Nozzle Pressure Drop (in Water)	0.762	0.82
Evaporator Coil Air Pressure Drop (in Water)	0.435	0.019

Refrigerant Side Conditions		
Expansion Valve		
Upstream Pressure (psia)	274.33	436.80
Upstream Temp A (F)	103.65	0.04
Upstream Temp B (F)	104.04	7.14
Upstream Temp C (F)	103.68	0.19
Upstream Average Temp (F)	103.79	
Upstream Subcooling A (F)	16.19	
Upstream Subcooling B (F)	15.80	
Upstream Subcooling C (F)	16.16	
Average Subcooling (F)	16.05	
Evap Exit Pressure (psia)	90.33	
Evap Exit Avg Temp A	46.75	
Evap Exit Avg Temp B	60.86	
Evap Exit Avg Temp C	64.18	
Circuit A Superheat (F)	1.31	
Circuit B Superheat (F)	15.41	
Circuit C Superheat (F)	18.74	
Overall Superheat (F)	7.22	
Circuit B Calculated Mass Flow (lbm/h)		
Circuit Temp 1 (F)	49.74	214.28
Circuit Temp 2 (F)	49.45	0.0300
Circuit Temp 3 (F)	49.28	0.08
Circuit Temp 4 (F)	48.54	1.13
Circuit Temp 5 (F)	48.45	1.00
Circuit Temp 6 (F)	48.80	0.0285
Circuit Temp 7 (F)	51.16	0.04
Circuit Temp 8 (F)	48.77	0.63
Circuit Temp 9 (F)	49.05	0.74
Turbine A Frequency (Hz)		
Turb A Vol Flow (ft3/min)	0.419	37.26
Turb A Density (lbm/ft3)	1.506	27.39
Turb A Mass Flow (lb/h)	1.227	35.35
Turbine C Frequency (Hz)	0.419	
Turb C Vol Flow (ft3/min)	1.369	
Turb C Density (lbm/ft3)	1.227	
Turb C Mass Flow (lb/h)	4.196	
% Total Mass Flow Thru A	0.648	
% Total Mass Flow Thru B	0.558	
% Total Mass Flow Thru C	0.557	

SMART DISTRIBUTOR SUMMARY SHEET
 DATA FILENAME: E020605A.dat SUMMARY FILENAME: E020605A.sum

Air-Side Conditions		Range	Total Air-Side Capacity: 23983.95	Range
Indoor Dry-Bulb :	73.983	0.42	Sensible Cap (Btu/h): 17310.40	393.40
Indoor Wet-Dew (F):	60.310	0.20	Latent Cap (Btu/h): 6673.55	380.89
Indoor Exit Dry-Bulb:	53.630	0.28	EvapAir Delta T (F): 20.85	229.49
Indoor Exit Dew (F):	53.463	0.20	Air/Ref Cap Prcnt Diff: -1.22	0.43
			Sensible Heat Ratio: 0.722	2.30
Indoor Airflow (CFM):	762.67	7.99	SCFM per Ton: 377.23	0.0076
Indoor Airflow (SCFM):	753.95	7.96	(0.075 lb/ft3 standard air)	
Evap Inlet Humidity Ratio (lbH2O/lbAir):	0.011431			
Evap Exit Humidity Ratio (lbH2O/lbAir):	0.009575			
Barometric Pressure (in HG):	29.24	Nozzle Temp (F): 60.85	0.37	
Air Chamber Nozzle Pressure Drop (in Water):	0.762	0.016		
Evaporator Coil Air Pressure Drop (in Water):	0.428	0.012		

Refrigerant Side Conditions				
Expansion Valve				
Upstream Pressure (psia):	271.09	0.365	Ref-side Cap (Btu/h) :	23689.75
Upstream Temp A (F):	104.46	0.262	Ref-side Cap (tons):	1.97
Upstream Temp B (F):	105.00	0.612	Refrigerant Mdot (lbm/h):	344.83
Upstream Temp C (F):	104.66	0.350	Coriolis Density (lbm/ft3):	82.15
Upstream Average Temp (F):	104.71		Upstream R22 Tsat (F):	118.89
Upstream Subcooling A (F):	14.43	0.237		
Upstream Subcooling B (F):	13.89	0.603		
Upstream Subcooling C (F):	14.24	0.330		
Average Subcooling (F):	14.19			
Evap Exit Pressure (psia):	90.36	0.486	Turbine A Frequency (Hz):	209.06
Evap Exit Avg Temp A:	55.17	3.217	Turb A Vol Flow (ft3/min):	0.0293
Evap Exit Avg Temp B:	55.33	2.528	Turb A Density (lbm/ft3):	70.39
Evap Exit Avg Temp C:	54.76	2.600	Turb A Mass Flow (lb/h):	123.75
Circuit A Superheat (F):	9.70	3.061	Turbine C Frequency (Hz):	206.71
Circuit B Superheat (F):	9.87	2.685	Turb C Vol Flow (ft3/min):	0.0298
Circuit C Superheat (F):	9.29	2.600	Turb C Density (lbm/ft3):	70.36
Overall Superheat (F)	12.49	1.533	Turb C Mass Flow (lb/h):	125.86
			Turb C Calculated Mass Flow (lbm/h):	95.22
Evap Circuit Temp 1 (F):	49.38	0.091	Total Mass Flow Thru A:	35.89
Evap Circuit Temp 2 (F):	49.90	0.373	Total Mass Flow Thru B:	27.61
Evap Circuit Temp 3 (F):	49.48	0.557	Total Mass Flow Thru C:	36.50
Evap Circuit Temp 4 (F):	48.28	0.279		
Evap Circuit Temp 5 (F):	48.19	0.467		
Evap Circuit Temp 6 (F):	48.64	0.279		
Evap Circuit Temp 7 (F):	51.45	0.278		
Evap Circuit Temp 8 (F):	48.50	0.558		
Evap Circuit Temp 9 (F):	49.50	1.069		

SMART DISTRIBUTOR SUMMARY SHEET

DATA FILENAME: E020607A.dat SUMMARY FILENAME: E020607A.sum

Air-Side Conditions		Range	Total Air-Side Capacity:	23732.88	Range
Indoor Dry-Bulb :	79.851	0.39	Sensible Cap (Btu/h):	17252.27	459.67
Indoor Inlet Dew (F):	50.360	0.11	Latent Cap (Btu/h):	6480.61	350.17
Indoor Exit Dry-Bulb:	59.725	0.19	Evap Air Dew Pt (m):	20.59	153.02
Indoor Exit Dew (F):	55.721	0.15	Air/Ref Cap Prct Diff:	-0.48	0.22
			Sensible Heat Ratio:	0.727	3.41
Indoor Airflow (CFM):	769.76	7.65	SCFM per Ton:	384.78	0.0062
Indoor Airflow (SCFM):	760.95	7.53	(0.075 lb/ft ³ standard air)		
Evap Inlet Humidity Ratio (lbH2O/lbAir):			0.011451		
Evap Exit Humidity Ratio (lbH2O/lbAir):			0.009888		
Barometric Pressure (in HG)	29.24		Nozzle Temp (F):	60.70	0.84
Air Chamber Nozzle Pressure Drop (in Water):			0.776	0.015	
Evaporator Coil Air Pressure Drop (in Water):			0.340	0.008	

Refrigerant Side Conditions					
Expansion Valve					
Upstream Pressure (psia):	273.97	0.809	Ref-side Cap (Btu/h):	23619.08	522.68
Upstream Temp A (F):	105.06	0.810	Ref-Hiwe Cap (tons):	1.97	0.04
Upstream Temp B (F):	105.52	0.262	Refrigerant Mdot (lbm/h):	344.39	1.78
Upstream Temp C (F):	105.08	0.524	Coriolis Density (lbm/ft ³):	82.28	0.08
Upstream Average Temp (F):	105.22		Upstream R22 Tsat (F):	119.69	
Upstream Subcooling A (F):	14.63	0.644			
Upstream Subcooling B (F):	14.17	0.297			
Upstream Subcooling C (F):	14.62	0.524			
Average Subcooling (F):	14.47				
Vap Exit Pressure (psia):	90.83	0.486	Turbine A Frequency (Hz):	221.44	1.00
Vap Exit Avg Temp A:	55.73	1.283	Turb A Vol Flow (ft ³ /min):	0.0309	0.00
Vap Exit Avg Temp B:	55.97	1.747	Turb A Density (lbm/ft ³):	70.29	0.09
Vap Exit Avg Temp C:	55.76	2.343	Turb A Mass Flow (lb/h):	130.53	0.71
Cir-uit A Superheat (F):	10.04	1.419	Turbine C Frequency (Hz):	198.44	1.00
Cir-uit B Superheat (F):	10.23	1.668	Turb C Vol Flow (ft ³ /min):	0.0287	0.00
Cir-uit C Superheat (F):	10.02	2.656	Turb C Density (lbm/ft ³):	70.29	0.08
Overall Superheat (m)	12.83	1.223	Turb C Mass Flow (lb/h):	121.09	0.59
Cir-uit Temp 1 (F):	49.92	0.279	Calculated Mass Flow (lbm/h):	92.76	8.08
Cir-uit Temp 2 (F):	51.11	0.557	Total Mass Flow (m/hr):	37.90	0.93
Cir-uit Temp 3 (F):	50.37	0.649	Total Mass Flow (m/hr):	26.93	1.81
Circuit Temp 4 (m):	49.15	0.558	Total Mass Flow (m/hr):	35.16	0.93
Circuit Temp 5 (m):	49.04	0.325			
Circuit Temp 6 (F):	49.12	0.368			
Circuit Temp 7 (F):	53.23	0.644			
Circuit Temp 8 (F):	49.02	0.558			
Circuit Temp 9 (F):	49.96	0.279			

SMART DISTRIBUTOR SUMMARY SHEET
 DATA FILENAME: E020607B.dat SUMMARY FILENAME: E020607B.sum

Air-Side Conditions		Range	Total Air-Side Capacity: 23191.63	Range
Indoor Dry-Bulb :	78.867	0.30	Sensible Cap (Btu/h): 17080.76	450.61
Indoor Inlet Dew (F) :	80.810	0.12	Latent Cap (Btu/h): 6110.87	474.14
Indoor Exit Dry-Bulb :	80.086	0.16	EvapAir Delta T (F): 20.41	116.49
Indoor Exit Dew (F) :	81.842	0.10	Air/Ref Cap Prcnt Diff: -0.36	0.43
			Sensible Heat Ratio: 0.736	3.03
			SCFM per Ton: 393.27	0.0062
Indoor Airflow (CFM) :	769.56	8.57		
Indoor Airflow (SCFM) :	760.05	8.42	(0.075 lb/ft3 standard air)	
Evap Inlet Humidity Ratio (ϕ H2O/lbAir) :			0.011430	
Evap Exit Humidity Ratio (ϕ H2O/lbAir) :			0.009745	
Barometric Pressure (in ϕ G) :	29.24		Nozzle Temp (F): 61.10	0.73
Air Chamber Nozzle Pressure (in Water) :			0.775	0.017
Evaporator Coil Air Pressure Drop (in Water) :			0.413	0.014

Refrigerant Side Conditions				
Expansion Valve				
Upstream Pressure (psia) :	269.24	0.365	Ref-side Cap (Btu/h) :	23106.51
Upstream Temp A (F) :	104.31	0.697	Ref-side Cap (tons) :	1.93
Upstream Temp B (F) :	104.74	0.700	Refrigerant Mdot (lbm/h) :	340.01
Upstream Temp C (F) :	104.37	0.654	Coriolis Density (lbm/ft3) :	82.09
Upstream Average Temp (F) :	104.48		Upstream R22 Tsat (F) :	118.36
Upstream Subcooling A (F) :	14.05	0.732		
Upstream Subcooling B (F) :	13.62	0.736		
Upstream Subcooling C (F) :	13.99	0.646		
Average Subcooling (F) :	13.88			
Evap Exit Pressure (psia) :	90.73	0.365	Turbine A Frequency (Hz) :	217.50
Evap Exit Avg Temp A :	46.35	0.304	Turb A Vol Flow (ft3/min) :	0.0304
Evap Exit Avg Temp B :	60.82	0.728	Turb A Density (lbm/ft3) :	70.41
Evap Exit Avg Temp C :	65.84	0.860	Turb A Mass Flow (lb/h) :	128.53
Circuit A Superheat (F) :	0.70	0.520	Turbine C Frequency (Hz) :	194.29
Circuit B Superheat (F) :	15.17	0.963	Turb C Vol Flow (ft3/min) :	0.0282
Circuit C Superheat (F) :	20.19	1.126	Turb C Density (lbm/ft3) :	70.40
Overall Superheat (F) :	1.81	1.038	Turb C Mass Flow (lb/h) :	118.94
			Turb B Calculated Mass Flow (lbm/h) :	92.54
Evap Circuit Temp 1 (F) :	49.66	0.513	% Total Mass Flow Thru A :	37.80
Evap Circuit Temp 2 (F) :	50.55	0.276	% Total Mass Flow Thru B :	27.21
Evap Circuit Temp 3 (F) :	49.87	0.464	% Total Mass Flow Thru C :	34.98
Evap Circuit Temp 4 (F) :	48.90	0.512		
Evap Circuit Temp 5 (F) :	48.60	0.651		
Evap Circuit Temp 6 (F) :	48.94	0.648		
Evap Circuit Temp 7 (F) :	52.71	0.555		
Evap Circuit Temp 8 (F) :	48.88	0.604		
Evap Circuit Temp 9 (F) :	49.12	0.512		

SMART DISTRIBUTOR SUMMARY SHEET
 DATA FILENAME: E020610A.dat SUMMARY FILENAME: E020610A.sum

Air-Side Conditions				Range
Indoor Dry-Bulb	: 78.897	Total Air-Side Capacity:	23226.10	446.20
Indoor Inlet Dew (F)	: 60.349	Sensible Cap (Btu/h)	: 6802.07	476.20
Indoor Exit Dry-Bulb	: 60.164	Latent Cap (Btu/h)	: 6424.03	235.43
Indoor Exit Dew (F)	: 58.729	EvapAir Delta T (F)	: 20.15	0.44
		Air/Ref Cap Prnt Diff:	: -0.85	3.18
		Sensible Heat Ratio:	: 0.723	0.0112
Indoor Airflow (CFM)	: 766.90	SCFM per Ton:	391.30	
Indoor Airflow (SCFM)	: 757.36	(0.075 lb/ft3 standard air		
Evap Inlet Humidity Ratio (lbH2O/lbAir)	: 0.011447			
Evap Exit Humidity Ratio (lbH2O/lbAir)	: 0.009668			
Barometric Pressure (in HG)	: 29.24	Nozzle Temp (F)	: 61.39	≤0
Air Chamber Nozzle Pressure Drop (in Water)	: 0.769		0.012	
Evaporator Coil Air Pressure Drop (in Water)	: 0.409		0.012	

Refrigerant Side Conditions				
Expansion Valve				
Upstream Pressure (psia)	: 274.91	0.487	Ref-size Cap (Btu/h)	: 23028.12
Upstream Temp A (F)	: 105.46	0.524	Ref-size Cap (tons)	: 1.92
Upstream Temp B (F)	: 106.05	0.524	Refrigerant Mdot (lbm/h)	: 386.43
Upstream Temp C (F)	: 105.62	0.262	Coriolis Mdot (lbm/ft3)	: 82.44
Upstream Average Temp (F)	: 105.71		Upstream R Tsat (F)	: 119.98
Upstream Subcooling A (F)	: 14.52	0.593		
Upstream Subcooling B (F)	: 13.93	0.663		
Upstream Subcooling C (F)	: 14.36	0.331		
Average Subcooling (F)	: 14.27			
Evap Exit Pressure (psia)	: 91.15	0.486	Turbine A Frequency (Hz)	: 201.47
Evap Exit Avg Temp A:	567.2	1.720	Turb A Vol Flow (ft3/min)	: 0.0283
Evap Exit Avg Temp B:	561.8	1.652	Turb A Density (lbm/ft3)	: 70.23
Evap Exit Avg Temp C:	566.3	2.112	Turb A Mass Flow (lb/h)	: 119.23
Circuit A Superheat (F)	: 107.3	1.824	Turbine C Frequency (Hz)	: 203.89
Circuit B Superheat (F)	: 101.9	1.808	Turb C Vol Flow (ft3/min)	: 0.0294
Circuit C Superheat (F)	: 106.4	1.957	Turb C Density (lbm/ft3)	: 70.21
Overall Superheat (F)	: 128.9	1.268	Turb C Mass Flow (lb/h)	: 124.02
		Circuit B Calculated Mass Flow (lbm/h)	: 93.18	5.88
Evap Circuit Temp 1 (F)	: 49.2	0.558	% Total Mass Flow Thru A	: 35.44
Evap Circuit Temp 2 (F)	: 50.0	0.557	% Total Mass Flow Thru B	: 27.70
Evap Circuit Temp 3 (F)	: 49.9	0.510	% Total Mass Flow Thru C	: 36.86
Evap Circuit Temp 4 (F)	: 48.8	0.605		
Evap Circuit Temp 5 (F)	: 48.9	0.512		
Evap Circuit Temp 6 (F)	: 48.8	0.558		
Evap Circuit Temp 7 (F)	: 52.9	0.556		
Evap Circuit Temp 8 (F)	: 48.8	0.558		
Evap Circuit Temp 9 (F)	: 51.2	1.392		

SMART DISTRIBUTOR SUMMARY SHEET

DATA FILENAME: E020611A.dat SUMMARY FILENAME: E020611A.sum

Air-Side Conditions		Range	Metal Air-Side Capacity:	23033.79	Range
Indoor Dry-Bulb :	78.524	0.22	Sensible Cap (Btu/h):	16747.09	239.47
Indoor Inlet Dew (F):	80.597	0.11	Latent Cap (Btu/h):	6286.70	210.65
Indoor Exit Dry-Bulb:	80.564	0.24	EvapAir Delta T (F):	20.05	141.28
Indoor Exit Dew (F):	81.598	0.15	Air/Ref Cap Prcnt Diff:	1.14	0.22
			Sensible Heat Ratio:	0.727	2.25
			SCFM per Ton:	395.17	0.0059
Indoor Airflow (CFM):	768.41	7.65	(0.075 lb/ft3 standard air)		
Indoor Airflow (SCFM):	758.53	7.57	0.011467		
Evap Inlet Humidity Ratio (lbH2O/lbAir):			0.009729		
Evap Exit Humidity Ratio (lbH2O/lbAir):			Nozzle Temp (F):	61.63	0.37
Barometric Pressure (in HG):	29.24		Nozzle Temp (F):	0.772	0.015
Air Chamber Nozzle Pressure Drop (in Water):			0.406	0.006	
Evaporator Coil Air Pressure Drop (in Water):					

Refrigerant Side Conditions					
Expansion Valve					
Upstream Pressure (psia):	289.57	1.027	Ref-sive Cap (Btu/h):	23295.57	0.90.2E
Upstream Temp A (F):	104.07	0.299	Ref-sive Cap (tons):	1.90	0.00
Upstream Temp B (F):	104.49	0.525	Refrigerant Mdot (lbm/h):	342.69	7.23
Upstream Temp C (F):	104.19	0.262	Coriolis Density (lbm/ft3):	82.15	0.30
Upstream Average Temp (F):	104.25		Upstream R22 Tsat (F):	124.07	
Upstream Subcooling A (F):	20.00	0.825			
Upstream Subcooling B (F):	19.58	0.725			
Upstream Subcooling C (F):	19.89	0.555			
Average Subcooling (F):	19.82				
Evap Exit Pressure (psia):	90.45	0.482	Turbine A Frequency (Hz):	50574.87	565315 00
Evap Exit Avg Temp A:	46.14	0.372	Turb A Vol Flow (ft3/min):	0.6098	8.68
Evap Exit Avg Temp B:	59.66	1.532	Turb A Density (lbm/ft3):	70.45	0.11
Evap Exit Avg Temp C:	67.10	1.200	Turb A Mass Flow (lb/h):	2578.31	36720 Z5
Circuit A Superheat (F):	0.62	0.326	Turbine C Frequency (Hz):	180.33	195.00
Circuit B Superheat (F):	14.15	1.532	Turb C Vol Flow (ft3/min):	0.0263	0.03
Circuit C Superheat (F):	21.58	1.357	Turb C Density (lbm/ft3):	70.43	0.04
Overall Superheat (F):	1.37	0.437	Turb C Mass Flow (lb/h):	111.12	109.96
			Turb C Calculated Mass Flow (lbm/h):	2346.75	36617.35
vap Circuit Temp 1 (F):	48.67	0.324	% Total Mass Flow Thru A:	757.96	10799.68
vap Circuit Temp 2 (F):	50.15	0.251	% Total Mass Flow Thru B:	690.37	10768.28
vap Circuit Temp 3 (F):	48.75	0.325	% Total Mass Flow Thru C:	32.41	32.15
vap Circuit Temp 4 (F):	48.66	0.093			
vap Circuit Temp 5 (F):	48.38	0.605			
vap Circuit Temp 6 (F):	48.65	0.649			
vap Circuit Temp 7 (F):	52.21	0.278			
vap Circuit Temp 8 (F):	49.02	0.465			
vap Circuit Temp 9 (F):	49.24	0.558			

SMART DISTRIBUTOR SUMMARY SHEET
 DATA FILENAME: E020612A.dat SUMMARY FILENAME: E020612A.sum

Air-Side Conditions		Range	Total Air-Side Capacity:	23591.22	Range
Indoor Dry-Bulb :	73.802	0.40	Sensible Cap (Btu/h):	16924.82	284.07
Indoor Inlet Dew (F):	60.323	0.21	Latent Cap (Btu/h):	6666.40	234.35
Indoor Exit Dry-Bulb:	53.765	0.28	EvapAir Delta T (F):	20.49	213.13
Indoor Exit Dew (F):	53.458	0.25	Air/Ref Cap Prcnt Diff:	-1.34	0.22
			Sensible Heat Ratio:	0.717	2.63
			SCFM per Ton:	381.56	0.0078
Indoor Airflow (CFM):	758.94	7.46	(0.075 lb/ft3 standard air)		
Indoor Airflow (SCFM):	750.11	7.31	0.011436		
Evap Inlet Humidity Ratio (lbH2O/lbAir):			0.009573		
Evap Exit Humidity Ratio (lbH2O/lbAir):			Nozzle Temp (F):	60.70	0.37
Barometric Pressure (in HG):	29.24		0.754	0.015	
Air Chamber Nozzle Pressure Drop (in Water):			0.407	0.009	
Evaporator Coil Air Pressure Drop (in Water):					

Refrigerant Side Conditions					
Expansion Valve					
Upstream Pressure (psia):	310.59	0.244	R ₂₂ -side Cap (Btu/h):	23275.77	482.97
Upstream Temp A (F):	103.56	0.612	Ref-side Cap (tons):	1.94	0.04
Upstream Temp B (F):	104.04	0.175	R ₂₂ refrigerant Mdot (lbm/h):	337.47	6.41
Upstream Temp C (F):	103.73	0.568	Coriolis Density (1 m/ft3):	81.98	0.14
Upstream Average Temp (F):	103.78		Upstream R22 T _{sat} (F):	129.68	
Upstream Subcooling A (F):	26.13	0.675			
Upstream Subcooling B (F):	25.64	0.208			
Upstream Subcooling C (F):	25.95	0.631			
Average Subcooling (F):	25.91				
Evap Exit Pressure (psia):	90.71	0.365	Turbine A Frequency (Hz):	196.14	1.00
Evap Exit Avg Temp A:	55.49	2.574	Turb A Vol Flow (ft3/min):	0.0276	0.00
Evap Exit Avg Temp B:	54.96	2.852	Turb A Density (lbm/ft3):	70.52	0.09
Evap Exit Avg Temp C:	53.96	1.681	Turb A Mass Flow (lb/h):	116.73	0.65
Circuit A Superheat (F):	9.79	2.574	Turbine C Frequency (Hz):	207.21	2.00
Circuit B Superheat (F):	9.27	2.696	Turb C Vol Flow (ft3/min):	0.0299	0.00
Circuit C Superheat (F):	8.26	1.681	Turb C Density (lbm/ft3):	70.50	0.09
Overall Superheat (F)	11.96	1.978	Turb C Mass Flow (lb/h):	126.40	1.26
			Turb C Calculated Mass Flow (lbm/h):	94.34	6.24
Evap Circuit Temp 1 (F):	49.35	0.226	% Total Mass Flow Thru A:	34.59	0.47
Evap Circuit Temp 2 (F):	49.98	0.651	% Total Mass Flow Thru B:	27.95	1.31
Evap Circuit Temp 3 (F):	49.52	0.326	% Total Mass Flow Thru C:	37.46	0.84
Evap Circuit Temp 4 (F):	48.52	0.373			
Evap Circuit Temp 5 (F):	48.33	0.652			
Evap Circuit Temp 6 (F):	48.72	0.370			
Evap Circuit Temp 7 (F):	52.06	0.413			
Evap Circuit Temp 8 (F):	48.51	0.186			
Evap Circuit Temp 9 (F):	50.51	2.041			

SMART DISTRIBUTOR SUMMARY SHEET
 DATA FILENAME: E020613A.dat SUMMARY FILENAME: E020613A.sum

Air-Side Conditions		Range	Total Air-Side Capacity: 22705.13	Range
Indoor Dry-Bulb :	80.129	0.43	Sensible Cap (Btu/h): 16720.22	318.70
Indoor Inlet Dew (F):	60.324	0.25	Latent Cap (Btu/h): 5984.91	567.51
Indoor Exit Dry-Bulb:	60.575	0.17	EvapAir Delta T (F): 20.03	300.83
Indoor Exit Dew (F):	58.043	0.15	Air/Ref Cap Prnt Diff: 2.77	0.85
			Sensible Heat Ratio: 0.736	3.22
Indoor Airflow (CFM):	768.35	7.35	SCFM per Ton: 400.67	0.0156
Indoor Airflow (SCFM):	758.10	7.27	(0.075 lb/ft3 standard air)	
Evap Inlet Humidity Ratio (lbH2O/lbAir):			0.011436	
Evap Exit Humidity Ratio (lbH2O/lbAir):			0.009781	
Barometric Pressure (in HG):	29.24		Nozzle Temp (F): 61.82	0.27
Air Chamber Nozzle Pressure Drop (in Water):	0.771		0.015	
Evaporator Coil Air Pressure Drop (in Water):	0.423		0.005	

Refrigerant Side Conditions				
Expansion Valve				
Upstream Pressure (psia):	283.27	0.852	Ref-side Cap (Btu/h):	23333.33
Upstream Temp A (F):	104.99	0.567	Ref-side Cap (tons):	1.94
Upstream Temp B (F):	105.27	0.524	Refrigerant Mdot (lbm/h):	544.67
Upstream Temp C (F):	105.14	0.524	Coriolis Density (lbm/ft3):	-82.34
Upstream Average Temp (F):	105.13		Upstream R22 Ts5t (F):	-22.31
Upstream Subcooling A (F):	17.32	0.431		
Upstream Subcooling B (F):	17.04	0.451		
Upstream Subcooling C (F):	17.17	0.592		
Average Subcooling (F):	17.18			
Evap Exit Pressure (psia):	90.90	0.243	Turbine A Frequency (Hz):	222.71
Evap Exit Avg Temp A:	46.23	0.233	Turb A Vol Flow (ft3/min):	0.0311
Evap Exit Avg Temp B:	58.64	1.144	Turb A Density (lbm/ft3):	70.30
Evap Exit Avg Temp C:	66.51	0.770	Turb A Mass Flow (lb/h):	131.27
Circuit A Superheat (F):	0.44	0.389	Turbine C Frequency (Hz):	196.14
Circuit B Superheat (F):	12.85	1.300	Turb C Vol Flow (ft3/min):	0.0284
Circuit C Superheat (F):	20.73	0.926	Turb C Density (lbm/ft3):	70.28
Overall Superheat (F)	1.08	0.482	Turb C Mass Flow (lb/h):	119.79
			Turb C Mass Flow (lbm/h):	93.61
Circuit B Calculated Mass Flow				38.09
Evap Circuit Temp 1 (F):	50.10	0.557	% Total Mass Flow Thru A:	27.16
Evap Circuit Temp 2 (F):	50.11	0.557	% Total Mass Flow Thru B:	34.76
Evap Circuit Temp 3 (F):	50.10	0.604	% Total Mass Flow Thru C:	
Evap Circuit Temp 4 (F):	49.31	0.558		
Evap Circuit Temp 5 (F):	49.22	0.558		
Evap Circuit Temp 6 (F):	49.10	0.648		
Evap Circuit Temp 7 (F):	52.38	0.645		
Evap Circuit Temp 8 (F):	49.28	0.371		
Evap Circuit Temp 9 (F):	49.08	0.093		

DATA FILENAME E020≤20A.dat SUMMARY FILENAME: E020≤20A sum SMART DISTRIBUTOR SUMMARY H≤ET

Air-Side Conditions		Range	Total Air-Side Capacity: 23465.20	Range
Indoor Dry-Bulb : 78.961		0.31	Sensible Cap (Btu/h): 17050.84	560.85
Indoor Inlet Dew (F): 80.128		0.30	Latent Cap (Btu/h): 6414.34	438.61
Indoor Exit Dry-Bulb: 80.004		0.18	EvapAir Delta T (F): 20.42	488.23
Indoor Exit Dew (F): 83.487		0.15	Air/Ref Cap Prcnt Diff: -1.13	0.43
			Sensible Heat Ratio: 0.727	3.58
			SCFM per Ton: 387.89	0.0151
Indoor Airflow (CFM): 767.80		11.63	(0.075 lb/ft3 standard air)	
Indoor Airflow (SCFM): 758.49		11.56	0.011356	
Evap Inlet Humidity Ratio (lbH2O/lbAir):			0.009583	
Evap Exit Humidity Ratio (lbH2O/lbAir):			Nozzle Temp (F): 60 93 0 09	
Barometric Pressure (in HG): 29.24			0.771 0.023	
Air Chamber Nozzle Pressure Drop (in Water):			0.415 0.015	
Evaporator Coil Air Pressure Drop (in Water):				

Refrigerant Side Conditions				
Expansion Valve				
Upstream Pressure (psia):	318.93	0.974	Ref-side Cap (Btu/h) :	23109.58
Upstream Temp A (F) :	103.95	0.350	Ref-side Cap (tons) :	1.93
Upstream Temp B (F) :	104.32	0.088	Refrigerant Mdot (lbm/h) :	336.95
Upstream Temp C (F) :	104.05	0.568	Coriolis Density (lbm/ft3) :	32.07
Upstream Average Temp (F) :	104.11		Upstream R22 Tsat (F) :	131.81
Upstream Subcooling A (F) :	27.85	0.423		
Upstream Subcooling B (F) :	27.48	0.205		
Upstream Subcooling C (F) :	27.75	0.680		
Average Subcooling (F) :	27.70			
Evap Exit Pressure (psia):	90.53	0.486	Turbine A Frequency (Hz) :	191.06
Evap Exit Avg Temp A:	53.89	5.563	Turb A Vol Flow (ft3/min) :	0.0269
Evap Exit Avg Temp B:	54.92	2.849	Turb A Density (lbm/ft3) :	70.46
Evap Exit Avg Temp C:	56.77	2.821	Turb A Mass Flow (lb/h) :	113.77
Circuit A Superheat (F) :	8.38	5.877	Turbine C Frequency (Hz) :	209.06
Circuit B Superheat (F) :	9.41	3.139	Turb C Vol Flow (ft3/min) :	0.0301
Circuit C Superheat (F) :	11.26	3.056	Turb C Density (lbm/ft3) :	70.45
Overall Superheat (F)	11.90	2.422	Turb C Mass Flow (lb/h) :	127.35
Circuit B Calculated Mass Flow (lbm/h) :				
≤vap Circuit Temp 1 (F) :	49.60	0.279	% Total Mass Flow Thru A :	95.82
≤vap Circuit Temp 2 (F) :	49.56	0.372	% Total Mass Flow Thru B :	33.77
≤vap Circuit Temp 3 (F) :	49.29	0.094	% Total Mass Flow Thru C :	28.44
≤vap Circuit Temp 4 (F) :	48.31	0.094		37.80
≤vap Circuit Temp 5 (F) :	48.22	0.559		
≤vap Circuit Temp 6 (F) :	48.82	0.558		
≤vap Circuit Temp 7 (F) :	51.56	0.346		
≤vap Circuit Temp 8 (F) :	48.77	0.352		
≤vap Circuit Temp 9 (F) :	50.13	3.803		

DATA FILENAME: E020621A.dat SUMMARY FILENAME: E020621A.sum

Air-Side Conditions			Range	Total Air-Side Capacity:	22434.90	Range
Indoor Dry-Bulb :		73.97°	0.46	Sensible Cap (Btu/h):	16483.48	441.26
Indoor Inlet Dew (F):		60.42°	0.21	Latent Cap (Btu/h):	5951.42	284.76
Indoor Exit Dry-Bulb:		60.85°	0.16	EvapAir Delta T (F):	19.60	389.14
Indoor Exit Dew (F):		58.21°	0.15	Air/Ref Cap Prcnt Diff:	2.90	0.22
				Sensible Heat Ratio:	0.735	3.38
Indoor Airflow (CFM):		774 ±3	7	SCFM per Ton:	008.33	0.0106
Indoor Airflow (SCFM):		763.52	7.18	(0.075 lb/ft3 swamp/d air)		
Evap Inlet Humidity Ratio (lbH2O/lbAir):				0.011476		
Evap Exit Humidity Ratio (lbH2O/lbAir):				0.009842		
Barometric Pressure (in HG):		29.24		Nozzle Temp (F):	61 °F	0 °F
Air Chamber Nozzle Pressure Drop (in Water):				0.783	0.015	
Evaporator Coil Air Pressure Drop (in Water):				0.397	0.013	

Refrigerant Side Conditions						
Expansion Valve						
Upstream Pressure (psia):		302.15	1.218	Ref-side Cap (Btu/h) :	23083.84	624.23
Upstream Temp A (F):		103.97	0.568	Ref-side Cap (tons):	1.92	0.03
Upstream Temp B (F):		104.39	0.262	Refrigerant Mdot (lbm/h):	339.33	9.43
Upstream Temp C (F):		103.86	0.568	Coriolis Density (lbm/ft3):	82.02	0.13
Upstream Average Temp (F):		104.07		Upstream R22 Tsat (F):	127.44	
Upstream Subcooling A (F):		23.48	0.697			
Upstream Subcooling B (F):		23.06	0.367			
Upstream Subcooling C (F):		23.59	0.633			
Average Subcooling (F):		23.38				
Evap Exit Pressure (psia):		91.18	0.608	Turbine A Frequency (Hz):	217.86	2.00
Evap Exit Avg Temp A:		46.39	0.558	Turb A Vol Flow (ft3/min):	0.0305	0.00
Evap Exit Avg Temp B:		60.66	1.233	Turb A Density (lbm/ft3):	70.46	0.09
Evap Exit Avg Temp C:		68.09	0.972	Turb A Mass Flow (lb/h):	128.83	1.14
Circuit A Superheat (F):		0.44	0.636	Turbine C Frequency (Hz):	191.09	2.00
Circuit B Superheat (F):		14.71	1.274	Turb C Vol Flow (ft3/min):	0.0277	0.00
Circuit C Superheat (F):		22.15	1.148	Turb C Density (lbm/ft3):	70.48	0.09
Overall Superheat (F)		0.80	0.715	Turb C Mass Flow (lb/h):	117.27	1.21
				Calculated Mass Flow (lbm/h):	93.22	9.55
Circuit Temp 1 (F):		50.41	1.114	% Total Mass Flow Thru A:	37.97	1.11
Circuit Temp 2 (F):		50.86	0.603	% Total Mass Flow Thru B:	27.47	2.14
Circuit Temp 3 (F):		50.21	0.557	% Total Mass Flow Thru C:	34.56	1.03
Circuit Temp 4 (F):		49.20	0.651			
Circuit Temp 5 (F):		48.95	0.279			
Circuit Temp 6 (F):		49.26	0.603			
Circuit Temp 7 (F):		52.93	1.200			
Circuit Temp 8 (F):		49.69	0.837			
Circuit Temp 9 (F):		48.89	0.604			

SMART DISTRIBUTOR SUMMARY SHEET
 DATA FILENAME: E020624A.dat SUMMARY FILENAME: E020624A.sum

Air-Side Conditions		Range	Total Air-Side Capacity	23455.84	Range
Indoor Dry-Bulb :	~9.94E	0.23	Sensible Cap (Btu/h):	16834.92	506.67
Indoor Inlet Dew (F):	≤0.37E	0.31	Latent Cap (Btu/h):	6620.92	440.93
Indoor Exit Dry-Bulb:	≤0.21E	0.23	EvapAir Delta T (F):	20.14	194.35
Indoor Exit Dew (F):	35.62E	0.25	Air/Ref Cap Prcnt Diff:	-1.51	0.43
			Sensible Heat Ratio:	0.718	5.46
Indoor Airflow (CFM):	768.99	7.34	SCFM per Ton:	388.48	0.0080
Indoor Airflow (SCFM):	759.35	7.23	(0.075 lb/ft3 standard air)		
Evap Inlet Humidity Ratio (lbH2O/lbAir):			0.011459		
Evap Exit Humidity Ratio (lbH2O/lbAir):			0.009631		
Barometric Pressure (in HG):	29.24		Nozzle Temp (F):	61.07	0 ≤0
Air Chamber Nozzle Pressure Drop (in Water):			0.773	0.015	
Evaporator Coil Air Pressure Drop (in Water):			0.409	0.010	

Refrigerant Side Conditions					
Expansion Valve					
Upstream Pressure (psia):	315.48	0.487	Ref-side Cap (Btu/h):	23100.49	153.85
Upstream Temp A (F):	105.60	0.523	Ref-side Cap (tons):	1.33	0.07
Upstream Temp B (F):	106.33	0.262	Refrigerant Mdot (lbm/h):	338.35	12.54
Upstream Temp C (F):	105.90	0.524	Coriolis Density (lbm/ft3):	32.45	0.16
Upstream Average Temp (F):	105.94		Upstream R22 Tsat (F):	130.31	
Upstream Subcooling A (F):	25.31	0.61E			
Upstream Subcooling B (F):	24.58	0.41E			
Upstream Subcooling C (F):	25.02	0.46E			
Average Subcooling (F):	24.97				
Evap Exit Pressure (psia):	90.66	0.486	Turbine A Frequency (Hz):	187.88	1.00
Evap Exit Avg Temp A:	55.73	2.848	Turb A Vol Flow (ft3/min):	0.0265	0.00
Evap Exit Avg Temp B:	55.12	2.851	Turb A Density (lbm/ft3):	70.21	0.0E
Evap Exit Avg Temp C:	54.49	2.901	Turb A Mass Flow (lb/h):	111.58	0.62
Circuit A Superheat (F):	10.19	3.004	Turbine C Frequency (Hz):	215.88	2.00
Circuit B Superheat (F):	9.57	3.008	Turb C Vol Flow (ft3/min):	0.0310	0.00
Circuit C Superheat (F):	8.95	3.058	Turb C Density (lbm/ft3):	70.16	0.0E
Overall Superheat (F)	11.89	2.136	Turb C Mass Flow (lb/h):	130.67	1.27
			Turb C Calculated Mass Flow (lbm/h):	96.10	12.24
Evap Circuit Temp 1 (F):	49.53	0.603	Total Mass Flow Thru A:	32.94	1.23
Evap Circuit Temp 2 (F):	50.03	0.32E	Total Mass Flow Thru B:	28.40	2.62
Evap Circuit Temp 3 (F):	49.50	0.604	Total Mass Flow Thru C:	38.62	1.41
Evap Circuit Temp 4 (F):	48.36	0.093			
Evap Circuit Temp 5 (F):	48.28	0.652			
Evap Circuit Temp 6 (F):	48.65	0.558			
Evap Circuit Temp 7 (F):	52.31	0.645			
Evap Circuit Temp 8 (F):	48.69	0.372			
Evap Circuit Temp 9 (F):	50.68	2.876			

APPENDIX B. CAPACITY UNCERTAINTY

Table B.1 lists the relative uncertainty in the air-side capacity for two representative tests at low and high evaporator capacity. Two tests are shown below, with the first test being a typical test at a capacity comparable to a majority of the other tests for all coils. The second test listed in Table B.1 shows a worst case test for COIL-W in parallel flow with an extremely low capacity. For the majority of tests, the uncertainty in the evaporator capacity was at the 4 % to 5 % level. A complete description of the propagation of error technique used to calculate uncertainty is given in Payne and Domanski (2001).

Table B.1: Relative Uncertainties of Two Evaporator Tests

Test Name	Coil Designation	Capacity, kW (Btu/h)	Uncertainty Description	Capacity, kW (Btu/h)	Percent Uncertainty at a 95 % Confidence Limit on the Mean
E020416B	Enhanced-cut	7.8 (26546)	<i>Typical of all tests</i>	7.8 (26546)	4.2
W020311B	Wavy	0.90 (3078)	Worst <i>case</i>	0.90 (3078)	8.9

APPENDIX C. USER'S INSTRUCTION FOR THE EVAP-COND VERSION USED IN THIS STUDY

A CD attached to this report contains a version of EVAP-COND that was specifically developed for this study. The following pages describe how to install and use the model. As needed for this study, this version of EVAP-COND simulates only evaporators with multiple inlets using the option that solicits refrigerant outlet saturation temperatures and global superheat. This option is identified in the figure below with the EVAPORATOR OPERATING CONDITIONS. The condenser, which normally is included in the EVAP-COND package is not provided here.

The attached CD package contains the following two files:

EV-CD.exe - self-extracting file with all files needed for
executing EVAP-COND.

EVAP-COND instructions.pdf - file with visual instructions on how to use EVAP-COND. (You need Version **5** of Adobe Reader to read this file.). The instructions are also included in this appendix.

Installation of EVAP-COND on your PC

Execute file EV-CD.exe to expand it on your hard drive. You will be prompted to select a directory where you want the program to reside. When the installation is completed, you should see EVAP-COND directory and two subdirectories called FLUIDS and MIXTURES.

In the main directory (EVAP-COND), EVAP-COND.exe is the interface. EVAP5.exe is the evaporator. Files with the affix.dat are example cases of input data used in this study. Files with the affix.opc extension contain corresponding operating conditions.

Next step

Refer to the following pages or EVAP-COND instructions.pdf for further information about EVAP-COND capabilities and limitations. They will also assist you in your first evaporator simulation run. It is recommended for the user to follow the steps described there to familiarize yourself with the model. Because of constant upgrading of the model, the simulation results you are going to obtain may not be the same as those presented in EVAP-COND instructions.pdf.

Control of the option to simulate with or without longitudinal fin conduction

The user can control the option of using longitudinal fin conduction in a simulation by accessing file TUNE.TXT selecting 0 or 1 for the flag, as it is explained in the file, and saving the file. TUNE.TXT is located in the EVAP-COND directory.

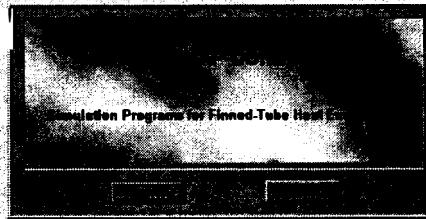
The following pages contain general visual instructions for using EVAP-COND as they are presented in the file EVAP-COND instructions.pdf located on the attached CD. The option developed for this project is marked and available in this package is marked.

EVAP- COND INSTRUCTIONS

NAPCOND is a software package that contains NIST's simulation models for a finned-tube evaporator (EVAP5) and condenser (COND5). The following pages provide basic instructions on how to use this package. The instructions include preparation of input data, execution of the program, and examination of simulation results.

Capabilities include:

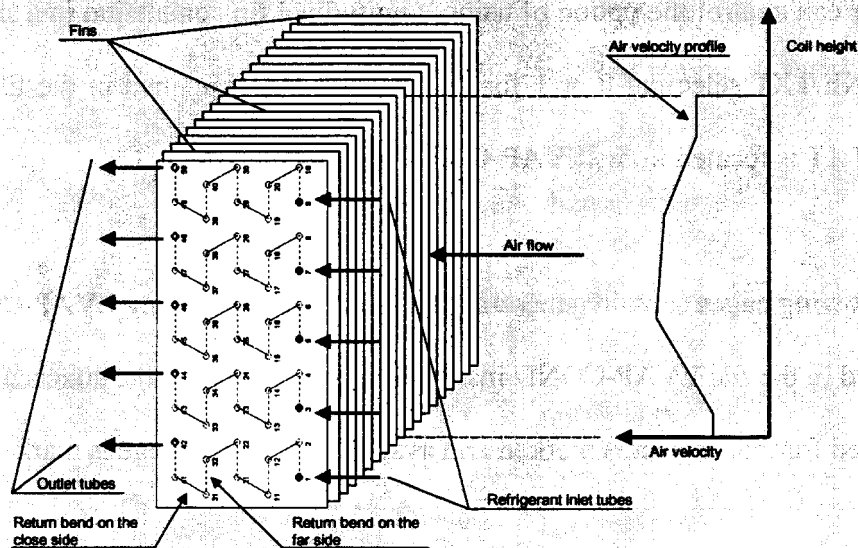
- tube-by-tube simulation
- non-uniform air distribution
- simulation of refrigerant distribution
- condenser model capable of simulations above the critical point
- 10 refrigerants and refrigerant mixtures
- REFPROP6 refrigerant properties



Piotr A Domanski
National Institute of Standards and Technology
Building and Fire Research Laboratory
Gaithersburg, MD, USA

Smart Distributor Version, Aug. 5, 2002

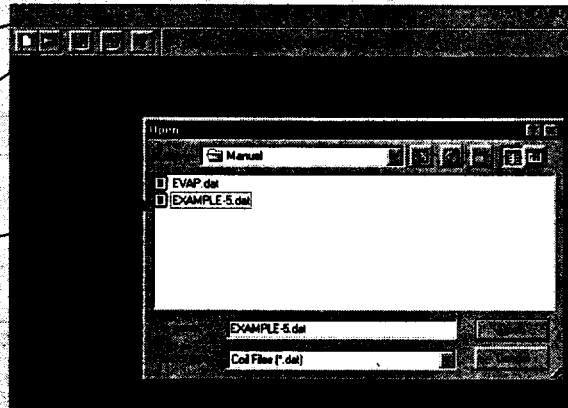
EVAPORATOR REPRESENTATION



LOADING A FILE

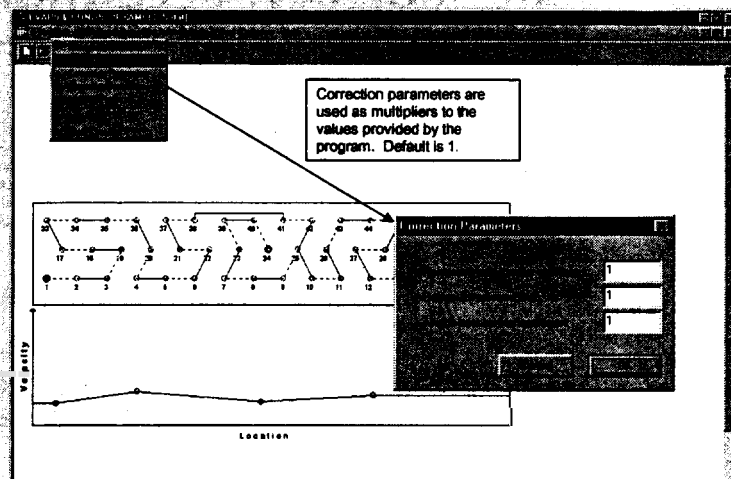
After starting the program, click on the "open file" button on the power bar or select "Open" on the pull down menu

Open file EXAMPLE-5 to continue this tutorial.



PREPARING A SIMULATION RUN

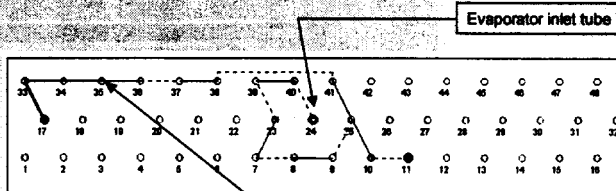
Correction parameters are used as multipliers to the values provided by the program. Default is 1.



REFRIGERANT CIRCUIT DESIGN

Follow the steps below to design a circuitry:

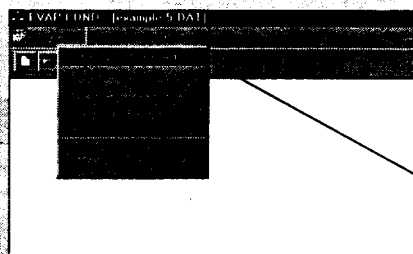
1. place the pointer on the tube
2. press the left mouse button
3. drag the pointer to the next tube
4. release the left button.



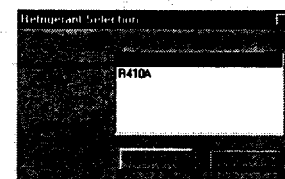
Option:

You may remove a part of the circuit by positioning the pointer on a given tube and clicking twice with the left button.

REFRIGERANT SELECTION



EXAMPLE-5 was set up to use refrigerant inlet pressure and quality as input data (see Operating Conditions). Since the specified inlet pressure is for R22, use the pull-down menu to select R22.



COIL DESIGN DATA

Coil Design Data

EXAMPLE 6

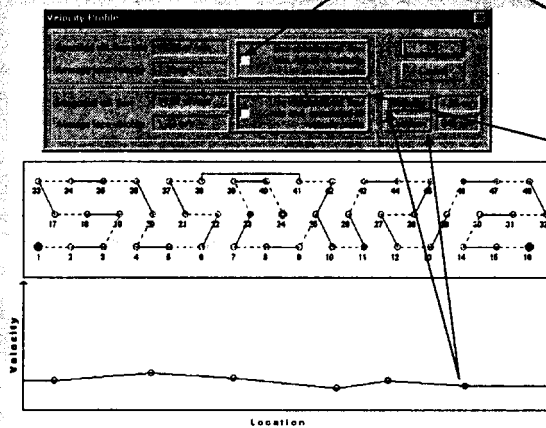
16
16
16
0
0

454.025
3.2202
10.0076
25.4
22.225
Smooth
0.366713

0.2032
2.00406
Wavy
0.221968

Value 1 must be used for this version of EVAP-COND.

AIR VELOCITY PROFILE



Recall that the operating conditions input data included the volumetric flow rate of air. Before you leave this window you must decide between the two options:

- to use the previously specified vol. flow rate and have the velocity profile scaled to match that value (recommended)

or

- to disregard the previously specified vol. flow rate and calculate a new volumetric flow rate from the velocity profile

To specify velocity at a given point, place the pointer at that point and click with the left button. The window above shows the coordinates. Up to sixteen velocity points may be specified.

Click on a given point to remove it.

The Velocity Profile window must be open to make air velocity profile changes.

EVAPORATOR OPERATING CONDITIONS

(Eight options)

This option was used for simulation runs for this project

Input includes estimated refrigerant mass flow rate, which is later iterated by EVAP5.
Inlet quality is imposed at 0.20.

Input includes refrigerant mass flow rate.

This option includes a refrigerant distributor. Condenser subcooling and evaporator superheat are imposed to be 5 °C (9 °F).

Input includes estimated refrigerant mass flow rate, which is later iterated so the least superheated tube has the specified minimum superheat.
Inlet quality is imposed at 0.20.

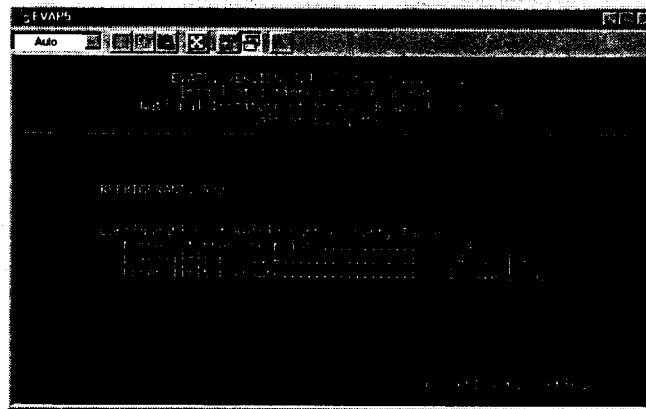
All input options include air inlet temperature, pressure, relative humidity, and volumetric flow rate.

The mark indicates the currently selected option.

EXECUTION OF EVAP5

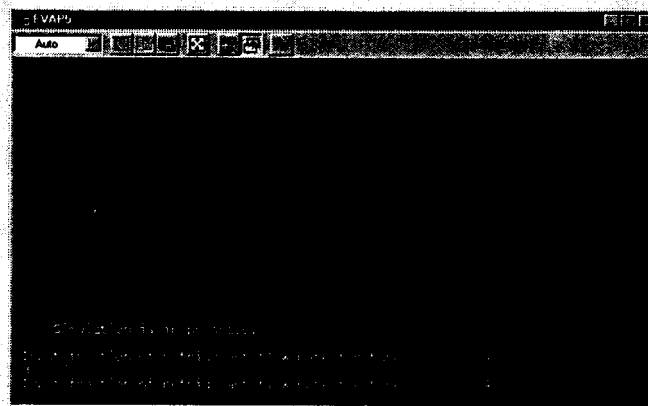
Use the pull-down menu to execute EVAP5.

EVAPS OPENING WINDOW



EVAPS SOLICITS REFRIGERANT DISTRIBUTION

This window appears only in this version of EVAP- COND for the simulation option used for this study



SIMULATION SUMMARY (cont.)

(Complete printout of file si.res)

5.0 Source: Notepad

File Edit View Window Help

EVAP5 SIMULATION SUMMARY

Coil ID EXAMPLE-5

REFRIGERANT R22

REFRIGERANT SIDE

Refrigerant mass flow rate	120.0	[kg/h]
Sensible capacity	3.735	[kW]
Latent capacity	1.677	[kW]
Total capacity	5.413	[kW]
Outlet saturated temp and superheat	7.0	6.2 [C]
Inlet and outlet temperatures	8.7	11.3 [C]
Inlet and outlet pressures	655.0	622.9 [kPa]
Inlet and outlet qualities	0.200	1.000

AIR SIDE

Air volumetric flow rate	15.0	[m ³ /min]
Air temperature distribution [C]	26.7	21.0 17.8 13.7
Air humidity distribution [%]	5000	6638 7411 8877

CONDITION OF REFRIGERANT LEAVING OUTLET TUBES

Tube #	Quality (-)	Temperature (C)	Superheat (C)	Ref	M	Fract (-)
1	0.989	7.6	0.0	0	522	
16	1.000	23.0	16.0	0	476	

Multiplier for refig. heat transfer coeff	1.00
Multiplier for refrigerant pressure drop	1.00
Multiplier for air-side heat trans coeff	1.00

24

HOW TO SIMULATE EVAPORATOR ?

(An example using the existing file EXAMPLE-5.dat)

Run Windows Explorer and go to the directory containing EVAP-COND.exe

Double-click on EVAP-COND.exe to start the program

Open file EXAMPLE-5.dat to simulate the evaporator. After the file is loaded you will see a schematic representing a side view of the evaporator. The red circle(s) indicates the inlet tube to the evaporator. The blue circles indicate the outlet tubes. The horizontal line at the bottom of the screen indicates the air velocity profile at the evaporator inlet.

Review Input Data. Click on the **Edit/Coil Design** menu item to review the evaporator design information. You may select either the SI or British system of units for your input data and simulation results.

Click on the **Edit/Operating Conditions/Evaporator/inlet pressure and quality** menu item to review operation conditions. Note that the loaded option has a mark on the left-hand side. Since EVAP5 simulates performance tube-by-tube from the inlet to outlet, the options that specify any outlet refrigerant parameter involve iterative calls to the option that specifies refrigerant inlet pressure and quality until the larger outlet parameters are obtained (e.g. saturation temperature and superheat).

Click on the **Edit/Velocity Profile** menu item to review the air velocity profile. You may use the air mass flow rate specified earlier in the **Operating Conditions** window or integrate the air velocity profile. In general, the first option is recommended unless very detailed and accurate local measurements of the velocity profile were taken. You may change the air velocity profile using a mouse by clicking the left button.

Run a simulation. Click on the **Run Simulation** menu item and select EVAP5. An MS-DOS window will appear and will give you a message when a simulation run is successfully completed.

Examine local and global simulation results. EVAP5 writes global simulation results to file SI.res (SI system of units) and BT.res (British system of units). The same information is provided in the pull-down menu in the units selected for data input.

HOW TO PREPARE YOUR DATA FILE ?

Start with **Edit/Coil Design** menu item. Input all information.

Select **Edit/Operating Conditions** menu item to input operating conditions data

Select **Edit/Velocit Profile** to change the velocity profile using a mouse (left button)

Specify refrigerant circuitry

If you are coding evaporator circuitry, start with one of the inlet tubes and proceed downstream. If you are coding condenser circuitry, start with one of the outlet tubes and proceed upstream, i.e., in either case you have to start from the side that is closer to the saturated liquid line

To draw a return bend, point the mouse on a tube, press the left button, drag the mouse to the next tube, and release

If you want to modify a circuitry, you may delete a part of it starting from a given tube and ending by the exit tube by pointing the mouse on the given tube and double-clicking the left button

Once a circuit is coded, it can be used for both evaporator and condenser simulations based on specified operating conditions

COMMENTS

SUGGESTIONS

QUESTIONS

?

Piotr A. Domanski
National Institute of Standards and Technology
Building and Fire Research Laboratory
Gaithersburg, MD, USA
Piotr.Domanski@NIST.gov

BIBLIOGRAPHY

ANSYASHRAE Standard **51-1985** or ANSI/AMCA Standard **210**. *Laboratory methods of testing fans for rating*. American Society of Heating, Refrigerating and Air-conditioning Engineers. **1791** Tullie Circle NE, Atlanta, GA, USA.

ANSYASHRAE Standard **37-1988**. *Methods of testing for rating unitary air conditioning and heat pump equipment*. American Society of Heating, Refrigerating and Air-conditioning Engineers. **1791** Tullie Circle NE, Atlanta, GA, USA.

ARI, **1999**. "Positive Displacement Refrigerant Compressor and Compressor Units", Standard **540-1999**, Air-conditioning and Refrigeration Institute, Arlington, VA.

ASHRAE, **2001**. *ASHRAE Handbook*, Fundamentals Volume, p. **3.14**, American Society of Heating, Refrigerating and Air Conditioning Engineers, Inc., Atlanta, GA.

Bergles, A.E., Collier, J.G., Delhay, J.M., Hewitt, G.F., and Mayinger, F., **1981**. *Two-Phase Flow and Heat Transfer in the Power and Process Industries*, p. **146-147**, Hemisphere Publishing Corp., New York, NY.

Chen J. C., **1966**, Correlation for Boiling Heat Transfer to Saturated Fluids in Convective Flow, *I&EC Process Design and Development*, Vol. **5**, No. **3**.

Chi, J., **1979**. "A Computer Model HTPUMP for Simulation of Heat Pump Steady-State Performance", National Bureau of Standards, Internal Report, Washington, D.C.

Chwalowski, M., Didion, D. A., and Domanski, P. A., **1989**, Verification of evaporator computer models and analysis of performance of an evaporator coil, *ASHRAE Trans.*, Vol. **95**, No. **1**.

Domanski, P.A., and Didion, D.A., **1983**. "Computer Modeling of the Vapor Compression Cycle with Constant Flow Area Expansion Device", *Building Science Series 155*, National Bureau of Standards, Gaithersburg, MD.

Domanski, P.A., **1990**. "Rating Procedure for Mixed Air-Source Unitary Heat Pumps Operating in the Heating Mode", NISTIR **90-4298**, National Institute of Standards and Technology, Gaithersburg, MD.

Domanski, P.A., **1991**. "Simulation of an Evaporator with Nonuniform One Dimensional Air Distribution", *ASHRAE Transactions*, Paper No. **NY-91-13-1**, Vol. **97**, Part 1.

Domanski, P.A. and McLinden, M.O., **1992**. A Simplified Cycle Simulation Model for the Performance Rating of Refrigerants and Refrigerant Mixtures, *Int. Journal of Refrigeration*, Vol. **15**, No 2, pp. **81-88**.

Domanski, P.A., 1999a. Evolution of Refrigerant Application, Proc. International Congress on Refrigeration, Milan, Italy.

Domanski, P.A., 1999b, "Finned-Tube Evaporator Model With a Visual Interface", 20th Int. Congress of Refrigeration, Sydney, Australia, September 19-24, 1999, International Institute of Refrigeration, Paris.

Ellison R.R., Crewick F.A., Ficher S.K., Jackson W.L., 1981, A computer model for air-cooled refrigerant condenser with specified refrigerant circuiting. ASHRAE Trans.

Gray D.L., Webb R.L., 1986, Heat transfer and friction correlations for plate fin-tube heat exchangers having plain fins, Proceedings of the 9th International Heat Transfer Conference, San Francisco.

Gungor K. E., Winterton R. H. S., 1986, **A General Correlation for Flow Boiling in Tubes and Annuli**, *International Journal of Heat and Mass Transfer*, Vol. 29, No. 3.

Heun, M.K., Crawford, R.R., 1994. Longitudinal Fin Conduction in Multipass Cross-Counterflow Finned-Tube Heat Exchangers, ASHRAE Transactions, Vol. 100, **Part 1**, pp. 382-389

Judge J., Radermacher R., 1997, **A heat exchanger model for mixtures and pure refrigerant cycle simulations**, International Journal of Refrigeration, Vol. 20.

Jung, D.S., Didion, D.A., 1989, *Horizontal Flow Boiling Heat Transfer using Refrigerant Mixtures*, ER-6364, EPRI Project 8006-2.

Kandlikar S. G., 1990, A General Correlation for Saturated Two-Phase **Flow Boiling Heat Transfer Inside Horizontal and Vertical Tubes**, *Transactions of the ASME, Journal of Heat Transfer*, Vol. 112.

Kandlikar S.G., 1991, A model for correlating flow boiling heat transfer in augmented tubes and compact evaporators, Journal of Heat Transfer, Vol. 113.

Kays, W.M., London, A.L., 1984, *Compact Heat Exchangers*, McGraw-Hill.

Kirby, E. S., C. W. Bullard, and W. E. Dunn, 1998, Effect of Airflow Nonuniformity on Evaporator Performance, *Transactions of the American Society of Heating, Refrigeration, and Air Conditioning Engineers*, Vol. 104, No. 2.

Kim, N.H., Yun, J.H., and Webb, R.L., 1997. "Heat transfer and friction correlations for wavy plate fin-and-tube heat exchangers", Journal of Heat Transfer 119, 560-567.

Klimenko V.V., 1988, A general correlation for two-phase forced flow heat transfer for two-phase forced flow heat transfer, Int. J. Heat Mass Transfer, Vol. 39, No. 3.

- Lee, J., Domanski, P. A., 1997. ***Impact of Air and Refrigerant Maldistributions on the Performance of Finned-Tube Evaporators with R22 and R-407C***, Report DOE/CE/23810-81 for ARI, National Institute of Standards and Technology, Gaithersburg, MD.
- Liang S.Y., Wong T.N., Nathan G.K., 2001, Numerical and experimental studies of refrigerant circuitry of evaporator coils, *International Journal of Refrigeration*, Vol. 24.
- McLinden, M.O., Klein, S.A., Lemmon, E.W., and Peskin, A.P., 1998. ***NIST Standard Reference Database 23***, Version 6.01 (REFPROP), National Institute of Standards and Technology, Gaithersburg, MD.
- McQuiston F.C., 1978, Correlation of heat, mass and momentum transport coefficients for plate-fin-tube heat transfer surface, *ASHRAE Trans.*, Vol. 84, No. 1.
- McQuiston, F.C., and Parker, J.D, 1982. ***Heating, Ventilating, and Air Conditioning***, J.Wiley & Sons.
- Nakayama, W., and Xu, L.P., 1983. Enhanced fins for air-cooled heat exchangers -heat transfer and friction correlations, *Proceedings of the 1st ASME/JSME Thermal Engineering Joint Conference*, 495-502.
- Oliet, C., Perez-Segarra, C.D., Danov, S., Oliva, A., 2002. Numerical Simulations of Dehumidifying Fin-and tube Heat Exchangers. Model Strategies and Experimental Comparisons, *Int. Refrig. Conf. at Purdue University*, W. Lafayette, IN, July 15-19.
- Payne, W.V. and Domanski, P. A., 2001, A comparison of rating water-source heat pumps using ARI standard 320 and ISO standard 13256-1, NISTIR 6803, National Institute of Standards and Technology, Gaithersburg, Maryland, USA.
- Petukhov, B.S., 1970. "Heat transfer and friction in turbulent pipe flow with variable physical properties", ***Advances in Heat Transfer***, Vol. 6., p. 503-564, Academic Press, New York.
- Pierre, B., 1964. "Flow Resistance with Boiling Refrigerants", ***ASHRAE Journal***, September issue.
- Ranganayakulu, Ch. et. al. 1996. ***The effects of longitudinal heat conduction in compact plate-fin and tube-fin heat exchangers using a finite element method*** *Int. J. Heat Mass Transfer*, Vol. 40, No. 6, pp. 1261-1277.
- Romero-Mendez, R., Sen, M., Yang, K.T., McClain, R.L., 1997. Effect of tube-to-tube conduction on plate-fin and tube heat exchanger performance, *Int. J. Heat Mass transfer*, Vol. 40, No. 16, pp 3909-3916.
- Shah M. M., 1976, A New Correlation for Heat Transfer During Boiling Flow Through Pipes, ***ASHRAE Transactions***, Vol. 82.

Sheffield, J.W., Wood, R.A., and Sauer, H.J., 1988. "Experimental Investigation of Thermal Conductance of Finned Tube Contacts", *Experimental Thermal and Fluid Science*, Elsevier Science Publishing Co., Inc., New York, NY.

Schlager, L.M., Pate, M.B., Bergles, A.E., 1989. "Heat Transfer and Pressure Drop during Evaporation and Condensation of R22 in Horizontal Micro-fin Tubes", *Int. J. Refrig.*, Vol. 12, No. 1.

Schlichting, H., 1968. *Boundary-Layer Theory*, Sixth Edition, p. 590, McGraw-Hill, Inc.

Wang, C.C., Jang, J.Y., and Chiou, N.F., 1999a. "A heat transfer and friction correlation for wavy fin-and-tube heat exchangers", *International Journal of Heat Mass Transfer* 42, 1919-1924.

Wang, C.C., Lee, C.J., Chang, C.T., and Lin, S.P., 1999b. "Heat transfer and friction correlation for compact louvered fin-and-tube heat exchangers", *International Journal of Heat Mass Transfer* 42, 1945-1956.

Wang, C.C., Chi, K.Y., and Chang, C.J., 2000, "Heat transfer and friction characteristics of plain fin-and-tube heat exchangers", part 1: correlation, *International Journal of Heat Mass Transfer* 43, 2693-2700.

Wang C.C., Lee W.S., Sheu W.J., 2001. A comparative study of compact enhanced fin-and-tube heat exchangers, *International Journal of Heat Mass Transfer*, Vol. 44.

Webb, R.L., 1990. "Air-side heat transfer correlations for flat and wavy plate fin-and-tube geometries", *ASHRAE Transactions* 96, Pt.2, 445-449.

